



LIBRARY
Michigan State
University

This is to certify that the

dissertation entitled

Exploratory Synthesis of New M/As $_{x}^{Q}Q_{y}(Q = S, Se)$ Compounds with Thioarsenate and Selenoarsenate Ligands by the Hydro (Solvo) Thermal Technique

presented by

Jun-Hong Chou

has been accepted towards fulfillment of the requirements for

Doctor degree in Philosophy

Date 2 16 1995

MSU is an Affirmative Action/Equal Opportunity Institution

0-12771

PLACE IN RETURN BOX to remove this checkout from your record.

TO AVOID FINES return on or before date due.

DATE DUE	DATE DUE	DATE DUE

MSU is An Affirmative Action/Equal Opportunity Institution



EXPLORATORY SYNTHESIS OF NEW $M/As_xQ_y(Q=S,Se)$ COMPOUNDS WITH THIOARSENATE AND SELENOARSENATE LIGANDS BY THE HYDRO(SOLVO)THERMAL TECHNIQUE

Ву

Jun-Hong Chou

A DISSERTATION

Submitted to

Michigan State University
in partial fulfillment of the requirements
for the degree of

DOCTOR OF PHILOSOPHY
Department of Chemistry
1995

ABSTRACT

EXPLORATORY SYNTHESIS OF NEW $M/As_xQ_y(Q = S, Se)$ COMPOUNDS WITH THIOARSENATE AND SELENOARSENATE LIGANDS BY THE HYDRO(SOLVO)THERMAL TECHNIQUE

Ву

Jun-Hong(Richard) Chou

The hydro(solvo)thermal technique was explored to synthesize new metal/As_xQ_y (Q = S, Se) compounds with thioarsenate and selenoarsenate ligands. With thioarsenate ligands, $[As_xS_y]^{n-}$, we have synthesized eleven new compounds. The remarkable feature exhibited by the compounds described in this dissertation is the complex condensation reactions exhibited by the thioarsenate polyanions.(see eq 1-4)

$$AsS_2SH^{2-} + AsS_2SH^{2-} = [As_2S_5]^{4-} + H_2S$$
 (Eq. 1)

$$[As_2S_5]^{4-} + H_2S \longrightarrow [As_2S_4SH]^{3-} + HS^{1-}$$
 (Eq. 2)

$$[As_2S_4SH]^{3-} + AsS_2SH^{2-} \longrightarrow [As_3S_7]^{5-} + H_2S$$
 (Eq. 3)

$$[As_3S_7]^{5}$$
 + H_2S = $[As_3S_6SH]^{4}$ + HS^{1} (Eq. 4)

These condensation reaction were probably catalyzed by the protonation of the terminal sulfide groups. The compounds include (Ph₄P)₂[InAs₃S₇], (Ph₄P)₂[SnAs₄S₉],

(Me₄N)₂Rb[BiAs₆S₁₂], (Ph₄P)₂[NiAs₄S₈], (Me₄N)₂[Mo₂O₂As₂S₇], (Ph₄P)₂[Pt(As₃S₅)₂], (Ph₄P)₂K[Pt₃(AsS₄)₃], (Ph₄P)₂K[Pd₃(AsS₄)₃], (Ph₄P)₂[Hg₂As₄S₉], (Me₄N)[HgAs₃S₆], and K[Ag₃As₂S₅]. Further exploration using selenoarsenate ligands, [As_xSe_y]ⁿ-, has allowed us to investigate the coordination chemistry of the [As_xSe_y]ⁿ- with metals like Hg and Ag. These reactions have resulted in the formation of variety of new compounds including (Me₄N)[HgAsSe₃], (Et₄N)[HgAsSe₃], (Ph₄P)₂[Hg₂As₄Se₁₁], β -Ag₃AsSe₃, K₅[Ag₂As₃Se₉], and (Me₃NH)[Ag₃As₂Se₅].

In this dissertation the synthesis, characterization and properties of the above compounds will be discussed.

TO MY WIFE, HSUPING CHOU, AND CHILDREN, TIFFANY AND DANIEL CHOU

ACKNOWLEDGMENT

I sincerely like to thank my research advisor, Professor Mercouri G. Kanatzidis. No of the work described in this dissertation would have been possible without his patient guidance, encouragement, dedication, and support. I would also like to thank the other members of my committee: Professor H. A. Eick, Professor, J. McCracken, and Professor J. Allison.

I would also like to express my appreciation to each member of the Kanatzidis group, past and present, for their kindness and friendship, which make my graduate school a wonderful experience.

Finally, I would like to express my deepest gratitude to my wife, Hsu-Ping, and children, Tiffany and Daniel Chou, for their understanding and encouragement throughout this thesis work. Tiffany, we now can go to the Disney World like I promise you before.

Financial support given by National Science Foundation, ACS-PRF, and Center for Fundamental Material Research, and the Department of Chemistry at Michigan State University are gratefully acknowledged.

TABLE OF CONTENTS

	Pa	ge
LIST OF TABLE	ES	. x
LIST OF FIGUR	ÆSx	vii
CHAPTER 1.	A Review of Metal/ $[E_xQ_y]^{n-}$ Systems (E = As, Sb; Q) =
	S, Se)	1
Reference	S	32
CHAPTER 2.	HYDROTHERMAL SYNTHESIS OF M/As_xS_y ($M = In$	3+,
	Sn ⁴⁺ , Bi ³⁺) COMPOUNDS. SYNTHESIS AND	
	CHARACTERIZATION OF (Ph4P)2[InAs3S7],	
	(Ph4P) ₂ [SnAs ₄ S ₉] AND (Me ₄ N) ₂ Rb[BiAs ₆ S ₁₂]	37
1. Introdu	ction	39
2. Experis	mental Section	40
2.1	Reagents	40
2.2	2 Syntheses	40
	(Ph ₄ P) ₂ [InAs ₃ S ₇]	41
	(Ph4P) ₂ [SnAs4S9]	41
	(Me4N)2Rb[BiAs6S12]	41
2.3	Physical Measurements	41
	X-ray crystallography	
3. Results	and discussion	57
3.1	Syntheses and description of structures	57
3.2	Physicochemical studies	73
Reference	S	85

CHAPTER 3.	HYDROTHERMAL SYNTHESIS OF M/As_xS_y (M = Ni^2	+,
	Mo ⁵⁺) COMPOUNDS. SYNTHESIS AND STRUCTURAL	
	CHARACTERIZATION OF (Ph4P)2[Ni2As4S8], and	
	(Me ₄ N) ₂ [Mo ₂ O ₂ As ₂ S ₇]	8
1. Introduc	etion	0
2. Experin	nental Section9	2
2.1	Reagents 9	12
2.2	Syntheses9)2
	(Ph ₄ P) ₂ [Ni ₂ As ₄ S ₈]9)2
	(Me ₄ N) ₂ [Mo ₂ O ₂ As ₂ S ₇])3
2.3	Physical Measurements 9	13
2.4	X-ray crystallography 9	3
3. Results	and discussion	13
3.1	Syntheses and description of structures 10)3
3.2	Physicochemical studies 11	5
References		:2
CHAPTER 4.	HYDRO(SOLVO)THERMAL SYNTHESIS OF DISCRETE	
	MOLECULAR M/As _x S _y (M = Pt ⁴⁺ , Pt ²⁺ Pd ²⁺) ANIONS	S.
	SYNTHESIS AND STRUCTURAL CHARACTERIZATION	N
	OF (Ph ₄ P) ₂ [Pt(As ₃ S ₅) ₂](I), (Ph ₄ P) ₂ K[Pt ₃ (AsS ₄) ₃](II),	
	AND (Ph ₄ P) ₂ K[Pd ₃ (AsS ₄) ₃](III)	6
1. Introduc	tion	8
2. Experin	ental Section	9
2.1	Reagents	9
2.2	Syntheses	0
	(Ph ₄ P) ₂ [Pt(As ₃ S ₅) ₂]	0

	(Ph ₄ P) ₂ K[Pt ₃ (AsS ₄) ₃]	. 130
	(Ph ₄ P) ₂ K[Pd ₃ (AsS ₄) ₃]	. 130
2.3	Physical Measurements	131
2.4	X-ray crystallography	131
3. Results	and discussion	145
3.1	Syntheses and description of structures	145
3.2	Physicochemical studies	159
Reference	S	167
CHAPTER 5	HYDROTHERMAL SYNTHESIS OF M/As_xQ_y ($M = 1$	Hg ²⁺ ,
	Q = S, Se) COMPOUNDS. SYNTHESIS AND	
	CHARACTERIZATION OF (Ph4P)2[Hg2As4S9](I),	
	$(Me_4N)[HgAs_3S_6](II), (Me_4N)[HgAsSe_3](III),$	
	(Et4N)[HgAsSe ₃](IV), and (Ph ₄ P) ₂ [Hg ₂ As ₄ Se ₁₁](V)
1. Introdu	ction	173
2. Experin	mental Section	174
2.1	Reagents	174
2.2	Syntheses	174
	(Ph4P)2[Hg2As4S9]	175
	(Me4N)[HgAs3S6]	175
	(Me4N)[HgAsSe3]	175
	(Et4N)[HgAsSe3]	. 176
	(Ph4P)2[Hg2As4Se11]	176
2.3	Physical Measurements	176
2.4	X-ray crystallography	176
	and discussion	
	Syntheses and description of structures	
	Physicochemical studies	216

Reference	s	230
CHAPTER 6	HYDRO(METHANO)THERMAL SYNTHESIS OF	
	M/As_xQ_y (M = Ag^{2+} , Q = S, Se) COMPOUNDS.	
	SYNTHESIS AND CHARACTERIZATION OF	
	Ag3AsSe3(I), (Me3NH)[Ag3As2Se5](II),	
	K ₅ [Ag ₂ As ₃ Se ₉](III), and K[Ag ₃ As ₂ S ₅](IV)	233
1. Introdu	ction	236
2. Experir	mental Section	238
2.1	Reagents	238
2.2	Syntheses	239
	β-Ag ₃ AsSe ₃	239
	(Me ₃ NH)[Ag ₃ As ₂ Se ₅]	240
	K ₅ [Ag ₂ As ₃ Se ₉]	240
	K[Ag ₃ As ₂ S ₅]	241
2.3	Physical Measurements	241
2.4	X-ray crystallography	241
3. Results	and discussion	255
3.1	Syntheses and description of structures	255
3.2	Physicochemical studies	292
Reference	S	303
CHAPTER 7	CONCLUSIONS	306
Reference	3	212

LIST OF TABLES

	Page
2 - 1	Crystallographic Data for (Ph ₄ P) ₂ [InAs ₃ S ₇](I),
	$(Ph_4P)_2[SnAs_4S_9](II), \ and \ (Me_4N)_2Rb[BiAs_6S_{12}](III) \ \ 46$
2-2	Selected Atomic Coordinates and Estimated
	Standard Deviations (esd's) of (Ph ₄ P) ₂ [InAs ₃ S ₇]
2-3	Selected Atomic Coordinates and Estimated
	Standard Deviations (esd's) of (Ph ₄ P) ₂ [SnAs ₄ S ₉] 50
2-4	Selected Atomic Coordinates and Estimated
	Standard Deviations (esd's) of (Me ₄ N) ₂ Rb[BiAs ₆ S ₁₂] 52
2-5	Calculated and Observed X-ray Powder
	Diffraction Pattern of (Ph ₄ P) ₂ [InAs ₃ S ₇] (I)
2-6	Calculated and Observed X-ray Powder
	Diffraction Pattern of (Ph ₄ P) ₂ [SnAs ₄ S ₉](II)
2-7	Calculated and Observed X-ray Powder
	Diffraction Pattern of (Me ₄ N) ₂ Rb[BiAs ₆ S ₁₂](III)
2-8	Selected Distances (Å) in (Ph ₄ P) ₂ [InAs ₃ S ₇] with Standard
	Deviations in Parentheses 58
2-9	Selected Angles (Deg) in (Ph ₄ P) ₂ [InAs ₃ S ₇] with Standard
	Deviations in Parentheses 59
2-10	Selected Distances (Å) in (Ph ₄ P) ₂ [SnAs ₄ S ₉] with Standard
	Deviations in Parentheses
2-11	Selected Angles (Deg) in (Ph ₄ P) ₂ [SnAs ₄ S ₉] with Standard
	Deviations in Parentheses
2-12	Selected Distances (Å) in (Me ₄ N) ₂ Rb[BiAs ₆ S ₁₂] with
	Standard Deviations in Parentheses

2-13	Selected Angles (Deg) in (Me ₄ N) ₂ Rb[BiAs ₆ S ₁₂] with
	Standard Deviations in Parentheses
2-14	Frequencies (cm ⁻¹) of Raman and Infrared Spectral
	Absorptions of (Ph ₄ P) ₂ [InAs ₃ S ₇](I), (Ph ₄ P) ₂ [SnAs ₄ S ₉](II),
	and (Me ₄ N) ₂ Rb[BiAs ₆ S ₁₂](III)
2-15	TGA data for (Ph ₄ P) ₂ [InAs ₃ S ₇](I), (Ph ₄ P) ₂ [SnAs ₄ S ₉](II),
	and (Me ₄ N) ₂ Rb[BiAs ₆ S ₁₂](III)
3 - 1	Crystallographic Data for (Ph4P)2[Ni2As4S8](I), and
	(Me ₄ N) ₂ [Mo ₂ O ₂ As ₂ S ₇](II)
3 - 2	Selected Atomic Coordinates and Estimated
	Standard Deviations (esd's) of (Ph ₄ P) ₂ [Ni ₂ As ₄ S ₈](I) 96
3-3	Selected Atomic Coordinates and Estimated Standard
	Deviations (esd's) of (Me ₄ N) ₂ [Mo ₂ O ₂ As ₂ S ₇](II)
3-4	Calculated and Observed X-ray Powder
	Diffraction Pattern of (Ph ₄ P) ₂ [NiAs ₄ S ₈](I) 101
3-5	Calculated and Observed X-ray Powder
	Diffraction Pattern of (Me ₄ N) ₂ [Mo ₂ O ₂ As ₂ S ₇](II) 102
3 - 6	Selected Distances (Å) in (Ph ₄ P) ₂ [Ni ₂ As ₄ S ₈] with
	Standard Deviations in Parentheses 107
3 - 7	Selected Angles (Deg) in (Ph ₄ P) ₂ [Ni ₂ As ₄ S ₈] with
	Standard Deviations in Parentheses 107
3 - 8	Selected Distances (Å) in (Me ₄ N) ₂ [Mo ₂ O ₂ As ₂ S ₇] with
	Standard Deviations in Parentheses 111
3 - 9	Selected Angles (Deg) in (Me ₄ N) ₂ [Mo ₂ O ₂ As ₂ S ₇] with
	Standard Deviations in Parentheses 112
3-10	Frequencies (cm ⁻¹) of Infrared Spectral Absorptions of
	(Ph ₄ P) ₂ [NiAs ₄ S ₈](I) ₂ and (Me ₄ N) ₂ [Mo ₂ O ₂ As ₂ S ₇](II) 115

3-11	TGA Data for $(Ph_4P)_2[NiAs_4S_8](I)$,
	and (Me ₄ N) ₂ [Mo ₂ O ₂ As ₂ S ₇](II)
4 - 1	Crystallographic Data for (Ph ₄ P) ₂ [Pt(As ₃ S ₅) ₂](I) and
	(Ph ₄ P) ₂ K[Pt ₃ (AsS ₄) ₃]·1.5 H ₂ O(II)
4 - 2	Selected Atomic Coordinates and Estimated
	Standard Deviations (esd's) of (Ph ₄ P) ₂ [Pt(As ₃ S ₅) ₂](I) 135
4-3	Selected Atomic Coordinates and Estimated Standard
	Deviations (esd's) of $(Ph_4P)_2K[Pt_3(AsS_4)_3]\cdot 1.5H_2O(II)$ 137
4 - 4	Selected Atomic Coordinates and Estimated Standard
	Deviations (esd's) of (Ph ₄ P) ₂ K[Pd ₃ (AsS ₄) ₃]·3CH ₃ OH(III)
4-5	Calculated and Observed X-ray Powder
	Diffraction Pattern of (Ph ₄ P) ₂ [Pt(As ₃ S ₅) ₂](I)
4 - 6	Calculated and Observed X-ray Powder
	Diffraction Pattern of (Ph ₄ P) ₂ K[Pt ₃ (AsS ₄) ₃]·1.5H ₂ O(II). 143
4-7	Calculated and Observed X-ray Powder
	Diffraction Pattern of (Ph ₄ P) ₂ K[Pd ₃ (AsS ₄) ₃]·
	3CH ₃ OH(III)144
4 - 8	Selected Distances (Å) in the [Pt(As ₃ S ₅) ₂] ² - with Standard
	Deviations in Parentheses
4 - 9	Selected Angles (Deg) in the [Pt(As ₃ S ₅) ₂] ² - with Standard
	Deviations in Parentheses 148
4-10	Selected Distances (Å) in the $[M_3(AsS_4)_3]^{3-}$ (M = Pt, Pd)
	with Standard Deviations in Parentheses 154
4-11	Selected Angles (Deg) in the $[M_3(AsS_4)_3]^{3-}$ (M = Pt, Pd)
	with Standard Deviations in Parentheses

4-12	Far-IR spectral Data for (Ph ₄ P) ₂ [Pt(As ₃ S ₅) ₂](I),
	$Ph_4P)_2K[Pt_3(AsS_4)_3]\cdot 1.5 H_2O(II)$, and
	(Ph ₄ P) ₂ K[Pd ₃ (AsS ₄) ₃]·3 MeOH(III)
4-13	TGA Data for $(Ph_4P)_2[Pt(As_3S_5)_2](I)$, $(Ph_4P)_2K[Pt_3(AsS_4)_3]$.
	1.5 $H_2O(II)$, and $(Ph_4P)_2K[Pd_3(AsS_4)_3]$.
	3MeOH(III)
5 - 1	Crystallographic Data for (Ph ₄ P) ₂ [Hg ₂ As ₄ S ₉](I),
	Me4N)[HgAs3S6](II)
5-2	Crystallographic Data for (Me ₄ N)[HgAsSe ₃](III),
	$(Et_4N)[HgAsSe_3](IV)$, and $(Ph_4P)_2[Hg_2As_4Se_{11})](V)$ 181
5-3	Selected Atomic Coordinates and Estimated
	Standard Deviations (esd's) of (Ph ₄ P) ₂ [Hg ₂ As4S ₉] 183
5 - 4	Selected Atomic Coordinates and Estimated
	Standard Deviations (esd's) of (Me ₄ N)[HgAs ₃ Se ₆] 185
5 - 5	Selected Atomic Coordinates and Estimated
	Standard Deviations (esd's) of (Me ₄ N)[HgAsSe ₃] 186
5-6	Selected Atomic Coordinates and Estimated
	Standard Deviations (esd's) of (Et4N)[HgAsSe3] 187
5-7	Selected Atomic Coordinates and Estimated
	Standard Deviations (esd's) of (Ph ₄ P) ₂ [Hg ₂ As ₄ Se ₁₁] 188
5 - 8	Calculated and Observed X-ray Powder
	Diffraction Pattern of (Ph ₄ P) ₂ [Hg ₂ As ₄ S ₉] 192
5 - 9	Calculated and Observed X-ray Powder
	Diffraction Pattern of (Me ₄ N)[HgAs ₃ S ₆]
5-10	Calculated and Observed X-ray Powder
	Diffraction Pattern of (Me ₄ N)[HgAsSe ₃] 194
5-11	Calculated and Observed X-ray Powder

	Diffraction Pattern of (Et ₄ N)[HgAsSe ₃]
5-12	Calculated and Observed X-ray Powder
	Diffraction Pattern of (Ph ₄ P) ₂ [Hg ₂ As ₄ Se ₁₁] 196
5-13	Selected Distances (Å) in (Ph ₄ P) ₂ [Hg ₂ As ₄ S ₉] with
	Standard Deviations in Parentheses
5-14	Selected Angles (Deg) in (Ph ₄ P) ₂ [Hg ₂ As ₄ S ₉] with
	Standard Deviations in Parentheses
5-15	Selected Distances (Å) in (Me ₄ N)[HgAs ₃ S ₆](II) with
	Standard Deviations in Parentheses
5-16	Selected Angles (Deg) in (Me ₄ N)[HgAs ₃ S ₆](II) with
	Standard Deviations in Parentheses 204
5-17	Selected Distances (Å) and Angles (Deg) in
	(Me ₄ N)[HgAsSe ₃] (III) and (Et ₄ N)[HgAsSe ₃] (IV) with
	Standard Deviations in Parentheses
5-18	Selected Distances (Å) in (Ph ₄ P) ₂ [Hg ₂ As ₄ Se ₁₁] with
	Standard Deviations in Parentheses
5-19	Selected Angles (Deg) in in (Ph ₄ P) ₂ [Hg ₂ As ₄ Se ₁₁] with
	Standard Deviations in Parentheses
5-20	Frequencies (cm-1) of Raman and Infrared Spectral
	Absorptions of (Ph ₄ P) ₂ [Hg ₂ As ₄ S ₉] (I), (Me ₄ N)[HgAs ₃ S ₆]
	(II), (Me ₄ N)[HgAsSe ₃] (III), (Et ₄ N)[HgAsSe ₃] (IV), and
	(Ph ₄ P) ₂ [Hg ₂ As ₄ Se ₁₁] (V)
5-21	TGA Data for (Ph4P) ₂ [Hg ₂ As ₄ S ₉] (I), (Me ₄ N)[HgAs ₃ S ₆] (II),
	(Me ₄ N)[HgAsSe ₃] (III), (Et ₄ N)[HgAsSe ₃] (IV), and
	(Ph ₄ P) ₂ [Hg ₂ As ₄ Se ₁₁] (V)
6 - 1	Crystallographic Data for β-Ag ₃ AsSe ₃ (I)
	(MeaNH)[AgaAsaSes](II)

6-2	Crystallographic Data for K ₅ [Ag ₂ As ₃ Se ₉](III)
	K[Ag ₃ As ₂ S ₅](IV)244
6-3	Selected Atomic Coordinates and Estimated
	Standard Deviations (esd's) of β-Ag ₃ AsSe ₃ (I)
6-4	Selected Atomic Coordinates and Estimated
	Standard Deviations (esd's) of
	(Me ₃ NH)[As ₃ As ₂ Se ₅](II)
6 - 5	Selected Atomic Coordinates and Estimated
	Standard Deviations (esd's) of K ₅ [Ag ₂ As ₃ Se ₉](III) 247
6-6	Selected Atomic Coordinates and Estimated
	Standard Deviations (esd's) of K[Ag ₃ As ₂ S ₅](IV)
6-7	Calculated and Observed X-ray Powder
	Diffraction Pattern of β-Ag ₃ AsSe ₃ (I)
6 - 8	Calculated and Observed X-ray Powder
	Diffraction Pattern of(Me ₃ NH)[As ₃ As ₂ Se ₅](II)
6-9	Calculated and Observed X-ray Powder
	Diffraction Pattern of K ₅ [Ag ₂ As ₃ Se ₉](III)
6-10	Calculated and Observed X-ray Powder
	Diffraction Pattern of K[Ag ₃ As ₂ S ₅](IV)
6-11	Selected Distances (Å) in β-Ag ₃ AsSe ₃ with Standard
	Deviations in Parentheses
6-12	Selected Angles (Deg) in β-Ag ₃ AsSe ₃ with Standard
	Deviations in Parentheses
6-13	Selected Distances (Å) (with Standard Deviations in
	Parenthesesa) in the [Ag ₃ As ₂ Se ₅] ¹ - layer
6-14	Selected Angles (Deg) (with Standard Deviations in
	Parentheses ^a) in the [Ag ₃ As ₂ Se ₅] ¹ - layer

6-15	Selected Distances (Å) of K ₅ [Ag ₂ As ₃ Se ₉] with Standard	
	Deviations in Parentheses	6
6-16	Selected Angles (Deg) of [Ag2As3Se9]5- with Standard	
	Deviations in Parentheses	7
6-17	Selected Distances (Å) in K[Ag ₃ As ₂ S ₅] with Standard	
	Deviations in Parentheses	5
6-18	Selected Angles (Deg) in [Ag ₃ As ₂ S ₅] ¹ with Standard	
	Deviations (in Parentheses	36
6-19	Frequencies (cm ⁻¹) of Raman and Infrared Spectral	
	Absorptions of Ag ₃ AsSe ₃ (I), (Me ₃ NH)[Ag ₃ As ₂ Se ₅] (II),	
	K ₅ [Ag ₂ As ₃ Se ₉] (III), and K[Ag ₃ As ₂ S ₅] (IV))2
7 - 1	Various [As _x S _y] ⁿ - polyanions	8
7-2	Various [As _x Se _y] ⁿ - polyanions	18
7-3	Various $[As_xQ_y]^{n-}$ (Q = S, Se) anions found in this	
	work)9
7 - 4	Different binding modes found in the [As _x Q _y] ⁿ -	
	anions	0
7-5	Some other known $[As_xQ_y]^{n-}$ (Q = S, Se, Te) anions 31	1

LIST OF FIGURES

	rage
1 - 1	Structure of [As ₆ S ₁₂] ⁶ - anion
1 - 2	Structure relation of [PbS ₃] layers and [TlS ₅] chains in
	PbTlAs ₃ S ₆ 4
1-3	The square pyramidal ribbon of MS_5 (M = Pb, Sb) in
	Pb/Sb/S sulfosalts 6
1 - 4	Packing diagram of Ag ₇ S ₂ (AsS ₄) viewed down the a
	axis 7
1-5	(A) Structure of [SAsS ₇] anion. (B) Packing diagram of
	(Ph4P)[SAsS7]9
1-6	The structure of [As(Se ₂)(Se)] infinite chain found in
	compounds MAsSe ₃ (M = K, Rb, Cs)
1 - 7	Two views of the $[As_3S_6]^{3-}$ anion
1 - 8	Structure of the [As ₄ S ₆] ² - anion
1-9	Structure of the [Sb ₁₂ Se ₂₀] ⁴ - anion
1-10	(A) Structure of Cp'3Ti2O(AsS3). (B) Structure of the
	[Mo ₂ O ₂ As ₄ S ₁₄] ² - anion
1-11	Structure of the [Se=W(PSe ₄)(PSe ₂)] anion 18
1-12	Structure of the [W ₂ As ₂ Se ₁₃] ² - anion
1-13	Structure of the [MoAs ₂ Se ₁₀] ² - anion
1-14	Structure of the $[M(CO)_2(As_3Se_3)]^{2-}$ (M = W, Mo) anion 23
1-15	Ortep drawing of a [As ₈ S ₁₃] ² - layer in Cs ₂ As ₈ S ₁₃ 26
1-16	Ortep drawing of a [As ₈ S ₁₃] ² - chain in Rb ₂ As ₈ S ₁₃
1-17	(A) View of KCu ₂ AsS ₃ down the b axis showing the
	copper arsenic sulfide connectivity in a layer.

	(B) View of KCu ₂ AsS ₃ down the c axis				
1 - 18	Packing diagram of KCu ₄ AsS ₄				
2 - 1	Structure and labeling scheme of $[InAs_3S_7]_{n^{2n}}$				
2-2	Packing diagram of (Ph ₄ P) ₂ [InAs ₃ S ₇]. (A) view down the				
	c-axis. (B) view down the b-axis				
2-3	Strucuture and labeling scheme of [SnAs ₄ S ₉] _n ²ⁿ 66				
2-4	Packing diagram of (Ph ₄ P) ₂ [SnAs ₄ S ₉]. (A) Showing the				
	crossing section. (B) Showing the One-dimensional				
	chains 67				
2-5	Structure and labeling scheme of				
	one $[BiAs_6S_{12}]_n^{3n-}$ layer				
2-6	Packing diagram of (Me ₄ N) ₂ Rb[BiAs ₆ S ₁₂]				
2-7	Far-IR spectra of (A) (Ph ₄ P) ₂ [InAs ₃ S ₇], (B)				
	$(Ph_4P)_2[SnAs_4S_9]$, and $(C) (Me_4N)_2Rb[BiAs_6S_{12}]$				
2-8	TGA diagrams of (A) [InAs ₃ S ₇] and				
	(B) (Ph ₄ P) ₂ [SnAs ₄ S ₉]77				
2-9	TGA diagram of (Me ₄ N) ₂ Rb[BiAs ₆ S ₁₂]78				
2-10	Optical absorption spectra of (A) (Ph ₄ P) ₂ [InAs ₃ S ₇],				
	and (B) (Ph ₄ P) ₂ [SnAs ₄ S ₉]				
2-11	Optical absorption spectrum of (Me ₄ N) ₂ Rb[BiAs ₆ S ₁₂] 81				
3-1	Structure and labeling scheme of				
	one [NiAs4S8] _n ²ⁿ - chain				
3-2	Packing diagram of (Ph ₄ P) ₂ [NiAs ₄ S ₈].				
	(A) view down the a-axis. (B) view down the c-axis 107				
3-3	Structure and labeling scheme of one				
	$[Mo_2O_2As_2S_7]_{n^2}^{n-1}$ chain				
3 - 4	Packing diagram of (Me ₄ N) ₂ [Mo ₂ O ₂ As ₂ S ₇]				

3-5	Far-IR spectra (CsI pellets) of (A) (Ph ₄ P) ₂ [NiAs ₄ S ₈], and		
	(B) (Me ₄ N) ₂ [Mo ₂ O ₂ As ₂ S ₇]116		
3-6	TGA diagrams of (A) (Ph ₄ P) ₂ [NiAs ₄ S ₈], and (B)		
	(Me ₄ N) ₂ [Mo ₂ O ₂ As ₂ S ₇]		
3 - 7	Optical absorption spectra of (A) (Ph ₄ P) ₂ [NiAs ₄ S ₈], and (B)		
	(Me ₄ N) ₂ [Mo ₂ O ₂ As ₂ S ₇]		
4 - 1	Packing diagram of (Ph ₄ P) ₂ [Pt(As ₃ S ₅) ₂] 149		
4-2	Structure and labeling scheme of [PtAs ₆ S ₁₀] ² 150		
4-3	Packing diagram of (Ph ₄ P) ₂ K[Pt ₃ (AsS ₄) ₃] 156		
4-4	Structure and labeling scheme of [Pt ₃ (AsS ₄) ₃] ³ 157		
4-5	Structure and labeling scheme of [Pd ₃ (AsS ₄) ₃] ³ 158		
4-6	Far-IR spectral Data for (A) (Ph ₄ P) ₂ [Pt(As ₃ S ₅) ₂](I), (B)		
	$(Ph_4P)_2K[Pt_3(AsS_4)_3]\cdot 1.5\ H_2O(II)$, and		
	(C) (Ph ₄ P) ₂ K[Pd ₃ (AsS ₄) ₃]·3 MeOH(III)		
4-7	TGA diagrams of (A) $(Ph_4P)_2[Pt(As_3S_5)_2](I)$, (B)		
	(Ph ₄ P) ₂ K[Pt ₃ (AsS ₄) ₃]·1.5 H ₂ O(II)		
4 - 8	TGA diagram of (Ph ₄ P) ₂ K[Pd ₃ (AsS ₄) ₃]·1.5 H ₂ O(III) 164		
5-1	Packing diagram of (Ph ₄ P) ₂ [Hg ₂ As ₄ S ₉]		
5-2	Structure and labeling scheme of		
	one $[Hg_2As_4S_9]_{n^{2n}}$ chain		
5-3	Packing diagram of (Me ₄ N)[HgAs ₃ S ₆]		
5-4	Structure and labeling scheme of		
	one $[HgAs_3S_6]_{n^{n-}}$ layer		
5-5	Packing diagram of (Me ₄ N)[HgAsSe ₃]		
5-6	Structure and labeling scheme of		
	one [HgAsSe ₃] _n ⁿ - chain		
5 - 7	Packing diagram of (Ph ₄ P) ₂ [Hg ₂ As ₄ Se ₁₁]		

5 - 8	Structure and labeling scheme of
	one $[Hg_2As_4Se_{11}]_{n^{2n}}$ chain
5-9	Far-IR spectra of (A) $(Ph_4P)_2[Hg_2As_4S_9](I)$, (B)
	(Me ₄ N)[HgAs ₃ S ₆](II)
5-10	Far-IR spectra of (A) (Me ₄ N)[HgAsSe ₃](III), (B)
	(Et ₄ N)[HgAsSe ₃](IV), and (C) (Ph ₄ P) ₂ [Hg ₂ As ₄ Se ₁₁](V) 218
5-11	TGA diagrams of (A) (Ph ₄ P) ₂ [Hg ₂ As ₄ S ₉](I), (B)
	(Me ₄ N)[HgAs ₃ S ₆](II)221
5-12	TGA diagrams of (A) (Me ₄ N)[HgAsSe ₃](III), (B)
	(Et4N)[HgAsSe3](IV)
5-13	TGA diagram of (Ph ₄ P) ₂ [Hg ₂ As ₄ Se ₁₁]
5-14	Optical absorption spectra of (A) (Ph ₄ P) ₂ [Hg ₂ As ₄ S ₉](I),
	(B) (Me ₄ N)[HgAs ₃ S ₆](II)
5-15	Optical absorption spectra of (A) (Me ₄ N)[HgAsSe ₃](III),
	(B) (Et4N)[HgAsSe ₃](IV)
5-16	Optical absorption spectrum
	of(Ph ₄ P) ₂ [Hg ₂ As ₄ Se ₁₁](V)
6 - 1	Structure and labeling scheme of Ag ₃ AsSe ₃ .
	(A) β-form. (B) α-form
6-2	Stereoview of the β-Ag ₃ AsSe ₃ (I)
6-3	Packing diagrams of β-Ag ₃ AsSe ₃ (I). (A) view down the b-
	axis. (B) Stereoview down the b-axis. (C) view down the
	c-axis. (D) stereoview down the c-axis
6 - 4	(A). Structure and labeling scheme of one [Ag3As2Se5]
	layer. (B) Stereoview
6-5	Packing diagrams of (Me ₃ NH)[Ag ₃ As ₂ Se ₅](II). (A) view
	down the c-axis. (B) view down the a-axis

6-6	Packing diagram of (Me ₃ NH)[Ag ₃ As ₂ Se ₅](II) showing the
	hydrogen bonding between the Se and H 274
6-7	Structure and labeling scheme of
	one [Ag ₂ As ₃ Se ₉]n ⁵ⁿ⁻ layer
6 - 8	Packing diagram of K ₅ [Ag ₂ As ₃ Se ₉]. (A) view down the a-
	axis. (B) view down the b-axis
6-9	The coordination environments of K+ in K ₅ [Ag ₂ As ₃ Se ₉].
	The open circles represent Se atoms
6-10	(A) Structure and labeling scheme of one [Ag ₃ As ₂ S ₅] _n ⁿ -
	layer. (B) Stereoview
6-11	Packing diagram of K[Ag ₃ As ₂ S ₅]. (A) view down the b-
	axis. (B) view down the c-axis
6-12	The coordination environments of K+ in K[Ag ₃ As ₂ S ₅].
	The open circles represent S atoms
6-13	Far-IR spectra of (A) Ag ₃ AsSe ₃ , (B)
	(Me ₃ NH)[Ag ₃ As ₂ Se ₅]293
6-14.	Far-IR spectra of (A) K ₅ [Ag ₂ As ₃ Se ₉], (B) and
	K[Ag ₃ As ₂ S ₅]294
6-15	Optical absorption spectra of (A) Ag ₃ AsSe ₃ (I) and (B)
	(Me ₃ NH)[Ag ₃ As ₂ Se ₅](II)
6-16	Optical absorption spectra of (A) K ₅ [Ag ₂ As ₃ Se ₉](III)
	and (B) K[Ag ₃ As ₂ S ₅](IV)
6-17	DTA data of Ag ₃ AsSe ₃ (I). (A) First cycle. (B) Second
	cycle
6-18	TGA diagram of β-Ag ₃ AsSe ₃ (I)
6-19	TGA diagram of (Me ₃ NH)[Ag ₃ As ₂ Se ₅]

CHAPTER 1

A Review of Metal/ $[E_xQ_y]^{n}$. Systems (E = As, Sb; Q = S, Se)

IJ 10 (1) روم ادار r. 1"2 713 į. V 1 M: je

The chemistry of metal/As_xS_y has been studied in mineralogy for a very long time. There is a large number of minerals which belong to a class of structurally interesting compounds known as sulfosalts. These sulfosalts have the general formula of $M_x E_y Q_z$ (M = metal, E = As, Sb, Bi; Q = S, Se, Te). Examples include Ag_3AsS_3 , 1 Ag3AsSe3,² HgSb4S8,³ TlHgAs3S6,⁴ Tl₃AsS4⁵, Pb₃As4S9.⁶ There are several characteristic features in these compounds. First, the metals are usually soft heavy metals, like Ag, Tl, Pb, Au, Hg. Second, they often have very complicated 3-dimensional dense packed structures. Third, the building blocks are mostly thio- or seleno- arsenates and antimonates with tri- or pentavalent group 15 elements. The interest in the sulfosalts stems not only from their great structural diversity but also because of interesting physical properties that are characteristic of these compounds. For example Ag3AsS3 and A g₃AsSe₃ are well known for their nonlinear optical properties.⁷ Most of these compounds were formed in the earth's crust through the reaction of metal sulfides with group 15/16 sulfides at elevated temperatures or through hydrothermal reaction in superheated water. From a synthetic point of view, this area of chemistry is relatively unexplored, although there is increasing evidence that **Example 2.** The paying more attention to the mixed group 15/16 **hemistry.** For example, Ag₃AsSe₃ does not occur in nature like the *Somorphous Ag3AsS3 (proustite, pyragyrite). It was synthesized by using a mixture of Ag/As/Se in a sealed silica tube at 1000 °C.8 ther example of a synthetic sulfosalt is PbTlAs₃S₆ which was

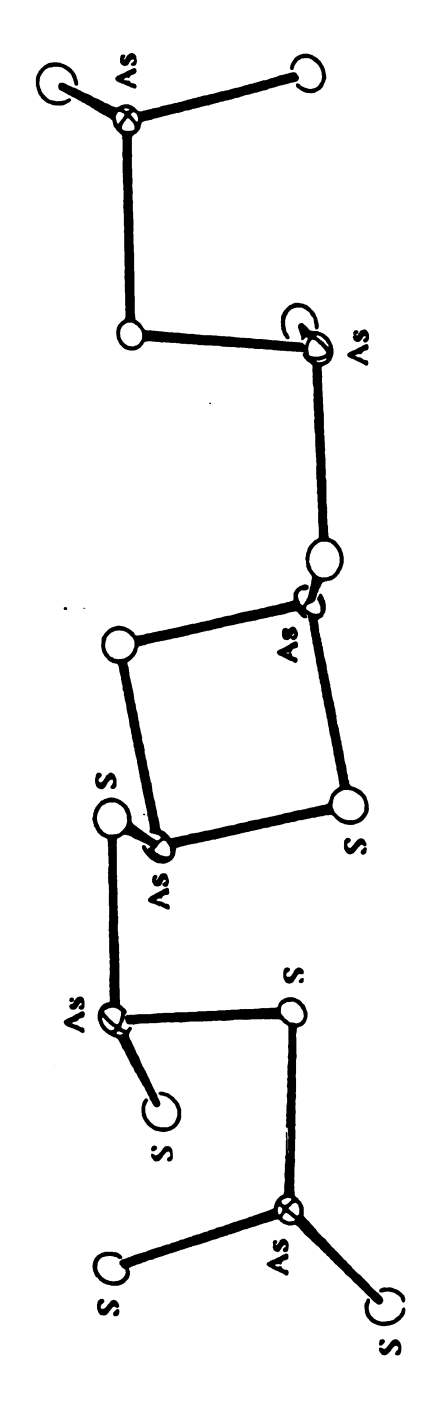


Figure 1-1. Structure of the [As₆S₁₂]⁶- anion.

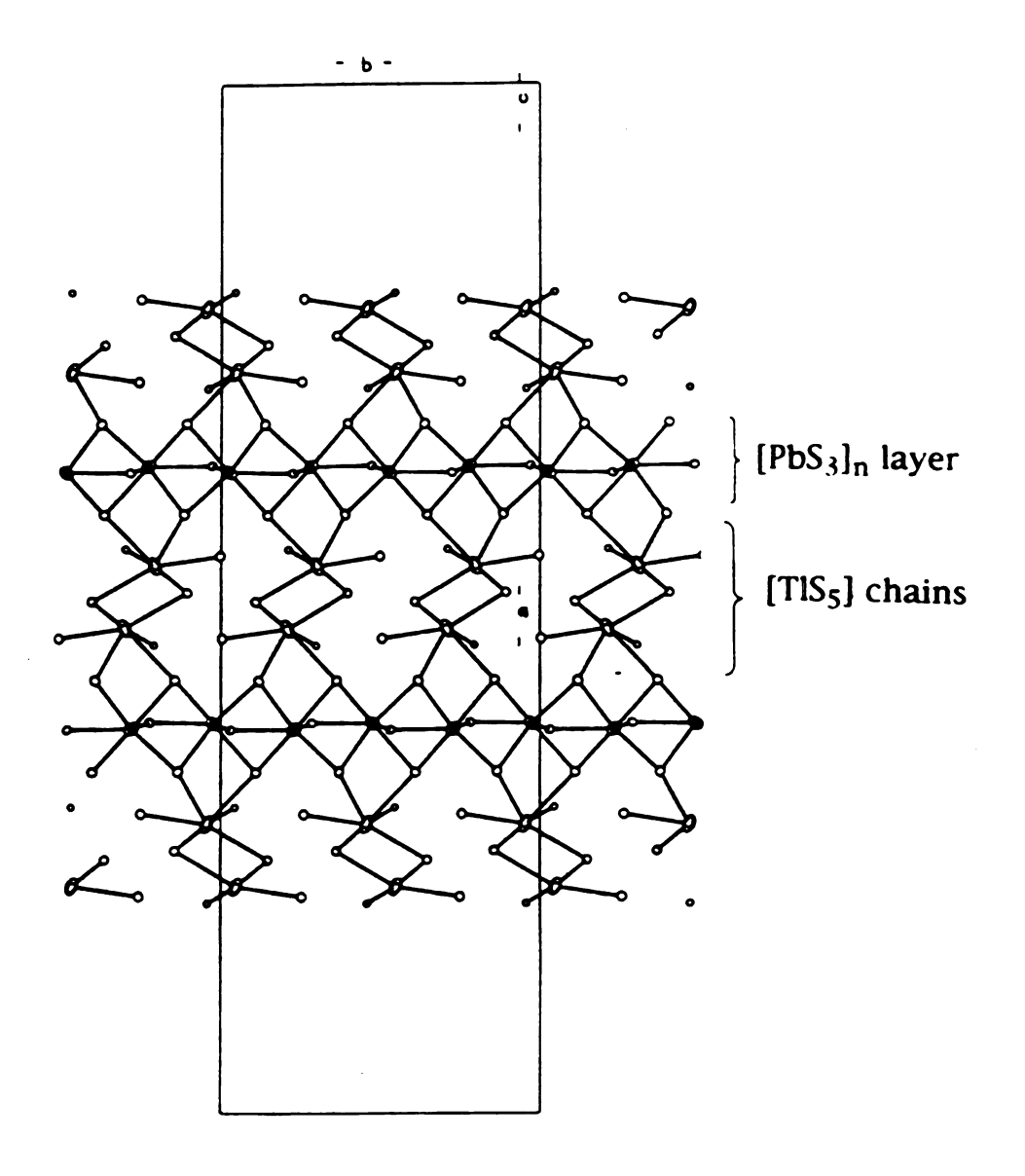


Figure 1-2. Structural relation of [PbS₃] layers and [TlS₅] chains in PbTlAs₃S₆.

ij. ::1 <u>;</u>22 lay: riet V).: **X**. X. 7:: λ., Rece ļi. Itt 11. : Pi itiç C. **3**. ! Œ: £ 4 ;

synthesized by using a mixture of Tl₂S/PbS/As₂S₃ by a hydrothermal reaction.⁹ The structure contains unique chainlike [As₆S₁₂]⁶ ligands; see Figure 1-1. The Pb is coordinated by seven S atoms forming PbS₃ layers which are interconnected by TlS₅ double chains; see figure 1-The most studied system in sulfosalts, from a synthetic point of view, is probably the Pb/Sb/S system. A detailed phase diagram, 10 published in 1979, indicated that six ternary compounds are possible between PbS and Sb₂S₃: Pb₇Sb₄S₁₃, ¹¹ Pb₃Sb₂S₆, ¹² Pb₅Sb₄S₁₁ (boulangerite), ¹³ Pb₂Sb₂S₅, ¹⁴ Pb₄Sb₆S₁₃ (robinsonite), ¹⁵ and PbSb₂S₄ (Zinckenite).¹⁶ Three of them are known as natural minerals and the other three can be synthesized from elemental lead, antimony and sulfur in sealed silica tubes at temperatures in excess of 1000 °C. Recently, a number of compounds was reported in this system that were previously unknown including Pb₅Sb₆S₁₄,¹⁷ Pb₇Sb₄S₁₃,¹¹ Pb4Sb4Se₁₀,¹⁸ and PbSb₂Se₄.¹⁹ They all have very complicated three-dimensional dense packed structures. The common feature of these compounds is the ribbons built of the square pyramid MS₅ (M = Pb, Sb), see Figure 1-3. Different width and binding modes of the ribbons give different structures. A unique modification of the known sulfosalt, CuAg₂AsS₄, is seen in (NH₄)Ag₂AsS₄.²⁰ The sites that were previously held by the Cu atoms are now occupied by NH₄+ cations. The compound was synthesized by using elemental Ag, As, S in a stainless steel autoclave with an ammonia solution (25%) at 220 Also, The compound Ag7S2(AsS4) has been synthesized by hydrothermal technique.²¹ There are three crystallographically independent Ag atoms which are surrounded by two, three, and four

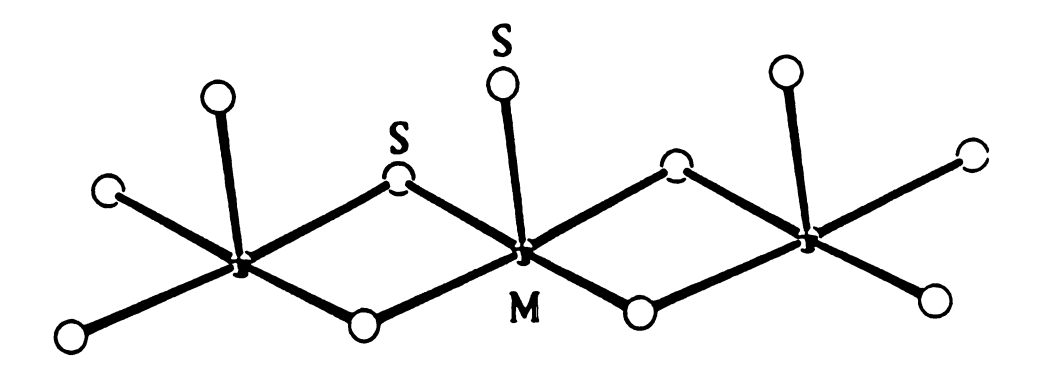
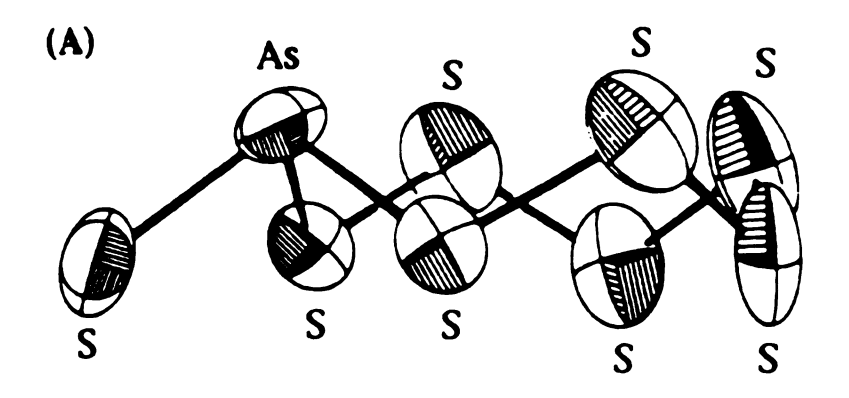


Figure 1-3. The square pyramidal ribbon of MS_5 (M = Pb, Sb) in Pb/Sb/S sulfosalts.

S atoms. These Ag polyhedra and AsS4 tetrahedra form a threedimensional framework, see Figure 1-4. The above examples suggest that the chemistry is very broad and structurally diverse, and that opportunities exist for synthetic chemists to explore for new materials ("synthetic minerals").

We have studied metal polychalcogenides in our lab for a long time. It has been demonstrated that polychalcogenide ligands of various chain lengths can act as building blocks and can connect metal ions together to form compounds ranging from molecular complexes to one-dimensional, two-dimensional, and even three-dimensional solid state compounds.²² These polychalcogenide ligands can coordinate to virtually all metal ions. In addition, since each member of the chain contains at least two lone pairs of electrons, one or all members of polychalcogenide ligands can ligate the metal ions.

Conceptually, the mixed $[As_xS_y]^{n-}$ anions can be viewed as an extension of the well-known polychalcogenide ligands, see Scheme 1, since the As- ion is isoelectronic to S. The best example of this concept is the compound $(Ph_4P)[SAsS_7]$, see Figure 1-5, prepared from the reaction of $[As_2SCl_5]^-$ and $S_5^{2-}.2^3$ The eight-member crown shaped ring compound is isoelectronic with elemental S_8 . Because of the charge on the As- ion, the Ph_4P^+ cations are needed for charge balance. The introduction of the trivalent As element should dramatically increase the potential connectivity of the building blocks and lead to more complicated structures.



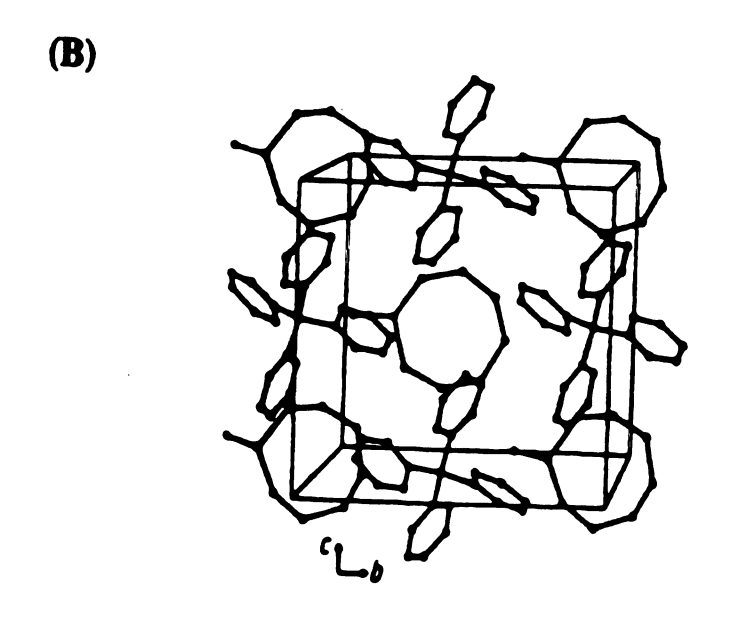


Figure 1-5. (A) Structure of [SAsS₇] anion. (B) Packing diagram of (Ph₄P)[SAsS₇].

Ý

Ċ

$$\begin{bmatrix} s & s & s \end{bmatrix}^{2} = \begin{bmatrix} s & s & s \end{bmatrix}^{3}$$

Scheme 1-1

Despite the great potential for structural variation, the chemistry of the metal/As_xS_y has not been as intensely studied as that of the metal/polychalcogenides. The simple reason may be the absence of suitable starting materials, in contrast to the polychalcogenide anions, which are soluble in polar organic solvents like DMF, so the chemistry can be easily carried out in solution. Also the alkali metal/polychalcogenides, A_xQ_y, form melts at relative low temperature (200 °C to 600 °C), so reactions can be carried out in molten salts. The alkali metal/As_xS_y system usually forms solid state compounds, which are not soluble in common organic solvents. For example, $MAsSe_3^{24}$ and $MAsSe_2^{25}$ (M = K, Rb, Cs) all have onedimensional chain-like structures. MAsSe₃ (M = K, Rb, Cs) were prepared by hydrothermal reaction of the respective alkali carbonate with As₂Se₃ at a temperature of 135 °C. Their X-ray structural analyses revealed that the compounds contain polyselenoarsenate anion, (AsSe₃)_nⁿ-, in which As atoms are bonded with a terminal monoselenide and connected to the neighboring As atom through a diselenide. The compound can be best described as MAs(Se₂)(Se); see Figure 1-6. The MAsSe₂ (M = K, Rb, Cs) were prepared by methanothermal reaction of M_2CO_3 (M = K, Rb, Cs) with As_2Se_3 at a temperature of 130 °C. The structures are basically the

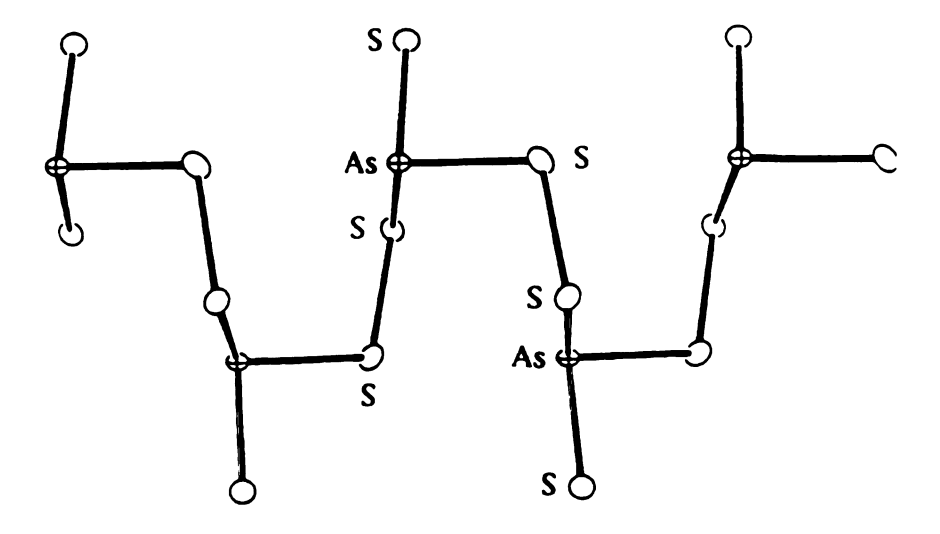


Figure 1-6. The structure of $[As(Se_2)(Se)]^-$ infinite chains found in the compounds MAsSe₃ (M = K, Rb, Cs).

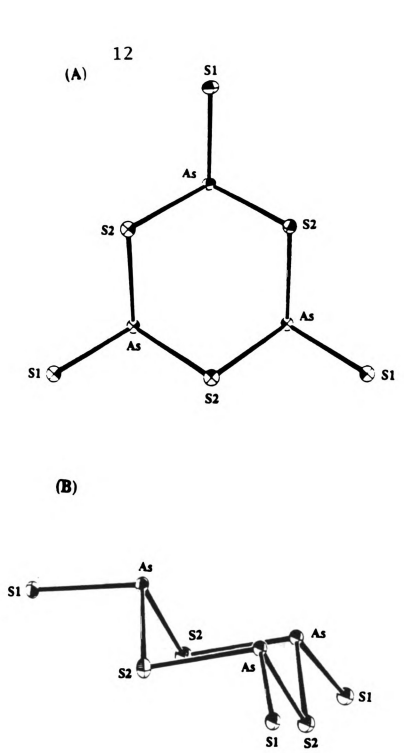


Figure 1-7. Two views of the $[As_3S_6]^3$ - anion.

same as those of the MAsSe₃ but the diselenides are now replaced by monoselenides.

There are a variety of synthetic methods to prepare the mixed $[As_xS_y]^{n-}$ anions; most of them involve some kind of a nucleophilic attack. For example ethylenediamine can react with As2S3 to give [As₃S₆]³-.²⁶ The structure of [As₃S₆]³- is shown in Figure 1-7. It contains discrete cyclic [As₃S₆]³- anions with a six-member As₃S₃ ring in the chair conformation. Similarly, piperidine can attack As4S4 to form the thioarsenate anion [As4S₆]²-, see Figure 1-8.²⁷ It is also a molecular compound with discrete [As4S₆]²- anions. The structure of the [As4S₆]²- anion is related to that of As4S₄ by replacement of an As-As bond with two [As-S] units. By using the same principle, the selenium analog can also be synthesized with ethylenediamine and As4Se4 in DMF.28 Simple reduction of the binary phases with alkali metals also yields some interesting results. For example, As₂Te₃ reacts with K in ethylenediamine and with Ph₄P+ to yield (Ph₄P)₂[As₁₀Te₃].²⁹ Recently, Kolis and coworkers reported that simple reduction of antimony selenide in DMF by using potassium metal leads to formation of a salt with the formula (Ph₄P)₄[Sb₁₂Se₂₀],³⁰ see Figure 1-9. By the classical definition, this is the largest molecular Zintl ion characterized.

Rauchfuss and co-workers reported the isolation of a compound with the formula $Cp'_3Ti_2O(AsS_3)$ ($Cp' = \eta^5-CH_3C_5H_4$).³¹ This compound which contains $[AsS_3]^{3-}$ ligands bridged across two Ti centers used all three S atoms. The lone pair on the As atom is not involved with the bonding to metal ions. It also contains an oxo bridge which could

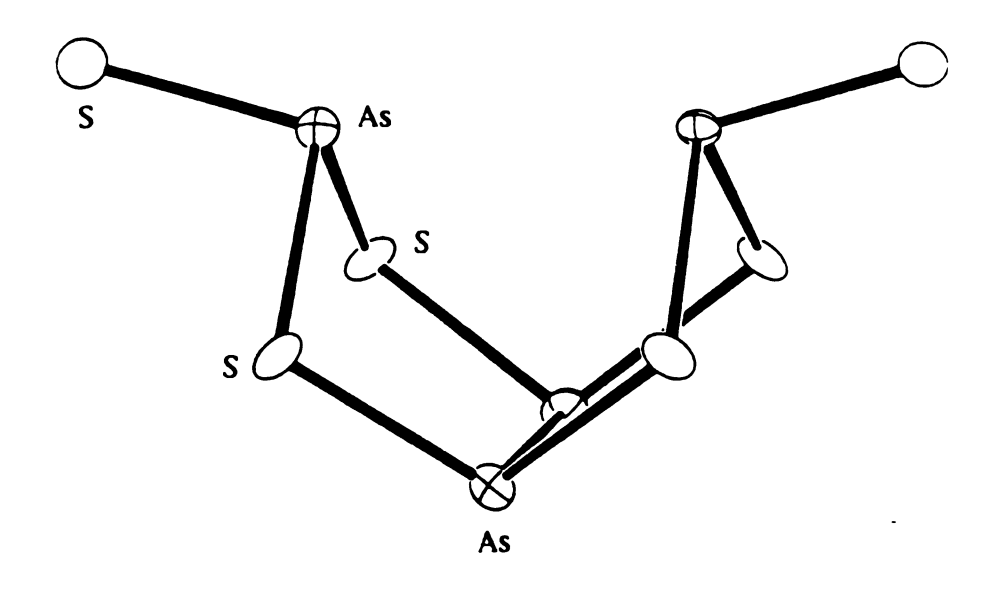


Figure 1-8. Structure of the $[As_4S_6]^{2-}$ anion.

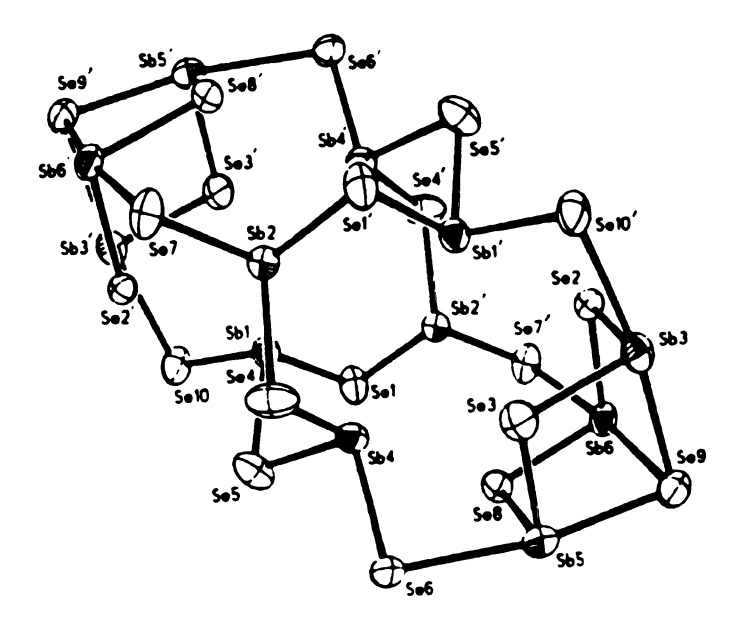


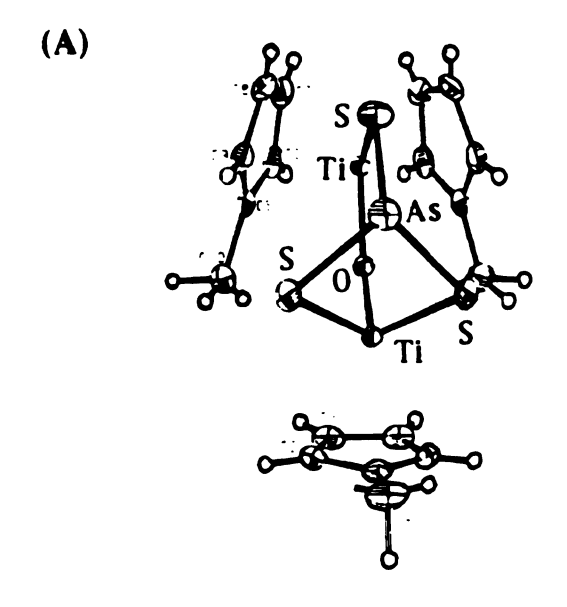
Figure 1-9. Structure of the [Sb₁₂Se₂₀]⁴⁻ anion.

have come from the solvent. This is an important compound because it demonstrates that molecular $[As_xS_y]^{n-}$ anions can act as ligands toward transition metals, see Figure 1-10(A). In the same paper, they also found that tetrathiomolybdate, MoS_4^{2-} , acts as a nucleophile and attacks As_4S_4 to form the complex $[Mo_2O_2As_4S_{14}]^{2-}$, see Figure 1-10(B). The origin of the oxo group probably is adventitious water in the solvent. This compound contains the highly unusual $[As_4S_{12}]^{4-}$ ligand and further indicates the great potential new chemistry that $[As_xS_y]^{n-}$ can provide.

Kolis et al. also have also contributed toward the related class of $[P_xSe_y]^{n-}$ ligands. They found that WSe_4^{2-} readily attacks P_4Se_4 glass to form the first reported metal phosphorus selenide compound, $(Ph_4P)_2[Se=W(PSe_4)(PSe_2)]$, see Figure 1-11.³² It represents the first example of a coordinated $[PSe_4]^{3-}$ ligand. It also contains the highly unusual side-bonded $[PSe_2]^{-}$ group. Related reactions of $MoSe_4^{2-}$ and WSe_4^{2-} with As_4Se_4 in DMF also lead to a series of novel clusters.³³

$$(Ph_4P)_2[WSe_4] + As_4Se_4 \xrightarrow{DMF} (Ph_4P)_2[W_2(\mu-Se)_3(AsSe_5)_2]$$

$$(Ph_4P)_2[MoSe_4] + As_4Se_4 \xrightarrow{DMF} (Ph_4P)_2[Mo(AsSe_5)_2]$$



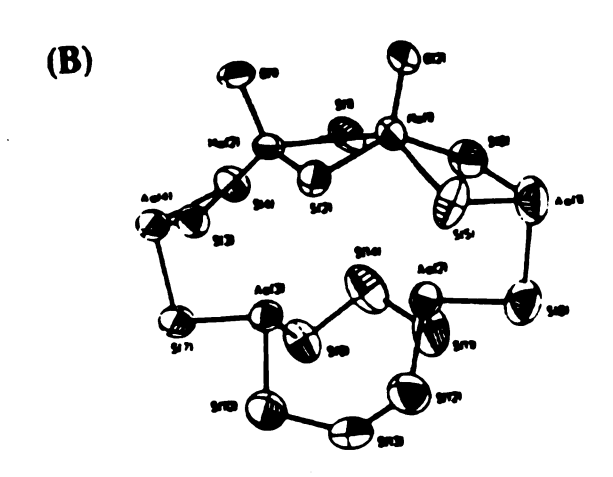


Figure 1-10. (A) Structure of $Cp'_3Ti_2O(AsS_3)$. (B) Structure of the $[Mo_2O_2As_4S_{14}]^{2-}$ anion.

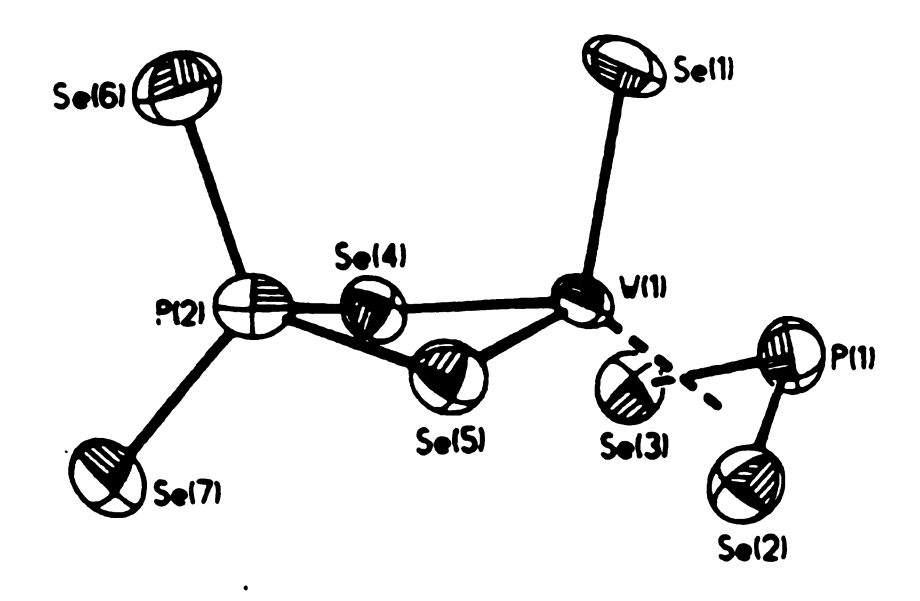


Figure 1-11. Structure of the [Se=W(PSe₄)(PSe₂)] anion.

The [W₂As₂Se₁₃]²- anion consists of two tungsten centers each of which is ligated by six selenium atoms in an irregular coordination environment; see Figure 1-12. Three selenides bridge the metal centers, and each tungsten atom is also ligated by a tridentate AsSe₅ group. The overall shape of each fragment is that of a "bird cage" similar to the familiar As₄Se₃ shape. Each tridentate fragment can be considered a trianion, making the tungsten atoms formally 5+. The W-W distance is 2.903 Å, which is well within accepted bonding distance. The [MoAs₂Se₁₀]²- anion is a monomer with Mo in the 4+ oxidation state (see figure 1-13). It contains one molybdenum atom chelated by two AsSe₅ groups. The fact that the tungsten ion in [W₂As₂Se₁₃]²- has a 5+ oxidation state is probably because tungsten is much harder to reduce than molybdenum.

It was also found that many of the soluble anionic clusters will react with metal carbonyls to form novel transition metal complexes. This so-called oxidative decarbonylation reaction is well known for polychalcogenide ligands and metal carbonyls.³⁴ Now it can be extended to the $[As_xSe_y]^{n-}$ anions.³⁵

$$M(CO)_6 + [As_2Se_6]^2 - DMF = [M(AsSe_5)_2]^2 \cdot (M = Mo, W)$$

$$M(CO)_6 + [As_4Se_6]^2 - DMF = [M(CO)_2(As_3Se_3)_2]^2 - (M = Mo, W)$$

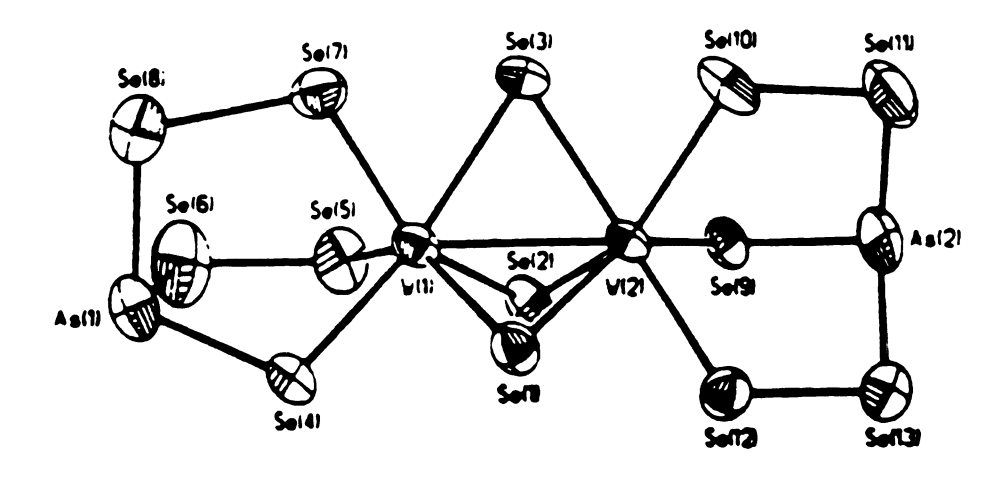


Figure 1-12. Structure of the $[W_2As_2Se_{13}]^{2-}$ anion.

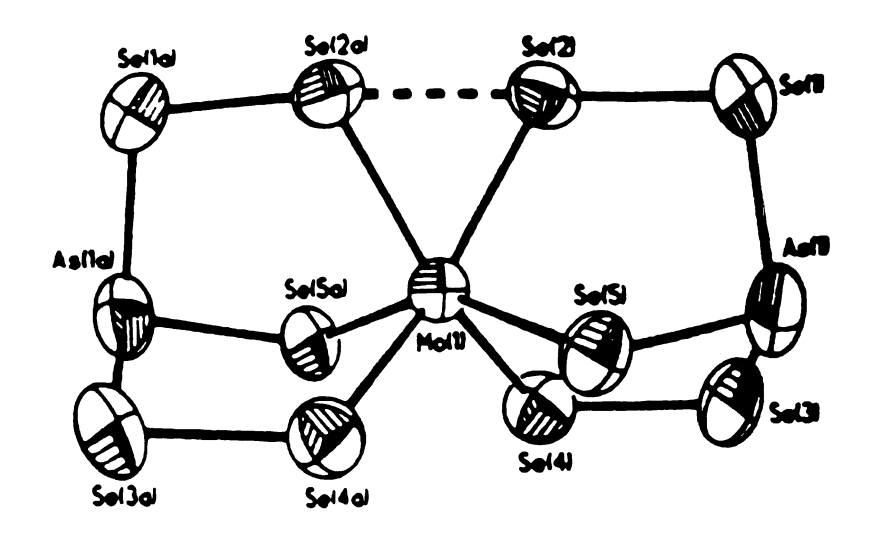


Figure 1-13. Structure of the $[MoAs_2Se_{10}]^{2-}$ anion.

The molecule $[WAs_2Se_{10}]^{2-}$ is isostructural with a molybdenum analog shown above. The $[M(CO)_2(As_3Se_3)]^{2-}$ (M=W, Mo) anion contain a central metal atom which is coordinated by two arsenic and one selenium atom of two identical As_3Se_3 ligands; see Figure 1-14. Each ligand cage combines with the metal to complete the formation of two corner-sharing birdcage structures. The two cages are related by two noncrystallographic mirror planes passing through the center of the molecule. There are also two CO molecules coordinated to the metal. The geometry around the metal can best be described as bicapped trigonal prismatic.

There is an increasing interest in developing new and unusual synthetic techniques to help stabilize new compounds that otherwise might not be possible by traditional methods. Recently, a great deal of attention has been paid to the use of superheated fluids as a synthetic technique.³⁶ Superheated fluids are solvents which are heated above their boiling point, with enough pressure to keep them in the fluid state. There are several advantages offered by superheated fluids. The solubility and the activities of the reactants are greatly increased with the elevation of temperature. The superheated fluids promote crystal growth which is very important for characterization since the isolated compounds are usually new materials, and single-crystal X-ray analysis is essential. The operating temperatures are below those used for molten salt reactions. This technique gives access to a lower temperature regime where metastable compounds that were previously unreachable can now be accessed. Water is the most common fluid in this method.

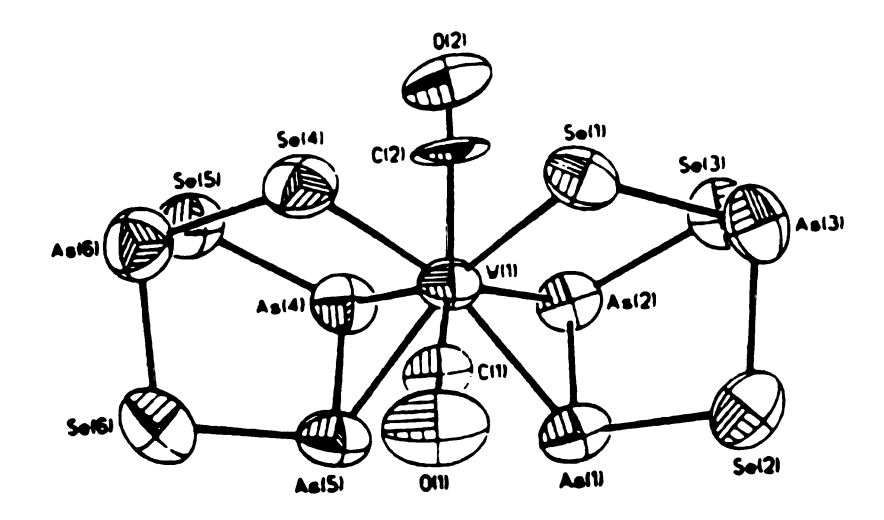


Figure 1-14. Structure of the $[M(CO)_2(As_3Se_3)]^{2-}$ (M = W, Mo) anion.

but recently a variety of other solvents have been used successfully as well.

Schäfer et al. have prepared a large number of ternary alkali metal antimony sulfides using the hydrothermal technique. The dimensionality of these compounds extends from molecular to three-dimensional. Examples include Cs₂Sb₈S₁₃,³⁷ K₂Sb₄S₇,³⁸ K₂Sb₄S₇.H₂O,³⁹ α,β-Rb₂Sb₄S₇,⁴⁰ Cs₂Sb₄S₇.⁴¹ The last four compounds, although isoelectronic, all have different structures. These results demonstrate the broad structural flexibility of the A/Sb/S (A= alkali metal) system.

Sheldrick et al. have investigated the M/15/16 system (M = alkali metal) using superheated water and methanol and have shown that a host of ternary phases can be prepared by reacting alkali metal carbonate with binary 15/16 phases.⁴²⁻⁴⁷ For example:

$$Rb_{2}CO_{3} + Sb_{2}Se_{3} \xrightarrow{175^{\circ}C/MeOH} RbSb_{3}Se_{5}$$

$$Rb_{2}CO_{3} + Sb_{2}S_{3} \xrightarrow{140^{\circ}C/MeOH} Rb_{2}Sb_{4}Se_{7}$$

$$Cs_{2}CO_{3} + As_{2}Se_{3} \xrightarrow{130^{\circ}C/MeOH} CsAsSe_{2}$$

This technique has led to a wide variety of new ternary phases with structures that range from one-dimensional infinite chains to two-dimensional layers to very complicate three-dimensional

structures. Two examples, Cs₂As₈S₁₃⁴⁸ and Rb₂As₈S₁₃,⁴⁹ demonstrate this astonishing structural diversity. Cs2As8S13 is prepared hydrothermally at 180 °C and possess a two-dimensional layered structure. The X-ray structure analysis revealed that the polyanion (As₈S₁₃)_n²ⁿ is composed of individual As₄S₄ eight-member rings, which are each connected to three other rings via As-S-As bridges, giving rise to an infinite layered structure; see Figure 1-15. Rb2As8S13 is also prepared hydrothermally at 200 °C. The polyanion (As₈S₁₃)_n²ⁿ- is composed of As₃S₃ six-member rings, which are connected to one another via bridging AsS₃ pyramids, giving rise to an infinite one-dimensional double chain structure; see Figure 1-16. The main structural differences between Cs2As8S13 and Rb2As8S13 arise from the two different As_xS_y rings, As₄S₄ and As₃S₃. This may be explained by the cation size effect. The larger As4S4 eightmember rings, whose sizes were just right for Cs cations, were stabilized by the larger Cs cations while the Rb cations stabilized the smaller As₃S₃ six-member rings.

Recently, the same methodology was adopted by Parise et al. with small modification. They used tetraalkyl ammonium ions, Instead of alkali metals, as the counterions. With the large counterions more open frameworks can be attained. Examples include (Me4N)[Sb₃S₅],⁵⁰ (Et₄N)[Sb₃S₅], and (N₂C₄H₈)[Sb₄S₇].⁵¹ (Et₄N)[Sb₃S₅], and (N₂C₄H₈)[Sb₄S₇] are layered compounds with the organic cation sitting between the layers. In the case of [Sb₃S₅]_nⁿ-, a counterion size effect is observed. The smaller tetramethylammonium salt, (Me₄N)[Sb₃S₅], has a three-dimensional

Figure 1-15. Ortep drawing of a $[As_8S_{13}]^{2-}$ layer in $Cs_2As_8S_{13}$.

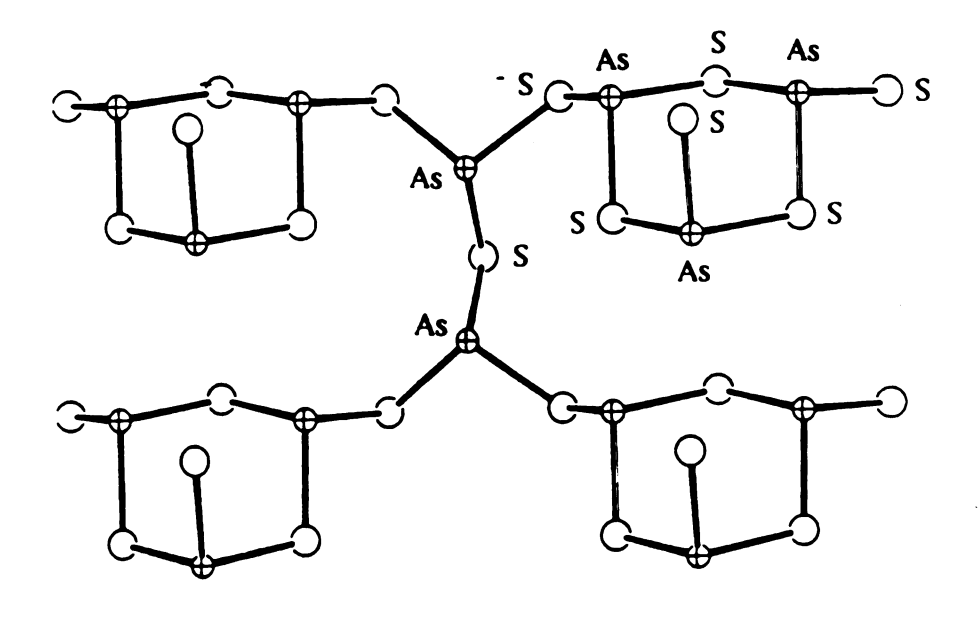


Figure 1-16. Ortep drawing of a $[As_8S_{13}]^{2-}$ chain in $Rb_2As_8S_{13}$.

structure while the large tetraethylammonium salts, (Et4N)[Sb₃S₅], possesses a two-dimensional layered structure.

Kolis et al. have demonstrated recently that superheated ethylenediamine is also a suitable solvent for synthesis of new metal mixed15/16 compounds. They have synthesized two new quaternary phases by reaction between KAsS₂ and Cu powder in superheated ethylenediamine.⁵²

$$Cu + KAsS_2 = \frac{300^{\circ}C/en}{KCu_2AsS_3 + KCu_4AsS_4}$$

The KCu₂AsS₃ compound possesses a two-dimensional layered structure with the K cations situated in the gallery region. Each layer is a complex structure consisting of formal Cu⁺ ions linked in a complicated manner by a series of trigonal AsS₃³- groups; see Figure 1-17. One unusual feature of this compound is that Cu(1) and Cu(2) are tetrahedrally coordinated by three three sulfur atoms and the lone pair from the arsenic atoms of an AsS₃³- group. The KCu₄AsS₄ compound has an extremely compicated three-dimensional structure with copper ions ligated by AsS₃³- groups as well as S²- ions; see Figure 1-18.

The development of useful technologies often depends on the availability of the solid-state materials with appropriate physical and chemical properties. The exploratory synthesis of these new materials is often accomplished by traditional high-temperature fusion reactions method. This method has led to several discoveries with great potential impact on technology ranging from the high-temperature superconductors to the next-generation nonlinear

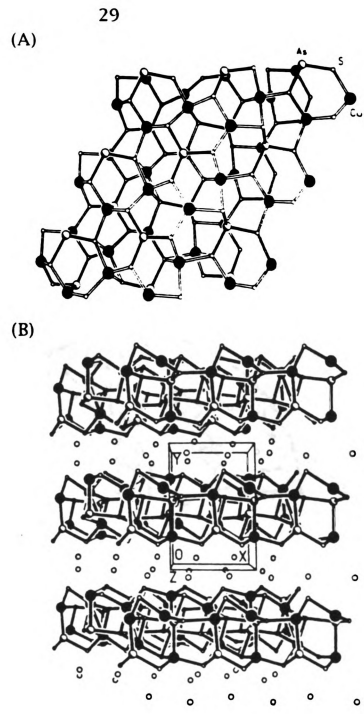


Figure 1-17. (A) View of KCu₂AsS₃ down the b axis showing the copper arsenic sulfide connectivity in a layer. (B) View of KCu2AsS3 down the caxis.

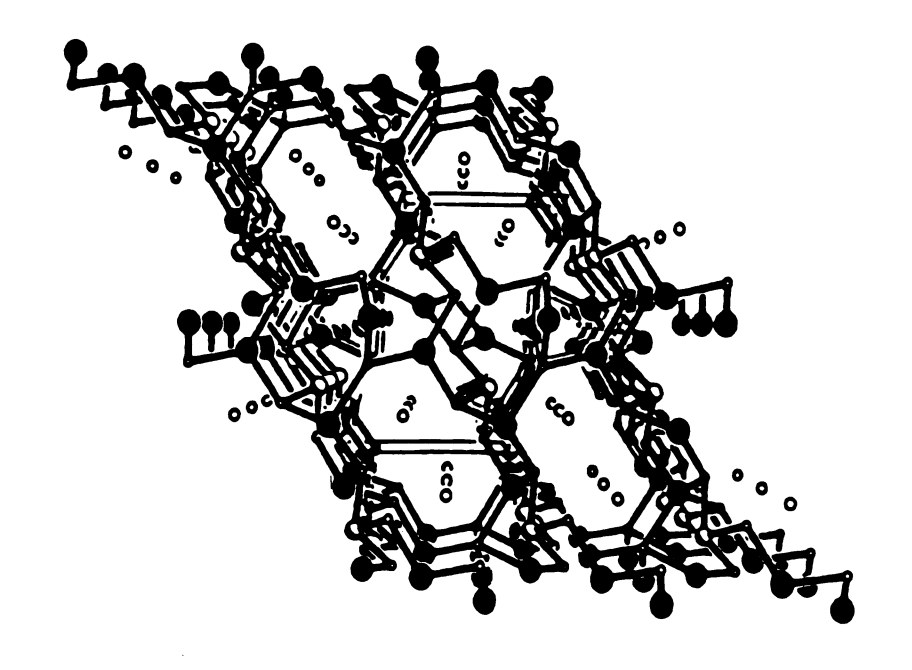


Figure 1-18. Packing diagram of KCu₄AsS₄.

optical materials. However, new synthetic methodologies are needed to advance solid-state chemistry. From all the results presented above, the chemistry of $M_x E_y Q_z$ (M = metal; E = As, Sb, Bi; Q = S, Se, Te) shows great promise for discovering new materials. We decided to investigate $\text{metal}/(As_x S_y)^{z-}$ and $\text{metal}/(As_x S_y)^{z-}$ systems by using the hydrothermal and methanothermal techniques. In the following chapters we present the synthesis, structure, and physicochemical characterization of several newly discovered $[M_x As_y Q_z]^{n-}$ compounds.

REFERENCES

- 1. Wuensch, B. J. in P. H. Ribbe (Ed.), Sulfide Mineralogy,
 Mineralogical Society of America, Blacksburg, 21-43.
- 2. Y. Takeuchi, R. Sadanaga, Z. Kristallogr. 1969, 130, 346-361.
- 3. Niizeki, N.; Buerger, M. J., Z. Kristallogr. 1957, 109, 129-157.
- 4. Engel, P.; Nowacki, W.; Balic-Zunic, T.; Scavnicar, S. Z. Kristallogr. 1982, 161, 159-166.
- Wilson, J. R.; Gupta, P. K.; Robison, P. D.; Criddle, A. J. American Mineralogist 1993, 78, 1096-1103.
- 6. Marumo, F.; Nowacki, W. Z. Kristallogr. 1967, 124, 409-419.
- 7. Sakai, K.; Koide, T.; Matsumoto, T.; Acta Cryst. 1978, b34, 3326-3328.
- 8. Bogget, D. M.; Gibson, A. F. Phys. Lett. 1968, 28, 33-37.
- 9. Bali'c-Zuni'c, T.; Engel, P. Z. Kristallogr. 1983, 165, 261-269.
- 10. Salanci, B. Neues Jahrb. Mineral Abh. 1979, 135, 315-326.
- 11. Skowron, A.; Boswell, F. W.; Corbett, J. M.; Taylor, N. J. J. Soild State Chem. 1994, 112, 307-311.
- 12. Smith, P. P. K.; Hyde, B. G. Acta Cryst. 1983, C39, 1498-1502.
- 13. Skowron, A.; Brown, I. D. Acta Cryst. 1990, C46, 531-534.

- 14. Skowron, A.; Brown, I. D. Acta Cryst. 1990, C46, 534-536.
- 15. Skowron, A.; Brown, I. D. Acta Cryst. 1990, C46, 527-531.
- Tilley, R. D. J.; Wright, A. C.; Smith, D. J. Proc. R. Soc. London Ser.
 1986, 408, 9-22.
- 17. Skowron, A.; Brown, I. D.; Tilley, R. D. J. Solid State Chem. 1992, 97. 199-211.
- 18. Skowron, A.; Brown, I. D. Acta Cryst. 1990, C46, 2287-2291.
- Skowron, A.; Brown, I. D.; Tilley, R. D. J. Solid State Chem. 1992,
 97, 251-254.
- 20. Auernhammer, M.; Effenberger, H.; Irran, E.; Pertlik, F.; Rosenstingl, J. J. Solid State Chem. 1993, 106, 421-426.
- 21. Pertlik, F. J. Solid State Chem. 1994, 112, 170-175.
- (a) Ansari, M.; Ibers, J. A. Coord. Chem. Rev. 1990, 100, 223-266.
 (b) Kanatzidis, M. G. Comments Inorg. Chem. 1990, 10, 161-195.
 (c) Huang, S.-P.; Kanatzidis, M. G. Coord. Chem. Rev. 1994, 130, 509-621.
 (d) Kolis, J. W. Coord. Chem. rev. 1990, 105, 195-219.
 (e) Roof, L. C.; Kolis, J. W. Chem. Rev. 1993, 93, 1037-1080.
- 23. Siewert, B.; Müller, U. Z. Anorg. Allg. Chem. 1991, 595, 211-215.
- 24. Sheldrick, W.; Häusler, H.-J. Z. Anorg. Allg. Chem. 1988, 561, 139-148.

- 25. Sheldrick, W.; Kaub, J. Z. Anorg. Allg. Chem. 1986, 535, 179-185.
- 26. Sheldrick, W.; Kaub, J. Z. Naturforsch. 1985, 40b, 19-21.
- 27. Sheldrick, G. M.; Porter, E. J. J. Chem. Soc. (A) 1971, 3130-3132.
- Ansari, M. A.; Ibers, J. A.; O'neal, S. C.; Pennington, W. T.; Kolis, J. W. Polyhedron, 1992, 11, 1877-1881.
- 29. Haushalter, R. C. J. Chem. Soc. Chem. Commun. 1987, 196-198.
- 30. Martin, T. M.; Wood, P. T.; Kolis, J. W. Inorg. Chem. 1994, 33, 1587-1588.
- 31. Zank, G. A.; Rauchfuss, T. B.; Wilson, S. R. J. Am. Chem. Soc. 1984, 106, 7621-7623.
- 32. O'Neal, S. C.; Pennington, W. T.; Kolis, J. W. Angew. Chem. Int. Ed. Engl. 1990, 29, 1486-1487.
- O'Neal, S. C.; Pennington, W. T.; Kolis, J. W. J. Am. Chem. Soc.
 1991, 113, 710-712.
- 34. Kolis, J. W. Coord. Chem. Rev. 1990, 105, 195-219.
- 35. O'Neal, S. C.; Pennington, W. T.; Kolis, J. W. *Inorg. Chem.* 1992, 31, 888-894.
- (a) Parise, J. B. Science, 1991, 251, 293-294. (b) Parise, J. B. J. Chem. Soc. Chem. Commun. 1990, 22, 1553-1554. (c) Stein, A.;
 Keller, S. W.; Mallouk, T. C. Science 1993, 259, 1558-1564. (d)

Soghomonian, V.; Chen, Q.; Haushalter R. C.; Zubieta, J.; O'Connor, C. J. Science, 1993, 259, 1596-1599. (e) Soghomonian, V.; Chen, Q.; Haushalter R. C.; Zubieta, J. Inorg. Chem. 1994, 33, 1700-1704. (f) Warren, C. J.; Dhingra, S. S.; Ho, D. M.; Haushalter R. C.; Bocarsly, A. B. Inorg. Chem. 1994, 33, 2704-2711. (g) Khan. M. I.; Lee, Y.-S.; O'Connor, C. J.; Haushalter R. C.; Zubieta, J. Inorg. Chem. 1994, 33, 3855-3856. (h) Davis, M. E. Science, 1993, 262, 1543-1546. (i) Kim, K.-W.; Kanatzidis, M. G. J. Am. Chem. Soc. 1992, 114, 4878-4883. (j) Liao. J.-H. Kanatzidis, M. G. J. Am. Chem. Soc. 1990, 112, 7400-7402.

- 37. Volk, K.; Schäfer, H. Z. Anorg. Allg. Chem. 1975, 414, 220-230.
- 38. Eisenmann. B.; Schäfer, H. Z. Naturforsch. 1979, 34b, 1637-1640.
- 39. Graf, H.; Schäfer, H. Z. Naturforsch. 1979, 34b, 383-385.
- (a) Dittmar, V. G.; Schäfer, H. Z. Anorg. Allg. Chem. 1978, 441,
 93-97. (b) Sheldrick, W. S.; Haüsler, H.-J. Z. Anorg. Allg. Chem.
 1988, 557, 105-111.
- 41. Dittmar, V. G.; Schäfer, H. Z. Anorg. Allg. Chem. 1978, 441, 98-102.
- 42. Sheldrick, W. S.; Haüsler, H.-J. Z. Anorg. Allg. Chem. 1988, 557, 98-104.
- 43. Sheldrick, W. S.; Haüsler, H.-J. Z. Anorg. Allg. Chem. 1988, 557, 105-111.

- 44. Sheldrick, W. S.; Haüsler, H.-J. Z. Anorg. Allg. Chem. 1988, 561, 139-148.
- 45. Sheldrick, W. S.; Haüsler, H.-J. Z. Anorg. Allg. Chem. 1988, 561, 149-156.
- 46. Sheldrick, W.; Kaub, J. Z. Anorg. Allg. Chem. 1986, 535, 114-118.
- 47. Sheldrick, W.; Kaub, J. Z. Anorg. Allg. Chem. 1986, 535, 179-185.
- 48. Sheldrick, W.; Kaub, J. Z. Naturforsch. 1985, 40b, 1130-1133.
- 49. Sheldrick, W.; Kaub, J. Z. Naturforsch. 1985, 40b, 571-573.
- 50. Parise, J. B. Science, 1991, 251, 293-294.
- 51. Parise, J. B.; Ko, Y. Chem. Mater. 1992, 4, 1446-1450.
- Jerome, J. E.; Wood, P. T.; Pennington, W. T. Kolis, J. W. Inorg.
 Chem. 1994, 33, 1733-1734.

CHAPTER 2

HYDROTHERMAL SYNTHESIS OF M/As_XS_Y (M = In³⁺, Sn⁴⁺, Bi³⁺) COMPOUNDS. SYNTHESIS AND CHARACTERIZATION OF $(Ph_4P)_2[InAs_3S_7], \ (Ph_4P)_2[SnAs_4S_9] \ AND$ $(Me_4N)_2Rb[BiAs_6S_{12}]$

ABSTRACT

By using hydrothermal synthesis technique (Ph₄P)₂[InAs₃S₇], (Ph₄P)₂[SnAs₄S₉], and (Me₄N)₂Rb[BiAs₆S₁₂] were synthesized from mixtures of InCl₃/2K₃AsS₃/4Ph₄PBr, SnS₂/3K₃AsS₃/4Ph₄PBr, and BiCl₃/2Rb₃AsS₃/4Me₄NCl, respectively. (Ph₄P)₂[InAs₃S₇] crystallizes in the monoclinic space group $P2_1/c$ (No. 14) with a = 19.078(9) Å, b = 14.436(3) Å, c = 19.325(6) Å, $\beta=106.11(3)^{\circ}$, V = 5111(4) Å³, Z = 4. $[InAs_3S_7]_{n^2}^{n-1}$ is a one-dimensional chain structure consisting of trigonal bipyramidal In³⁺ ions and [As₃S₇]⁵⁻ units formed by cornersharing [AsS₃]³- units. (Ph₄P)₂[SnAs₄S₉] crystallizes in the triclinic space group P-1(No. 2) with a = 13.476(3) Å, b = 18.365(5) Å, c = 18.365(5)11.348(2) Å, $\alpha = 107.28(2)$, $\beta = 96.90(3)^{\circ}$, $\gamma = 96.92(2)$, V = 5111(4)Å³, Z = 2. [SnAs₄S₉]_n²ⁿ also has a one-dimensional chain structure with octahedral Sn⁴⁺ ions and [As₄S₉]⁶⁻ units formed by cornersharing [AsS₃]³ units. The mixed salt (Me₄N)₂Rb[BiAs₆S₁₂] crystallizes in the trigonal R-3(h) space group (No. 148) with a=9.978(1) Å, c = 28.337(5) Å, V = 2356(1) Å³, Z = 3. [BiAs₆S₁₂]_n³ⁿ possesses a two-dimensional structure. Three As atoms and six S atoms form a unique cyclic [As₃S₆]³- unit in a chair conformation, which is connected to three Bi atoms via terminal S atoms. The Bi³⁺ is in a nearly perfect octahedral geometry. The Me₄N⁺ and Rb⁺ cations reside in the interlayer gallery. The Rb+ cations are coordinated to six S atoms, forming a trigonal antiprism. The solid state optical spectra of these compounds are reported.

1. Introduction

Several important classes of solid-state compounds such as silicate, borate, and phosphate minerals contain building blocks which are assembled from the condensation of elementary units like SiO_4^{4-} , BO_3^{3-} , PO_4^{3-} , etc.¹ This condensation gives rise to a large variety of rings, chains, and layers and results in great structural diversity among these minerals. By comparison, condensation in main-group thiometalates is less common. Examples include ternary thioborates,² thiogermanates,³ and thioarsenates.⁴ An elementary structural unit which may have great potential for condensation is the pyramidal AsS_3^{3-} unit. This condensation properity is demonstrated in species such as $[As_8S_{13}]^{2-}$,⁵ $[As_4S_6]^{2-}$,⁶ and $[As_3S_6]^{2-}$.⁷ Similar units were recently reported to occur in the molecular compounds $[M(CO)_2(As_3Se_3)_2]^{2-}$ (M = Mo, W),⁸ $[Mo_2O_2As_4S_14]^{2-}$,⁹ $[MoAs_2Se_{10}]^{2-}$, and $[W_2As_2Se_{13}]^{2-}$,¹⁰

From the examples above, it is clear that the thioarsenic anions are interesting ligands and excellent building blocks for potentially to an enormous variety of complexes and solids. With this in mind, we initiated exploration of the systems R_4E^+ (R = alkyl, Ph; E = N, $P)/M^{n+}/AsS_3^{3-}$ (M = main group element) using hydrothermal technique with the aim of obtaining novel frameworks containing either AsS_3^{3-} or its condensates. We report here our initial results from this promising approach, P1 which include the isolation of three new polymeric compounds, P1 which include the isolation of three new polymeric compounds, P3 which include the isolation of three new polymeric compounds, P4 which include the isolation of three new polymeric compounds, P4 which include the isolation of three new polymeric compounds, P4 which include the isolation of three new polymeric compounds, P4 which include the isolation of three new polymeric compounds, P4 which include the isolation of three new polymeric compounds, P4 which include the isolation of three new polymeric compounds, P4 which include the isolation of three new polymeric compounds, P4 which include the isolation of three new polymeric compounds, P4 which include the isolation of three new polymeric compounds, P4 which include the isolation of three new polymeric compounds, P4 which include the isolation of three new polymeric compounds, P4 which include the isolation of three new polymeric compounds, P4 which include the isolation of three new polymeric compounds, P4 which include the isolation of three new polymeric compounds are necessarily and P5 which is the include the isolation of three new polymeric compounds are necessarily and P5 which is the include the isolation of three necessarily are necessarily and P5 which is the include the isolation of the necessarily are necessarily are necessarily and P5 which is the include the isolation of the necessarily are necessarily are necessarily are neces

2. Experimental Section

2.1 Reagents

Chemicals. Chemicals in this work, other than solvents, were used as obtained. (i) BiCl₃, 98% purity, InCl₃, 99% purity, tetraphenylphosphonium bromide (Ph₄PBr), 98% purity, tetramethylammonium chloride, (Me₄NCl), 99% purity, Aldrich Chemical Company, Inc., Milwaukee, WI. (ii) sulfur powder, sublimed, J. T. Baker Chemical Co., Phillipsberg, NJ. (iii) potassium metal, analytical reagent, Mallinckrodt Inc., Paris, KY; (iv) arsenic sulfide, As₂S₃, ~100 mesh, 99% purity, Cerac Inc. Milwaukee WI. (v) Methanol, anhydrous, Mallinckrodt Inc., Paris, KY; diethyl ether, ACS anhydrous, EM Science, Inc., Gibbstown, NJ.

2.2 Syntheses

All syntheses were carried out under dry nitrogen atmosphere in a Vacuum Atmosphere Dri-Lab glovebox except where specifically indicated otherwise.

A 3 A s S 3 (A = K, Rb, Cs) were synthesized by using stoichiometric amounts of alkali metal, arsenic sulfide (As_2S_3) , and sulfur in liquid ammonia. The reaction gives a yellow brown powder upon evaporation of ammonia.

(Ph₄P)₂[InAs₃S₇]: A Pyrex tube (~4 mL) containing InCl₃ (55 mg, 0.25 mmol), K₃AsS₃ (144 mg, 0.5 mmol), Ph₄PBr (419 mg, 1.0 mmol), and 0.5 mL of water was sealed under vacuum and kept at 120 °C for 2 days. The large pale yellow transparent chunky crystals

were isolated in water and washed with methanol and ether (yield 74.5 % based on In). SEM/EDS analysis on these crystals showed a P:In:As:S ratio of 1.6:1:1.4:7.2.

(Ph₄P)₂[SnAs₄S₉]: A Pyrex tube (~4 mL) containing SnS₂ (55 mg, 0.25 mmol), K₃AsS₃ (144 mg, 0.5 mmol), Ph₄PBr (419 mg, 1.0 mmol), and 0.5 mL of water was sealed under vacuum and kept at 120 °C for 2 days. The large orange transparent chunky crystals were isolated in water and washed with methanol and ether (yield 74.5 % based on Sn). SEM/EDS analysis on these crystals showed a P:Sn:As:S ratio of 1.6:1:1.2:6.2.

(Me₄N)₂Rb[BiAs₆S₁₂]: BiCl₃ (63 mg, 0.2 mmol) was mixed with 2 equiv of Rb₃AsS₃ (171 mg, 0.4 mmol) and 4 equiv of Me₄NCl (88 mg, 0.8 mmol), and the mixture was sealed under vacuum with 0.3 mL of H₂O in a Pyrex tube (~4 mL). The reaction was run at 120 °C for 1 week. Washing the reaction mixture with methanol and ether afforded dark red cube-like single crystals of (Me₄N)₂Rb[BiAs₆S₁₂] (45 mg, yield of 30 % based on Bi). SEM/EDS analysis on these crystals showed a Rb:Bi:As:S ratio of 1:1.1:8:7.2.

FT-IR spectra of compounds were recorded as a solid in a CsI matrix. The sample was ground with dry CsI into a fine powder, and a pressure of about seven metric tons was applied to the mixture to make a translucent pellet. The spectra were record in the far-IR region (600-100 cm⁻¹, 4 cm⁻¹ resolution) with the use of a Nicolet 740 FT-IR spectrometer equipped with a TGS/PE detector and silicon

splitter. Raman spectra were recorded at room temperature with a Nicolet FT-Raman 950 spectrometer.

Quantitative microprobe analysis of the compounds was performed with JEOL JSM-35CF scanning electron microscope (SEM) equipped with a Tracor Northern Energy Dispersive Spectroscopy (EDS) detector. Single crystals of each sample were mounted on an aluminum stub which was coated with conducting graphite paint to avoid charge accumulation on the sample surface under bombardment of the electron beam during measurements. Energy Dispersive Spectra (EDS) were obtained by using the following experimental set-up:

X-ray detector position: 55 mm Take-off angle: 27 deg

Working distance: 39 mm Beam current: 200 picoamps

Accelerating voltage: 20 kv Accumulation time: 60 sec.

Window: Be

Optical diffuse reflectance measurements were made at room temperature with a Shimadzu UV-3101PC double beam, double-monochromator spectrophotometer. The instrument was equipped with an integrating sphere and controlled by a personal computer. The measurement of diffuse reflectivity can be used to obtain values for the band gap which agree rather well with values obtained by absorption measurements from single crystals of the same material. The digitized spectra were processed using the Kaleidagraph^{T M} software program. BaSO4 powder was used as reference (100%)

reflectance). Absorption data were calculated from the reflectance data by using the Kubelka-Munk function: 12

$$\alpha/S = \frac{(1-R)^2}{2R}$$

R is the reflectance at a given wavelength, α is the absorption coefficient and S is the scattering coefficient. The scattering coefficient has been shown to be practically wavelength independent for particles larger than 5 μ m which is smaller than the particle size of the samples used here.

Thermal Gravimetric Analysis (TGA) was performed on a Shimadzu TGA-50. The samples were heated to 800 °C at a rate of 10 °C/min. under a steady flow of dry N₂ gas.

Differential thermal analysis (DTA) was performed with a computer-controlled Shimadzu DTA-50 thermal analyzer. The ground single crystals were sealed in quartz ampules under vacuum. An quartz ampule of equal mass was sealed and placed on the reference side of the detector. The samples were heated to the desired temperature at 5 °C/min, then kept at that temperature for 10 min followed by cooling at 10 °C/min to 100 °C and finally rapid cooling to room temperature.

2.4. X-ray crystallography

 $(Ph_4P)_2[InAs_3S_7]$: The plate-like pale yellow crystal used for the study had approximate dimensions of 0.35 x 0.33 x 0.75 mm. The crystal was sealed inside a thin-walled glass capillary under air

and mounted on a goniometer head. Single-crystal X-ray diffraction data were collected at 23 °C on a Rigaku AFC6 diffractometer. A total of 8227 reflections were collected. All the nonhydrogen atoms except carbon were refined anisotropically. All hydrogen atom positions were calculated by assuming idealized geometry. Hydrogen atom contributions were included in the structure factor calculations, but their coordinates and temperature factors were not refined.

(Ph4P)₂[SnAs₄S₉]: A well shaped orange crystal with dimensions of 0.45 x 0.35 x 0.5 mm was mounted on a glass fiber. Single-crystal X-ray diffraction data were collected at 23 °C on a Rigaku AFC6 diffractometer. A total of 7220 reflections were collected. All the nonhydrogen atoms except carbon were refined anisotropically. All hydrogen atom positions were calculated and fixed without further refinement.

(Me₄N)₂Rb[BiAs₆S₁₂]: The single-crystal diffraction data were collected by Crystallics Compouny. A well shaped dark red cube-like crystal with dimensions of 0.34 x 0.45 x 0.52 mm was sealed inside a thin-walled glass capillary with epoxy. The crystal was oriented with an edge nearly parallel to the ψ axis of the diffractometer. Single-crystal X-ray diffraction data were collected at 23 °C on a computer-controlled four-circle Nicolet (Siemens) autodiffractometer. A total of 1233 reflections were collected. All nonhydrogen atoms except carbon were refined anisotropically. All hydrogen atom positions were calculated and fixed without further refinement.

The crystals did not show any significant decay as judged by three check reflections measured every 150 reflections throughout the data collection. The space group was determined by systematic absences and intensity statistics. The structures were solved by direct methods (SHELXS-86)¹³ with the TEXSAN software package¹⁴ and refined by full matrix least-squares methods. An empirical absorption correction (DIFABS)¹⁵ was applied to the isotropically refined data. All non-hydrogen atoms except nitrogen and carbon were refined anisotropically. All calculations were performed on a VAXstation 3100 Model 76 computer.

Table 2-1 summarizes the crystallographic data and details of the structure solution and refinement. The final atomic coordinates with their estimated standard deviation (esd's) are given in Table 2-2, 2-3, and 2-4.

Table 2.1 Crystallographic Data for $(Ph_4P)_2[InAs_3S_7](I)$, $(Ph_4P)_2[SnAs_4S_9](II)$, and $(Me_4N)_2Rb[BiAs_6S_{12}](III)$.

	I	II
Formula	C48H40P2InAs3S7	C48H40P2SnAs4S9
F. w.	1241.59	1384.38
a, Å	19.079(9)	13.476(2)
b, Å	14.436(3)	18.365(3)
c, Å	19.325(6)	11.348(2)
α, deg.	90.00	107.28(2)
β, deg.	106.11(3)	96.90(2)
γ, deg.	90.00	96.92(2)
Z, V, Å ³	4, 5111(4)	2, 2626(2)
Space Group	$P2_{1}/c$ (No. 14)	P-1 (No. 2)
color, habit	pale yellow, plate	orange, plate
D _{cal} , g/cm ³	1.62	1.75
Radiation	Cu Ka	Μο Κα
μ, cm ⁻¹	94.61	34.22
2θ _{max} , deg.	120.0	45.0
Absorption Correction	γ scan	ψ scan
Transmission Factor	0.71-1.40	0.83-1.15
Index ranges	$0 \le h \le 21, 0 \le k \le 16,$	$0 \le h \le 16, -22 \le k \le$
•	$-22 \le l \le 22$	$22, -13 \le l \le 13$
No. of Data coll.	8227	7220
Unique reflection	7971	6863
Data Used	3604	3891
$(F_0^2 > 3\sigma(F_0^2))$		
No. of Variables	550	340
Final Ra/Rwb, %	5.5/5.7	4.9/6.2

a R= $\Sigma(|Fo|-|Fc|)/\Sigma|Fo|$, b R_w= $\{\Sigma_w(|Fo|-|Fc|)^2/\Sigma_w|Fo|^2\}^{1/2}$

Table 2-1 (cont.)

	III
Formula	C ₈ H ₂₄ N ₂ RbBiAs ₆ S ₁₂
F. w.	1201.98
a, Å	9.978(1)
b, Å	9.978(1)
c, Å	28.337(5)
α, deg.	90.00
β, deg.	120.00
γ, deg.	90.00
Z, V, Å ³	3, 2356(1)
Space Group	R-3 (No. 148)
color, habit	dark red block
D _{cal} , g/cm ³	2.73
Radiation	Μο Κα
μ, cm ⁻¹	141.34
2θ _{max} , deg.	58.7
Absorption Correction	ψ scan
Transmission Factor	0.745-1.000
Index ranges	$0 \le h \le 13, 0 \le k \le 11, 0 \le l \le 34$
No. of Data coll.	1233
Unique reflection	1157
Data Used	906
$(F_0^2 > 3\sigma(F_0^2))$	
No. of Variables	40
Final Ra/Rwb, %	3.1/2.5

^a R= Σ (|Fo|-|Fc|)/ Σ |Fo|, ^b R_w={ Σ w(|Fo|-|Fc|)²/ Σ w|Fo|²} 1/2

Table 2-2. Selected Atomic Coordinates and Estimated Standard Deviations (esd's) of (Ph₄P)₂[InAs₃S₇]

atom	X	Y	Z	$B_{eq} a, (A^2)$
In	0.77261(5)	0.19922(6)	0.35422(4)	3.82(4)
Asi	0.78622(9)	0.2030(1)	0.54266(7)	4.48(7)
As2	0.8320(1)	0.2241(1)	0.71648(8)	4.48(7)
As3	0.6873(1)	0.0363(1)	0.4239(1)	5.47(8)
S1	0.7896(2)	0.3053(2)	0.4582(2)	$4.7(2)^{'}$
S2	0.6496(2)	0.1254(3)	0.3249(2)	5.5(2)
S 3	0.7510(2)	0.3362(2)	0.2642(2)	5.0(2)
S4	0.8045(2)	0.0439(2)	0.4341(2)	5.3(2)
S 5	0.8706(2)	0.1614(2)	0.2956(2)	4.8(2)
S6	0.7641(2)	0.3088(3)	0.6215(2)	5.3(2)
S7	0.6741(2)	0.1362(2)	0.5114(2)	5.5(2)
P1	0.8830(2)	-0.1772(2)	0.2150(2)	4.2(2)
P2	0.3851(2)	0.3795(2)	0.6678(2)	4.2(2)
C1	0.9335(7)	-0.1653(8)	0.3083(7)	3.7(6)
\mathbf{c}_{2}	0.9812(8)	-0.2310(9)	0.3417(7)	5.0(7)
C3	1.0214(8)	-0.218(1)	0.4139(8)	5.7(7)
C4	1.0137(8)	-0.140(1)	0.4478(8)	6.0(8)
C5	0.968(1)	-0.074(1)	0.416(1)	9(1)
C6	0.927(1)	-0.085(1)	0.346(1)	9(1)
C 7	0.8859(7)	-0.2957(9)	0.1900(7)	4.3(1)
C8	0.901(1)	-0.320(1)	0.127(1)	8(1)
C9	0.896(2)	-0.414(1)	0.107(1)	12(2)
C10	0.876(1)	-0.478(1)	0.147(1)	8(1)
C11	0.8612(8)	-0.456(1)	0.207(1)	5.3(8)
C12	0.8661(8)	-0.3629(9)	0.2304(7)	4.5(7)
C13	0.7879(8)	-0.145(1)	0.1972(7)	4.7(7)
C14	0.763(1)	-0.072(2)	0.225(1)	11(1)
C15	0.692(1)	-0.049(2)	0.206(1)	12(2)
C16	0.642(1)	-0.098(2)	0.160(1)	9(1)
C17	0.664(1)	-0.173(1)	0.131(1)	11(1)
C18	0.737(1)	-0.196(1)	0.149(1)	8(1)
C19	0.9256(8)	-0.1048(8)	0.1632(7)	4.0(6)
C20	0.8922(9)	-0.024(1)	0.132(1)	6.1(8)
C21	0.928(1)	0.032(1)	0.097(1)	8(1)
C22	0.997(1)	0.011(1)	0.092(1)	7(1)
C23	1.030(1)	-0.069(1)	0.123(1)	7(1)
C24	0.995(1)	-0.126(1)	0.1595(9)	5.9(8)

C25	0.4498(8)	0.296(1)	0.6543(8)	4.7(7)
C26	0.518(1)	0.323(1)	0.655(1)	6.4(9)
C27	0.567(1)	0.260(1)	0.646(1)	8(1)
C28	0.551(1)	0.171(2)	0.635(1)	9(1)
C29	0.487(1)	0.144(1)	0.638(1)	16(2)
C30	0.434(1)	0.207(1)	0.645(2)	14(2)
C31	0.4034(8)	0.485(1)	0.629(1)	5.0(7)
C32	0.404(1)	0.490(1)	0.558(1)	9(1)
C33	0.416(1)	0.569(2)	0.525(1)	12(1)
C34	0.422(1)	0.647(2)	0.561(2)	12(2)
C35	0.422(2)	0.649(2)	0.633(2)	13(2)
C36	0.410(1)	0.566(1)	0.665(1)	9(1)
C37	0.3934(7)	0.3925(8)	0.7619(8)	4.3(7)
C38	0.3356(8)	0.429(1)	0.7840(9)	5.3(8)
C39	0.341(1)	0.444(1)	0.855(1)	6.3(9)
C40	0.405(1)	0.423(1)	0.9057(9)	5.9(8)
C41	0.464(1)	0.387(1)	0.8856(9)	5.6(8)
C41	0.4571(7)	0.371(1)	0.8135(9)	4.8(7)
C43	0.2939(8)	0.347(1)	0.6225(8)	4.8(7)
C44	0.269(1)	0.261(1)	0.625(1)	10(1)
C45	0.197(1)	0.238(2)	0.589(2)	16(2)
C46	0.152(1)	0.303(3)	0.553(1)	11(1)
C47	0.174(1)	0.386(2)	0.551(2)	13(2)
C48	0.2464(9)	0.411(1)	0.585(1)	10(1)

^a B_{eq} =(4/3)[$a^2B_{11} + b^2B_{22} + c^2B_{33} + ab(\cos\gamma)B_{12} + ac(\cos\beta)B_{13} + bc(\cos\alpha)B_{23}$]

Table 2-3. Selected Atomic Coordinates and Estimated Standard Deviations (esd's) of (Ph₄P)₂[SnAs₄S₉]

$\begin{array}{c ccccccccccccccccccccccccccccccccccc$	
As1 0.7788(1) 0.3623(1) 0.5155(2) 3.03(7) As2 0.2450(1) -0.0252(1) 0.4641(2) 3.16(7) As3 1.2120(2) 0.4386(1) 0.4124(2) 4.9(1) As4 0.6563(1) 0.1887(1) 0.5132(2) 2.70(7) S1 0.3622(3) 0.0594(3) 0.6098(4) 3.1(2) S2 0.6509(3) 0.0698(3) 0.6710(4) 2.9(2) S3 0.8812(3) 0.3728(2) 0.3813(4) 3.6(2) S4 1.0880(4) 0.4785(3) 0.3092(4) 4.3(2) S5 1.1332(4) 0.4272(3) 0.5668(5) 4.1(2) S6 0.6661(3) 0.2597(2) 0.3797(4) 3.5(2) S7 0.2130(3) -0.1246(3) 0.5434(5) 3.6(2) S8 0.5184(3) 0.1095(2) 0.4002(4) 2.5(2) S9 0.6743(4) 0.4484(3) 0.5012(5) 4.6(2) P1 0.2250(3) 0.0449(2) 1.0017(4) 2.3(2) P2 0.2804(3) 0.4128(3) 0.9216(4) 2.8(2)	
As2 0.2450(1) -0.0252(1) 0.4641(2) 3.16(7) As3 1.2120(2) 0.4386(1) 0.4124(2) 4.9(1) As4 0.6563(1) 0.1887(1) 0.5132(2) 2.70(7) S1 0.3622(3) 0.0594(3) 0.6098(4) 3.1(2) S2 0.6509(3) 0.0698(3) 0.6710(4) 2.9(2) S3 0.8812(3) 0.3728(2) 0.3813(4) 3.6(2) S4 1.0880(4) 0.4785(3) 0.3092(4) 4.3(2) S5 1.1332(4) 0.4272(3) 0.5668(5) 4.1(2) S6 0.6661(3) 0.2597(2) 0.3797(4) 3.5(2) S7 0.2130(3) -0.1246(3) 0.5434(5) 3.6(2) S8 0.5184(3) 0.1095(2) 0.4002(4) 2.5(2) S9 0.6743(4) 0.4484(3) 0.5012(5) 4.6(2) P1 0.2250(3) 0.0449(2) 1.0017(4) 2.3(2) P2 0.2804(3) 0.4128(3) 0.9216(4) 2.8(2) C1 0.189(1) -0.0558(9) 0.993(1) 2.3(3) <td< td=""><td></td></td<>	
As3 1.2120(2) 0.4386(1) 0.4124(2) 4.9(1) As4 0.6563(1) 0.1887(1) 0.5132(2) 2.70(7) S1 0.3622(3) 0.0594(3) 0.6098(4) 3.1(2) S2 0.6509(3) 0.0698(3) 0.6710(4) 2.9(2) S3 0.8812(3) 0.3728(2) 0.3813(4) 3.6(2) S4 1.0880(4) 0.4785(3) 0.3092(4) 4.3(2) S5 1.1332(4) 0.4272(3) 0.5668(5) 4.1(2) S6 0.6661(3) 0.2597(2) 0.3797(4) 3.5(2) S7 0.2130(3) -0.1246(3) 0.5434(5) 3.6(2) S8 0.5184(3) 0.1095(2) 0.4002(4) 2.5(2) S9 0.6743(4) 0.4484(3) 0.5012(5) 4.6(2) P1 0.2250(3) 0.0449(2) 1.0017(4) 2.3(2) P2 0.2804(3) 0.4128(3) 0.9216(4) 2.8(2) C1 0.189(1) -0.0558(9) 0.993(1) 2.3(3) C2 0.195(1) -0.111(1) 0.884(1) 3.8(4) C3 </td <td></td>	
As4 0.6563(1) 0.1887(1) 0.5132(2) 2.70(7) S1 0.3622(3) 0.0594(3) 0.6098(4) 3.1(2) S2 0.6509(3) 0.0698(3) 0.6710(4) 2.9(2) S3 0.8812(3) 0.3728(2) 0.3813(4) 3.6(2) S4 1.0880(4) 0.4785(3) 0.3092(4) 4.3(2) S5 1.1332(4) 0.4272(3) 0.5668(5) 4.1(2) S6 0.6661(3) 0.2597(2) 0.3797(4) 3.5(2) S7 0.2130(3) -0.1246(3) 0.5434(5) 3.6(2) S8 0.5184(3) 0.1095(2) 0.4002(4) 2.5(2) S9 0.6743(4) 0.4484(3) 0.5012(5) 4.6(2) P1 0.2250(3) 0.0449(2) 1.0017(4) 2.3(2) P2 0.2804(3) 0.4128(3) 0.9216(4) 2.8(2) C1 0.189(1) -0.0558(9) 0.993(1) 2.3(3) C2 0.195(1) -0.111(1) 0.884(1) 3.8(4) C3 0.165(1) -0.189(1) 0.876(1) 4.2(4) C4	
S1 0.3622(3) 0.0594(3) 0.6098(4) 3.1(2) S2 0.6509(3) 0.0698(3) 0.6710(4) 2.9(2) S3 0.8812(3) 0.3728(2) 0.3813(4) 3.6(2) S4 1.0880(4) 0.4785(3) 0.3092(4) 4.3(2) S5 1.1332(4) 0.4272(3) 0.5668(5) 4.1(2) S6 0.6661(3) 0.2597(2) 0.3797(4) 3.5(2) S7 0.2130(3) -0.1246(3) 0.5434(5) 3.6(2) S8 0.5184(3) 0.1095(2) 0.4002(4) 2.5(2) S9 0.6743(4) 0.4484(3) 0.5012(5) 4.6(2) P1 0.2250(3) 0.0449(2) 1.0017(4) 2.3(2) P2 0.2804(3) 0.4128(3) 0.9216(4) 2.8(2) C1 0.189(1) -0.0558(9) 0.993(1) 2.3(3) C2 0.195(1) -0.111(1) 0.884(1) 3.8(4) C3 0.165(1) -0.189(1) 0.876(1) 4.2(4) C4 0.128(1) -0.203(1) 0.970(1) 4.2(4) C5	
S2 0.6509(3) 0.0698(3) 0.6710(4) 2.9(2) S3 0.8812(3) 0.3728(2) 0.3813(4) 3.6(2) S4 1.0880(4) 0.4785(3) 0.3092(4) 4.3(2) S5 1.1332(4) 0.4272(3) 0.5668(5) 4.1(2) S6 0.6661(3) 0.2597(2) 0.3797(4) 3.5(2) S7 0.2130(3) -0.1246(3) 0.5434(5) 3.6(2) S8 0.5184(3) 0.1095(2) 0.4002(4) 2.5(2) S9 0.6743(4) 0.4484(3) 0.5012(5) 4.6(2) P1 0.2250(3) 0.0449(2) 1.0017(4) 2.3(2) P2 0.2804(3) 0.4128(3) 0.9216(4) 2.8(2) C1 0.189(1) -0.0558(9) 0.993(1) 2.3(3) C2 0.195(1) -0.111(1) 0.884(1) 3.8(4) C3 0.165(1) -0.189(1) 0.876(1) 4.2(4) C4 0.128(1) -0.203(1) 0.970(1) 4.2(4) C5 0.124(1) -0.153(1) 1.079(2) 3.9(4) C6	
S3 0.8812(3) 0.3728(2) 0.3813(4) 3.6(2) S4 1.0880(4) 0.4785(3) 0.3092(4) 4.3(2) S5 1.1332(4) 0.4272(3) 0.5668(5) 4.1(2) S6 0.6661(3) 0.2597(2) 0.3797(4) 3.5(2) S7 0.2130(3) -0.1246(3) 0.5434(5) 3.6(2) S8 0.5184(3) 0.1095(2) 0.4002(4) 2.5(2) S9 0.6743(4) 0.4484(3) 0.5012(5) 4.6(2) P1 0.2250(3) 0.0449(2) 1.0017(4) 2.3(2) P2 0.2804(3) 0.4128(3) 0.9216(4) 2.8(2) C1 0.189(1) -0.0558(9) 0.993(1) 2.3(3) C2 0.195(1) -0.111(1) 0.884(1) 3.8(4) C3 0.165(1) -0.189(1) 0.876(1) 4.2(4) C4 0.128(1) -0.203(1) 0.970(1) 4.2(4) C5 0.124(1) -0.153(1) 1.079(2) 3.9(4) C6 0.154(1) -0.0759(9) 1.090(1) 2.7(3) C7	
S4 1.0880(4) 0.4785(3) 0.3092(4) 4.3(2) S5 1.1332(4) 0.4272(3) 0.5668(5) 4.1(2) S6 0.6661(3) 0.2597(2) 0.3797(4) 3.5(2) S7 0.2130(3) -0.1246(3) 0.5434(5) 3.6(2) S8 0.5184(3) 0.1095(2) 0.4002(4) 2.5(2) S9 0.6743(4) 0.4484(3) 0.5012(5) 4.6(2) P1 0.2250(3) 0.0449(2) 1.0017(4) 2.3(2) P2 0.2804(3) 0.4128(3) 0.9216(4) 2.8(2) C1 0.189(1) -0.0558(9) 0.993(1) 2.3(3) C2 0.195(1) -0.111(1) 0.884(1) 3.8(4) C3 0.165(1) -0.189(1) 0.876(1) 4.2(4) C4 0.128(1) -0.203(1) 0.970(1) 4.2(4) C5 0.124(1) -0.153(1) 1.079(2) 3.9(4) C6 0.154(1) -0.0759(9) 1.090(1) 2.7(3) C7 0.356(1) 0.0699(8) 0.997(1) 2.1(3) C8 <t< td=""><td></td></t<>	
S5 1.1332(4) 0.4272(3) 0.5668(5) 4.1(2) S6 0.6661(3) 0.2597(2) 0.3797(4) 3.5(2) S7 0.2130(3) -0.1246(3) 0.5434(5) 3.6(2) S8 0.5184(3) 0.1095(2) 0.4002(4) 2.5(2) S9 0.6743(4) 0.4484(3) 0.5012(5) 4.6(2) P1 0.2250(3) 0.0449(2) 1.0017(4) 2.3(2) P2 0.2804(3) 0.4128(3) 0.9216(4) 2.8(2) C1 0.189(1) -0.0558(9) 0.993(1) 2.3(3) C2 0.195(1) -0.111(1) 0.884(1) 3.8(4) C3 0.165(1) -0.189(1) 0.876(1) 4.2(4) C4 0.128(1) -0.203(1) 0.970(1) 4.2(4) C5 0.124(1) -0.153(1) 1.079(2) 3.9(4) C6 0.154(1) -0.0759(9) 1.090(1) 2.7(3) C7 0.356(1) 0.0699(8) 0.997(1) 2.1(3) C8 0.398(1) 0.029(1) 0.898(2) 3.2(2)	
S6 0.6661(3) 0.2597(2) 0.3797(4) 3.5(2) S7 0.2130(3) -0.1246(3) 0.5434(5) 3.6(2) S8 0.5184(3) 0.1095(2) 0.4002(4) 2.5(2) S9 0.6743(4) 0.4484(3) 0.5012(5) 4.6(2) P1 0.2250(3) 0.0449(2) 1.0017(4) 2.3(2) P2 0.2804(3) 0.4128(3) 0.9216(4) 2.8(2) C1 0.189(1) -0.0558(9) 0.993(1) 2.3(3) C2 0.195(1) -0.111(1) 0.884(1) 3.8(4) C3 0.165(1) -0.189(1) 0.876(1) 4.2(4) C4 0.128(1) -0.203(1) 0.970(1) 4.2(4) C5 0.124(1) -0.153(1) 1.079(2) 3.9(4) C6 0.154(1) -0.0759(9) 1.090(1) 2.7(3) C7 0.356(1) 0.0699(8) 0.997(1) 2.1(3) C8 0.398(1) 0.029(1) 0.898(2) 3.2(2)	
S7 0.2130(3) -0.1246(3) 0.5434(5) 3.6(2) S8 0.5184(3) 0.1095(2) 0.4002(4) 2.5(2) S9 0.6743(4) 0.4484(3) 0.5012(5) 4.6(2) P1 0.2250(3) 0.0449(2) 1.0017(4) 2.3(2) P2 0.2804(3) 0.4128(3) 0.9216(4) 2.8(2) C1 0.189(1) -0.0558(9) 0.993(1) 2.3(3) C2 0.195(1) -0.111(1) 0.884(1) 3.8(4) C3 0.165(1) -0.189(1) 0.876(1) 4.2(4) C4 0.128(1) -0.203(1) 0.970(1) 4.2(4) C5 0.124(1) -0.153(1) 1.079(2) 3.9(4) C6 0.154(1) -0.0759(9) 1.090(1) 2.7(3) C7 0.356(1) 0.0699(8) 0.997(1) 2.1(3) C8 0.398(1) 0.029(1) 0.898(2) 3.2(2)	
S8 0.5184(3) 0.1095(2) 0.4002(4) 2.5(2) S9 0.6743(4) 0.4484(3) 0.5012(5) 4.6(2) P1 0.2250(3) 0.0449(2) 1.0017(4) 2.3(2) P2 0.2804(3) 0.4128(3) 0.9216(4) 2.8(2) C1 0.189(1) -0.0558(9) 0.993(1) 2.3(3) C2 0.195(1) -0.111(1) 0.884(1) 3.8(4) C3 0.165(1) -0.189(1) 0.876(1) 4.2(4) C4 0.128(1) -0.203(1) 0.970(1) 4.2(4) C5 0.124(1) -0.153(1) 1.079(2) 3.9(4) C6 0.154(1) -0.0759(9) 1.090(1) 2.7(3) C7 0.356(1) 0.0699(8) 0.997(1) 2.1(3) C8 0.398(1) 0.029(1) 0.898(2) 3.2(2)	
S9 0.6743(4) 0.4484(3) 0.5012(5) 4.6(2) P1 0.2250(3) 0.0449(2) 1.0017(4) 2.3(2) P2 0.2804(3) 0.4128(3) 0.9216(4) 2.8(2) C1 0.189(1) -0.0558(9) 0.993(1) 2.3(3) C2 0.195(1) -0.111(1) 0.884(1) 3.8(4) C3 0.165(1) -0.189(1) 0.876(1) 4.2(4) C4 0.128(1) -0.203(1) 0.970(1) 4.2(4) C5 0.124(1) -0.153(1) 1.079(2) 3.9(4) C6 0.154(1) -0.0759(9) 1.090(1) 2.7(3) C7 0.356(1) 0.0699(8) 0.997(1) 2.1(3) C8 0.398(1) 0.029(1) 0.898(2) 3.2(2)	
P1 0.2250(3) 0.0449(2) 1.0017(4) 2.3(2) P2 0.2804(3) 0.4128(3) 0.9216(4) 2.8(2) C1 0.189(1) -0.0558(9) 0.993(1) 2.3(3) C2 0.195(1) -0.111(1) 0.884(1) 3.8(4) C3 0.165(1) -0.189(1) 0.876(1) 4.2(4) C4 0.128(1) -0.203(1) 0.970(1) 4.2(4) C5 0.124(1) -0.153(1) 1.079(2) 3.9(4) C6 0.154(1) -0.0759(9) 1.090(1) 2.7(3) C7 0.356(1) 0.0699(8) 0.997(1) 2.1(3) C8 0.398(1) 0.029(1) 0.898(2) 3.2(2)	
P2 0.2804(3) 0.4128(3) 0.9216(4) 2.8(2) C1 0.189(1) -0.0558(9) 0.993(1) 2.3(3) C2 0.195(1) -0.111(1) 0.884(1) 3.8(4) C3 0.165(1) -0.189(1) 0.876(1) 4.2(4) C4 0.128(1) -0.203(1) 0.970(1) 4.2(4) C5 0.124(1) -0.153(1) 1.079(2) 3.9(4) C6 0.154(1) -0.0759(9) 1.090(1) 2.7(3) C7 0.356(1) 0.0699(8) 0.997(1) 2.1(3) C8 0.398(1) 0.029(1) 0.898(2) 3.2(2)	
C1 $0.189(1)$ $-0.0558(9)$ $0.993(1)$ $2.3(3)$ C2 $0.195(1)$ $-0.111(1)$ $0.884(1)$ $3.8(4)$ C3 $0.165(1)$ $-0.189(1)$ $0.876(1)$ $4.2(4)$ C4 $0.128(1)$ $-0.203(1)$ $0.970(1)$ $4.2(4)$ C5 $0.124(1)$ $-0.153(1)$ $1.079(2)$ $3.9(4)$ C6 $0.154(1)$ $-0.0759(9)$ $1.090(1)$ $2.7(3)$ C7 $0.356(1)$ $0.0699(8)$ $0.997(1)$ $2.1(3)$ C8 $0.398(1)$ $0.029(1)$ $0.898(2)$ $3.2(2)$	
C2	
C3	
C4 0.128(1) -0.203(1) 0.970(1) 4.2(4) C5 0.124(1) -0.153(1) 1.079(2) 3.9(4) C6 0.154(1) -0.0759(9) 1.090(1) 2.7(3) C7 0.356(1) 0.0699(8) 0.997(1) 2.1(3) C8 0.398(1) 0.029(1) 0.898(2) 3.2(2)	
C5 0.124(1) -0.153(1) 1.079(2) 3.9(4) C6 0.154(1) -0.0759(9) 1.090(1) 2.7(3) C7 0.356(1) 0.0699(8) 0.997(1) 2.1(3) C8 0.398(1) 0.029(1) 0.898(2) 3.2(2)	
C6 0.154(1) -0.0759(9) 1.090(1) 2.7(3) C7 0.356(1) 0.0699(8) 0.997(1) 2.1(3) C8 0.398(1) 0.029(1) 0.898(2) 3.2(2)	
C7 0.356(1) 0.0699(8) 0.997(1) 2.1(3) C8 0.398(1) 0.029(1) 0.898(2) 3.2(2)	
C8 0.398(1) 0.029(1) 0.898(2) 3.2(2)	
C9 0.497(1) 0.051(1) 0.886(2) 3.4(4)	
0.771(1) $0.031(1)$ $0.000(2)$ $3.4(4)$	
C10 $0.553(1)$ $0.115(1)$ $0.968(2)$ $3.3(4)$	
C11 $0.515(1)$ $0.157(1)$ $1.069(2)$ $4.6(4)$	
C12 $0.415(1)$ $0.135(1)$ $1.083(2)$ $4.2(4)$	
C13 $0.153(1)$ $0.0586(9)$ $0.868(1)$ $2.7(3)$	
C14 0.191(1) 0.118(1) 0.827(2) 3.6(4)	
C15 $0.139(1)$ $0.129(1)$ $0.722(2)$ $4.4(4)$	
C16 $0.050(1)$ $0.080(1)$ $0.660(2)$ $4.2(4)$	
C17 $0.016(1)$ $0.022(1)$ $0.700(2)$ $3.7(4)$	
C18 $0.066(1)$ $0.010(1)$ $0.806(2)$ $3.3(4)$	
C19 0.194(1) 0.1044(8) 1.141(1) 2.4(3)	
C20 0.118(1) 0.151(1) 1.139(2) 3.1(3)	
C21 0.098(1) 0.199(1) 1.250(1) 4.1(4)	

C22	0.151(1)	0.203(1)	1.363(2)	4.4(4)
C23	0.223(1)	0.157(1)	1.368(2)	5.1(5)
C24	0.247(1)	0.110(1)	1.259(2)	3.3(4)
C25	0.344(1)	0.3773(9)	0.790(1)	2.6(3)
C26	0.376(1)	0.427(1)	0.725(2)	3.6(4)
C27	0.426(1)	0.395(1)	0.620(2)	4.4(4)
C28	0.441(1)	0.319(1)	0.591(2)	4.0(4)
C29	0.411(1)	0.274(1)	0.658(2)	3.6(4)
C30	0.364(1)	0.303(1)	0.762(2)	3.5(4)
C31	0.297(1)	0.5160(8)	0.979(1)	2.2(3)
C32	0.262(1)	0.554(1)	0.900(2)	3.4(4)
C33	0.272(1)	0.635(1)	0.945(2)	4.5(4)
C34	0.313(1)	0.675(1)	1.071(2)	4.7(4)
C35	0.342(1)	0.636(1)	1.147(2)	4.4(4)
C36	0.335(1)	0.554(1)	1.103(2)	4.3(4)
C37	0.147(1)	0.3757(9)	0.875(1)	2.7(3)
C38	0.106(1)	0.324(1)	0.759(2)	3.1(3)
C39	0.001(1)	0.303(1)	0.730(2)	4.8(4)
C40	-0.060(1)	0.329(1)	0.814(2)	4.8(4)
C41	-0.021(2)	0.384(1)	0.926(2)	5.4(5)
C41	0.083(1)	0.407(1)	0.959(2)	3.9(4)
C43	0.333(1)	0.3771(9)	1.042(1)	2.8(3)
C44	0.439(1)	0.395(1)	1.081(2)	3.8(4)
C45	0.486(1)	0.372(1)	1.175(2)	4.2(4)
C46	0.425(1)	0.331(1)	1.233(2)	4.3(4)
C47	0.322(1)	0.312(1)	1.197(2)	4.2(4)
C48	0.276(1)	0.337(1)	1.101(2)	3.4(4)

^a B_{eq} =(4/3)[$a^2B_{11} + b^2B_{22} + c^2B_{33} + ab(\cos\gamma)B_{12} + ac(\cos\beta)B_{13} + bc(\cos\alpha)B_{23}$]

52

Table 2-4. Selected Atomic Coordinates and Estimated Standard Deviations (esd's) of (Me₄N)₂Rb[BiAs₆S₁₂]

atom	X	Y	Z	B_{eq}^{a} , (A^2)
Bi	0.0000	0.0000	0.0000	1.01(2)
Rb	0.0000	0.0000	0.5000	5.00(8)
As	0.28307(8)	-0.16664(1)	0.02659(3)	1.30(2)
S 1	0.2390(2)	0.0110(2)	0.05874(7)	1.71(6)
S2	0.5102(2)	-0.1047(2)	0.06797(8)	1.74(6)
N	0.000	0.000	0.1928(5)	2.7(3)
C1	0.000	0.000	0.2453(4)	0.9(2)
<u>C2</u>	-0.155(1)	-0.033(2)	0.1739(4)	5.5(5)

^a $B_{eq} = (4/3)[a^2B_{11} + b^2B_{22} + c^2B_{33} + ab(\cos\gamma)B_{12} + ac(\cos\beta)B_{13} + bc(\cos\alpha)B_{23}]$

The compounds were examined by X-ray powder diffraction to determine phase purity and for identification. Accurate dhkl spacings (Å) were obtained from the powder patterns recorded on a calibrated (with FeOCl as internal standard) Phillips XRG-3000 computer-controlled powder diffractometer with graphite-monochromated Cu Kα radiation operating at 35 kV and 35 mA. The data were collected at a rate of 0.12°/min. Based on the atomic coordinates from X-ray single crystal diffraction study, X-ray powder patterns for all compounds were calculated, by the software package CERIUS. Calculated and observed X-ray powder patterns that show d-spacings and intensities of strong hkl reflections are complied in table 2-5 to 2-7.

Table 2-5. Calculated and Observed X-ray Powder Diffraction Pattern of (Ph₄P)₂[InAs₃S₇] (I)

h	k	l	d _{calc} (Å)	d _{obs} (Å)	I/I _{max} (obs, %)
1	0	0	18.3	18.2	8
0	1	1	11.4	11.2	100
1	1	0	11.3		
2	0	0	9.27	9.15	46
2	0	-2	7.67	7.59	10
1	0	2	7.48	7.35	10
0	2	0	7.22	7.15	16
2	1	1	6.61	6.55	13
1	2	-1	6.53	6.45	35
2	2	0	5.67	5.64	13
3	1	0	5.62	5.59	30
3	2	0	4.66	4.65	22
0	1	4	4.41	4.41	1 1
1	2	4	3.65	3.65	10
1	3	-5	3 00	3.00	1 2
0	4	5	2.587	2.575	8

Table 2-6. Calculated and Observed X-ray Powder Diffraction Pattern of (Ph₄P)₂[SnAs₄S₉](II)

_	· ·			
<u>h</u>	k l	d _{calc} (Å)	d_{obs} (Å)	I/I_{max} (obs, %)
1	-1 0	11.4	11.3	62
0	0 1	10.7	10.6	100
1	1 0	9.82	9.78	11
0	2 0	8.67	8.65	75
1	-1 1	8.07	8.01	6.5
1	-1 -1	7.54	7.50	7 1
2	0 0	6.61	6.55	21
1	-3 1	5 54		
0	2 -2	5.37	5.35	27
0	0 2	5.34	5.30	52
1	3 0	5.01		
1	-1 2	4.97	4.97	50
1	-1 -2	4.71	4.71	18
0	4 -1	4.54	4.54	21
2	0 -2	4.51	4.51	17
3	1 0	4 12		
2	4 0	3.39	3.37	10
3	3 1	2.929	2.927	13
0	6 3	2.697	2.697	1 2

Table 2-7. Calculated and Observed X-ray Powder Diffraction Pattern of (Me₄N)₂Rb[BiAs₆S₁₂](III)

h	k	1	d _{calc} (Å)	d _{obs} (Å)	I/I _{max} (obs, %)
0	0	3	9.44	9.43	100
1	0	2	7.28	7.27	35
1	1	0	4.90	4.88	20
1	0	5	4.71	4.70	33
2	0	4	3.64	3.64	10
1	1	6	3.40	3.40	30
1	0	8	3.27	3.25	15
2	1	1	3.19	3.18	20
2	1	1	3.13		
2	1	4	2 921	2.92	75
2	1	7	2.51		
2	1	8	2 377	2 37	10
4	1	0	1.851		

3. Results and discussion

3.1 Syntheses and description of structures

(Ph₄P)₂[InAs₃S₇] was prepared by heating InCl₃ with K₃AsS₃ and Ph₄PBr in H₂O at 120 °C. The compound, formed as pale yellow platelike crystals, and does not dissolve in common organic solvents consistent with a polymeric compound. The structure was determined by X-ray single-crystal diffraction analysis. $[InAs_3S_7]_{n^{2n}}$ has an unusual one-dimensional polymeric structure composed of In³⁺ ions and [As₃S₇]⁵⁻ units form by corner-sharing pyramidal [AsS₃]³- units, see Figure 2-1. The [As₃S₇]⁵- units engage in a remarkably complex multidentate coordination with two In³⁺ centers, using all five of their terminal sulfur atoms. To the best of our knowledge, the [As3S7]⁵ unit represents a new thioarsenate anion with potentially rich coordination chemistry. The In³⁺ ion is in a distorted trigonal bipyramidal environment with the axial bond angle, S3-In-S4, at 171.4(1)°. For comparsion, in indium/polysulfide systems, the In usually adopts tetrahedral geometry; examples include $[In_2S_{14}]^{2-}$ and $[In_2S_{16}]^{2-.18}$ In fact, trigonal bypyramidal indium polychalcogenide compounds are quite rare. include $[In_2Se_{21}]^{4-}$, 17 and $[In_2(S_4)_2(S_6)_2(S_7)]^{4-.18}$ It is interesting to point out that there are two six membered InAs₂S₃ rings, formed as the result of the [As₃S₇]⁵ unique binding mode, in the structure. These two six membered rings share 5 of the six atoms and as a result of that, one adopts a chair conformation while the other one has the boat conformation. The average distance between the In and the axial S atoms(S2 and S3), at 2.642(4) Å, is significantly longer than that between the equatorial S atoms, at 2.489(4) Å. The $[InAs_3S_7]_n^{2n}$ chains lie parallel to the crystallographic c axis and are separated by Ph₄P+ cations; see Figure 2-2(A) and (B). There are two types of As-S bonds in $[As_3S_7]^{5}$ unit. The average As-S distance of the type As-S-In, at 2.216(4) Å, is slightly shorter than that of the As-S-As type, at 2.279(4) Å. The S-As-S angles range from 95.3(1) to $107.8(1)^\circ$. The bond distances and angles are comparable to those in $[Mo_2O_2As_4S_{14}]^{2}$ and $[Mo_4O_4As_4S_{14}]^{4}$. Selected bond distances and bond angles are given in Table 2-8 and 2-9.

Table 2-8. Selected Distances (Å) in (Ph₄P)₂[InAs₃S₇] with Standard Deviations in Parentheses.^a

In - S1	2.474(4)	As1 - S7	2.271(5)
In - S2	2.496(4)	As2 - S3	2.189(4)
In - S3	2.589(3)	As2 - S5	2.234(4)
In - S4	2.696(4)	As2 - S6	2.285(4)
In - S5	2.499(4)	As3 - S2	2.251(4)
As1 - S1	2.214(4)	As3 - S4	2.192(5)
As1 - S6	2.276(4)	As3 - S7	2.287(4)

a The estimated standard deviations in the mean bond lengths and the mean bond angles are calculated by the equation $\sigma l = \{\Sigma_n(l_n - 1)^2/n(n-1)\}^{1/2}$, where l_n is the length (or angle) of the nth bond, l the mean length (or angle), and n the number of bonds.

Table 2-9. Selected Angles (Deg) in (Ph₄P)₂[InAs₃S₇] with Standard Deviations in Parentheses.^a

S1 - In - S2	110.6(1)	S3 - As2 - S5	98.3(1)
S1 - In - S3	91.8(1)	S3 - As2 - S6	104.0(2)
S1 - In - S4	95.3(1)	S5 - As2 - S6	99.1(1)
S1 - In - S5	123.8(1)	S2 - As3 - S4	97.2(2)
S2 - In - S3	102.1(1)	S2 - As3 - S7	101.0(2)
S2 - In - S4	79.8(1)	S4 - As3 - S7	102.7(2)
S2 - In - S5	125.3(1)	In - S1 - As1	99.2(1)
S3 - In - S4	171.4(1)	In - S2 - As3	89.6(1)
S3 - In - S5	82.2(1)	In - S3 - As2	88.8(1)
S4 - In - S5	89.9(1)	In - S4 - As3	85.8(1)
S1 - As1 - S6	95.3(1)	In - S5 - As2	90.1(1)
S1 - As1 - S7	107.8(1)	As1 - S6 - As2	90.5(1)
S6 - As1 - S7	97.3(2)	As1 - S7 - As3	100.2(2)

^aThe estimated standard deviations in the mean bond lengths and the mean bond angles are calculated by the equation $\sigma l = \{\Sigma_n(l_n - 1)^2/n(n-1)\}^{1/2}$, where l_n is the length (or angle) of the nth bond, l the mean length (or angle), and n the number of bonds.

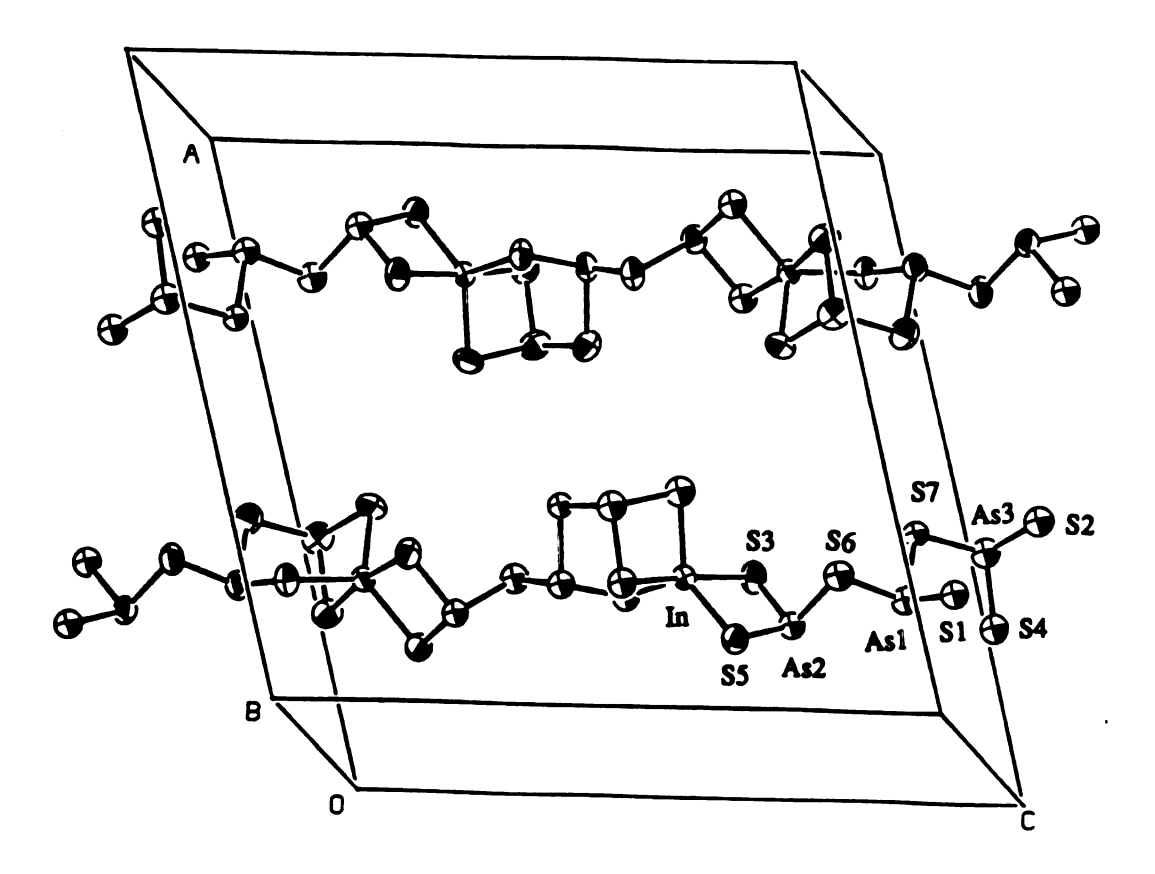


Figure 2-1. Structure and labeling scheme of $[InAs_3S_7]_n^{2n}$.

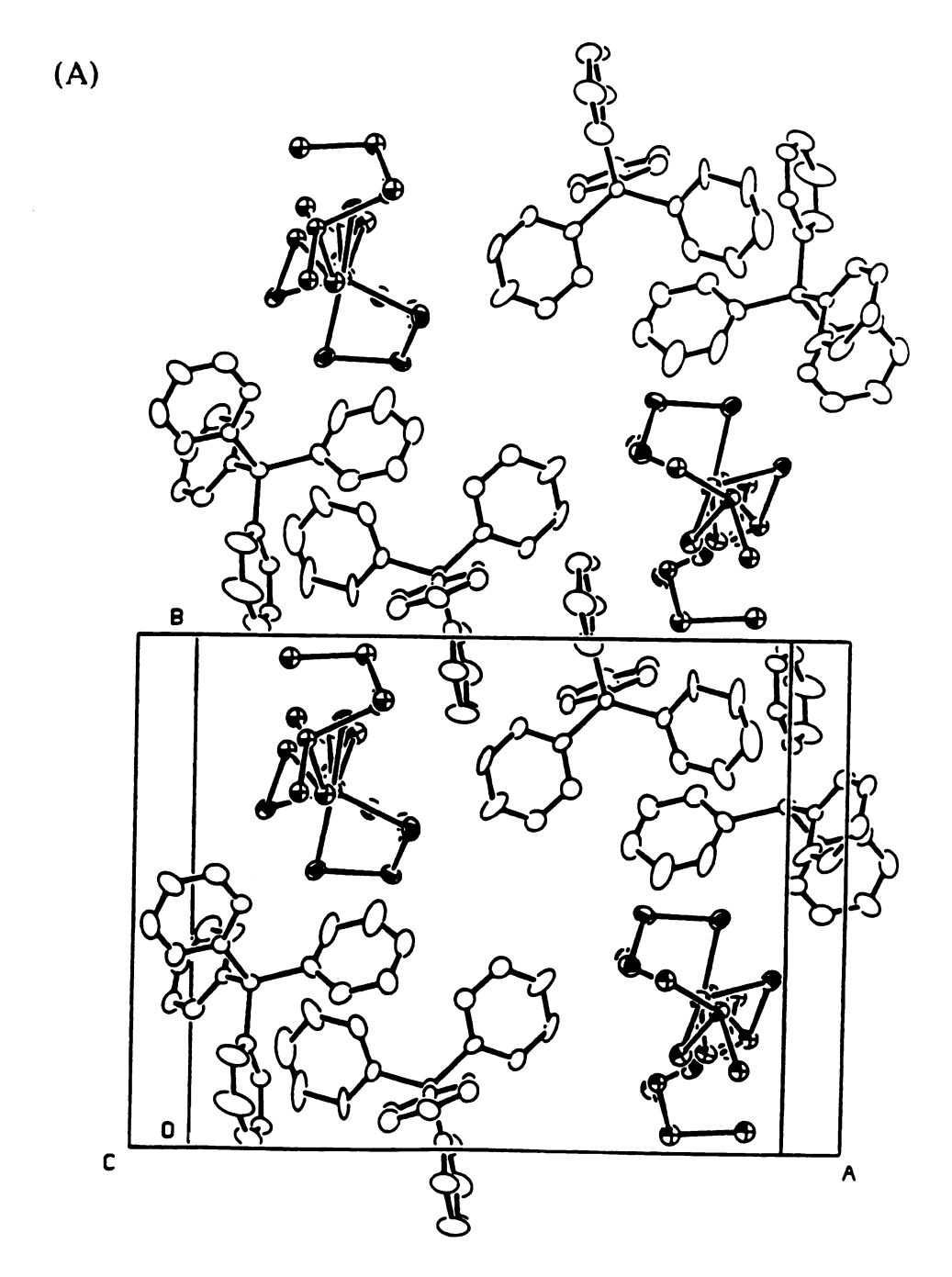
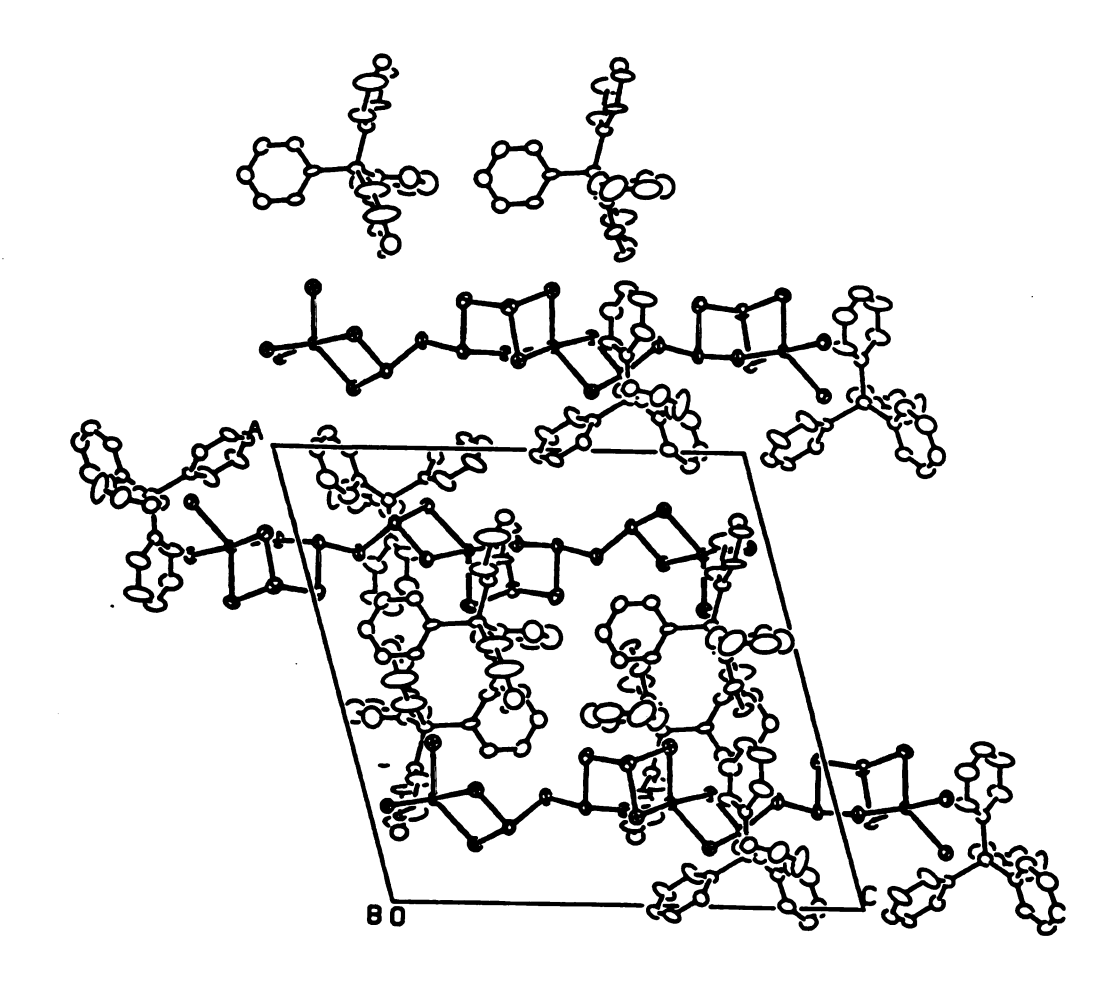


Figure 2-2. Packing diagram of $(Ph_4P)_2[InAs_3S_7]$. (A) view down the c-axis. (B) view down the b-axis.

(B)



(Ph₄P)₂[SnAs₄S₉](II) was prepared hydrothermally by heating SnS₂ with K₃A₅S₃ and Ph₄PBr in H₂O at 120 °C for four days. The reaction was initially run with the SnS₂/K₃AsS₃/Ph₄PBr ratio of 1:2:2 and gave a low yield. We later discovered that excess of cation, Ph₄PBr, not only increased the yield but also helped crystal growth which indicated that the Ph₄PBr is not just a cation but also a The compound does not dissolve in common organic mineralizer. solvents such as CH₃CN, DMF, and DMSO. The structure was determined X-ray single-crystal diffraction analysis. by $[SnAs_4S_9]_{n^{2n}}$ also has a one-dimensional polymeric chain-like structure composed of Sn⁴⁺ ions and [As₄S₉]⁶⁻ units formed by corner-sharing pyramidal [AsS₃]³- units; see Figure 2-3. The [As4S9]6- units, which can be viewed as the further condensation product between the [As3S7]⁵- unit and [AsS3]³- unit, use all their six terminal sulfur atoms connecting two Sn⁴⁺ centers together. [As4S9]⁶- also represents a new thioarsenate anion. When comparing the bonding modes of the two thioarsenate polyanions, [As₃S₇]⁵- and $[As_4S_9]^{6}$, we see the $[As_3S_7]^{5}$ units, in $(Ph_4P)_2[InAs_3S_7]$, use two and three terminal sulfur atoms at either end of the units to bond metal ions, while the [As4S9]6- units, in (Ph4P)2[SnAs4S9], have only one The $[SnAs_4S_9]_{n^{2n}}$ chains are well separated bonding arrangement. by Ph₄P⁺ cations, see Figure 2-4(A) and (B). The Sn⁴⁺ is in a distorted octahedral environment with the S1-Sn-S2 bond angle at 177.8(1)°. The average Sn-S distance at 2.550(4)Å is very close to those found in K₂S_nS₃.2H₂O,¹⁹ at 2.571Å, which is in the range of typical Sn-S distances in SnS₆ octahedra. The average S-As-S angle

Table 2-10. Selected Distances (Å) in (Ph₄P)₂[SnAs₄S₉] with Standard Deviations in Parentheses.^a

				_
Sn1 - S1	2.535(4)	As2 - S1	2.213(5)	
Sn1 - S2	2.548(4)	As2 - S2	2.243(5)	
Sn1 - S8	2.587(4)	As2 - S7	2.281(5)	
Sn2 - S3	2.558(4)	As3 - S4	2.244(6)	
Sn2 - S4	2.544(5)	As3 - S5	2.210(5)	
Sn2 - S5	2.528(5)	As3 - S9	2.298(5)	
As1 - S3	2.208(5)	As4 - S6	2.279(5)	
As1 - S6	2.292(5)	As4 - S7	2.287(5)	
As1 - S9	2.267(5)	As4 - S8	2.209(4)	

^aThe estimated standard deviations in the mean bond lengths and the mean bond angles are calculated by the equation $\sigma l = \{\Sigma_n(l_n - 1)^2/n(n-1)\}^{1/2}$, where l_n is the length (or angle) of the nth bond, l the mean length (or angle), and n the number of bonds.

Table 2-11. Selected Angles (Deg) in (Ph₄P)₂[SnAs₄S₉] with Standard Deviations in Parentheses.

S1 - Sn1 - S1	180.00	S6 - As1 - S9	93.1(2)
S1 - Sn1 - S2	98.2(1)	S1 - As2 - S2	96.7(2)
S1 - Sn1 - S2	81.8(1)	S1 - As2 - S7	103.8(2)
S1 - Sn1 - S8	90.6(1)	S2 - As2 - S7	102.1(2)
S1 - Sn1 - S8	89.4(1)	S4 - As3 - S5	97.1(2)
S2 - Sn1 - S2	180.00	S4 - As3 - S9	101.0(2)
S2 - Sn1 - S8	91.3(1)	S5 - As3 - S9	104.5(2)
S2 - Sn1 - S8	88.7(1)	S6 - As4 - S7	95.9(2)
S8 - Sn1 - S8	180.00	S6 - As4 - S8	94.1(2)
S3 - Sn2 - S3	180.00	S7 - As4 - S8	104.8(2)
S3 - Sn2 - S4	87.2(1)	Sn1 - S1 - As2	90.2(2)
S3 - Sn2 - S4	92.8(1)	Sn1 - S2 - As2	89.1(2)
S3 - Sn2 - S5	90.7(2)	Sn2 - S3 - As1	102.6(2)
S3 - Sn2 - S5	89.3(2)	Sn2 - S4 - As3	88.5(2)
S4 - Sn2 - S4	180.00	Sn2 - S5 - As3	89.7(2)
S4 - Sn2 - S5	82.3(2)	As1 - S6 - As4	96.1(2)
S4 - Sn2 - S5	97.7(2)	As2 - S7 - as4	99.7(2)
S5 - Sn2 - S5	180.00	Sn1 - S8 - As4	104.0(2)
S3 - As1 - S6	96.2(2)	As1 - S9 - As3	99.5(2)
S3 - As1 - S9	103.1(2)		

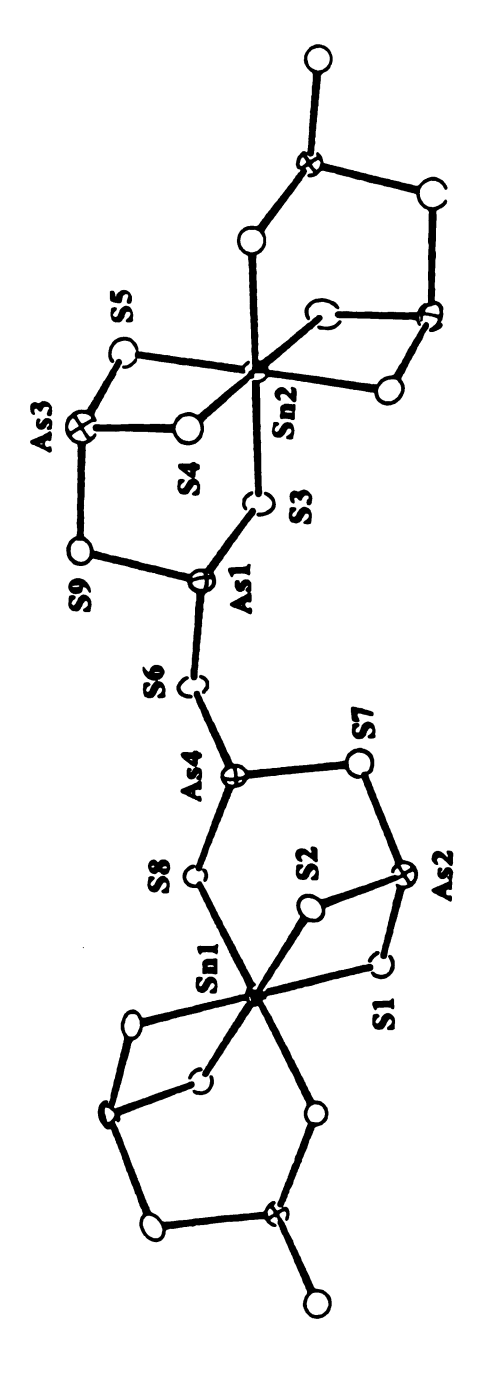


Figure 2-3. Structure and labeling scheme of $[SnAs4S9]_n^{2n}$.

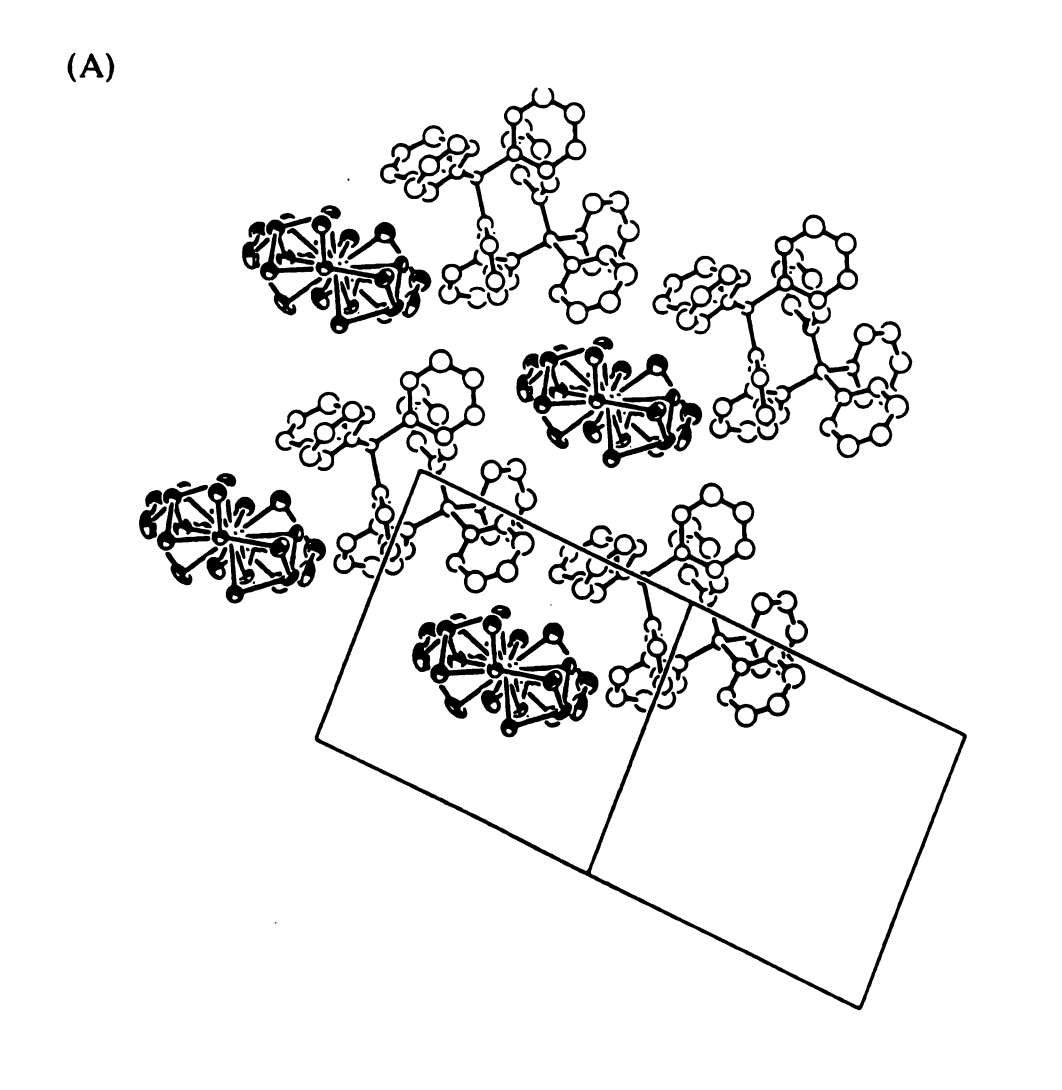
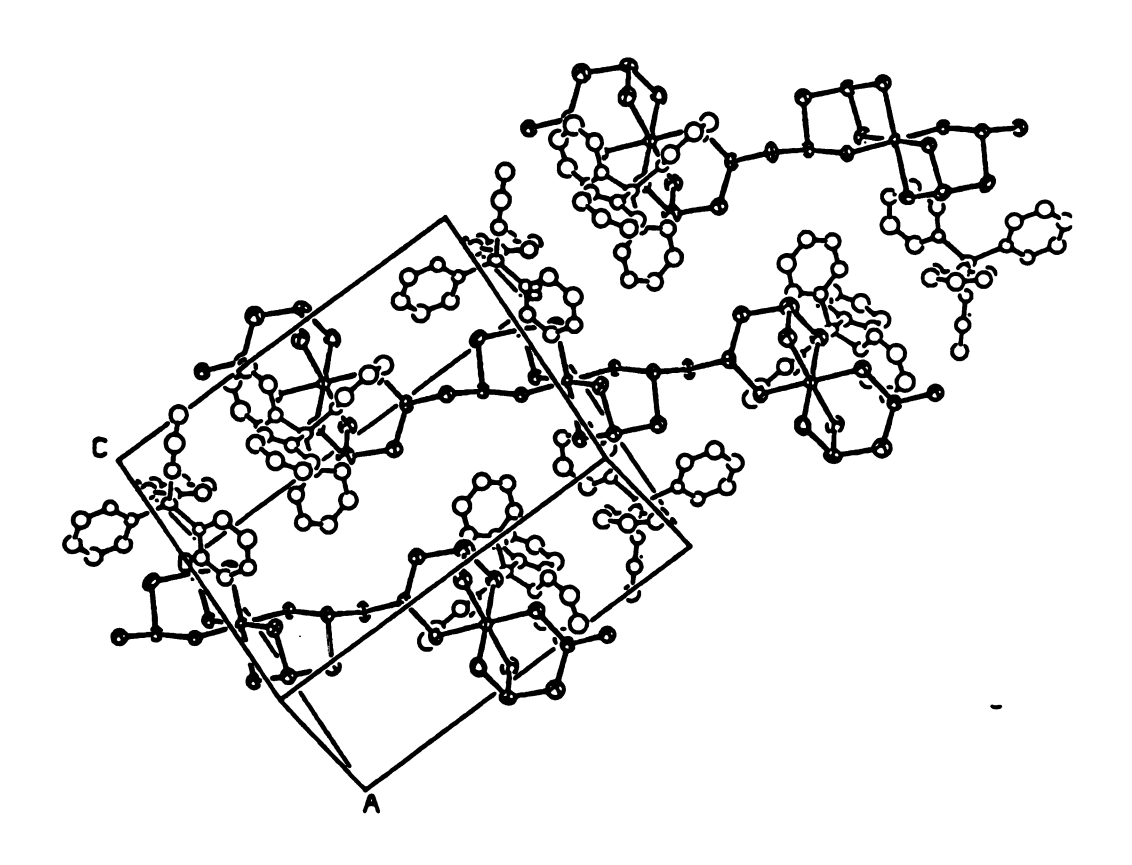


Figure 2-4. Packing diagram of $(Ph_4P)_2[SnAs_4S_9]$. (A) Showing the crossing section. (B) Showing the One-dimensional chains.

(B)



and As-S distance are normal compare to those in other arsenic sulfide compounds.9 Selected bond distances and angles are given in Tables 2-10 and 2-11. When comparing the structures of these two compounds, (Ph₄P)₂[InAs₃S₇] and (Ph₄P)₂[SnAs₄S₉], one can find several similarities. They both have one-dimensional chainlike structures which probably are the result of the large Ph₄P⁺ cations. They both contained unique thioarsenate ligands, [As₃S₇]⁵ and [As4S9]6-, formed by condensation reactions of the pyramidal [AsS3]3units. The main structural differences between the two compounds arise from the metal coordination. The In³⁺ ions, in [InAs₃S₇]²⁻. adopt trigonal bypyramid geometry while the Sn⁴⁺ ions, in [SnAs₄S₉]², take an octahedral environment. This imply that metal coordination preference may actually dictate the formation of the $[As_xS_y]^{n-}$ species.

 $(Me_4N)_2Rb[BiAs_6S_{12}]$ was synthesized by heating BiCl₃ with Rb₃AsS₃ and Me₄NCl in H₂O at 120 °C for one week. The anionic $[BiAs_6S_{12}]_n^{3n}$ possesses a two-dimensional layered structure with trigonal symmetry consisting of octahedral Bi³⁺ ions and $[As_3S_6]^3$ -cyclic units formed by three corner-sharing trigonal pyramidal $[AsS_3]^3$ - units; see Figure 2-5. The $[As_3S_6]^3$ - units were first observed as a discrete molecule in $(enH_2)_3(As_3S_6)_2$. The $[As_3S_6]^3$ - fragment in $(Me_4N)_2Rb[BiAs_6S_{12}]$ is located on a 3-fold axis with three As atoms and three S atoms forming a six-membered ring in a chair conformation. In $[As_3S_6]^3$ - the As-S bonds are separated into two types. The intra-ring As-S distance, at 2.312(2) Å, is significantly longer than the other As-S distance, at 2.189(3) Å. Similar distances were observed in $(As_3S_6)^3$ -20 Selected bond distances and angles are

Table 2-12. Selected Distances (Å) in (Me₄N)₂Rb[BiAs₆S₁₂] with Standard Deviations in Parentheses.^a

Bi - S1	2.830(2)	As - S2	2.296(3)
Rb - S2	3.461(2)	N - C1	1.49(1)
As - S1	2.190(3)	N - C2	1.49(1)
As - S2	2.312(2)		

Table 2-13. Selected Angles (Deg) in (Me₄N)₂Rb[BiAs₆S₁₂] with Standard Deviations in Parentheses.^a

S1 - Bi - S1	88.92(6)	S1 - As - S2	99.7(1)
S1 - Bi - S1	180.00	S2 - As - S1	91.96(7)
S1 - Bi - S1	91.08(6)	Bi - S1 - As	102.30(7)
S2 - Rb - S2	118.75(5)	Bi - S1 - As	92.47(6)
S2 - Rb - S2	118.75(5)	C1 - N - C2	111.1(6)
S1 - As - S1	89.33(9)	C2 - N - C2	107.8(6)
S1 - As - S2	97.34(8)		

^aThe estimated standard deviations in the mean bond lengths and the mean bond angles are calculated by the equation $\sigma l = \{\Sigma_n(l_n - 1)^2/n(n-1)\}^{1/2}$, where l_n is the length (or angle) of the nth bond, l the mean length (or angle), and n the number of bonds.

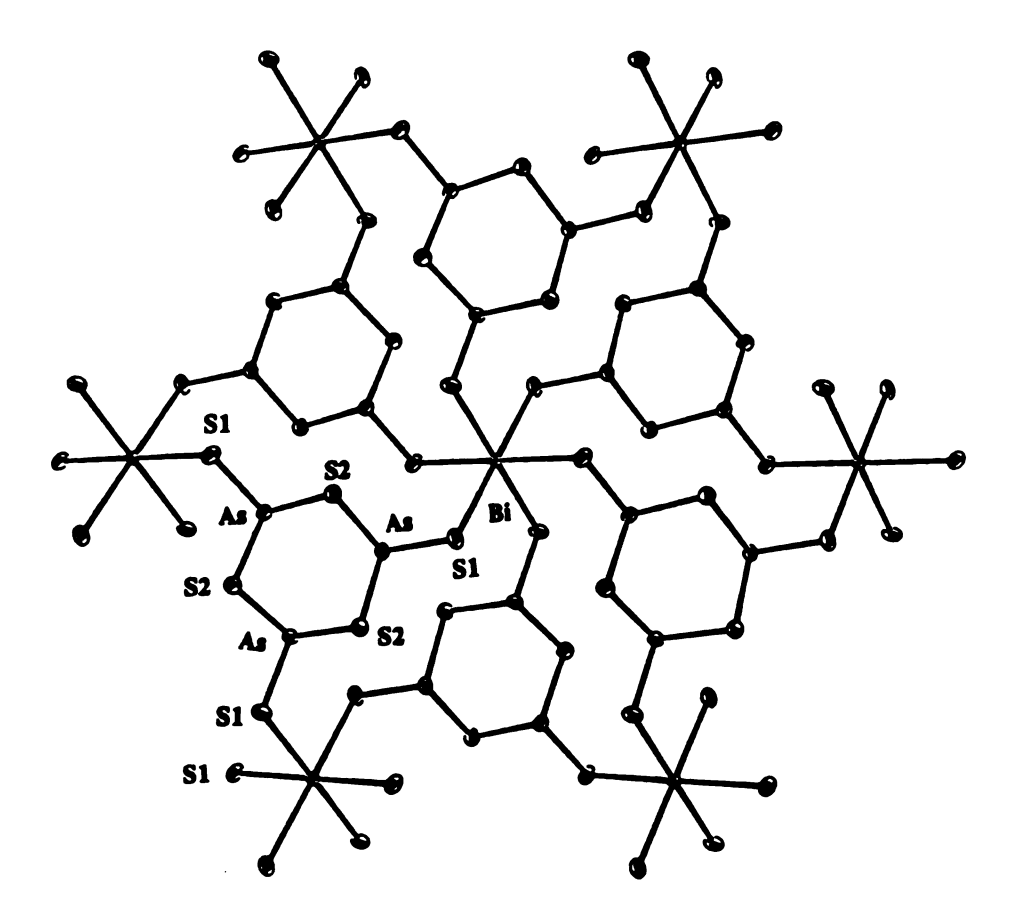


Figure 2-5. Structure and labeling scheme of one $[BiAs_6S_{12}]_n^{3n}$ -layer.

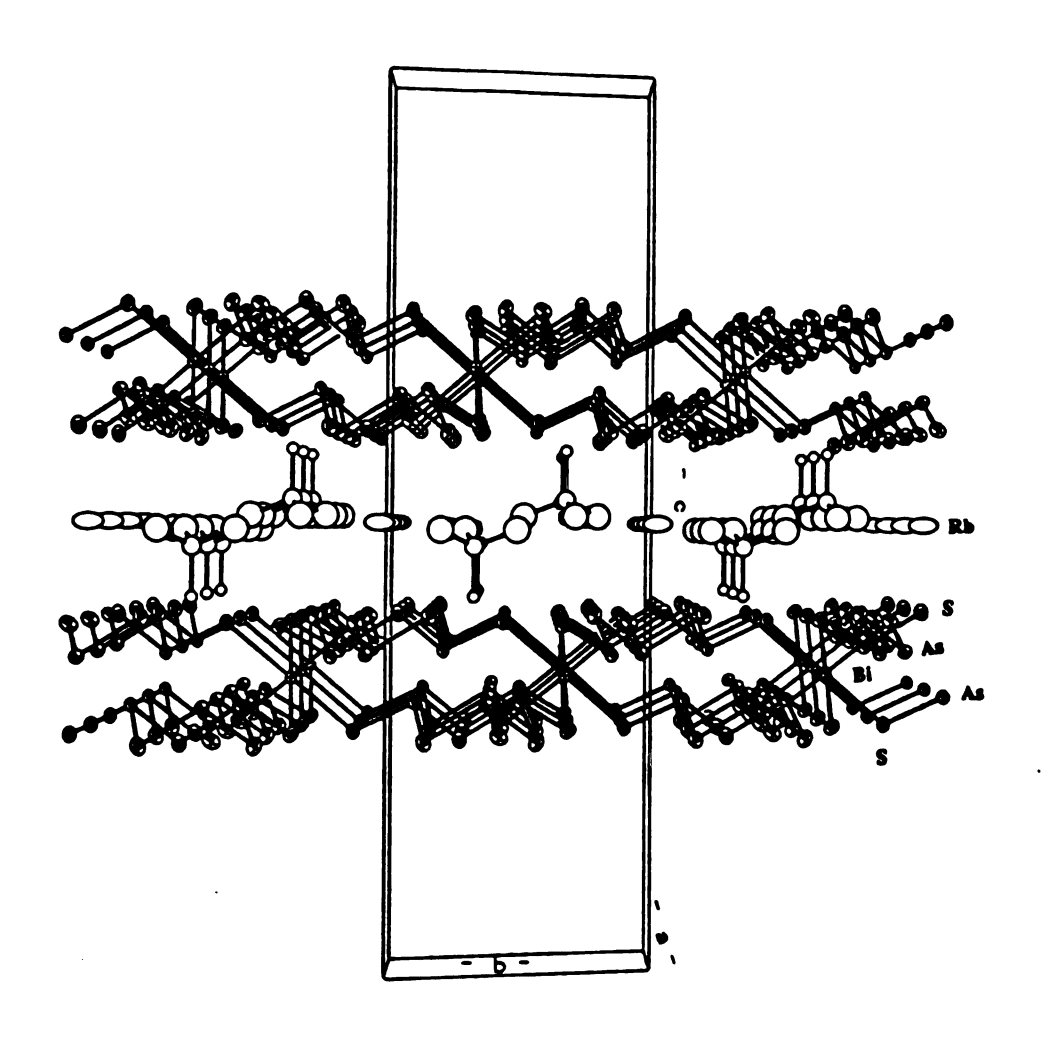


Figure 2-6. Packing diagram of (Me₄N)₂Rb[BiAs₆S₁₂].

given in Tables 2-12 and 2-13. The Bi³⁺ ion is in a nearly perfect octahedral geometry. The overall organization of the Bi3+ and the [As₃S₆]³- ions is CdCl₂-type with the cations in the Cd²⁺ and the anions in the Cl- sites, respectively. The Bi-S bond distance, at 2.830(2) Å, is in the normal range for the Bi-S bonds.²¹ The Me₄N+ and the Rb⁺ cations are located between the $[BiAs_6S_{12}]_n^{3n}$ layers, see Figure 2-6, which are spaced 9.445 Å apart The Rb+ and $[As_3S_6]^{3-}$ ions share a common C_3 axis so that each Rb+ ion is coordinated to six bridging S atoms from two [As₃S₆]³- units, one above and one below, in a trigonal antiprismatic fashion. The Rb...S distance is 3.458(2) Å. We noticed that the same As₃S₃ six membered rings previously seen in the Rb₂As₈S₁₃,²² which is also a Rb salt, were also found in (Me₄N)₂Rb[BiAs₆S₁₂]. It is possible that the Rb cation is just the right size to coordinate to six sulfur atoms from two [As₃S₆]³- units and that this structure type may not be stable for either the smaller K cation or the larger Cs cation. Hence, the Rb here may act both as cation and as structure directing One can then speculate that the larger As4S4 eight template. membered rings might possibly coordinate with the larger Cs as the cation as seen in Cs₂As₈S₁₃.²³ The larger space generated by the Cs cations may also need larger organic cations, such as Et4N+, to be filled. The lone electron pair on Bi3+ is stereochemically inactive and apparently is delocalized around the Bi nucleus. This is common for octahedral Bi³⁺ sites and has been found earlier in other Bi-S compounds such as KBiS₂.¹⁹

3.2 Physicochemical studies

In the far-IR region all complexes reported here exhibit spectral absorptions due to As-S and M-S stretching vibrations as shown in Figure 2-7. Observed absorption frequencies of all the complexes are given in table 2-14.

Table 2-14. Frequencies (cm⁻¹) of Raman and Infrared Spectral Absorptions of (Ph₄P)₂[InAs₃S₇](I), (Ph₄P)₂[SnAs₄S₉](II), and (Me₄N)₂Rb[BiAs₆S₁₂](III).

Compounds	Infrared	Raman
(Ph4 P) ₂ [InAs ₃ S ₇]	400(s), 373(s, sh)	395(s), 375(m), 352(m)
	346(m), 284(s, br)	329(w), 301(m), 253(m)
	225(m), 205(m)	186(m), 154(w)
(Ph4 P) ₂ [SnAs ₄ S ₉]	387(m), 374(m)	409(w), 387(m), 380(m)
	340(m, sh), 288(s)	341(s), 292(m), 256(m)
	250(m, br), 211(m)	199(m), 155(w)
	198(m)	
$(Me_4N)_2Rb[BiAs_6S_{12}]$	389(s), 370(w)	
	354(m), 302(s, br)	
	186(s, br) 154(w)	

^{*} s: strong, m; medium, w: weak, sh: shoulder.

In the Far-IR spectra, see Figure 2-7, of $(Ph_4P)_2[InAs_3S_7]$, $(Ph_4P)_2[SnAs_4S_9]$, and $(Me_4N)_2Rb[BiAs_6S_{12}]$, the peaks in the region of 250-400 cm⁻¹ could be attributed to As-S vibration modes. Similar assignments have been made in the far-IR spectra of other known

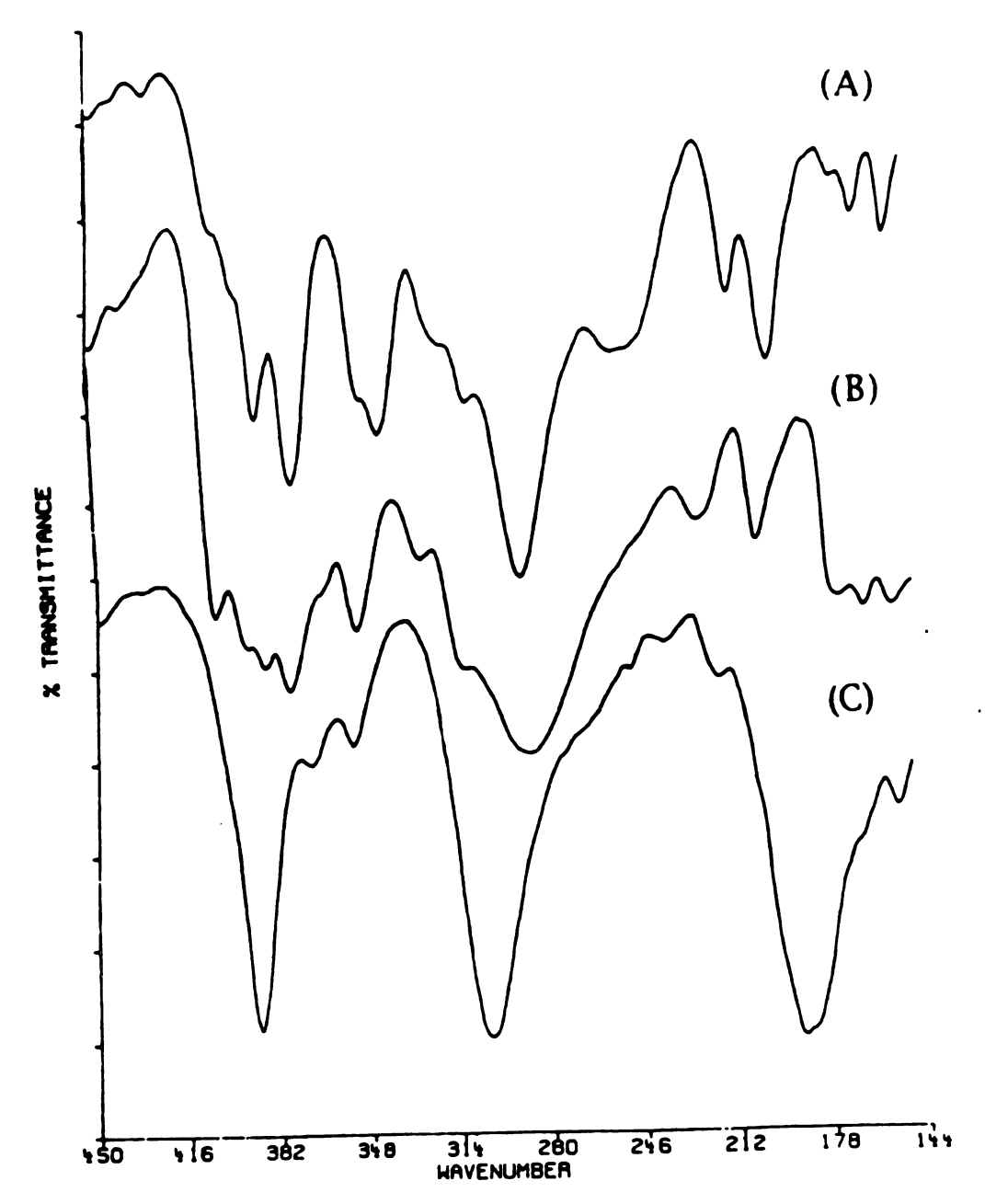


Figure 2-7. Far-IR spectra of (A) $(Ph_4P)_2[InAs_3S_7]$, (B) $(Ph_4P)_2[SnAs_4S_9]$, and (C) $(Me_4N)_2Rb[BiAs_6S_{12}]$

thioarsenate complexes.²⁴ Furthermore, the additional peaks in the IR spectra at 225 cm⁻¹ and 205 cm⁻¹ for (Ph₄P)₂[InAs₃S₇], at 211 cm⁻¹ and 198 cm⁻¹ for (Ph₄P)₂[SnAs₄S₉], and at 186 cm⁻¹ for (Me₄N)₂Rb[BiAs₆S₁₂] may be possible candidates of an M-S stretching vibration. Assigning the observed IR spectra of these compounds is difficult because As-S and M-S stretching frequencies fall in the same low frequency region of 150-350 cm⁻¹.

The Raman spectra of (I) and (II) were also recorded while the spectrum of (III) was not due to a large diffuse reflectance which obscured the area from 2000 cm⁻¹ to 200 cm⁻¹. There are numerous peaks between 150 and 450 cm⁻¹, see Table 2-13, just as in the far-IR spectra. The peaks in the range from 250 - 400 cm⁻¹ could be due to As-S vibration modes while the lower energy peaks, at 186 cm⁻¹ and 154 cm⁻¹ for (I) and 199 cm⁻¹ and 155 cm⁻¹ for (II), might be due to the M-S vibration mode.

Thermal Gravimetric Analysis (TGA) results for all compounds are summarized in Table 2-15 and shown in Figures 2-8 and 2-9.

Table 2-15. TGA data for $(Ph_4P)_2[InAs_3S_7](I)$, $(Ph_4P)_2[SnAs_4S_9](II)$, and $(Me_4N)_2Rb[BiAs_6S_{12}](III)$.

Compound	Temp. range (°C)	Weight loss (%)
(Ph ₄ P) ₂ [InAs ₃ S ₇]	224 - 600	78.3
$(Ph_4P)_2[SnAs_4S_9]$	290 - 600	67.8
$(Me_4N)_2Rb[BiAs_6S_{12}]$	120 - 750	65.2

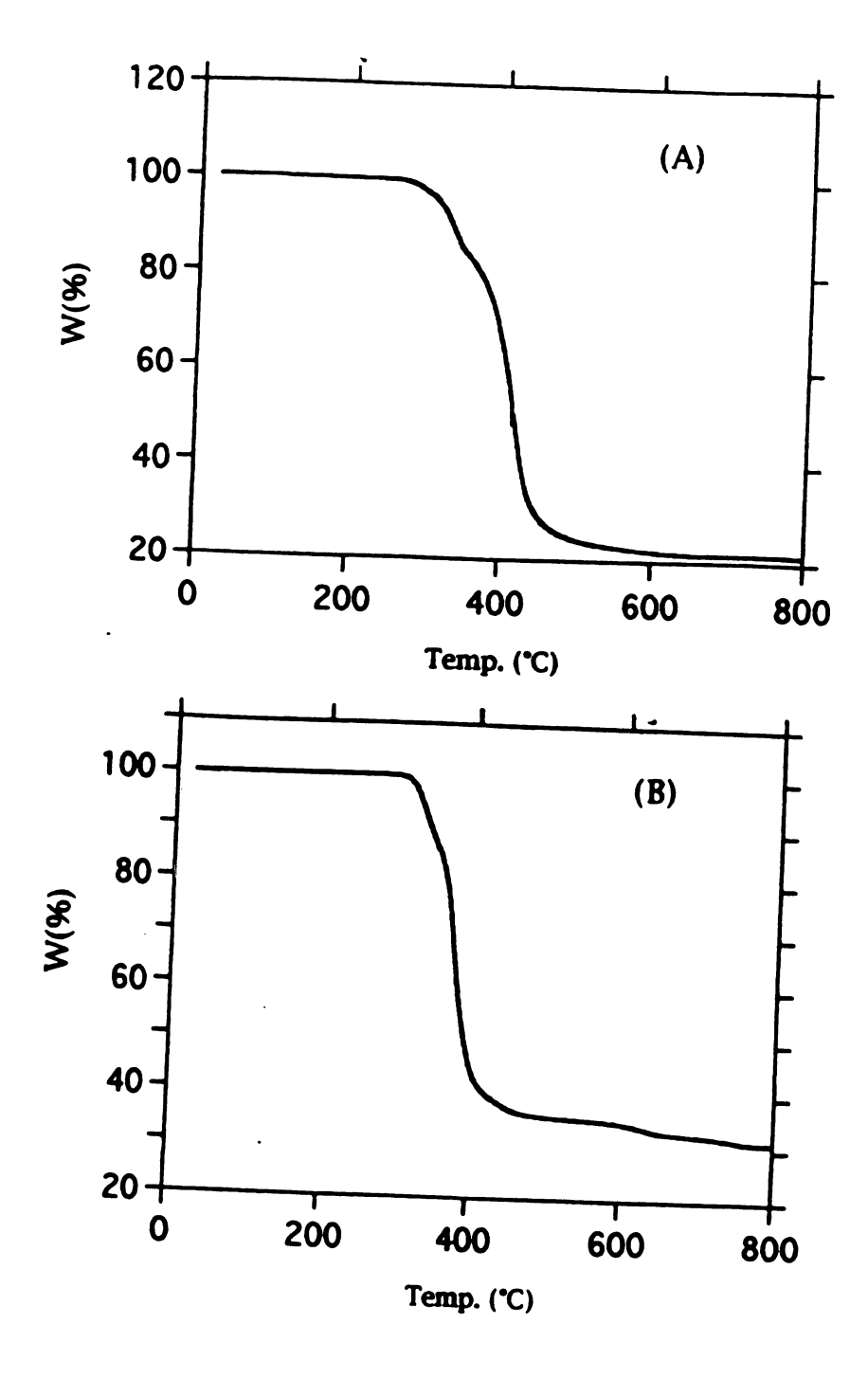


Figure 2-8. TGA diagrams of (A) $(Ph_4P)_2[InAs_3S_7]$ and (B) $(Ph_4P)_2[SnAs_4S_9]$.

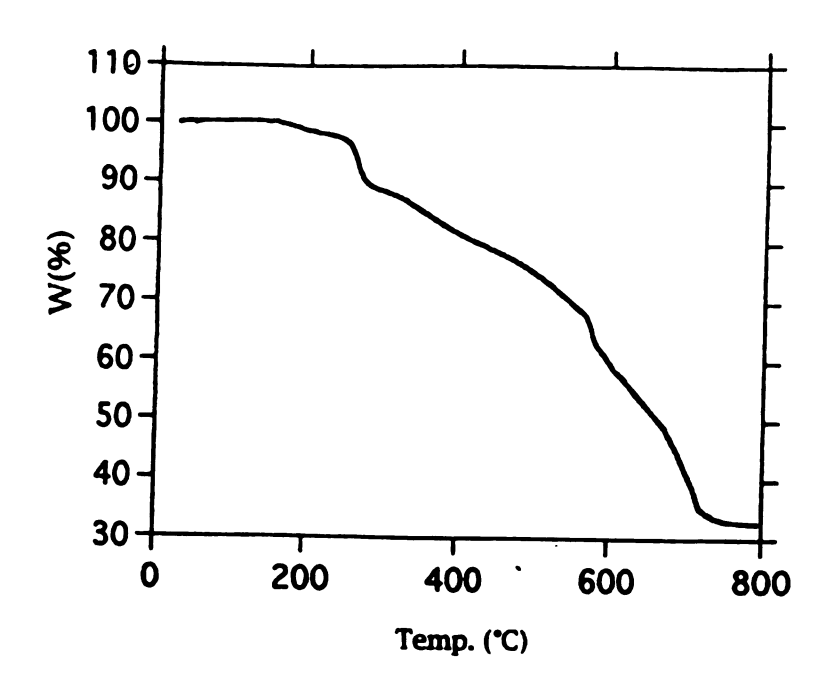


Figure 2-9. TGA diagram of (Me₄N)₂Rb[BiAs₆S₁₂].

(Ph₄P)₂[InAs₃S₇] shows a one step weight loss of 78.3 % in the temperature range of 224-600 °C probably as Ph₃PS, other organic species and various As_xS_y. The X-ray powder diffraction analysis of the final residue indicates the presence of InAs₂S₄ and other phases that can not be identified. (Ph₄P)₂[SnAs₄S₉] also shows a clean one step weight loss of 67.8 % in the temperature range of 290-600 °C. The final product was proved to be SnS(Herzenbergite) by X-ray powder diffraction. For (Me4N)₂Rb[BiAs₆S₁₂], a weight loss, 65.2 %, occurred gradually over the temperature range 120 to 750 °C. The final residue appears by SEM/EDS analysis to be Rb_{0.3}Bi₂S₃. From the TGA results, compounds (I) and (II) do show some thermal stability. There is no weight loss up to 200 and 290 °C for (I) and (II) The thermal behavior of (I) and (II) were further respectively. studied by DTA (differential thermal analysis). We did not observed any melting before the decomposition temperature. Visual inspection of the product, under the microscope, confirmed that no melting occurred. Slight discoloration of the crystals indicated the compounds were starting to decompose.

The optical properties of (Ph₄P)₂[InAs₃S₇], (Ph₄P)₂[SnAs₄S₉], and (Me₄N)₂Rb[BiAs₆S₁₂] were assessed by studying the UV-visible-near IR spectra of the material. The spectra confirm that these compounds are wide band-gap semiconductors. The optical absorption spectra of (Ph₄P)₂[InAs₃S₇](I) and (Ph₄P)₂[SnAs₄S₉](II), shown in Figure 2-10, exhibit an intense, steep absorption edge for both compounds, revealing optical bandgaps of 3.1 eV and 2.8 eV

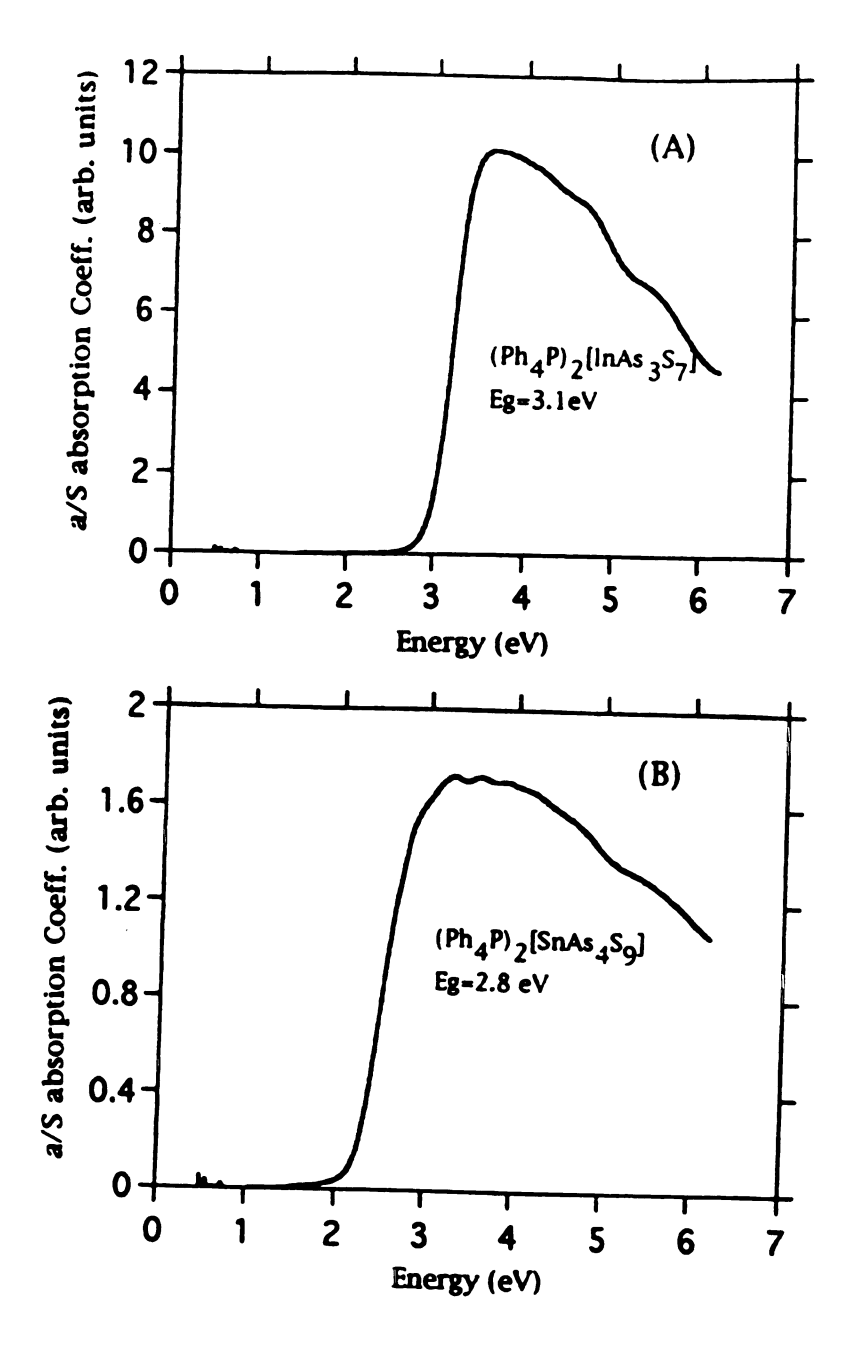


Figure 2-10. Optical absorption spectra of (A) $(Ph_4P)_2[InAs_3S_7]$, and (B) $(Ph_4P)_2[SnAs_4S_9]$.

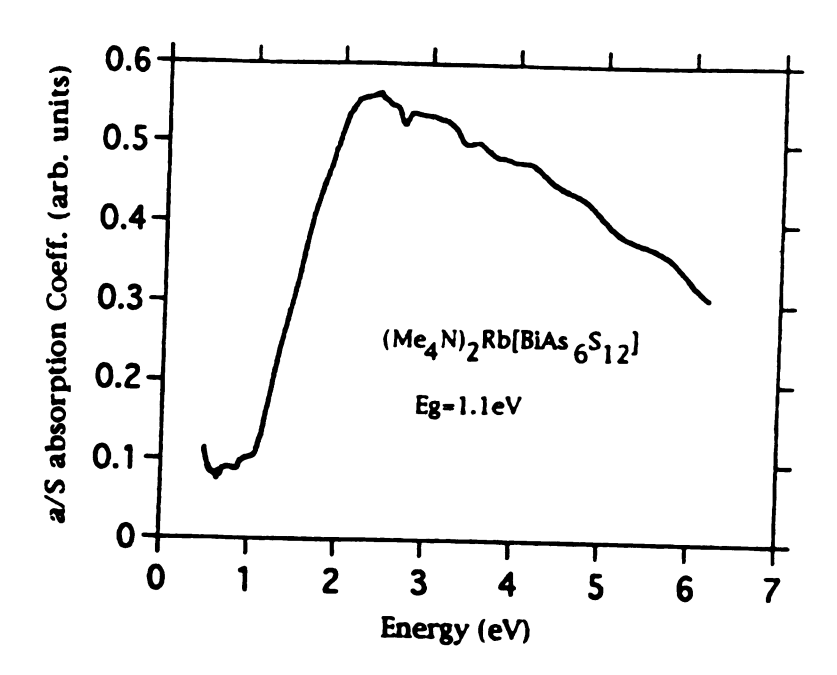


Figure 2-11. Optical absorption spectrum of $(Me_4N)_2Rb[BiAs_6S_{12}]$.

respectively. $(Me_4N)_2Rb[BiAs_6S_{12}](III)$ absorbs light strongly throughout the visible region with a λ_{max} of 520 nm; see Figure 2-11. Its electronic spectrum reveals an optical bandgap of 1.1 eV, which is within the range appropriate for efficient solar energy collection and suggests possible photoconductivity in this material. The absorption is probably due to a charge-transfer transition from a primarily sulfur-based valence band to a mainly metal-based conduction band.

Remarkably, despite the fact that the arsenic/sulfide source in all reactions was $[AsS_3]^{3-}$, we do not observe this discrete unit in the new structures. Rather, in $[InAs_3S_7]^{2-}$, $[SnAs_4S_9]^{2-}$, and $[BiAs_6S_{12}]^{3-}$, we find respectively the unusual chainlike $[As_3S_7]^{5-}$ $[As_4S_9]^{6-}$, and cyclic $[As_3S_6]^{3-}$ fragments which are formed from corner-sharing $[AsS_3]^{3-}$ units. These units result from condensation reactions in water in which several equilibria of the type shown in eqs. 2.1-2.4 must exist.

$$AsS_3^{3-} + AsS_3^{3-} = [As_2S_5]^{4-} + S^{2-}$$
 (Eq. 2.1)

$$[As_2S_5]^{4}$$
 + AsS_3^{3} \longrightarrow $[As_3S_7]^{5}$ + S^{2} (Eq. 2.2)

$$[As_3S_7]^{5}$$
 + AsS_3^{3} \longrightarrow $[As_4S_9]^{6}$ + S^{2} (Eq. 2.3)

$$[As_3S_7]^{5}$$
 \longrightarrow $[As_3S_6]^{3}$ + S^{2} (Eq. 2.4)

These condensation reactions parallel those found in the condensation of SiO₄⁴- and PO₄³- units.¹ Therefore, as in these

systems, one would expect that a variety of $[As_xS_y]^{n}$ species might be possible. It must be mentioned that the degree and extent of these equilibria are probably influenced by the presence of the metal ions in solution. In addition, however, these condensation reactions were probably facilitated by the protonation of the terminal sulfur atoms, see eqs 2-5 and 2-6

$$\begin{bmatrix} S \\ AS \\ S \end{bmatrix}^{3} + H^{+} \longrightarrow \begin{bmatrix} S \\ AS \\ S \end{bmatrix}^{2} \cdot (eq 2-5)$$

$$\begin{bmatrix} S \\ AS \\ S \end{bmatrix}^{4} + H_{2}S \cdot (eq 2-6)$$

In conclusion, the successful hydrothermal synthesis of $(Ph4P)_2[InAs_3S_7]$, $(Ph4P)_2[SnAs_4S_9]$, and $(Me_4N)_2Rb[BiAs_6S_{12}]$ by using AsS_3^{3-} as starting material opens exciting possibilities for the further exploration of metal/arsenic/sulfide and related systems. Key to this is the complex condensation equilibria which exist among various $[As_xS_y]^{n-}$ species in the reaction medium. As in other labile systems, the size of the counter-cations is expected to influence the structural dimensionalities of the covalent framework. From comparing the structure of $(Ph_4P)_2[InAs_3S_7](I)$ and $(Ph_4P)_2[SnAs_4S_9](II)$, we noticed that the metal coordination preference also play a major role in the formation of different $[As_xS_y]^{n-}$ species. Different coordination geometry may dictate the formation of different $[As_xS_y]^{n-}$ species. It is interesting, for example, that the one-dimensional chain structure

of $[InAs_3S_7]^{2-}$ was isolated with the large Ph_4P^+ ion, while the two-dimensional framework of $[BiAs_6S_{12}]^{3-}$ formed with the small Me_4N^+ and Rb^+ cations. Although the controlled synthesis of specific $[As_xS_y]^{n-}$ ligands may be challenging, the above equilibria should undoubtedly be exploited for the synthesis of new thioarsenates and related compounds.

REFERENCES

- 1. (a) Liebau, F. Structural Chemistry of Silicates; Springer: New York, 1985. (b) Day, V. W.; Klemperer, W. G.; Mainz, V. V.; Millar, D. M. J. Am. Chem. Soc. 1985, 107, 8262-8264. (c) Cotton, F. A.; Wilkinson, G. Advanced Inorganic Chemistry; John Wiley & Sons: New York, 1988, pp 421-430.
- (a) Chopin, F.; Turrell, G. J. Mol. Struct. 1969, 3, 57-65. (b)
 Krebs, B.; Diercks, H. Acta Crystallogr. 1975, A31, 566-585. (c)
 Krebs, B. Angew. Chem., Int. Ed. Engl. 1983, 22, 113-134 and references cited therein.
- (a) Krebs, B.; Pohl, S.; Schiwy, W. Angew. Chem., Int. Ed. Engl.
 1970, 9, 897-898. (b) Krebs, B.; Pohl, S.; Schiwy, W. Z. Anorg.
 Allg. Chem. 1972, 393, 241-252. (c) Pohl, S.; Schiwy, W.;
 Weinstock, B.; Krebs. B. Z. Naturforsch. 1973, B28, 565-569. (d)
 Pohl, S.; Krebs. B. Z. Anorg. Allg. Chem. 1976, 424, 265-272.
- (a) Sommer, V. H.; Hoppe, R. Z. Anorg. Allg. Chem. 1977, 430, 199-210.
 (b) Sinning, H.; Muller, U. Z. Anorg. Allg. Chem. 1989, 568, 49-54.
 (c) Sinning, H.; Muller, U. Z. Anorg. Allg. Chem. 1988, 564, 37-45.
 (d) Siewert, B.; Muller, U. Z. Anorg. Allg. Chem. 1992, 609, 82-88.
 (e) Siewert, B.; Muller, U. Z. Anorg. Allg. Chem. 1991, 595, 211-215.
- 5. Sheldrick, W. S.; Kaub, J. Z. Naturforsch. 1985, 40B, 1130-1133.

- 6. Porter, E. J.; Sheldrick, G. M. J. Chem. Soc. Dalton. Trans. 1971, 3130-3134.
- 7. Sheldrick, W. S.; Kaub, J. Z. Naturforsch. 1985, 40b, 19-21.
- 8. O'Neal, S. C.; Penington, W. T.; Kolis, T. W. *Inorg. Chem.* 1992, 31, 888-894.
- Zank, G. A.; Rauchfuss, T. B.; Wilson, S. R. J. Am. Chem. Soc.
 1984, 106, 7621-7623.
- O'Neal, S. C.; Penington. W. T.; Kolis, T. W. J. Am. Chem. Soc.
 1991, 113, 710-712.
- 11. Chou, J.-H.; Kanatzidis. M. G. Unpublished results.
- (a) Wendlandt, W. W.; Hecht, H. G. "Reflectance Spectroscopy",
 Interscience Publishers, 1966. (b) Kotüm, G. "Reflectance
 Spectroscopy", springer Verlag, New York, 1969. (c) Tandon, S.
 P.; Gupta, J. P. Phys. Stat. Sol. 1970, 38, 363-367.
- Sheldrick, G. M. In Crystallographic Computing 3; Sheldrick, G.
 M.; Kruger, C.; Goddard, R., Eds.; Oxford University Press: Oxford,
 U.K., 1985; pp 175-189.
- 14. TEXSAN: Single Crystal Structure Analysis Package, Version 5.0, Molecular Structure Corp., Woodland, TX.
- 15. Walker, N.; Stuart, D. Acta Crystallogr. 1983, 39A, 158-166.
- CERIUS: Single Crystal Structure Analysis Software, Version 5.0,
 Molecular Simulations Inc. Cambridge, UK.

- 17. Dhingra, S.; Kanatzidis, M. G. Inorg. Chem. 1989, 28, 2024-2026.
- 18. Dhingra, S. S.; Kanatzidis, M. G. *Inorg. Chem.* 1993, 32, 3300-3305.
- 19. Schiwy, W.; Blutau, C.; Gäthje, D.; Krebs. B. Z. Anorg. Allg. Chem. 1975, 412, 1-10.
- 20. (a) en = ethylenediamine. (b) Sheldrick, W. S.; Kaub, J. Z.

 Naturforsch. 1985, 40B 19-21.
- 21. Schmitz, D.; Bronger, W. Z. Naturforsch. 1974, 29B, 438-439.
- 22. Sheldrick, W.; Kaub, J. Z. Naturforsch. 1985, 40b, 1130-1133.
- 23. Sheldrick, W.; Kaub, J. Z. Naturforsch. 1985, 40b, 571-573.
- 24. Peresh, E. Y.; Golovei, M. I.; Berul, S. I. Izv. Akad. Nauk SSR Neorg. Mater. 1971, 7, 27-30.
- (a) Huang, S.-P.; Kanatzidis, M. G. Inorg. Chem. 1991, 30, 1455-1466.
 (b) Kim, K.-W.; Kanatzidis. M. G. J. Am. Chem. Soc. 1992, 114, 4878-4883.

CHAPTER 3

HYDROTHERMAL SYNTHESIS OF M/As_xS_y ($M = Ni^2+$, Mo^5+) COMPOUNDS. SYNTHESIS AND STRUCTURAL CHARACTERIZATION OF $(Ph_4P)_2[Ni_2As_4S_8](I)$, and $(Me_4N)_2[Mo_2O_2As_2S_7](II)$

ABSTRACT

(Ph₄P)₂[Ni₂As₄S₈], and (Me₄N)₂[Mo₂O₂As₂S₇] were synthesized by hydrothermal reactions of NiCl₂/K₃A₅S₃/Ph₄PBr and MoO₃/K₃A₅S₃/Me₄NCl in a 1:3:4, and 1:2:4 molar ratio, respectively. The (Ph₄P)₂[Ni₂As₄S₈] compound crystallizes in the triclinic space group P-1(No. 2) with a = 10.613(3) Å, b = 13.230(2) Å, c = 9.617(2) \dot{A} , $\alpha = 93.53(2)$, $\beta = 96.69(2)^{\circ}$, $\gamma = 71.59(2)$, V = 1272(1) \dot{A}^3 , Z = 2. The $[Ni_2As_4S_8]_{n^{2n}}$ macroanion is a one-dimensional chain consisting of alternating square planar Ni²⁺ ions and [As₄S₈]⁴⁻ units, the latter formed by corner-sharing [AsS₃]³- units. The (Me₄N)₂[Mo₂O₂As₂S₇] compound crystallizes in the orthorombic space group Pbca(No. 61) with a = 18.176(4) Å, b = 17.010(2) Å, c = 16.556(7) Å, V = 5118(4) \dot{A}^3 , Z = 4. The $[Mo_2O_2As_2S_7]_{n^2}^{n-1}$ macroanion also has a onedimensional chain-like structure and contains Mo₂O₂S₂ fragments linked by [As₂S₅]⁴- units into a one-dimensional chain. The solid state optical and vibrational spectra of these compounds are reported.

1. Introduction

The incorporation of main group thiometallates in solid state extended frameworks in combination with transition and other main group metals promises to yield new solids with properties varying from semiconductivity to microporosity. The latter property could be achieved with large organic templates around which an open structure can assemble. At this stage use of organic counterions such as Ph₄P+ and R₄N+ seems appropriate. Although there is substantial precedent for hydrothermal (or solvothermal) synthesis of solids with thio- and chalcogeno- anions in the lattice^{1, 2, 3}, the use of the basic [AsS₃]³- anion has been limited. Recently, we have shown that hydrothermal exploratory investigations of the systems R_4E^+ (E = P, R = Ph; E=N, R = alkyl)/ $M^{n+}/[AsS_3]^{3-}$, (where M is a main group element) can lead to novel polymeric materials containing unusual thioarsenate polyanions as building blocks. These compounds include (Ph₄P)₂[InAs₃S₇] and (Me₄N)₂Rb[BiAs₆S₁₂].⁴ The former has a one-dimensional chain structure and contains unusual chain-like [As3S7]⁵ units while the latter is a mixed salt with a twodimensional layered structure featuring cyclic [As₃S₆]³- units. In these compounds the [AsS₃]³- anion shows a facile condensation ability that results in higher nuclearity [As_xS_y]ⁿ units which are found coordinated to the metal cations. These reactions (see chapter 2) are probably catalyzed by protonation of the terminal sulfide groups. Kolis et al. have also demonstrated that superheated ethylenediamine is also a suitable solvent for synthesis of new metal/As_xS_y compounds. They have reported two new quaternary

phases, KCu₂AsS₃ and KCu₄AsS₄, formed by reacting KAsS₂ with Cu powder in superheated ethylenediamine.⁵ By using a strong base, however, as the reaction solvent, the condensation reactions mentioned above, between the [AsS₃]³- units are not favored and the resulting compounds tend to contain only the most basic thioarsenic anion, [AsS₃]³-, as the building block.

In order to investigate further this tendency for condensation, and being aware of the wealth of different structure types exhibited by other condensable units (e. g. $[SiO_4]^{4-6}$, $[PO_4]^{3-7}$), we explored the hydrothermal behavior of the $R_4E^+/M^{n+}/[AsS_3]^{3-}$ (E = P, R = Ph; E = N, R = Me, M = transition metal) system. There are several examples of early transition metal complexes which contain discrete thioarsenate ligands. The very first complex, $Cp'_3Ti_2O(AsS_3)$ ($Cp' = \eta^5-CH_3C_5H_4$) synthesized by Rauchfuss and co-workers, demonstrated that the thioarsenate anion, $[AsS_3]^{3-}$, could be used as ligands toward transition metals. They also reported a Mo compound, $[Mo_2O_2As_4S_{14}]^{2-}$, which contains the highly unusual $[As_4S_{12}]^{4-}$ ligand and further indicates the great potential new chemistry that $[As_xS_y]^{n-}$ can provide.

Here we report the successful synthesis of two new polymeric compounds by using transition metals. The two novel low-dimensional compounds, $(Ph_4P)_2[Ni_2As_4S_8]$, and $(Me_4N)_2[Mo_2O_2As_2S_7]$ also feature higher order $[As_xS_y]^{n}$ units derived from the condensation of the $[AsS_3]^{3}$ anion, which are different from those found in $(Ph_4P)_2[InAs_3S_7]$ and $(Me_4N)_2Rb[BiAs_6S_{12}]$. These

compounds are new members of a rare group of crystalline inorganic solid state compounds that contain organic cations. 9-14

2. Experimental Section

2.1 Reagents

Chemicals. Chemicals in this work, other than solvents, were used as obtained. NiCl₂, 98% purity, purity, MoO₃, 99% purity, tetraphenylphosphonium bromide (Ph₄PBr), 98% purity, tetramethylammonium chloride, (Me₄NCl), 99% purity, Aldrich Chemical Company, Inc., Milwaukee, WI. A₃AsS₃ (A = K, Rb, Cs) were synthesized by using stoichiometric amounts of alkali metal, arsenic sulfide (As₂S₃), and sulfur in liquid ammonia. The reaction gives a yellow brown powder upon evaporation of ammonia.

2.2 Syntheses

All syntheses were carried out under dry nitrogen atmosphere in a Vacuum Atmosphere Dri-Lab glovebox except were specifically mentioned.

(Ph₄P)₂[Ni₂As₄S₈]: A mixture of 0.025g (0.2 mmol) NiCl₂, 0.172g (0.6 mmol) K₃AsS₃ and 0.419g (1 mmol) Ph₄PBr was sealed in thick wall Pyrex tube (~ 4mL) under vacuum with 0.3 mL of water. The reaction was carried out at 110 °C for one week. The product was isolated by washing off excess starting material and KCl with H₂O, methanol, and ether to give 0.105g (76% yield) of dark brown plate-like crystals. SEM/EDS analysis on these crystals showed the P:Ni:As:S ratio as 2:1:1.8:9.1.

(Me₄N)₂[Mo₂O₂As₂S₇]: The reaction mixture of 0.02g (0.2 mmol) MoO₃, 0.057g (0.4 mmol) K₃AsS₃ and 0.13g (0.12 mmol) Me₄NCl was prepared as above. The mixture was heated to $110\,^{\circ}$ C for 3 days. Large yellow chunky crystals were isolated in H₂O and washed with methanol and ether. (Yield = 88% based on Mo) SEM/EDS analysis on these crystals showed the Mo:As:S ratio as 1.1:1:6.2.

2.3. Physical Measurements

The instruments and experimental setups for Infrared measurements, optical diffuse reflectance measurements, thermal analysis, and quantitative microprobe analysis on SEM/EDS are the same as those in Chapter 2.

2.4 X-ray crystallography

 $(Ph_4P)_2[Ni_2As_4S_8]$: A well shaped dark brown crystal with dimensions of 0.65 x 0.55 x 0.25 mm was mounted on a glass fiber. Single-crystal X-ray diffraction data were collected at room temperature on a Rigaku AFC6 diffractometer and the ω -2 θ scan technique was used. A total of 2878 independent reflections were collected. All the nonhydrogen and non-carbon atoms were refined anisotropically. All hydrogen atom positions were calculated and fixed without further refinement.

(Me4N)₂[Mo₂O₂As₂S₇]: A well shaped orange crystal with dimensions of 0.45 x 0.35 x 0.5 mm was mounted on a glass fiber. Single-crystal X-ray diffraction data were collected at room

temperature on a Rigaku AFC6 diffractometer and the ω -20 scan technique was used. A total of 3769 independent reflections were All the nonhydrogen atoms except carbon were refined All hydrogen atom positions were calculated and anisotropically. fixed without further refinement. During the structure refinement carbon found that a atom (C5) in one the we tetramethylammonium cations was slightly disordered. The occupancy of the two positions C5 and C5' were refined to be about 50% each.

The crystals did not showed any significant decay as judged by three check reflections measured every 150 reflections throughout the data collection. The space group was determined by systematic absences and intensity statistics. All the structures were solved by direct methods (SHELXS-86)¹⁵ and refined with the TEXSAN¹⁶ software package. An empirical absorption correction (DIFABS¹⁷) was applied to the isotropically refined data. All nonhydrogen atoms except nitrogen and carbon were refined anisotropically. All calculations were performed on a VAXstation 3100 Model 76 computer. Table 3-1 summarizes crystallographic data and details of the structure solution and refinement. The final atomic coordinates with their estimated standard deviations (esd's) are given in Tables 3-2 and 3-3.

Table 3-1. Summary of Crystallographic Data and Structural Analysis for (Ph₄P)₂[Ni₂As₄S₈](I), and (Me₄N)₂[Mo₂O₂As₂S₇](II).

	I	ΙΙ
Formula	C ₄₈ H ₄₀ P ₂ NiAs ₄ S ₈	C ₈ H ₂₄ N ₂ Mo ₂ O ₂ As ₂ S ₇
F. w.	1351.1	745.72
a, Å	10.612(4)	18.176(4)
b, Å	13.230(2)	17.010(2)
c, Å	9.617(2)	16.556(7)
α, deg.	93.53(1)	90.00
β, deg.	96.69(2)	90.00
γ, deg.	71.59(2)	90.00
Z, V, Å ³	2, 1272(1)	4, 5118(4)
Space Group	P-1 (No. 2)	Pbca(No. 61)
color, habit	dark brown, plate	orange yellow, plate
D _{calc} , g/cm ³	1.69	1.94
Radiation	Μο Κα	Μο Κα
μ, cm ⁻¹	73.76	40.75
2θ _{max} , deg.	45.0	45.0
Absorption Correction	ψ scan	ψ scan
Transmission Factors	0.73-1.13	0.96-1.02
Index ranges	$0 \le h \le 11, -14 \le k \le$	$0 \le h \le 20, \ 0 \le k \le 22,$
·	$14, -10 \le l \le 10$	$0 \le 1 \le 20$
No. of Data coll.	2989	3859
Unique reflections	2878	3769
Data Used	1984	1874
$(F_0^2 > 3\sigma(F_0^2))$		
No. of Variables	286	196
Final Ra/Rwb, %	3.7/4.3	4.9/6.4

^a R= Σ (|Fo|-|Fc|)/ Σ |Fo|, ^b R_w={ Σ w(|Fo|-|Fc|)²/ Σ w|Fo|²} 1/2

Table 3-2. Selected Atomic Coordinates and Estimated Standard Deviations (esd's) of (Ph₄P)₂[Ni₂As₄S₈](I).

atom	X	Y	Z	B_{eq} a, (A^2)
Ni	0.50000	0.50000	0.00000	3.4(1)
As1	0.7376(1)	0.31671(7)	0.1454(1)	4.44(6)
As2	0.8697(1)	0.46009(7)	-0.0314(1)	4.00(6)
S 1	1.0617(3)	0.4380(2)	-0.1377(2)	5.1(2)
S 2	0.9398(2)	0.2983(2)	0.0646(2)	4.2(1)
S 3	0.5966(2)	0.3278(2)	-0.0452(3)	5.0(1)
S4	0.6608(2)	0.4927(2)	0.1695(2)	4.6(1)
P1	1.1891(2)	0.1744(2)	0.4976(2)	3.4(1)
C1	1.1655(9)	0.0844(6)	0.3592(8)	3.5(1)
C2	1.041(1)	0.0827(6)	0.3073(8)	4.0(5)
C3	1.026(1)	0.0070(8)	0.207(1)	5.2(7)
C4	1.137(1)	-0.0688(8)	0.159(1)	6.1(8)
C5	1.261(1)	-0.0669(7)	0.209(1)	6.0(1)
C 6	1.277(1)	0.0106(7)	0.308(1)	5.0(1)
C7	1.2995(8)	0.2410(6)	0.449(1)	4.1(5)
C8	1.291(1)	0.2701(7)	0.310(1)	5.2(6)
C9	1.378(1)	0.3228(8)	0.276(1)	6.0(7)
C10	1.466(1)	0.3455(8)	0.377(2)	6.7(8)
C11	1.475(1)	0.3176(9)	0.513(1)	6.9(8)
C12	1.392(1)	0.2646(6)	0.547(1)	5.6(7)
C13	1.0314(8)	0.2672(6)	0.5286(8)	3.1(5)
C14	0.9817(9)	0.3635(6)	0.4621(8)	3.6(5)

C15	0.858(1)	0.4329(6)	0.486(1)	4.5(6)
C16	0.7849(9)	0.4058(7)	0.579(1)	4.7(6)
C17	0.833(1)	0.3100(8)	0.6469(9)	4.7(6)
C18	0.9561(9)	0.2419(6)	0.6209(9)	4.2(5)
C19	1.2574(9)	0.0998(6)	0.6525(9)	4.2(5)
C20	1.258(1)	0.1549(7)	0.783(1)	5.8(6)
C21	1.310(1)	0.091(1)	0.905(1)	7.4(8)
C22	1.362(1)	-0.010(1)	0.897(1)	7.5(9)
C23	1.360(1)	-0.0638(8)	0.74491)	6.6(7)
C24	1.308(1)	-0.0106(7)	0.651(1)	4.9(6)

^a $B_{eq}=(4/3)[a^2B_{11} + b^2B_{22} + c^2B_{33} + ab(\cos\gamma)B_{12} + ac(\cos\beta)B_{13} + bc(\cos\alpha)B_{23}]$

Table 3-3. Selected Atomic Coordinates and Estimated Standard Deviations (esd's) of (Me₄N)₂[Mo₂O₂As₂S₇](II).

atom	X	Y	Z	$B_{eq}^{a}, (A^2)$
Mo1	0.6397(1)	0.7862(1)	0.1285(1)	1.85(7)
Mo2	0.6021(1)	0.9237(1)	0.2174(1)	1.83(7)
As1	0.6469(1)	0.6090(1)	0.051691)	2.5(1)
As2	0.5127(1)	1.0394(1)	0.3516(1)	2.6(1)
S1	0.4868(3)	0.9961(3)	0.2268(3)	3.0(3)
S 2	0.5847(3)	0.9331(3)	0.3632(3)	2.4(2)
S 3	0.6654(3)	0.8132(3)	0.2640(3)	2.4(2)
S4	0.5425(3)	0.8728(3)	0.1040(3)	2.3(2)
S5	0.5672(3)	0.7071(3)	0.0345(3)	2.7(3)
S 6	0.6650(3)	0.6543(3)	0.1768(3)	2.6(3)
S 7	0.5830(3)	0.4969(3)	0.0728(3)	2.6(3)
O1	0.7135(7)	0.8096(7)	0.0719(7)	2.5(6)
O2	0.6652(7)	0.9920(7)	0.1887(8)	2.6(7)
N1	0.299(1)	0.045(1)	0.094(1)	2.5(8)
N2	0.594(1)	0.235(1)	0.165(1)	4(1)
C1	0.354(1)	0.112(1)	0.107(1)	3(1)
C2	0.292(1)	-0.003(1)	0.169(1)	4(1)
C3	0.229(1)	0.074(2)	0.070(2)	8(2)
C4	0.330(2)	-0.007(2)	0.028(2)	6(2)
C5	0.511(3)	0.219(3)	0.164(3)	5(1)

C5'	0.515(2)	0.231(2)	0.196(2)	1.5(9)
C6	0.611(2)	0.311(3)	0.134(3)	3(1)
C6'	0.620(3)	0.317(3)	0.196(4)	6(1)
C7	0.612(2)	0.188(3)	0.101(3)	12(1)
C8	0.633(3)	0.207(2)	0.235(3)	13(1)

^a $B_{eq}=(4/3)[a^2B_{11}+b^2B_{22}+c^2B_{33}+ab(\cos\gamma)B_{12}+ac(\cos\beta)B_{13}+bc(\cos\alpha)B_{23}]$

The compounds were examined by X-ray powder diffraction to determine phase purity and for identification. Accurate dhk1 spacings (Å) were obtained from the powder patterns recorded on a calibrated (with FeOCl as internal standard) Phillips XRG-3000 computer-controlled powder diffractometer with graphite-monochromated Cu Kα radiation operating at 35 kV and 35 mA. The data were collected at a rate of 0.12°/min. Based on the atomic coordinates from X-ray single crystal diffraction study, X-ray powder patterns for all compounds were calculated, by the software package CERIUS. Calculated and observed X-ray powder patterns that show d-spacings and intensities of strong hkl reflections are complied in Tables 3-4 to 3-5.

Table 3-4. Calculated and Observed X-ray Powder Diffraction Pattern of (Ph₄P)₂[NiAs₄S₈](I).

h	k	l	d _{calc} (Å)	d_{obs} (Å)	1/1 _{max} (obs, %)
0	1	0	12.54	12.5	100
1	0	1	10.00	9.98	11
0	0	1	9.55	9.53	35
0	1	-1	7.70	7.68	22
0	1	1	7.50	7.50	70
1	1	-1	7.11	7.10	20
1	1	1	6.33	6.32	11
1	2	0	6.26	6.25	27
1	-1	-1	5.72	5.71	11
1	-1	1	5.42	5.40	4 1
0	2	1	5.18	5.18	29
0	0	2	4.77	4 75	11
1	-2	0	4.69	4.68	22
0	1	2	4.42	4.41	65
2	2	-1			
1	0	2	4.14	4.14	12
3	2	-1	3.35		
0	3	-2	3.19	3.18	11
2	2	2	3.16	3.16	12
3	2	-2	2.953	2.951	1 4
2	3	2	2.86		

Table 3-5. Calculated and Observed X-ray Powder Diffraction Pattern of (Me₄N)₂[Mo₂O₂As₂S₇](II).

h	k	l	d _{calc} (Å)	d _{obs} (Å)	I/I _{max} (obs, %)
1	1	1	9.93	9.91	25
2	0	0	9.09	9.08	16
0	0	2	8.27	8.27	1 4
2	1	0	8.02	8.01	100
1	0	2	7.53	7.53	47
2	1	1	7.21	7.20	2 4
1	1	2	6.89	6.88	1 5
1	2	2	5.63	5.63	3 1
3	0	2	4.89	4.88	2 1
2	3	0	4.81	4.80	13
3	1	2	4.70	4.70	10
2 4	1 0	3 0	4.54	4.55	30
3 4	3 2	1 0	4.01	4.00	9
4	2	1	3.89		
3	5	1	2.919	2.917	9
2	7 1	1 7	2.324	2.323	12

3. Results and discussion

3.1 Syntheses and Description of structures

(Ph₄P)₂[NiAs₄S₈] was prepared by heating NiCl₂ with K₃AsS₃ and Ph₄PBr in H₂O at 120 °C. It is well known in metal polychalcogenide chemistry that different cations can stabilize different structure types. 19 Since, conceptually, thioarsenic anions are similar to polysulfide ligands, we did try other cations, such as tetraalkyl ammonium, in reactions with similar reactant ratios hoping that different compounds could be isolated. We noticed that in these reactions, however, the reaction mixture immediately turned into a black precipitate of NiS_x as soon as the water was added. No other product was observed after heating was completed. The same phenomena occured with the Ph₄PBr reaction, however, prolonged heating resulted the formation of dark brown plates of (Ph₄P)₂[NiAs₄S₈] as the major product along with small amount (5%) of black NiS precipitate. (Ph₄P)₂[NiAs₄S₈] does not dissolve in common organic solvents. The structure was determined by X-ray single-crystal diffraction analysis. [NiAs4Sg] n^{2n} has an unusual one-dimensional polymeric structure composed of Ni²⁺ ions and [As4S₈]⁴- units formed by corner-sharing pyramidal [AsS₃]³- units; see Figure 3-1. The $[Ni_2 A s_4 S_8]_{n^{2n}}$ chains are parallel to the crystallographic a-axis and well separated by Ph₄P⁺ cations, see Figure 3-2. The Ni²⁺ resides on an inversion center with Ni-S distance range from 2.202(2) to 2.222(2) Å. The unique feature of this compound is the [As4S8]⁴- ligand which can derive from the

condensation of four $[AsS_3]^{3-}$ units. Remarkably, the $[As_4S_8]^{4-}$ unit contains a four membered As_2S_2 ring with trans connections to the other AsS_3 units. A similar four membered ring in a cis connection, $[As_6S_{12}]^{6-}$, has recently been found in the sulfosalt PbTlAs₃S₆.²⁰ The $[As_4S_8]^{4-}$ units can also be viewed as the intramolecular condensation product of the $[As_4S_9]^{6-}$ units from $[SnAs_4S_9]^{2-}$, see scheme 1. The $[As_4S_8]^{4-}$ represents a new thioarsenate anion.

The Ni²⁺ ion is in an almost perfect square planar environment with bond angles of S3-Ni-S3 = 180.00, S3-Ni-S4 = 88.59(9) S3-Ni-S4 = 91.41(9), and S4-Ni-S4 = 180.00. The average As-S distance and the average S-As-S angles are well within the normal range found in other arsenic sulfide compounds.²¹ The average Ni-S bonding distance is normal at 2.212(2) Å. Selected bond distances and angles are contained in Tables 3-6 and 3-7. We can rationalize the formation of the $[As_4S_8]^{4-}$ unit simply by the coordination number of the metal ion. The coordination preference of the Ni centers in Ni/S compounds is square planar, as in our compound, with CN of four. A chainlike ligand connecting two Ni center together would need two available terminal sites on either end of the chain. The $[As_4S_9]^{6-}$ unit, however, has three terminal S atoms on either side of the chain, and in order to get rid of the two extra S atoms the $[As_4S_9]^{6-}$ anion

Table 3-6. Selected Distances (Å) in (Ph₄P)₂[Ni₂As₄S₈] with Standard Deviations in Parentheses.^a

Ni - S3	2.222(2)	Ni - S4	2.202(2)
As1 - S2	2.303(3)	As1 - S3	2.208(3)
As1 - S4	2.218(2)	As2 - S1	2.314(3)
As2 - S1	2.250(2)	As2 - S2	2.250(2)

Table 3-7. Selected Angles (Deg) in (Ph₄P)₂[Ni₂As₄S₈] with Standard Deviations in Parentheses.^a

S3 - Ni - S3	180.00	S3 - Ni - S4	88.59(9)
S3 - Ni - S4	91.41(9)	S4 - Ni - S4	180.00
S2 - As1 - S3	104.8(1)	S2 - As1 - S4	99.81(9)
S3 - As1 - S4	88.51(9)	S1 - As2 - S1	89.53(9)
S1 - As2 - S2	95.48(9)	S1 - As2 - S2	102.5(1)
As2 - S1 - As2	90.47(9)	As1 - S2 - As2	93.99(9)
As1 - S3 - Ni	90.69(9)	As1 - S4 - Ni	90.97(9)

^aThe estimated standard deviation in the mean bond lengths and the mean bond angles are calculated by the equation $\sigma l = \{\Sigma_n(l_n - 1)^2/n(n-1)\}^{1/2}$, where l_n is the length (or angle) of the nth bond, l the mean length (or angle), and n the number of bonds.

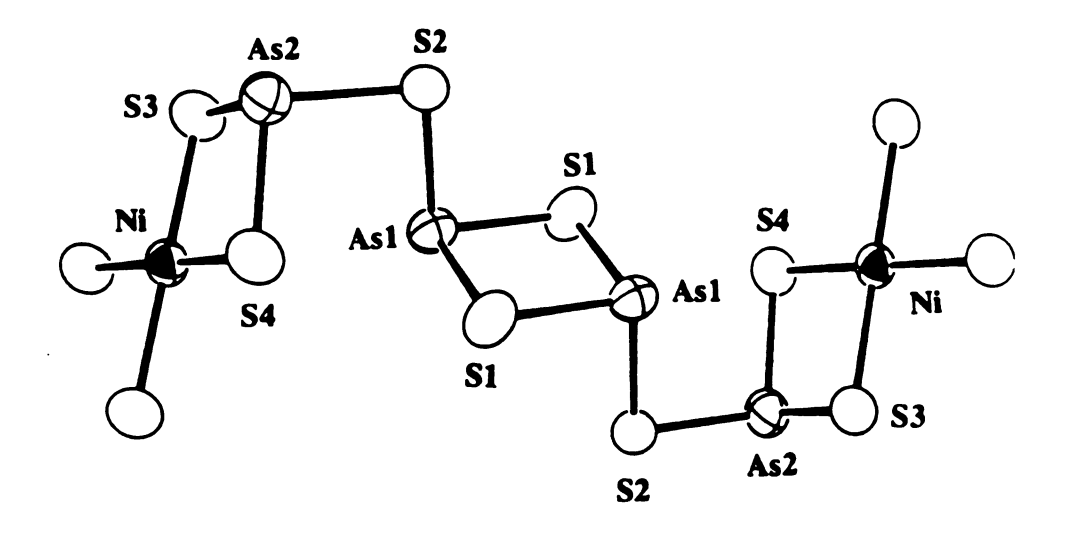


Figure 3-1. Structure and labeling scheme of one $[NiAs_4S_8]_n^{2n}$ chain.

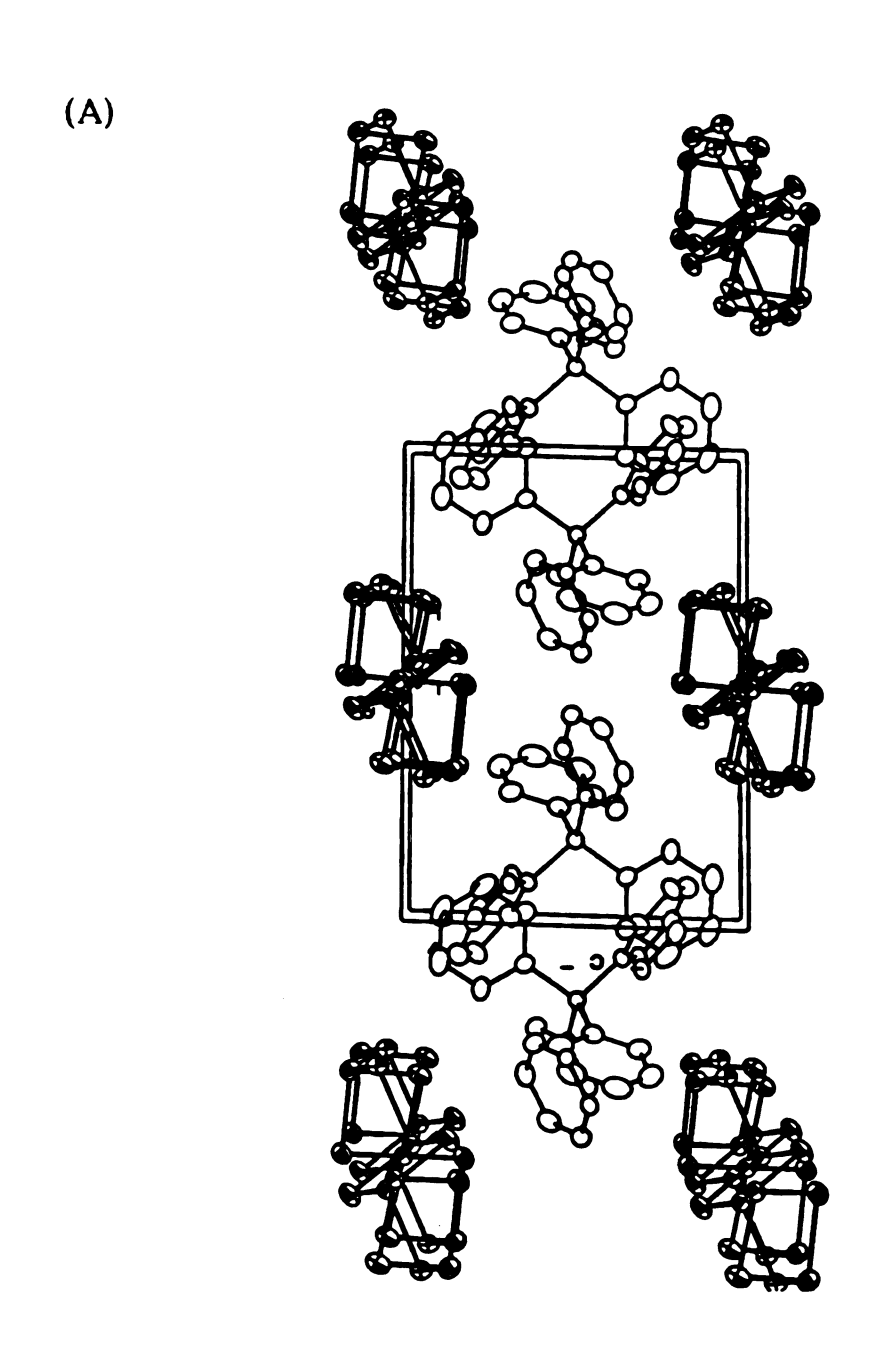
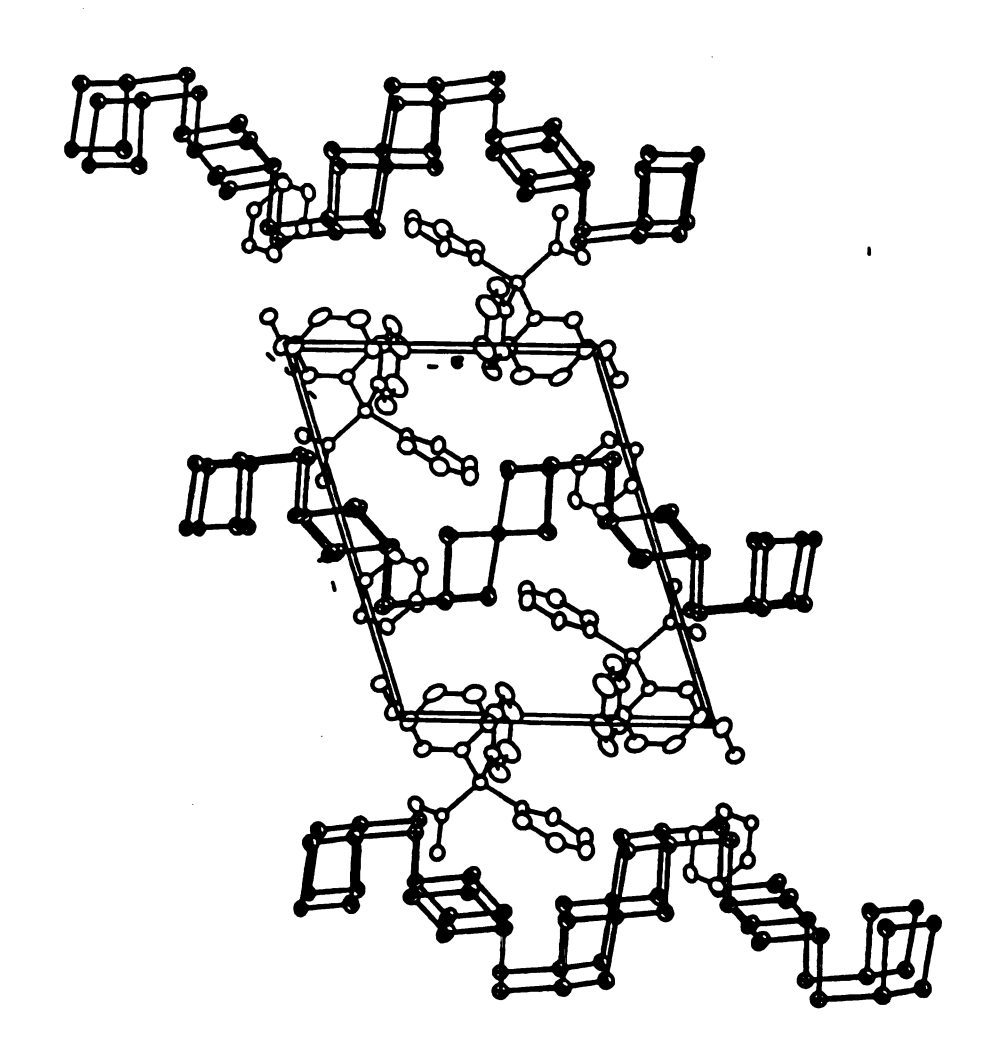


Figure 3-2 Packing diagram of $(Ph_4P)_2[NiAs_4S_8]$. (A) view down the a-axis. (B) view down the c-axis

(B)



undergoes intramolecular condensation. One can argue that the $[As_4S_8]^{4-}$ and not the $[As_2S_5]^{4-}$ unit is of the more appropriate length to accommodate the required number of Ph₄P⁺ cations. Large cations need large empty space, generated by longer thioarsenic polyanions, in order to form a stable crystal lattice. The empty space generated by the $[As_2S_5]^{4-}$ units may be too small for Ph₄P⁺ cations.

The (Me₄N)₂[Mo₂O₂As₂S₇] was prepared by heating a mixture of MoO₃/K₃A₅S₃/2Me₄NCl in sealed Pyrex tube with H₂O for one week. Other cations were also tried without much success. The only other cation that afforded crystalline products was Et4N+. The crystal quality of the Et4N+ salt, however, was poor and prohibited further characterization. The structure of (Me₄N)₂[Mo₂O₂As₂S₇], determined by X-ray single-crystal diffraction analysis, revealed that it also contains a one-dimensional chain structure consisting of distorted square pyramidal Mo⁵⁺ ions and linear [As₂S₅]⁴⁻ units formed by corner sharing of the [AsS₃]³- units, see Figure 3-3 and 3-4. The unique feature of this compound is that we still observe the well known Mo₂O₂S₂ fragment which has been seen many times in Mo-S chemistry, for examples, in $[Mo_2O_2S_2(S_2)_2]^{2-2}$, $[Mo_2O_2S_2(S_2)_2]^{2-2}$ and [Mo₂O₂S₂(S₃O₂)]^{2-.24} In these cases, however, the compounds are usually molecular species. With the introduction of the trivalent As atom, we increase the conductivity of the ligands thus forming a polymeric compound. The Mo-Mo distance of 2.848(2)Å is similar to those found in the molecular compounds. There are two types of Mo-S bonds. The average distance between the Mo atoms and bridging sulfur atoms, at 2.335(5)Å, is significantly shorter than the

average distance, at 2.435(5)Å, between the Mo atoms and the terminal S atoms in [As2S5]4- units. Similar results were observed in compound [Mo₂O₂A₅4S₁₄]². The average As-S distance and S-As-S angles are well within the normal range found in other metal thioarsenate compounds like [InAs₃S₇]²- and [SnAs₄S₉]²-. Selected bond distances and bond angles are contained in Tables 3-8 and 3-9. It is also noteworthy that in an earlier paper, without single crystal structure data, Rauchfuss proposed a structure for [Mo₄O₄A₅₄S₁₄]⁴where two [As₂S₅]⁴- units connect two Mo₂O₂S₂ units.⁸ The [As₂S₅]⁴been found earlier in the sulfosalts. unit has PbTlCuAs₂S₅(Wallisite),²⁵ PbTlAgAs₂S₅(Hatchite),²⁶ and Tl₂MnAs₂S₅.²⁷

It is interesting to point out that although the size difference between the cations seen in these two compounds, $(Ph4P)_2[Ni_2As_4S_8]$, and $(Me4N)_2[Mo_2O_2As_2S_7]$, is significant, the dimensionality of the two structures remains the same, unlike those found previously, $(Ph4P)_2[InAs_3S_7]$, $(Ph4P)_2[SnAs_4S_9]$, and $(Me4N)_2Rb[BiAs_6S_{12}]$, where the large cation, Ph_4P^+ , stabilized compounds with low dimensionality while the small cation, Me_4N^+ , stabilized a higher dimensional compound. A correlation, perhaps, can be made between these observations and the length of the thioarsenate ligands. We learned from metal polychalcogenide chemistry that large cations tend to stabilize large clusters and vise versa. In the present case, longer thioarsenate ligands, $[As_3S_7]^{5-}$, $[As_4S_8]^{4-}$, and $[As_4S_9]^{6-}$, create larger empty space that can only be filled with large cations, Ph_4P^+ . Changing from a large cation, Ph_4P^+ , to a small cation,

Me₄N+, the structure has two obvious choices. One is to increase the dimensionality of the compound, which we see in (Me₄N)₂Rb[BiAs₆S₁₂]; the other is to decrease the empty space by using a smaller ligand like [As₂S₅]⁴- in (Me₄N)₂[Mo₂O₂As₂S₇] and remain one-dimensional. A similar argument can be used to explain the structure of (Ph₄P)₂[Mo₂O₂As₄S₁₄] which retains the [As₂S₅]⁴- ligand and thus chooses to decrease its dimension to zero (i.e. cluster).

Table 3-8. Selected Distances (Å) in (Me₄N)₂[Mo₂O₂As₂S₇] with Standard Deviations in Parentheses.^a

Mo1 - Mo2	2.848(2)	Mo1 - S3	2.337(5)
Mo1 - S4	2.335(5)	Mo1 - S5	2.442(6)
Mo1 - S6	2.425(5)	Mo1 - O1	1.68(1)
Mo2 - S1	2.435(6)	Mo2 - S2	2.440(5)
Mo2 - S3	2.335(5)	Mo2 - \$4	2.334(5)
Mo2 - O2	1.70(1)	As1 - S5	2.230(6)
As1 - S6	2.236(6)	As1 - S7	2.260(6)
As2 - S1	2.245(6)	As2 - S2	2.240(5)
As2 - S7	2.262(6)		

^aThe estimated standard deviations in the mean bond lengths and the mean bond angles are calculated by the equation $\sigma l = \{\Sigma_n(l_n - 1)^2/n(n-1)\}^{1/2}$, where l_n is the length (or angle) of the nth bond, l the mean length (or angle), and n the number of bonds.

112
Table 3-9. Selected Angles (Deg) in (Me₄N)₂[Mo₂O₂As₂S₇] with
Standard Deviations in Parentheses.^a

Mo2 - Mo1 - S3	52.4(1)	Mo2 - Mo1 - S4	52.4(1)
Mo2 - Mo1 - S5	130.7(1)	Mo2 - Mo1 - S6	129.4(1)
Mo2 - Mo1 - O1	106.5(4)	S3 - Mo1 - S4	101.1(2)
S3 - Mo1 - S5	145.9(2)	S3 - Mo1 - S6	80.1(2)
S3 - Mo1 - O1	109.2(4)	S4 - Mo1 - S5	80.1(2)
S4 - Mo1 - S6	141.6(2)	S4 - Mo1 - O1	110.9(4)
S5 - Mo1 - S6	78.7(2)	S5 - Mo1 - O1	101.9(5)
S6 - Mo1 - O1	104.6(4)	Mo1 - Mo2 - S1	130.9(2)
Mo1 - Mo2 - S2	126.6(1)	Mo1 - Mo2 - S3	52.5(1)
Mo1 - Mo2 - S4	52.4(1)	Mo1 - Mo2 - O2	104.8(4)
S1 - Mo2 - S2	78.0(2)	S1 - Mo2 - S3	144.1(2)
S1 - Mo2 - S4	80.8(2)	S1 - Mo2 - O2	104.7(5)
S2 - Mo2 - S3	77.9(2)	S2 - Mo2 - S4	139.5(2)
S2 - Mo2 - O2	108.6(4)	S3 - Mo2 - S4	101.3(2)
S3 - Mo2 - O2	108.0(5)	S4 - Mo2 - O2	110.0(5)
S5 - As1 - S6	87.4(2)	S5 - As1 - S7	108.5(2)
S6 - As1 - S7	102.9(2)	S1 - As2 - S2	86.3(2)
S1 - As2- S7	104.1(2)	S2 - As2 - S7	98.3(2)
Mo2 - S1 - As2	92.5(5)	Mo2 - S2 - As2	92.5(2)
Mo1 - S3 - Mo2	75.1(2)	Mo1 - S4 - Mo2	75.2(2)
Mo1 - S5 - As1	88.9(2)	Mo1 - S6 - As1	89.2(2)

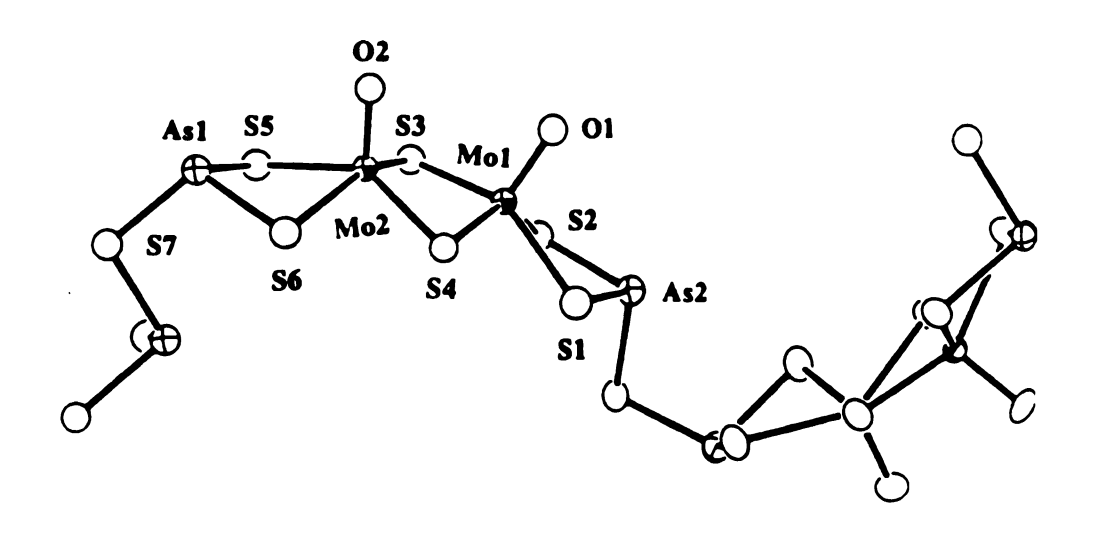


Figure 3-3. Structure and labeling scheme of one $[Mo_2O_2As_2S_7]_n^{2n}$ -Chain.

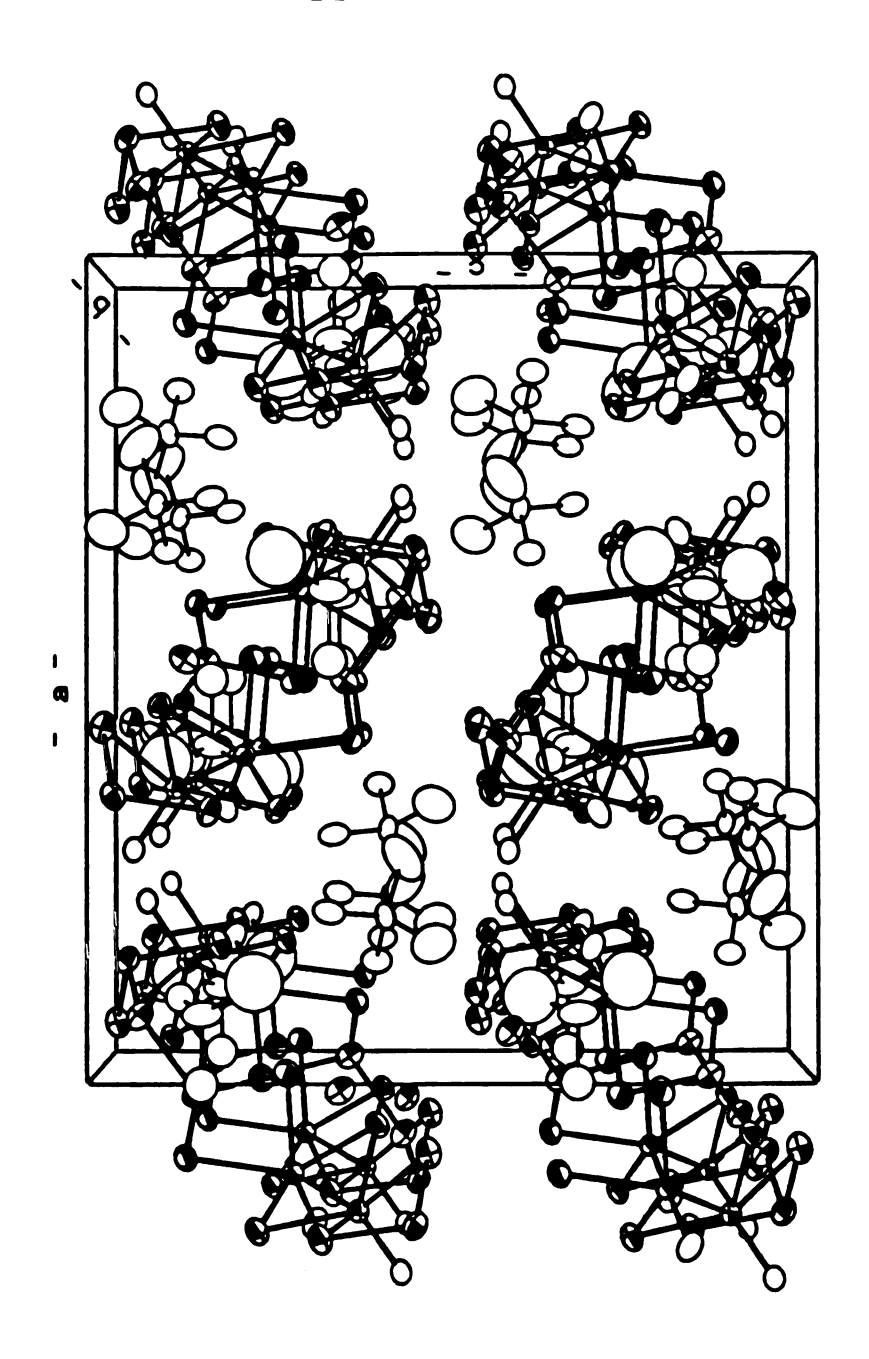


Figure 3-4. Packing diagram of (Me₄N)₂[Mo₂O₂As₂S₇].

3.2 Physicochemical studies

In the far-IR region all complexes reported here exhibit spectral absorptions due to As-S and M-S stretching vibrations as shown in Figure 3-5. Observed absorption frequencies of all the complexes are given in Table 3.10.

Table 3.10. Frequencies (cm⁻¹) of Infrared Spectral Absorptions of (Ph₄P)₂[NiAs₄S₈](I), and (Me₄N)₂[Mo₂O₂As₂S₇](II).

Compounds	Infrared	Raman
(Ph ₄ P) ₂ [NiAs ₄ S ₈]	465(w), 406(m)	395(s), 386(m), 352(m)
	386(m), 364(m)	314(s), 301(m), 253(m)
	339(w), 320(m)	178(m)
	288(s), 212(w)	
(Me ₄ N) ₂ [Mo ₂ O ₂ As ₂ S ₇]	930(s), 460(s)	930(s), 421(m), 402(m)
	407(s, sh), 361(s)	362(s), 274(m), 222(m)
	319(s, br), 238(m)	190(m), 170(w)
	219(m), 206(w)	

^{*} s: strong, m; medium, w: weak, sh: shoulder.

In the Far-IR spectra of (Ph₄P)₂[NiAs₄S₈], and (Ph₄P)₂[Mo₂O₂As₂S₇], the peaks in the region of 200-400 cm⁻¹ could be attributed to As-S vibration modes. Similar assignments have been made in the far-IR spectra of other known thioarsenic complexes.²⁹ The additional peak in the IR spectra, 460 cm⁻¹, for (Me₄N)₂[Mo₂O₂As₂S₇], might be assigned to a Mo-S stretching vibration. For comparison, 455 cm⁻¹

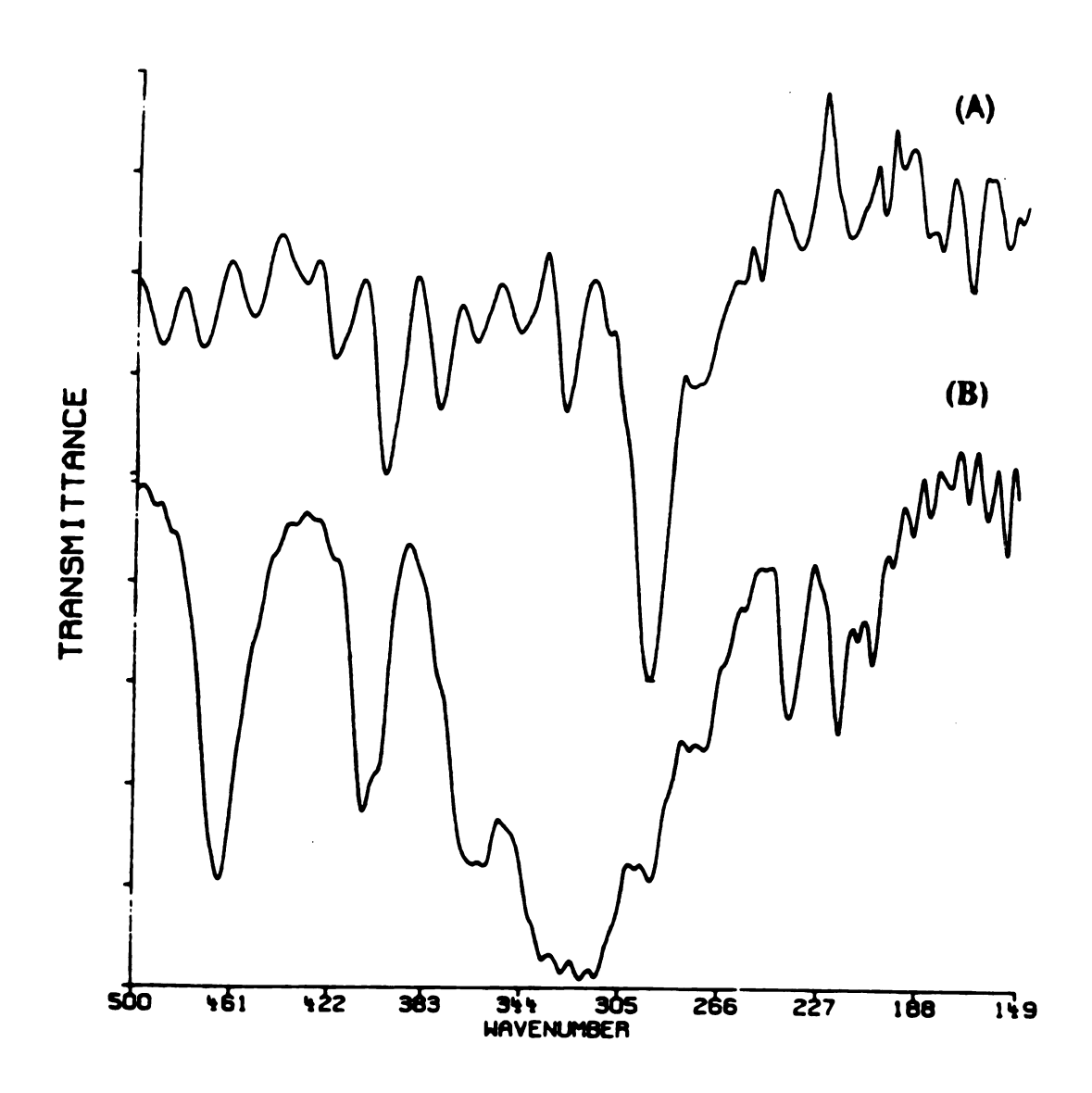


Figure 3-5. Far-IR spectra (CsI pellets) of (A) $(Ph_4P)_2[NiAs_4S_8]$, and (B) $(Me_4N)_2[Mo_2O_2As_2S_7]$.

was assigned as an Mo-S_b (bridging S atoms) vibrational frequency in [Mo₂O₂As₄S₁₄]²-,⁸ [Mo₂S₆]²-, [Mo₂S₇]²-, and [Mo₂S₉]²-.³⁰ We also observed the Mo=O stretching mode in (Me₄N)₂[Mo₂O₂As₂S₇] at 938 cm⁻¹. The major difficulty in assigning the observed IR spectra of these compounds arises from the fact that As-S and M-S stretching frequencies fall in the same low frequency region of 150-450 cm⁻¹. FT-Raman spectra of (I) and (II) were also collected (see Table 3-10). There are numerous peaks in the range between 150 to 400 cm⁻¹, just as in the far-IR spectra. Again, specific assignments were difficult since these peaks can be assigned to either the As-S or M-S vibration modes.

Thermal Gravimetric Analysis (TGA) results for all compounds are summarized in Table 3-11 and shown in Figure 3-6.

Table 3.9. TGA Data for $(Ph_4P)_2[NiAs_4S_8](I)$, and $(Me_4N)_2[Mo_2O_2As_2S_7](II)$.

Temp. range (°C)	Weight loss (%)
218 - 485	79.5
250-335	25.9
450-750	30.1
	218 - 485 250-335

(Ph₄P)₂[NiAs₄S₈] shows a one step weight loss of 79.5 % in the temperature range of 218-485 °C, probably as Ph₃PS, other organic species and various As_xS_y. An X-ray powder diffraction analysis of

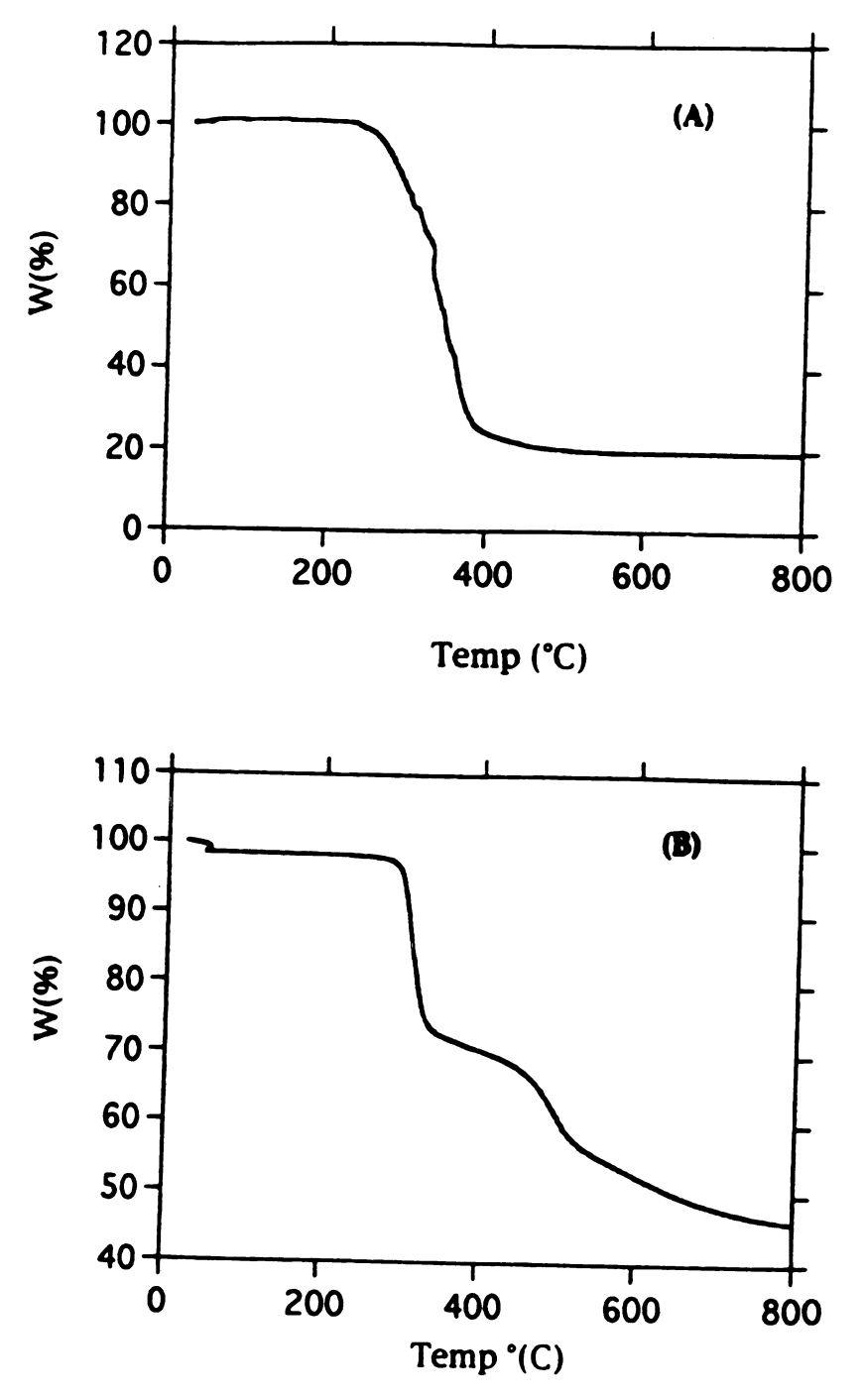


Figure 3-6. TGA diagrams of (A) $(Ph_4P)_2[NiAs_4S_8]$, and (B) $(Me_4N)_2[Mo_2O_2As_2S_5]$.

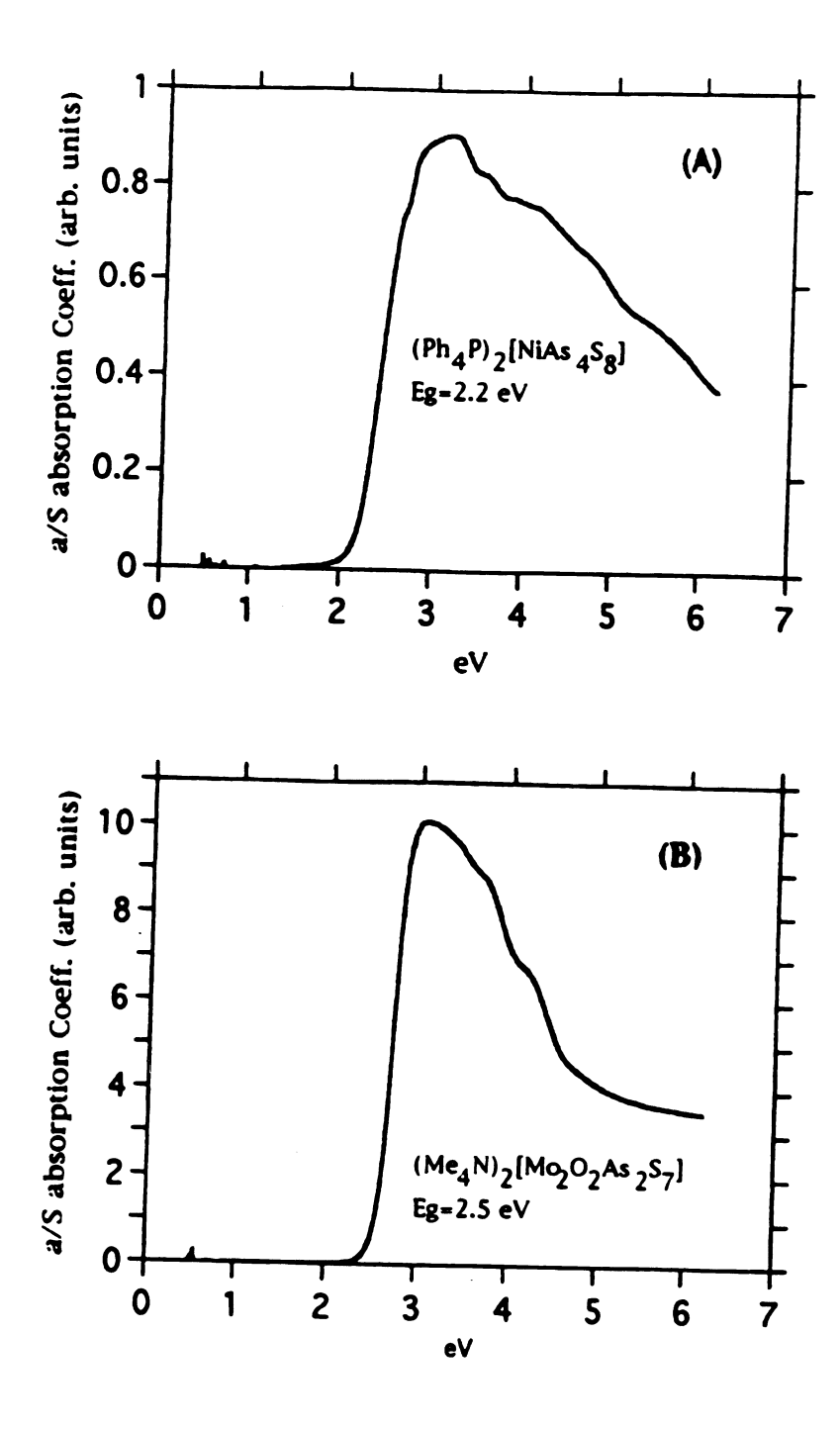


Figure 3-7. Optical absorption spectra of (A) $(Ph_4P)_2[NiAs_4S_8]$, and (B) $(Me_4N)_2[Mo_2O_2As_2S_5]$.

that can not be identified. (Me₄N)₂[Mo₂O₂As₂S₇] shows a two step weight loss in the temperature range of 250-335 and 450-750 °C. The first step is probably due to loss of Me₃N and Me₂S. In the (Me₄N)₂[Mo₂O₂As₂S₇] case, weight loss continues above 800 °C. The final product was proved to be MoS₂ by X-ray powder diffraction. The thermal behavior of both compounds was further investigated by differential thermal analysis (DTA). Neither shows any melting before the decomposition temperature.

The optical properties of (Ph₄P)₂[NiAs₄S₈] and (Me₄N)₂[Mo₂O₂As₂S₇] were assessed by studying the UV-visible-near IR spectra of the material. The spectra confirm that they are wide band-gap semiconductors. The optical absorption spectrum of (Ph₄P)₂[NiAs₄S₈], shown in Figure 3-7(A), exhibits an intense, steep absorption edge, revealing an optical bandgap of 2.2 eV. The spectrum of (Me₄N)₂[Mo₂O₂As₂S₇] also shows a similar absorption edge with a corresponding bandgap at 2.5 eV, see Figure 3-7(B). The absorption is probably due to a charge-transfer transition from a primarily sulfur-based valence band to a mainly metal-based conduction band.

In conclusion, hydrothermal synthesis methods readily promote synthesis and crystallization of new compounds which in many cases can not be achieved by classical solution technique. Using AsS3³ as starting material has given access to new and exciting metal/arsenic/sulfide chemistry and promises to do so for other unexplored systems as well. The key to this chemistry is the

condensation equilibria which exist in the reaction medium as well as the coordination preferences of the metal ions. Further investigations are needed to explore the existence of other novel $[As_xS_y]^{n-}$ anions and the possibility of using them as building blocks toward new solid state materials.

REFERENCES

- (a) Liao, J.-H.; Kanatzidis, M. G. Inorg. Chem. 1992, 31, 431-439.
 (b) Liao, L.-H.; Kanatzidis, M. G. J. Am. Chem. Soc. 1990, 112, 7400-7402.
 (c) Huang, S.-P.; Kanatzidis, M. G. J. Am. Chem. Soc. 1992, 114, 5477-5478.
- (a) Sheldrick, W. S. Z. Anorg. Allg. Chem. 1988, 562, 23-30. (b)
 Shedrick, W. S.; Hanser, H.-J. Z. Anorg. Allg. Chem. 1988, 557,
 98-104. (c) Shedrick, W. S.; Hanser, H.-J. Z. Anorg. Allg. Chem.
 1988, 557, 105-110.
- a) Wood, P. T.; Pennington, W. T.; Kolis, J. W. Inorg. Chem. 1993,
 32, 129-130. b) Wood, P. T.; Pennington, W. T.; Kolis, J. W. J.
 Chem. Soc. Chem. Commun. 1993, 25, 235-236.
- 4. Chou, J.-H.; Kanatzidis, M. G. Inorg. Chem. 1994, 33, 1001-1002.
- Jerome, J. E.; Wood, P. T.; Pennington, W. T. Kolis, J. W. Inorg.
 Chem. 1994, 33, 1733-1734.
- 6. Liebau, F. Structural Chemistry of Silicates, Springer, New York 1985.
- 7. Cotton, F. A.; Wilkinson, G. Advanced Inorganic Chemistry John wiley & Sons, New York 1988, 421-430.
- 8. Zank, G. A.; Rauchfuss, T. B.; Wilson, S. R. J. Am. Chem. Soc. 1984, 106, 7621-7623.

- 9. (a) Huang, S.-P.; Kanatzidis, M. G. J. Am. Chem. Soc. 1989, 111, 760-761.
- 10. Huang, S.-P.; Kanatzidis, M. G. Inorg. Chem. 1991, 30, 1455-1466.
- 11. Dhingra, S.; Kanatzidis, M. G. Science, 1992, 258, 1769-1772.
- 12. Kim, K.-W.; Kanatzidis, M. G. J. Am. Chem. Soc. 1993, 115, 5871-5872.
- (a) Parise, J. B. Science, 1991, 251, 293-294. (b) Parise, J. B. J. Chem. Soc. Chem. Commun. 1990, 22, 1553-1554. (c) Stein, A.;
 Keller, S. W.; Mallouk, T. C. Science 1993, 259, 1558-1564.
- (a) Soghomonian, V.; Chen, Q.; Haushalter R. C.; Zubieta, J.;
 O'Connor, C. J. Science, 1993, 259, 1596-1599. (b)
 Soghomonian, V.; Chen, Q.; Haushalter R. C.; Zubieta, J. Inorg.
 Chem. 1994, 33, 1700-1704. (c) Warren, C. J.; Dhingra, S. S.; Ho,
 D. M.; Haushalter R. C.; Bocarsly, A. B. Inorg. Chem. 1994, 33, 2704-2711. (d) Khan. M. I.; Lee, Y.-S.; O'Connor, C. J.; Haushalter R. C.; Zubieta, J. Inorg. Chem. 1994, 33, 3855-3856.
- Sheldrick, G. M. In Crystallographic Computing 3; Sheldrick, G.
 M.; Kruger, C.; Goddard, R., Eds.; Oxford University Press: Oxford,
 U.K., 1985; pp 175-189.
- 16. TEXSAN: Single Crystal Structure Analysis Package, Version5.0, Molecular Structure Corp., Woodland, TX.
- 17. Walker, N.; Stuart, D. Acta Crystallogr. 1983, 39A, 158-166.

- 18. CERIUS: Single Crystal Structure Analysis Software, Version 5.0, Molecular Simulations Inc. Cambridge, UK.
- (a) Huang, S.-P.; Kanatzidis, M. G. Inorg. Chem. 1991, 30, 1455-1466.
 (b) Kim, K.-W.; Kanatzidis. M. G. J. Am. Chem. Soc. 1992, 114, 4878-4883.
- 20. Bali'c-Zuni'c, T.; Engel, P. Z. Kristallogr. 1983, 165, 261-269.
- (a) Sommer, H.; Hoppe, R. Z. Anorg. Allg. Chem. 1977, 430, 199.
 (b) Sheldrick, W. S.; Kaub, J. Z. Naturforsch. 1985, 40b, 571-573.
 (c) Jerome, J. E.; Wood, P. T.; Pennington, W. T.; Kolis, J. W. Inorg. Chem. 1994, 33, 1733-1734.
- 22. Clegg, W.; Mohan, N.; Müller, A.; Neumann, A.; Ritter, W.; Sheldrick, G. M. *Inorg. Chem.* 1980, 19, 2066-2074.
- 23. Müller, A.; Römer, M.; Römer, C.; Reinsch-Vogell, U.; Bögge, H.; Schimanski, U. Monatsh. Chem. 1985, 116, 711-719.
- 24. Müller, A.; Reinsch-Vogell, U.; Krickemeyer, E.; Bögge, H. Angew. Chem. Int. Ed. Engl. 1982, 21, 796-782.
- 25. Takeuchi, Y.; Ohmasa, M. Z. Kristallogr. 1968, 127, 349-365.
- 26. Marumo, F.; Nowacki, W. Z. Kristallogr. 1967, 125, 249-265.
- Gostojic, M.; Edenharter, A.; Nowacki, W.; Engel, P. Z. Kristallogr.
 1982, 158, 43-51.

- (a) Huang, S.-P.; Kanatzidis, M. G. Inorg. Chem. 1991, 30, 1455-1466.
 (b) Kim, K.-W.; Kanatzidis. M. G. J. Am. Chem. Soc. 1992, 114, 4878-4883.
- 29. Peresh, E. Y.; Golovei, M. I.; Berul, S. I. Izv. Akad. Nauk SSR Neorg. Mater. 1971, 7, 27-30.
- 30. Hadjikyriacou, A. I.; Coucouvanis, D. *Inorg. Chem.* 1987, 26, 2400-2408.

CHAPTER 4

HYDRO(SOLVO)THERMAL SYNTHESIS OF DISCRETE MOLECULAR M/As_xS_y ($M = Pt^{4+}$, Pt^{2+} Pd^{2+}) ANIONS. SYNTHESIS AND STRUCTURAL CHARACTERIZATION OF $(Ph_4P)_2[Pt(As_3S_5)_2](I)$, $(Ph_4P)_2K[Pt_3(AsS_4)_3](II)$, AND $(Ph_4P)_2K[Pd_3(AsS_4)_3](III)$.

ABSTRACT

 $(Ph_4P)_2[Pt(As_3S_5)_2](I)$ and $(Ph_4P)_2K[Pt_3(AsS_4)_3]\cdot 1.5H_2O(II)$ were svnthesized hydrothermally from a mixture PtCl₂/3K₃A₅S₃/4Ph₄PBr and PtCl₂/2K₃A₅S₃/4Ph₄PBr, respectively, in 0.3 mL of water heated at 110 °C for one day. Both crystallize in the triclinic space group P-1 (No. 2) with unit cell dimensions a =13.104(3)Å, b = 20.519(4)Å, c = 11.559(2)Å, $\alpha = 105.72(2)$ °, $\beta =$ $108.09(2)^{\circ}$, $\gamma = 75.11(2)^{\circ}$, V = 2793(2) Å³, Z = 2 for $(Ph_4P)_2[Pt(As_3S_5)_2]$, and a = 14.655(2)Å, b = 17.852(3)Å, c =14.253(2)Å, $\alpha = 109.65(2)$ °, $\beta = 118.89(2)$ °, $\gamma = 72.08(3)$ °, V = 118.89(2)°, $\gamma = 118.89(2)$ °, $\gamma = 118.89(2)$ ° 3027(1)Å3, Z = 2 for $(Ph_4P)_2K[Pt_3(AsS_4)_3]\cdot 1.5H_2O$. (Ph₄P)₂K[Pd₃(AsS₄)₃]·3MeOH(III) was synthesized methanothermally by heating a mixture of PdCl₂/3K₃A₅S₃/4Ph₄PBr in 0.4 mL of MeOH at 110 °C for one day. (Ph₄P)₂K[Pd₃(AsS₄)₃]·3MeOH also crystallized in the triclinic space group P-1 (No. 2) with unit cell dimensions a =14.171(3)Å, b = 18.198(3)Å, c = 14.154(3)Å, $\alpha = 106.62(2)^{\circ}$, $\beta =$ 114.66(2)°, $\gamma = 73.88(2)$ °, V = 3125(2) Å³, Z = 2. (Ph₄P)₂[Pt(As₃S₅)₂] is a molecular cage compound consisting of [Pt(As₃S₅)₂]²- anions. The Pt atom has a 4+ formal oxidation state and is coordinated to four S atoms and two As atoms in octahedral fashion. The two As atoms are disposed in a cis-fashion around the metal center and the Pt-As bond length is 2.454(2)Å. The $[Pt_3(AsS_4)_3]^{3-}$ and $[Pd_3(AsS_4)_3]^{3-}$ anions are isostructural with essentially square planar Pt²⁺ and Pd²⁺ centers. The [AsS₄]³- ligand contains As³⁺ and represents a new isomer of the known tetrahedral As⁵⁺ species.

1. Introduction

Pt⁴⁺ complexes are both thermodynamically stable and kinetically inert. Those with halides, pseudo-halides and N-donor ligands are especially numerous. While oxygen-donor ligands such as OH- and acac (acac = acetylacetonate) also coordinate to Pt⁴⁺, sulfide and selenide, and especially P- and As- donor ligands, tend to reduce it to Pt^{+2} . Notable exceptions are $[Pt(S_5)_3]^{2-3}$ $[Pt_4S_4(S_3)_6]^{4-4}$ and $[Pt(Se_4)_3]^{2-.5}$ Pd⁴⁺ complexes, on the other hand, are very unstable and would rather stay at 2+ oxidation state with respect to polychalcogenide ligands. Recently, it has been shown that hydrothermal conditions offer significant advantages in new cluster and solid state compound synthesis.6.7.8 We have exploited the high reactivity and lability of the AsS₃³- pyramidal unit in conjunction main group elements (see chapter 2) and some transition metals (see chapter 3) and reported on the hydrothermal synthesis of several unusual one- and two-dimensional solids containing organic cations, including (Ph₄P)₂[InAs₃S₇],⁹ (Ph₄P)₂[SnAs₄S₉], $(Me_4N)_2Rb[BiAs_6S_{12}]_{,9}$ $(Ph_4P)_2[NiAs_4S_8]_{,1}$ and $(Me_4N)_2[Mo_2O_2As_2S_7]_{,2}$ Our work with AsS₃³- solutions thus far suggests the existence of very complex condensation equilibria in solution where a variety of $[As_xS_y]^{z}$ species might be present. The type and identity of [As_xSe_y]^{z-} fragment found in the isolated solids depends on the particular counterion present and on the metal size and coordination preference. Thus far, we have identified several types of $[As_xS_y]^{z-1}$ ligands including $[As_3S_6]^{3}$ -, $[As_2S_5]^{4}$ -, $[As_3S_7]^{5}$ -, $[As_4S_8]^{4}$ -, and [As4S916-. The chemistry of Pt2+ and Pt4+ polysulfides goes back to

the beginning of this century and even to this date it has proven remarkably complex, mostly due to the lability of S_x^{2-} species and redox processes in solution. The great lability of AsS_3^{3-} and its higher $[As_xS_y]^{2-}$ homologs, and the conceptual relationship of AsS_3^{3-} to S_x^{2-} (e.g. the former derives from S_x^{2-} via a S atom substitution by an isoelectronic As^- ion) raises interesting prospects for similar chemistry in the Pt/AsS_3^{3-} system. In fact, we observed not only the familiar Pt^{2+} vs. Pt^{4+} redox couple, but also an unusual kind of Pt-As bonding and several new thioarsenate ligands which emerge as new features in this chemistry. We describe here three unique clusters, $[Pt(As_3S_5)_2]^{2-}(I)$, $[Pt_3(AsS_4)_3]^{3-}(II)$, $[Pd_3(AsS_4)_3]^{3-}(III)$, formed under hydro(solvo)thermal conditions.

2. Experimental Section

2.1 Reagents

Chemicals. Chemicals, other than solvents, were used as obtained. $PtCl_2$, 98% purity, $PdCl_2$, 99% purity, tetraphenylphosphonium bromide (Ph_4PBr), 98% purity, Aldrich Chemical Company, Inc., Milwaukee, WI. A_3AsS_3 (A = K, Rb, Cs) were synthesized by using stoichiometric amounts of alkali metal, arsenic sulfide (As_2S_3), and sulfur in liquid ammonia. The reaction gives a yellow brown powder upon evaporation of ammonia.

2.2 Syntheses

All syntheses were carried out under a dry nitrogen atmosphere in a Vacuum Atmosphere Dri-Lab glovebox except were specifically mentioned.

(Ph₄P)₂[Pt(As₃S₅)₂](I): A Pyrex tube (~4 mL) containing a mixture of PtCl₂ (65mg, 0.25mmol), K₃AsS₃ (144mg, 0.75mmol), Ph₄PBr (419 mg, 1.0mmol) and 0.3 mL of water was sealed under vacuum and kept at 110 °C for one day. The large red platelike crystals that formed were isolated in methanol and washed with ether. (Yield=74.3 % based on Pt). Semiquantitative elemental analysis of the red crystals obtained by using a SEM/EDS technique gave the P:Pt:As:S ratio at 1.8:1.0:5.0:10.0.

(Ph₄P)₂K[Pt₃(AsS₄)₃]·1.5 H₂O(II): A mixture of PtCl₂ (65mg, 0.25mmol), K₃AsS₃ (96mg, 0.5mmol), Ph₄PBr (419 mg, 1.0mmol) and 0.3 mL of water was sealed under vacuum and kept at 110 °C for one day. A mixture of red plate-like crystals of (Ph₄P)₂[Pt(As₃S₅)₂] and yellow plate-like crystals of (Ph₄P)₂K[Pt₃(AsS₄)₃]·1.5 H₂O were isolated, by washing with methanol and ether, in 1:4 ratio with (Ph₄P)₂K[Pt₃(AsS₄)₃]·1.5 H₂O as the major product. (Yield = 85.4 %, based on Pt). Semiquantitative elemental analysis of the yellow crystals obtained by using a SEM/EDS technique gave the P:K:Pt:As:S ratio as 1.7:1:3:2:11.8.

(PH₄P)₂K[Pd₃(AsS₄)₃]·3MeOH(III): A Pyrex tube (~4 mL) containing a mixture of PdCl₂ (45mg, 0.25mmol), K₃AsS₃ (144mg, 0.75mmol), Ph₄PBr (419 mg, 1.0mmol) and 0.3 mL of methanol was

sealed under vacuum and kept at 110 °C for one day. The large red rod-like crystals that formed were isolated in methanol and washed with ether. (Yield=74.3 % based on Pd). Semiquantitaitive elemental analysis of the red crystals obtained by using a SEM/EDS technique gave the P:K:Pd:As:S ratio at 1.8:1.0:2.5:3.2:11.0.

2.3. Physical Measurements

The instruments and experimental setups for Infrared measurements, thermal analysis and quantitative microprobe analysis on SEM/EDS are the same as those described in Chapter 2.

2.4 X-ray crystallography

(Ph₄P)₂[Pt(As₃S₅)₂]: A well shaped dark red platelike crystal with dimensions of 0.55 x 0.55 x 0.35 mm was mounted on a glass fiber. Single-crystal X-ray diffraction data were collected at -100 °C on a Rigaku AFC6 diffractometer. A total of 7879 independent reflections was collected. All nonhydrogen and non-carbon atoms were refined anisotropically. All hydrogen atom positions were calculated and fixed without further refinement.

(Ph₄P)₂K[Pt₃(AsS₄)₃]·1.5 H₂O: The yellow platelike crystal used for the study had approximate dimensions of 0.45 x 0.53 x 0.35 mm. The crystal was mounted on a glass fiber. Single-crystal X-ray diffraction data were collected at -100 °C on a Rigaku AFC6 diffractometer. A total of 8545 reflections were collected. All

nonhydrogen and non-carbon atoms were refined anisotropically.

All hydrogen atom positions were calculated and fixed without further refinement.

(Ph₄P)₂K[Pd₃(AsS₄)₃]·3CH₃OH: The red rod-like crystal with dimensions of 0.55 x 0.65 x 0.75 mm was mounted on a glass fiber. Single-crystal X-ray diffraction data were collected at -100 °C on a Rigaku AFC6 diffractometer. A total of 8763 independent reflections was collected. All nonhydrogen and non-carbon atoms were refined anisotropically. All hydrogen atom positions were calculated and fixed without further refinement.

The crystals did not show any significant intensity decay as determined by monitoring 3 check reflections every 150 reflections throughout data collection. The structures were solved by direct methods (SHELXS-86)¹¹ and refined with the TEXSAN¹² software package. An empirical absorption correction (DIFABS¹³) was applied to the isotropically refined data. All non-hydrogen atoms except nitrogen and carbon were refined anisotropically. All calculations were performed on a VAXstation 3100 Model 76 computer.

Table 4.1 summarizes the crystallographic data and details of the structure solution and refinement. The final atomic coordinates with their estimated standard deviations (esd's) are given in Tables 4.2 - 4.4.

Table 4-1. Crystallographic Data for $(Ph_4P)_2[Pt(As_3S_5)_2](I)$ and $(Ph_4P)_2K[Pt_3(AsS_4)_3] \cdot 1.5 H_2O(II)$.

	I	ΙΙ
Formula	C48H40P2PtAs6S10	C48H43P2O1.5KPt3As3S12
F. w.	1642.6	1938.1
a, Å	13.104(2)	14.655(2)
b, Å	20.519(3)	17.852(2)
c, Å	11.559(2)	14.252(2)
α, deg.	105.72(2)	109.65(2)
β, deg.	108.09(2)	118.88(2)
γ, deg.	75.11(2)	72.08(2)
Z, V, Å ³	2, 2793(2)	2, 3027(2)
Space Group	P-1 (No. 2)	P-1 (No. 2)
color, habit	orange red, plate	yellow, plate
D _{calc} , g/cm ³	1.95	2.13
Radiation	Μο Κα	Μο Κα
μ, cm ⁻¹	65.09	91.68
2θ _{max} , deg.	45.0	45.0
Absorption Correction	ψ scan	ψ scan
Transmission Factors	0.76-1.12	0.66-1.25
Index ranges	$0 \le h \le 16$, $-24 \le k \le$	$0 \le h \le 17, -21 \le k \le$
	$24, -14 \le l \le 14$	$21, -17 \le 1 \le 17$
No. of Data coll.	7702	8319
Unique reflections	7316	7924
Data Used	3810	3908
$(F_0^2 > 3\sigma(F_0^2))$		
No. of Variables	364	390
Final Ra/Rwb, %	4.0/5.0	7.7/9.5

^a R= Σ (|Fo|-|Fc|)/ Σ |Fo|, ^b R_w={ Σ w(|Fo|-|Fc|)²/ Σ w|Fo|²}1/²

Table 4-1. (cont'd) Crystallographic Data for $(Ph_4P)_2K[Pd_3(AsS_4)_3] \cdot 3CH_3OH(III)$.

	III
Formula	C ₅₁ H ₅₂ P ₂ O ₃ KPd ₃ As ₃ S ₁₂
F. w.	1741.1
a, Å	14.171(3)
b, Å	18.198(5)
c, Å	14.154(3)
α, deg.	106.62(2)
β, deg.	114.66(2)
γ, deg.	83.88(2)
Z, V, Å ³	2, 3125(2)
Space Group	P-1 (No. 2)
color, habit	orange red, plate
D _{calc} , g/cm ³	1.85
Radiation	Μο Κα
μ, cm ⁻¹	29.58
$2\theta_{\text{max}}$, deg.	45.00
Absorption Correction	ψ scan
Transmission Factors	0.88-1.06
Index ranges	$0 \le h \le 15, -20 \le k \le 20,$
	$-15 \le 1 \le 15$
No. of Data coll.	8580
Unique reflections	8179
Data Used	6091
$(F_o^2 > 3\sigma(F_o^2))$	
No. of Variables	421
Final Ra/Rwb, %	3.4/4.4

^a R= $\Sigma(|Fo|-|Fc|)/\Sigma|Fo|$, ^b R_w= $\{\Sigma_w(|Fo|-|Fc|)^2/\Sigma_w|Fo|^2\}^{1/2}$

Table 4-2. Selected Atomic Coordinates and Estimated Standard Deviations (esd's) of (Ph₄P)₂[Pt(As₃S₅)₂](I).

atom	X	Y	Z	$B_{eq} a, (A^2)$
Pt	0.29073(6)	0.26542(4)	0.36578(6)	3.44(3)
As(1)	0.0160(2)	0.3817(1)	0.3141(2)	5.8(1)
As(2)	0.0477(2)	0.1895(1)	0.3083(2)	6.3(1)
As(3)	0.1891(2)	0.2489(1)	0.1458(2)	4.5(1)
As(4)	0.5286(2)	0.2677(1)	0.2587(2)	5.3(1)
As(5)	0.3832(2)	0.1489(1)	0.2874(2)	4.8(1)
As(6)	0.5711(2)	0.2172(1)	0.5698(2)	5.3(1)
S(1)	0.0609(4)	0.3462(3)	0.1317(4)	5.5(3)
S(2)	-0.0606(5)	0.2947(3)	0.3192(5)	7.0(3)
S(3)	0.0848(5)	0.1702(3)	0.1251(4)	6.0(3)
S(4)	0.1783(4)	0.3730(2)	0.4423(4)	5.0(2)
S(5)	0.2055(4)	0.2033(3)	0.4400(4)	5.1(3)
S (6)	0.4792(5)	0.1667(3)	0.1686(5)	5.7(3)
S(7)	0.6427(4)	0.2548(3)	0.4487(5)	5.8(3)
S(8)	0.5207(4)	0.1191(2)	0.4505(5)	5.5(3)
S(9)	0.3754(4)	0.3311(2)	0.2975(4)	4.7(2)
S(10)	0.4124(4)	0.2833(2)	0.5734(4)	4.6(2)
P(1)	0.6829(4)	0.4706(2)	0.8555(4)	3.7(2)
P(2)	0.2286(4)	0.0510(2)	0.6782(4)	3.9(2)
C(1)	0.681(1)	0.3924(8)	0.897(1)	4.3(4)
C(2)	0.582(2)	0.375(1)	0.890(2)	5.1(4)
C(3)	0.586(2)	0.318(1)	0.933(2)	5.8(4)
C(4)	0.682(2)	0.278(1)	0.976(2)	6.0(5)
C(5)	0.780(2)	0.293(1)	0.984(2)	6.4(5)
C(6)	0.779(1)	0.3498(9)	0.939(1)	4.5(4)
C(7)	0.711(1)	0.5356(8)	0.993(1)	3.6(3)
C(8)	0.721(1)	0.600(1)	0.983(2)	5.0(4)
C(9)	0.740(2)	0.651(1)	1.091(2)	5.7(4)
C(10)	0.747(1)	0.6387(9)	1.204(2)	4.7(4)
C(11)	0.736(2)	0.577(1)	1.215(2)	5.4(4)
C(12)	0.719(1)	0.5263(8)	1.110(1)	4.3(4)
C(13)	0.791(1)	0.4535(8)	0.782(1)	3.4(3)
C(14)	0.782(2)	0.411(1)	0.665(2)	6.1(5)
C(15)	0.868(2)	0.393(1)	0.608(2)	6.8(5)
C(16)	0.960(2)	0.419(1)	0.671(2)	7.0(5)
C(17)	0.973(2)	0.459(1)	0.785(2)	8.6(6)
C(18)	0.885(2)	0.476(1)	0.840(2)	7.2(5)

C(19)	0.550(1)	0.4975(8)	0.760(1)	3.7(3)
C(20)	0.507(2)	0.454(1)	0.647(2)	6.0(5)
C(21)	0.398(2)	0.475(1)	0.580(2)	7.0(5)
C(22)	0.337(2)	0.532(1)	0.625(2)	5.8(4)
C(23)	0.378(2)	0.575(1)	0.735(2)	6.2(5)
C(24)	0.485(2)	0.5573(9)	0.803(2)	4.9(4)
C(25)	0.223(1)	0.0098(8)	0.521(1)	3.3(3)
C(26)	0.149(2)	-0.032(1)	0.454(2)	5.6(4)
C(27)	0.141(2)	-0.064(1)	0.328(2)	6.1(5)
C(28)	0.206(2)	-0.047(1)	0.273(2)	6.8(5)
C(29)	0.277(2)	-0.004(1)	0.335(2)	6.0(5)
C(30)	0.287(1)	0.0241(9)	0.460(2)	4.8(4)
C(31)	0.125(1)	0.1278(8)	0.681(1)	4.0(4)
C(32)	0.125(2)	0.177(1)	0.792(2)	5.0(4)
C(33)	0.037(2)	0.230(1)	0.795(2)	6.6(5)
C(34)	-0.047(2)	0.237(1)	0.694(2)	6.1(5)
C(35)	-0.046(2)	0.191(1)	0.583(2)	5.5(4)
C(36)	0.039(1)	0.1362(9)	0.577(2)	4.5(4)
C(37)	0.357(1)	0.0733(8)	0.756(1)	4.1(4)
C(38)	0.383(2)	0.1345(9)	0.743(2)	5.0(4)
C(39)	0.487(2)	0.151(1)	0.804(2)	5.5(4)
C(40)	0.562(2)	0.107(1)	0.874(2)	5.7(4)
C(41)	0.541(2)	0.050(1)	0.890(2)	5.3(4)
C(42)	0.439(1)	0.0291(8)	0.827(1)	3.7(3)
C(43)	0.199(1)	-0.0043(8)	0.755(1)	3.6(3)
C(44)	0.235(1)	-0.0764(9)	0.725(2)	4.6(4)
C(45)	0.215(2)	-0.118(1)	0.785(2)	5.6(4)
C(46)	0.167(2)	-0.092(1)	0.881(2)	5.2(4)
C(47)	0.133(2)	-0.023(1)	0.914(2)	5.6(4)
C(48)	0.149(2)	0.022(1)	0.854(2)	5.4(4)

Table 4-3. Selected Atomic Coordinates and Estimated Standard Deviations (esd's) of (Ph₄P)₂K[Pt₃(AsS₄)₃]·1.5H₂O(II).

atom	X	Y	Z	$B_{eq}^{a}, (A^2)$
Pt(1)	0.3076(1)	0.2512(1)	0.9752(1)	3.18(8)
Pt(2)	0.0702(1)	0.1956(1)	0.8535(1)	3.30(8)
Pt(3)	0.1863(2)	0.2576(1)	1.1295(2)	4.4(1)
As(1)	0.3980(4)	0.3779(3)	1.2596(4)	5.5(3)
As(2)	0.1572(4)	0.2403(3)	0.6771(4)	5.0(3)
As(3)	-0.0973(5)	0.2500(5)	1.0013(6)	8.4(4)
K(1)	0.096(1)	0.4002(7)	0.958(1)	7.1(7)
S(1)	0.127(1)	0.1416(8)	1.003(1)	5.1(7)
S(2)	0.2360(9)	0.1370(5)	0.8622(9)	3.1(5)
S(3)	0.344(1)	0.1973(7)	1.120(1)	4.2(6)
S(4)	0.016(1)	0.2513(8)	0.703(1)	4.7(6)
S (5)	0.249(1)	0.3736(8)	1.257(1)	5.2(7)
S(6)	0.266(1)	0.3084(8)	0.831(1)	5.2(7)
S(7)	0.363(1)	0.3742(8)	1.089(1)	5.6(7)
S(8)	0.469(1)	0.2468(9)	1.260(1)	6.8(7)
S(9)	0.234(1)	0.1165(8)	0.707(1)	6.2(7)
S(10)	-0.094(1)	0.256(1)	0.848(1)	6.1(7)
S(11)	0.026(1)	0.317(1)	1.135(1)	8(1)
S(12)	-0.001(1)	0.124(1)	1.013(2)	9(1)
P(1)	0.5250(9)	0.1718(6)	0.633(1)	3.1(5)
P(2)	0.8292(9)	0.3118(7)	0.343(1)	3.4(5)
O(1)	-0.088(6)	0.443(5)	0.986(6)	8(2)
O(2)	-0.095(7)	0.464(6)	0.834(7)	27(2)
C(1)	0.346(3)	0.104(2)	0.534(3)	2.8(8)
C(2)	0.397(3)	0.155(2)	0.527(3)	2.1(7)
C(3)	0.965(4)	0.399(3)	0.537(4)	4(1)
C(4)	0.524(3)	0.278(2)	0.691(3)	3.4(8)
C(5)	0.946(3)	0.352(2)	0.433(3)	3.3(8)
C(6)	0.660(4)	0.085(3)	0.418(4)	6(1)
C(7)	0.758(3)	0.356(2)	0.224(3)	2.6(7)
C(8)	0.865(3)	0.200(2)	0.305(3)	2.9(8)
C(9)	0.722(4)	0.129(3)	0.639(4)	5(1)
C(10)	0.248(3)	0.092(2)	0.452(3)	3.4(8)
C(11)	0.505(4)	0.443(3)	0.765(4)	5(1)
C(12)	0.425(3)	0.409(2)	0.738(3)	3.0(8)
C(13)	0.758(4)	0.086(3)	0.480(4)	6(1)

C(14)	0.627(3)	0.048(3)	0.742(4)	4(1)	
C(15)	0.588(3)	0.111(3)	0.465(4)	4(1)	
C(16)	0.802(3)	0.403(2)	0.206(3)	3.7(9)	
C(17)	0.624(3)	0.134(3)	0.577(3)	3.9(9)	
C(18)	0.249(4)	0.185(3)	0.364(4)	5(1)	
C(19)	0.732(3)	0.290(3)	0.457(3)	3.8(9)	
C(20)	0.428(3)	0.326(3)	0.696(3)	3.8(9)	
C(21)	0.342(4)	0.195(3)	0.440(4)	5(1)	
C(22)	0.704(3)	0.425(3)	0.431(3)	4(1)	
C(23)	0.747(3)	0.344(3)	0.413(3)	3.5(9)	
C(24)	0.610(3)	0.313(3)	0.729(3)	4(1)	
C(25)	0.675(4)	0.318(3)	0.517(4)	5(1)	
C(26)	0.526(4)	0.155(3)	0.816(4)	5(1)	
C(27)	0.566(3)	0.119(2)	0.739(3)	3.2(8)	
C(28)	0.601(4)	0.395(3)	0.769(4)	5(1)	
C(29)	0.546(4)	0.115(3)	0.899(4)	6(1)	
C(30)	0.602(4)	0.034(3)	0.891(4)	6(1)	
C(31)	0.648(4)	0.005(3)	0.824(4)	5(1)	
C(32)	0.199(4)	0.131(3)	0.366(4)	6(1)	
C(33)	0.793(4)	0.106(3)	0.585(4)	7(1)	
C(34)	0.741(5)	0.439(3)	0.112(5)	7(1)	
C(35)	0.650(5)	0.425(4)	0.052(5)	8(2)	
C(36)	0.655(4)	0.342(3)	0.155(4)	6(1)	
C(37)	0.649(4)	0.453(3)	0.497(4)	5(1)	
C(38)	0.628(4)	0.402(3)	0.537(4)	6(1)	
C(39)	1.114(4)	0.373(3)	0.468(4)	5(1)	
C(40)	1.027(4)	0.337(3)	0.398(4)	5(1)	
C(41)	1.127(4)	0.417(3)	0.565(4)	6(1)	
C(42)	1.049(4)	0.433(3)	0.607(4)	6(1)	
C(43)	0.923(4)	0.041(3)	0.261(4)	6(1)	
C(44)	0.963(4)	0.072(3)	0.365(4)	6(1)	
C(45)	0.929(4)	0.163(3)	0.389(4)	7(1)	
C(46)	0.830(4)	0.169(3)	0.200(4)	7(1)	
C(47)	0.860(5)	0.082(4)	0.177(5)	8(1)	
C(48)	0.594(5)	0.375(4)	0.053(5)	9(2)	

^a $B_{eq}=(4/3)[a^2B_{11} + b^2B_{22} + c^2B_{33} + ab(\cos\gamma)B_{12} + ac(\cos\beta)B_{13} + bc(\cos\alpha)B_{23}]$

Table 4-4. Selected Atomic Coordinates and Estimated Standard Deviations (esd's) of (Ph₄P)₂K[Pd₃(AsS₄)₃]·3CH₃OH(III).

atom	X	Y	Z	$B_{eq}^{a}, (A^2)$
Pd(1)	0.49331(4)	0.23698(3)	0.26342(4)	1.82(2)
Pd(2)	0.23334(4)	0.24512(3)	0.18603(4)	2.00(2)
Pd(3)	0.32695(5)	0.32174(3)	0.06042(5)	2.26(3)
As(1)	0.40500(6)	0.10223(5)	0.34925(6)	2.55(4)
As(2)	0.60793(7)	0.26619(5)	0.08872(7)	3.06(4)
As(3)	0.05403(8)	0.28677(7)	-0.07283(8)	4.56(5)
K(1)	0.3767(2)	0.1145(1)	0.0211(2)	4.2(1)
S(1)	0.6252(2)	0.1871(1)	0.1923(2)	2.69(9)
S(2)	0.5261(2)	0.1121(1)	0.2940(2)	2.71(9)
S (3)	0.4552(1)	0.3595(1)	0.2232(1)	2.24(8)
S(4)	0.3672(1)	0.2876(1)	0.3418(1)	2.06(8)
S(5)	0.2518(2)	0.1229(1)	0.2186(2)	2.74(9)
S (6)	0.1027(2)	0.2010(1)	0.0295(2)	4.0(1)
S(7)	0.2111(2)	0.3680(1)	0.1516(2)	2.77(9)
S(8)	0.4429(2)	0.2690(1)	-0.0282(2)	3.1(1)
S(9)	0.1986(2)	0.2816(1)	-0.1028(2)	3.7(1)
S(10)	0.3952(2)	0.2208(1)	0.4521(2)	2.84(9)
S(11)	0.5803(2)	0.3789(1)	0.1985(2)	3.5(1)
S(12)	0.0586(2)	0.3953(2)	0.0491(2)	4.9(1)
P(1)	0.6144(2)	0.3548(1)	0.7526(1)	1.85(8)
P(2)	0.0369(2)	0.1695(1)	0.4113(2)	2.06(8)
O(1)	0.0629(5)	0.3793(5)	0.7045(5)	6.0(4)
O(2)	0.5954(7)	0.0421(4)	-0.0056(6)	6.4(4)
O(3)	0.3531(7)	0.0473(5)	-0.1807(6)	7.9(5)
C(1)	0.4733(5)	0.3685(4)	0.7074(5)	1.9(1)
C(2)	0.4261(5)	0.3431(4)	0.7577(5)	2.0(1)
C(3)	0.3177(6)	0.3559(4)	0.7252(6)	2.1(1)
C(4)	0.2554(6)	0.3933(4)	0.6416(6)	2.2(1)
C(5)	0.3017(6)	0.4175(4)	0.5894(6)	2.6(1)
C(6)	0.4096(6)	0.4060(4)	0.6219(6)	2.2(1)
C(7)	0.6717(5)	0.2547(4)	0.7684(5)	1.9(1)
C(10)	0.7659(6)	0.1014(4)	0.7895(6)	2.6(2)
C(11)	0.8225(6)	0.1614(5)	0.8463(6)	3.0(2)
C(12)	0.7739(6)	0.2385(4)	0.8365(6)	2.6(1)
C(13)	0.6669(6)	0.4168(4)	0.8785(6)	2.1(1)
C(14)	0.7606(6)	0.4431(4)	0.9065(6)	2.6(1)

ЪС

C(15)	0.8038(6)	0.4860(5)	1.0081(6)	3.0(1)
C(16)	0.7561(6)	0.5010(5)	1.0799(6)	3.1(2)
C(17)	0.6650(7)	0.4758(5)	1.0536(7)	3.5(2)
C(18)	0.6190(6)	0.4343(5)	0.9523(6)	2.8(2)
C(19)	0.6478(5)	0.3761(4)	0.6557(5)	1.8(1)
C(20)	0.6568(5)	0.3186(4)	0.5687(5)	2.0(1)
C(21)	0.6724(6)	0.3384(4)	0.4894(6)	2.4(1)
C(22)	0.6767(6)	0.4136(4)	0.4940(6)	2.6(1)
C(23)	0.6658(6)	0.4713(4)	0.5794(6)	2.7(2)
C(24)	0.6516(6)	0.4528(4)	0.6600(6)	2.3(1)
C(25)	0.1750(5)	0.1372(4)	0.4862(5)	2.0(1)
C(26)	0.2256(6)	0.0628(4)	0.4570(6)	2.4(1)
C(27)	0.3265(6)	0.0358(5)	0.5223(6)	2.8(2)
C(28)	0.3764(6)	0.0832(5)	0.6150(6)	2.9(2)
C(29)	0.3275(6)	0.1581(5)	0.6440(6)	2.8(2)
C(30)	0.2265(6)	0.1864(4)	0.5795(6)	2.6(1)
C(31)	0.0153(6)	0.2677(4)	0.3954(5)	2.1(1)
C(32)	0.0889(6)	0.2914(4)	0.3745(6)	2.6(1)
C(33)	0.0661(6)	0.3636(5)	0.3497(6)	3.1(2)
C(34)	-0.0295(8)	0.4127(6)	0.3426(7)	4.6(2)
C(35)	-0.103(1)	0.3883(7)	0.3619(9)	6.3(3)
C(36)	-0.0802(8)	0.3157(6)	0.3894(8)	4.8(2)
C(37)	-0.0054(6)	0.1080(4)	0.2828(6)	2.4(1)
C(38)	-0.0276(8)	0.1355(6)	0.1933(8)	4.7(2)
C(39)	-0.065(1)	0.0863(7)	0.094(1)	6.7(3)
C(40)	-0.0777(8)	0.0133(6)	0.0842(8)	4.9(2)
C(41)	-0.0540(6)	-0.0145(5)	0.1730(7)	3.3(2)
C(42)	-0.0183(6)	0.0326(5)	0.2716(6)	3.0(2)
C(43)	-0.0399(5)	0.1615(4)	0.4809(5)	2.0(1)
C(44)	0.0028(6)	0.1699(5)	0.5912(6)	3.0(2)
C(45)	-0.0579(7)	0.1630(5)	0.6429(7)	3.5(2)
C(46)	-0.1566(6)	0.1442(5)	0.5858(6)	2.9(2)
C(47)	-0.1978(6)	0.1355(5)	0.4787(6)	3.0(2)
C(48)	-0.1403(6)	0.1450(4)	0.4253(6)	2.8(2)
C(49)	0.6122(8)	0.0694(6)	-0.0809(8)	4.9(2)
C(50)	0.2487(9)	0.0418(6)	-0.2444(8)	5.4(2)
C(51)	-0.042(1)	0.4046(7)	0.696(1)	6.5(3)

^a $B_{eq}=(4/3)[a^2B_{11} + b^2B_{22} + c^2B_{33} + ab(\cos\gamma)B_{12} + ac(\cos\beta)B_{13} + bc(\cos\alpha)B_{23}]$

for spa cal

co

da

co: pa

CE

d-s Ta The compounds were examined by X-ray powder diffraction for the purpose of phase purity and identification. Accurate dhk1 spacings (Å) were obtained from the powder patterns recorded on a calibrated (with FeOCl as internal standard) Phillips XRG-3000 computer-controlled powder diffractometer with praphite-monochromated Cu Kα radiation operating at 35 kV and 35 mA. The data were collected at a rate of 0.12°/min. Based on the atomic coordinates from X-ray single crystal diffraction study, X-ray powder patterns for all compounds were calculated by the software package CERIUS.¹⁴ Calculated and observed X-ray powder patterns that show d-spacings and intensities of strong hkl reflections are complied in Tables 4-5 to 4-7.

Table 4-5. Calculated and Observed X-ray Powder Diffraction Pattern of (Ph₄P)₂[Pt(As₃S₅)₂](I).

h	k l	d _{calc} (Å)	d _{obs} (Å)	I/I _{max} (obs, %)
1	0 0	12.23	12.21	10
1	1 0	11.36	11.35	82
0	0 2	10.75	10.74	47
0	1 -1	10.36	10.35	62
0	2 0	9.69	9.69	77
1	-1 0	9.56	9.55	4 1
1	0 -1	9.36	9.36	5 1
0	1 1	8.67	8.66	100
	2 -1	8.20	8.20	70
0	2 -1	8.08	8.08	15
1	-1 -1	7.53	7.53	10
	0 1	7.20	7.20	10
	1 1	6.69	6.68	1 2
	2 1	6.55	6.55	1 2
	3 0	6.22	6.22	17
0	3 -1	6.13	6.12	20
1	-2 -1	5.85	5.85	14
	2 -2	5.51	5.50	15
0	1 -2			
1	0 -2	5.47	5.47	15
	0 2	5.37	5.37	15
2	3 -1	5.28	5.28	15
0	3 1	5.09	5.08	15
1	4 -1	5.03	5.02	17
2	-1 1	4.60		
3	-1 0	3.84		
3	4 -1	3.71	3.71	10
2	-4 0	3.49	3.49	11
3	5 -2	3.26	3.26	15
	5 -3	2.945	2.941	10
2	-1 3	2.793		

Table 4-6. Calculated and Observed X-ray Powder Diffraction Pattern of (Ph₄P)₂K[Pt₃(AsS₄)₃]·1.5H₂O(II)

h	k l	d _{calc} (Å)	d _{obs} (Å)	I/I _{max} (obs, %)
1	0 0	12.6	12.5	20
0	0 1	12.2	12.1	62
1	1 -1	11.8	11.7	57
1	0 -1	11.5	11.4	10
1	-1 0	9.28	9.27	58
0	2 0	8.28	8.27	100
1	-1 -1	8.14	8.14	35
0	2 -1	7.69	7.68	67
1	2 0	7.56	7.55	12
1	0 1	7.34	7.34	9
2	0 -1	6.93	6.92	13
1	-1 1	6.79	6.79	15
1	3 0	4.75	4.75	12
0	4 -1	4.21	4.21	13
2	3 -5	2.79		

Table 4-7. Calculated and Observed X-ray Powder Diffraction Pattern of (Ph₄P)₂K[Pd₃(AsS₄)₃]·3CH₃OH(III).

h	k	l	d _{calc} (Å)	d _{obs} (Å)	I/I _{max} (obs, %)
1	0	0	12.67	12.66	75
0	0	1	12.61	12.60	38
0	1	-1	11.26	11.25	90
1	1	-1			
1	1	0	11.21	11.21	75
1	0	-1			
1	-1	0	9.40	9.40	45
0	1	1	9.33	9.33	95
0	2	0	8.57	8.55	100
1	-1	-1	8.22	8.22	34
1	0	1	764	7.64	19
1	1	-2	7.01	7.00	15
1	0	-2	6.71	6.71	17
0	2	1	6.53	6.53	16
1	3	-1	5.96		
1	2	1	5.69	5.70	22
0	3	1	4.86	4.86	20
2	1	1			
1	-2	-2	4.65	4.64	1 4
4	1	-3	3.28	3.28	20
1	5	-3	3.18	3.18	10

3. Results and discussion

3.1 Syntheses and Description of Structures

(Ph₄P)₂[Pt(As₃S₅)₂] was prepared by heating a mixture of PtCl₂/3K₃A₅S₃/4Ph₄PBr in a sealed Pyrex tube with 0.3 mL of H₂O The orange-red platelike crystals of (Ph₄P)₂[Pt(As₃S₅)₂] for one day. are relatively air stable and soluble in polar organic solvents such as DMF and CH₃CN and give orange-red solutions, indicative that the compound might be a molecular complex. The structure was determined by X-ray single-crystal diffraction analysis. (Ph₄P)₂[Pt(As₃S₅)₂] is a molecular cage compound with discrete [Pt(As₃S₅)₂]²⁻ anions which are well separated from the organic cation, see Figure 4-1. There are two unique features in this the most unusual [As₃S₅]³- units and, remarkably, the presence of a Pt-As bond. The [As₃S₅]³- anion represents a new thioarsenic anion and can be viewed as the two electron reduction product of a cyclic [As₃S₆]³- unit¹⁰, (see Eq. 4-1). This results in a negatively charged As atom in the [As₃S₅]³- unit which bonds to Pt⁴⁺. The total charge of each ligand is 3-, with each of the sulfur atoms in a 2- oxidation state. We then can assign the formal oxidation states of the two As atoms that are not connected to the metal center as 3+ while the Pt-bound arsenic is assigned 1+. However, it should be noted that despite the different oxidation states for the As atoms in the [As₃S₅]³- units, there is no notable difference in the As-S bond distances which vary from 2.177(5)Å to 2.291(5)Å.

The Pt metal resides in a distorted octahedral environment coordinated by two [As₃S₅]³- ligands through two S and one As atom respectively, see Figure 4-2. Although we started with Pt2+, the geometry of the metal atom indicates it is now in the 4+ oxidation state suggestive that Pt is the reducing agent for [As₃S₆]³-. There are only two other mononuclear Pt4+ polychalcogenide compounds, $[Pt(S_5)_3]^{2-3}$ and $[Pt(S_4)(S_5)_2]^{2-15}$ known. The average Pt-S bond distance where the sulfur atom is trans to an As atom is 2.428(5)Å, significantly longer than the other Pt-S bond distances at 2.355(5)Å. The latter distances are within the normal range (2.332Å to 2.479Å) for Pt-S bond distances found in $[Pt(S_4)_3]^{2-1}$. The As-S distances and S-As-S angles are normal based on those observed in previously characterized arsenic sulfur compounds. 16 To the best of our knowledge and with the exception of solid state platinum arsenides, this is the first observation of a platinum-arsenide bond and it is surprising, particularly considering it formed in aqueous solution. Selected distances and angles are given in Tables 4.8-4.9.

Table 4.8. Selected Distances (Å) in the [Pt(As₃S₅)₂]² with Standard Deviations in Parentheses.²

Pt - As(3)	2.453(2)	Pt - As(5)	2.455(2)
Pt - S(4)	2.430(5)	Pt - S(5)	2.351(5)
Pt - S(9)	2.358(5)	Pt - S(10)	2.425(5)
As(1) - S(1)	2.245(5)	As(1) - S(2)	2.285(7)
As(1) - S(4)	2.177(5)	As(2) - S(2)	2.253(7)
As(2) - S(3)	2.229(5)	As(2) - S(5)	2.189(6)
As(3) - S(1)	2.261(6)	As(3) - S(3)	2.291(5)
As(4) - S(6)	2.214(6)	As(4) - S(7)	2.281(6)
As(4) - S(9)	2.196(6)	As(5) - S(6)	2.277(5)
As(5) - S(8)	2.263(6)	As(6) - S(7)	2.282(6)
As(6) - S(8)	2.236(5)	As(6) - S(10)	2.177(5)

^aThe estimated standard deviations in the mean bond lengths and the mean bond angles are calculated by the equation $\sigma l = \{\Sigma_n(l_n - 1)^2/n(n-1)\}^{1/2}$, where l_n is the length (or angle) of the nth bond, l the mean length (or angle), and n the number of bonds.

Table 4.9. Selected Angles (Deg) in the $[Pt(As_3S_5)_2]^{2-}$ with Standard Deviations in Parentheses.^a

As(3)-Pt-As(5)	79.83(7)	As(3)-Pt-S(4)	98.3(1)
As(3)-pt-S(5)	100.5(1)	As(3)-Pt-S(9)	80.9(1)
As3-Pt-S(10)	171.9(1)	As(5)-Pt-S(4)	171.8(1)
As(5)-Pt-S(5)	81.9(1)	As(5)-Pt-S(9)	99.9(1)
As(5)-Pt-S(10)	97.7(1)	S(4)- Pt-S(5)	90.7(2)
S(4)-Pt-S(9)	87.6(2)	S(4)-Pt-S(10)	85.3(2)
S(5)-Pt-S(9)	177.9(2)	S(5)-Pt-S(10)	86.6(2)
S(9)-Pt-S(10)	92.1(2)	S(1)-Pt-S(2)	103.2(2)
S(1)-Pt-S(4)	100.1(2)	S(2)-Pt-S(4)	107.7(2)
S(2)-Pt-S(3)	102.6(2)	S(3)-Pt-S(5)	102.4(2)
Pt-As(3)-S(1)	104.7(1)	Pt-As(3)-S(3)	103.8(1)
S(1)-As(3)-S(3)	101.5(2)	S(6)-As(4)-S(7)	105.8(2)
S(6)-As(4)-S(9)	101.3(2)	S(7)-As(4)-S(9)	105.1(2)
Pt-As(5)-S(6)	103.5(1)	Pt-As(5)-S(8)	105.7(1)
S(6)-As(5)-S(8)	100.6(2)	S(7)-As(6)-S(8)	103.8(2)
S(7)-As(6)-S(10)	107.1(2)	S(8)-As(6)-S(10)	100.9(2)
As(1)-S(1)-As(3))106.5(2)	As(1)-S(2)-As(2)	115.8(2)
As(2)-S(3)-As(3)	105.9(2)	Pt-S(4)-As(1)	108.7(2)
Pt-S(5)-As(1)	108.7(2)	As(4)-S(5)-As(5)	106.2(2)
As(4)-S(7)-As(6)	114.9(2)	As(5)-S(8)-As(6)	106.5(2)
Pt-S(8)-As(4)	109.0(2)	Pt-S(9)-As(6)	109.0(2)

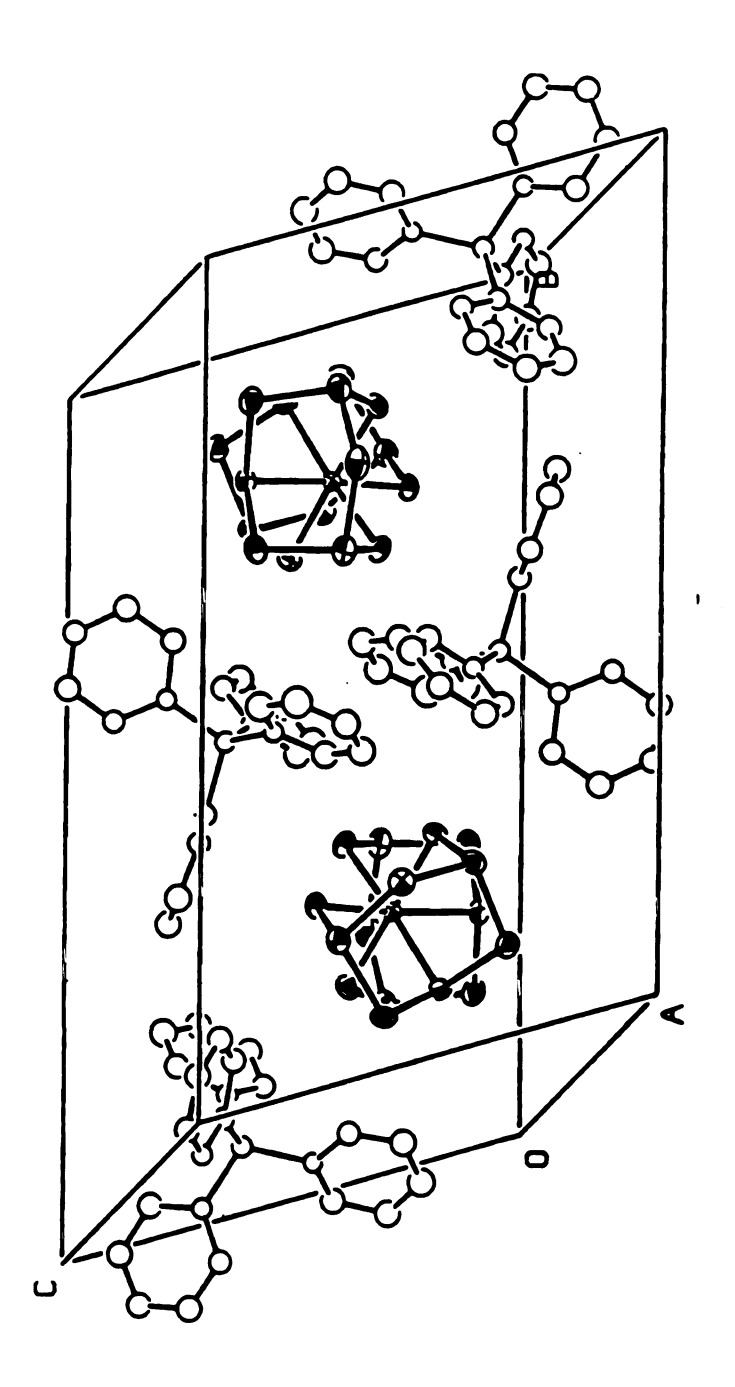


Figure 4-1. Packing diagram of (Ph₄P)₂[Pt(As₃S₅)₂].

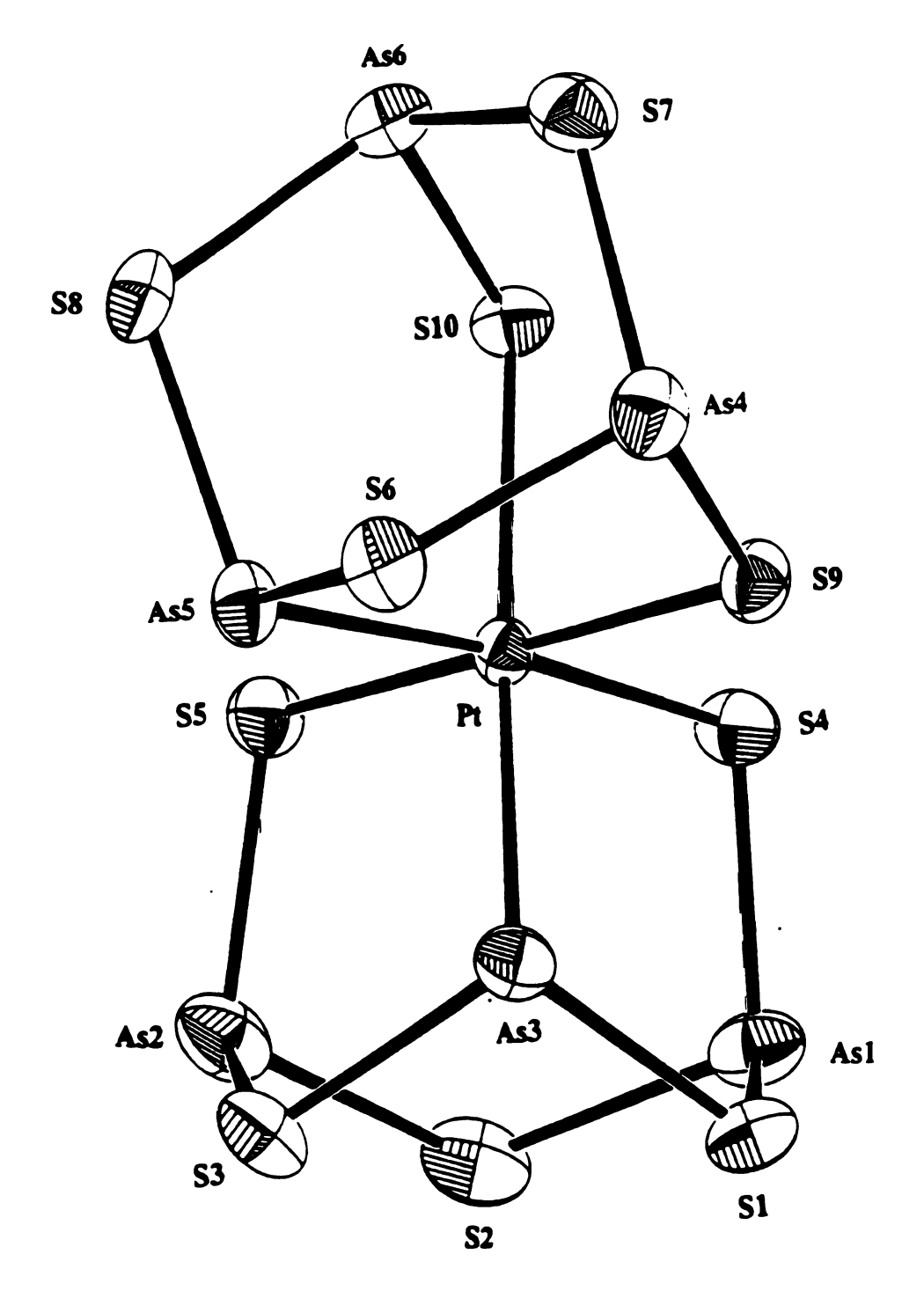


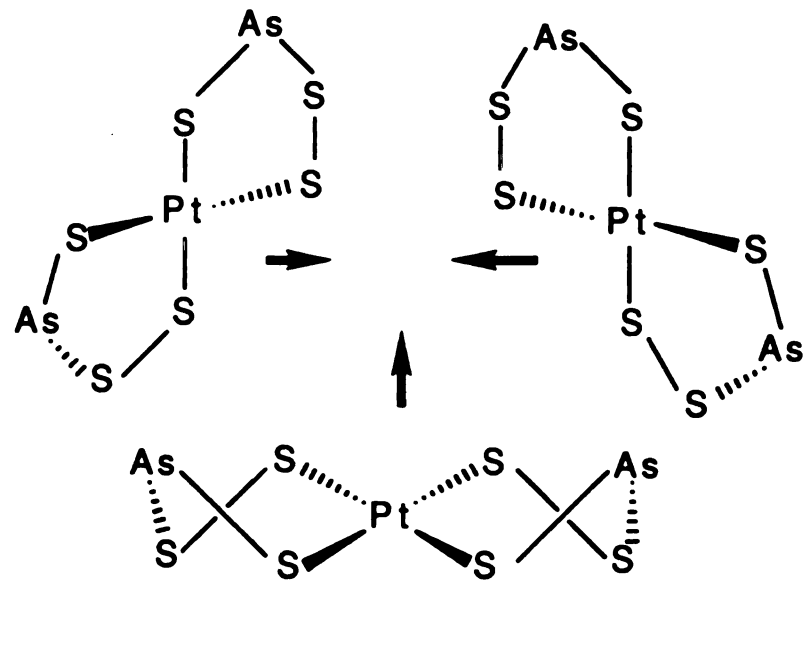
Figure 4-2. Structure and labeling scheme of $[PtAs_6S_{10}]^2$.

When the amount of AsS33- is decreased, the above redox chemistry is avoided and the Pt2+ cluster (Ph4P)2K[Pt3(AsS4)3]·1.5H2O while the very good vield Pd (Ph₄P)₂K[Pd₃(AsS₄)₃]·3MeOH(III), is synthesized by using the PdCl₂/K₃AsS₃/Ph₄PBr ratio of 1:2:6 in methanol at 110 °C for one The reaction gave bright-red rod-like crystals of day. (Ph₄P)₂K[Pd₃(AsS₄)₃]·3MeOH in good yield. The structure of the anion $[Pd_3(AsS_4)_3]^{3-}$ is the same as that of the Pt analog. The difference is that instead of being a hydrate it is a methylate with three CH₃OH molecules in the formula unit. The structure of the anion is showed in Figure 4-5. The selected distances and angles is given in the Table 4-10 and 4-11. (Ph₄P)₂K[Pt₃(AsS₄)₃] contains discrete trinuclear anions of [Pt₃(AsS₄)₃]³-, see Figure 4-3. The most unique feature of the compound is the presence of a new kind of [AsS4]³- ligands, which can be viewed as the oxidative coupling product between [AsS₃]³⁻ and S²⁻; see eq. 2. This anion contains As(III) and it is different from the well known tetrahedral [AsS4]3which is a As(V) species. The two isomers are related via an internal redox equilibrium according to eq. 3.

$$[AsS_3]^{3}$$
 + S^{2} - $[AsS_4]^{3}$ + $2e^{2}$ (eq. 2)

$$\begin{bmatrix} S & AS & -S \\ S & S \end{bmatrix}^3 \cdot \begin{bmatrix} S & AS & S \\ S & S \end{bmatrix}^3 \cdot (eq. 3)$$

Each $[AsS_4]^{3-}$ ligand that binds to two Pt atoms employs all its terminal S atoms, see Figure 4-4. A close inspection of the structure reveals the close relationship between the polychalcogenide and the thioarsenate ligands. The structure of $[Pt_3(AsS_4)_3]^{3-}$, can be viewed as three " $[Pt(AsS_3)_2]$ " units fused together, see sheeme 1. If the As atom in the AsS₃ unit is thought an S atom then the " $[Pt(AsS_3)_2]$ " becomes the known $[Pt(S_4)_2]^{2-}$ which was recently synthesized, methanothermally, by Dr. Kang-Woo Kim in our lab. 17



Scheme 1

The central cluster Pt_3S_3 core involving the atoms Pt(1), Pt(2), Pt(3), S(1), S(2), and S(3) is in a distorted "cyclohexane-chair"

conformation forming a partial cube which derives from a hypothetical Pt4S4 cube by removing a S and a Pt atom lying on a body diagonal. Interestingly, a cluster with a Pt4S4 cubane core has recently been described.⁴ Each Pt atom is coordinated by four sulfur atoms in a distorted square planar fashion with bond angles ranging from 84.0 (1)° to 179.0(1)°. The formal oxidation state of the metal center is 2+. The Pt-S bond distances range from 2.285(6)Å to 2.345(7)Å, while the As-S bond distances vary from 2.202(7)Å to 2.254(7)Å. Selected distances and angles are given in Tables 4.10-4.11.

Table 4-10. Selected Distances (Å) in the $[M_3(AsS_4)_3]^{3-}$ (M = Pt, Pd) with Standard Deviations in Parentheses.^a

[Pt ₃	$(AsS_4)_3]^{3}$	[Pd	3(AsS4)3] ³⁻
Pt(1) - S(3)	2.323(6)	Pd(1) - S(3)	2.322(2)
Pt(1) - S(2)	2.315(5)	Pd(1) - S(2)	2.330(2)
Pt(1) - S(7)	2.362(7)	Pd(1) - S(7)	2.331(2)
Pt(1) - S(6)	2.341(7)	Pd(1) - S(6)	2.318(2)
Pt(2) - S(1)	2.314(8)	Pd(2) - S(1)	2.332(2)
Pt(2) - S(4)	2.353(6)	Pd(2) - S(4)	2.321(2)
Pt(2) - S(2)	2.298(6)	Pd(2) - S(2)	2.326(2)
Pt(2) - S(10)	2.294(6)	Pd(2) - S(10)	2.316(2)
Pt(3) - S(3)	2.285(6)	Pd(3) - S(3)	2.319(2)
Pt(3) - S(11)	2.292(7)	Pd(3) - S(11)	2.333(2)
Pt(3) - S(1)	2.324(5)	Pd(3) - S(1)	2.334(2)
Pt(3) - S(5)	2.345(7)	Pd(3) - S(5)	2.313(2)
As(1) - S(7)	2.215(7)	As(1) - S(7)	2.235(2)
As(1) - S(5)	2.208(6)	As(1) - S(5)	2.227(2)
As(2) - S(6)	2.202(7)	As(2) - S(6)	2.227(2)
As(2) - S(4)	2.216(7)	As(2) - S(4)	2.207(2)
As(2) - S(9)	2.232(6)	As(2) - S(9)	2.235(2)
As(3) - S(11)	2.195(7)	As(3) - S(11)	2.232(3)
As(3) - S(10)	2.246(7)	As(3) - S(10)	2.207(2)
As(3) - S(12)	2.264(7)	As(3) - S(12)	2.216(3)
S(1) - S(12)	2.074(8)	S(1) - S(12)	2.055(3)
S(2) - S(9)	2.101(8)	S(2) - S(9)	2.091(3)
S(3) - S(8)	2.105(7)	S(3) - S(8)	2.079(3)

^aThe estimated standard deviations in the mean bond lengths and the mean bond angles are calculated by the equation $\sigma l = \{\Sigma_n(l_n - 1)^2/n(n-1)\}^{1/2}$, where l_n is the length (or angle) of the nth bond, l the mean length (or angle), and n the number of bonds.

[Pt ₃ (AsS ₄) ₃] ³ -	[Pd ₃ (AsS ₄) ₃] ³ -
S(2)-Pt(1)-S(3) 85.6(1)	S(2)-Pd(1)-S(3) 85.65(7)
S(2)-Pt(1)-S(7) 174.2(1)	S(2)-Pd(1)-S(7) 177.50(7)
S(3)-Pt(1)-S(7) 94.5(1)	S(3)-Pd(1)-S(7) 94.85(7)
S(2)-Pt(1)-S(6) 94.8(1)	S(2)-Pd(1)-S(6) 95.11(7)
S(3)-Pt(1)-S(6) 178.0(1)	S(3)-Pd(1)-S(6) 176.86(7)
S(6)-Pt(1)-S(7) 84.8(1)	S(6)-Pd(1)-S(7) 84.53(7)
S(1)-Pt(2)-S(2) 84.0(1)	S(1)-Pd(2)-S(2) 84.29(7)
S(1)-Pt(2)-S(10) 95.5(1)	S(1)-Pd(2)-S(10) 96.09(8)
S(2)-Pt(2)-S(10) 178.8(1)	S(2)-Pd(2)-S(10) 178.77(9)
S(1)-Pt(2)-S(4) 178.6(1)	S(1)-Pd(2)-S(4) 178.84(7)
S(2)-Pt(2)-S(4) 95.0(1)	S(2)-Pd(2)-S(4) 96.67(7)
S(4)-Pt(2)-S(10) 85.5(1)	S(4)-Pd(2)-S(10) 82.86(8)
S(1)-Pt(3)-S(3) 84.6(1)	S(1)-Pd(3)-S(3) 85.00(7)
S(1)-Pt(3)-S(11) 94.4(1)	S(1)-Pd(3)-S(11) 95.05(8)
S(3)-Pt(3)-S(11) 178.8(2)	S(3)-Pd(3)-S(11) 179.03(8)
S(1)-Pt(3)-S(5) 179.0(1)	S(1)-Pd(3)-S(5) 176.77(7)
S(3)-Pt(3)-S(5) 94.4(1)	S(3)-Pd(3)-S(5) 95.16(7)
S(5)-Pt(3)-S(11) 86.6(2)	S(5)-Pd(3)-S(11) 84.73(8)
S(5)-As(1)-S(7) 106.5(1)	S(5)-As(1)-S(7) 104.38(8)
S(5)-As(1)-S(8) 96.4(2)	S(5)-As(1)-S(8) 98.00(9)
S(7)-As(1)-S(8) 98.5(2)	S(7)-As(1)-S(8) 97.02(8)
S(4)-As(2)-S(9) 97.5(2)	S(4)-As(2)-S(9) 98.13(8)
S(4)-As(2)-S(6) 105.5(2)	S(4)-As(2)-S(6) 105.87(8)
S(6)-As(2)-S(9) 98.0(2)	S(6)-As(2)-S(9) 97.46(8)
S(10)-As(3)-S11 104.3(2)	S(10)-As(3)-S11 104.4(1)
S(11)-As(3)-S12 97.1(2)	S(11)-As(3)-S12 99.8(1)
S(10)-As(3)-S12 97.5(2)	S(10)-As(3)-S12 99.1(1)
Pt(2)-S(1)-Pt(3) 93.5(4)	Pd(2)-S(1)-Pt(3) 92.07(7)
Pt(2)-S(1)-S(12) 110.1(5)	Pd(2)-S(1)-S(12) 108.0(1)
Pt(3)-S(1)-S(12) 109.7(5)	Pd(3)-S(1)-S(12) 110.8(1)
Pt(1)-S(2)-Pt(2) 93.6(3)	Pd(1)-S(2)-Pt(2) 92.00(7)
Pt(1)-S(2)-S(9) 109.5(6)	Pd(1)-S(2)-S(9) 108.7(1)

^aThe estimated standard deviations in the mean bond lengths and the mean bond angles are calculated by the equation $\sigma l = \{\Sigma_n(l_n - 1)^2/n(n-1)\}^{1/2}$, where l_n is the length (or angle) of the nth bond, l the mean length (or angle), and n the number of bonds.

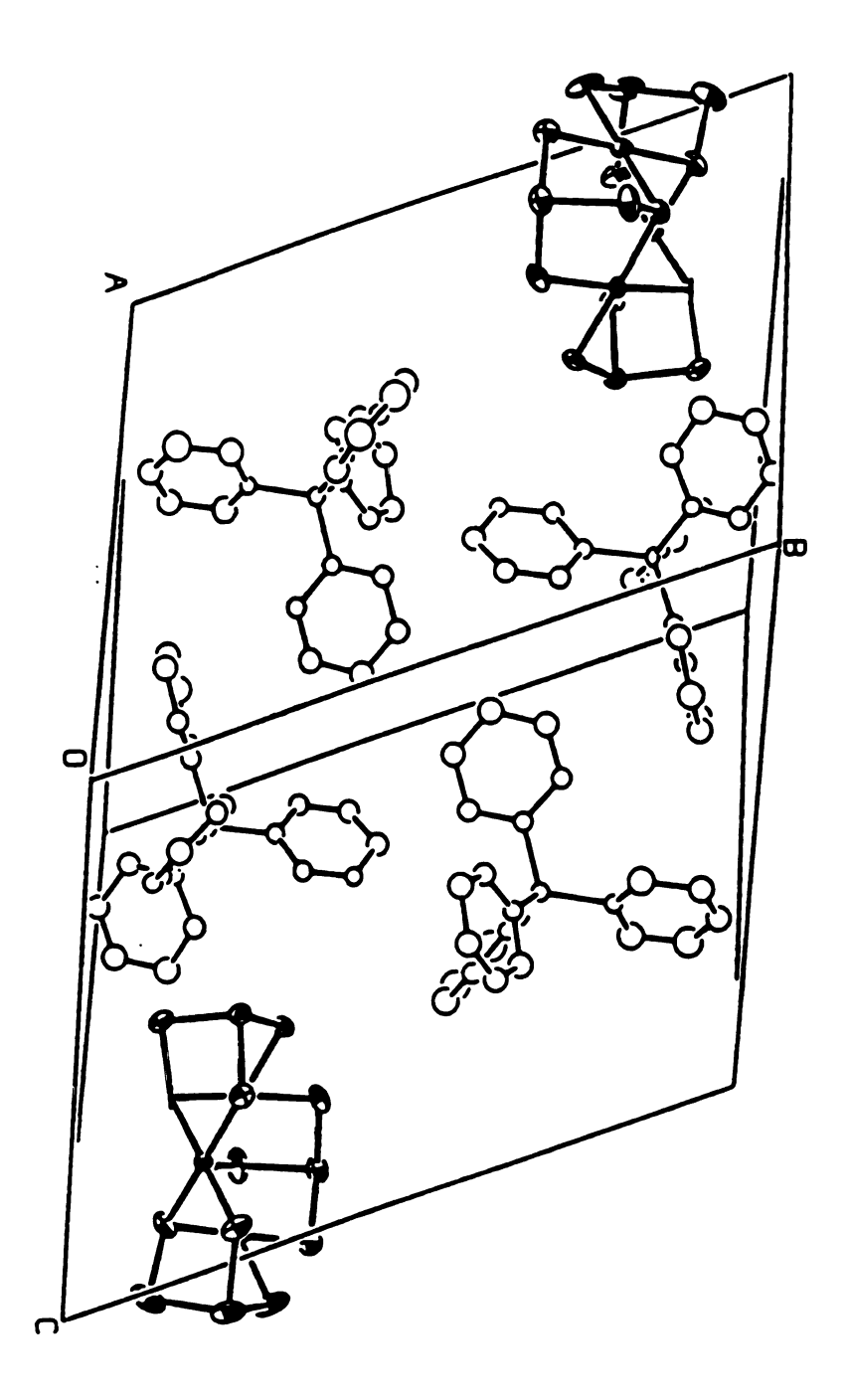


Figure 4-3. Packing diagram of (Ph₄P)₂K[Pt₃(AsS₄)₃].

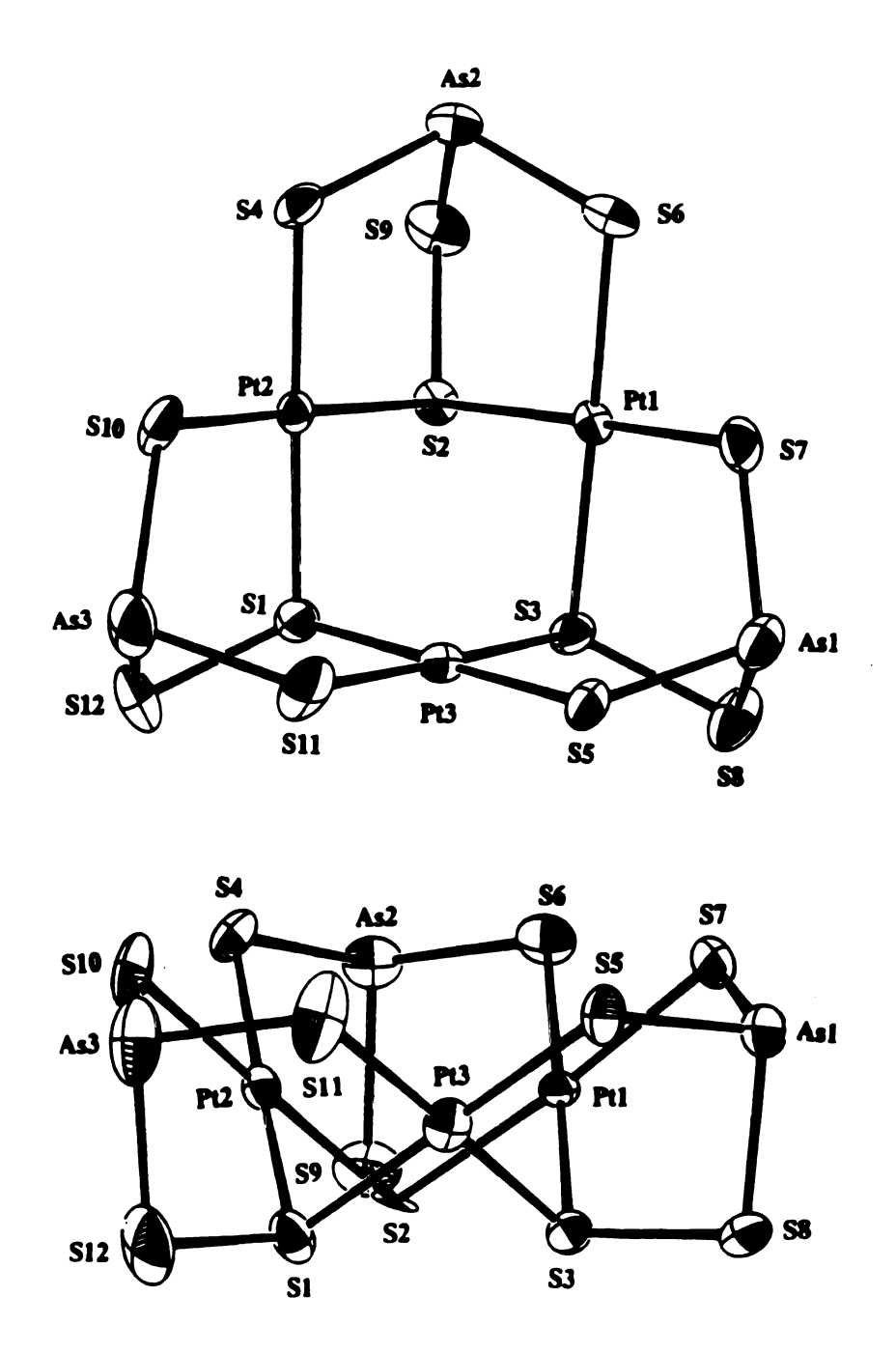


Figure 4-4. Structure and labeling scheme of $[Pt_3(AsS_4)_3]^3$ -.

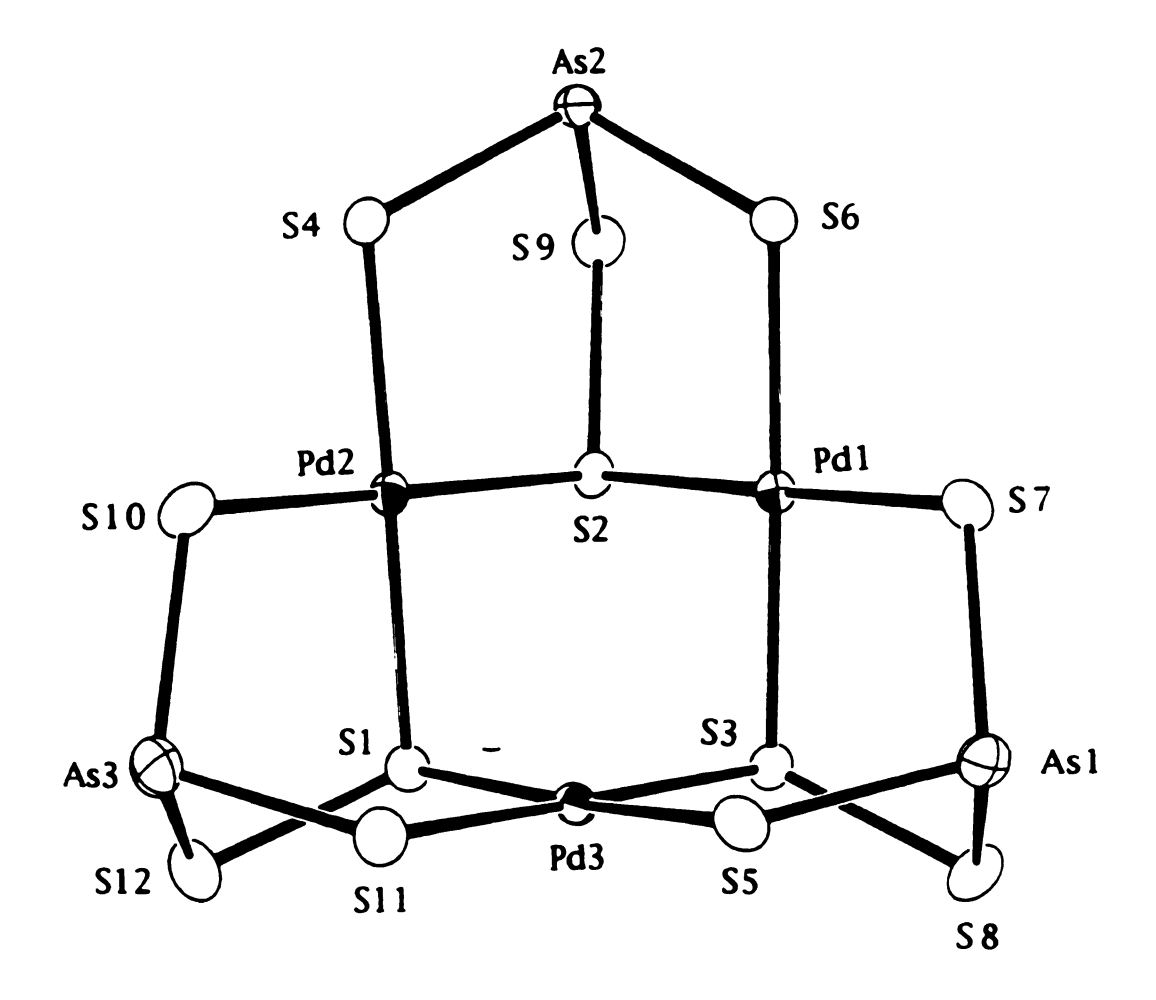


Figure 4-5. Structure and labeling scheme of $[Pd_3(AsS_4)_3]^3$.

3.2 Physicochemical studies

DMF (Ph₄ P)₂ [Pt(As₃S₅)₂] solutions of (Ph₄P)₂K[Pt₃(AsS₄)₃]·1.5H₂O are orange and yellow, respectively, and The far-IR spectra give featureless UV/Vis spectra. $(Ph_4P)_2[Pt(As_3S_5)_2](I)$, $(Ph_4P)_2K[Pt_3(AsS_4)_3]\cdot 1.5H_2O(II)$, and (Ph₄P)₂K[Pd₃(AsS₄)₃]·3MeOH(III) (see Figure 4-6) basically show three sets of absorptions. Observed absorption frequencies of all the complexes are given in Table 4-12. Absorptions in the range of 200-400 cm⁻¹ could be attributed to either M-S or As-S vibration modes. Similar assignments have been made in the far-IR spectra of other known thioarsenic complexes. 16 The additional low energy peaks, at 231 cm^{-1} and 203 cm^{-1} , in $(\text{Ph}_4\text{P})_2[\text{Pt}(\text{As}_3\text{S}_5)_2]$ could be due to M-As For comparsion, in the far-IR spectrum of vibration modes. (Ph₃P)₂Pt(S₄), the 315 and 326 cm⁻¹ peaks were assigned to the Pt-S modes. 17 vibration There is also a S-S vibration for $(Ph_4P)_2K[Pt_3(AsS_4)_3]\cdot 1.5H_2O$ and $(Ph_4P)_2K[Pd_3(AsS_4)_3]\cdot 3MeOH$ at 448 cm⁻¹ and 456 cm⁻¹, respectively. In the previously characterized metal polysulfide complexes, the S-S vibration modes occur in the Some representative example are as follows: similar region. $[Re_4S_{22}]^{4-}$ (465 cm⁻¹), ¹⁸ $[Pd_2S_{28}]^{4-}$ (482 and 453 cm⁻¹), ¹⁹ $[M(S_6)_2]^{2-}$ (M = Zn, Cd, Hg) (495 and 455 cm⁻¹).²⁰

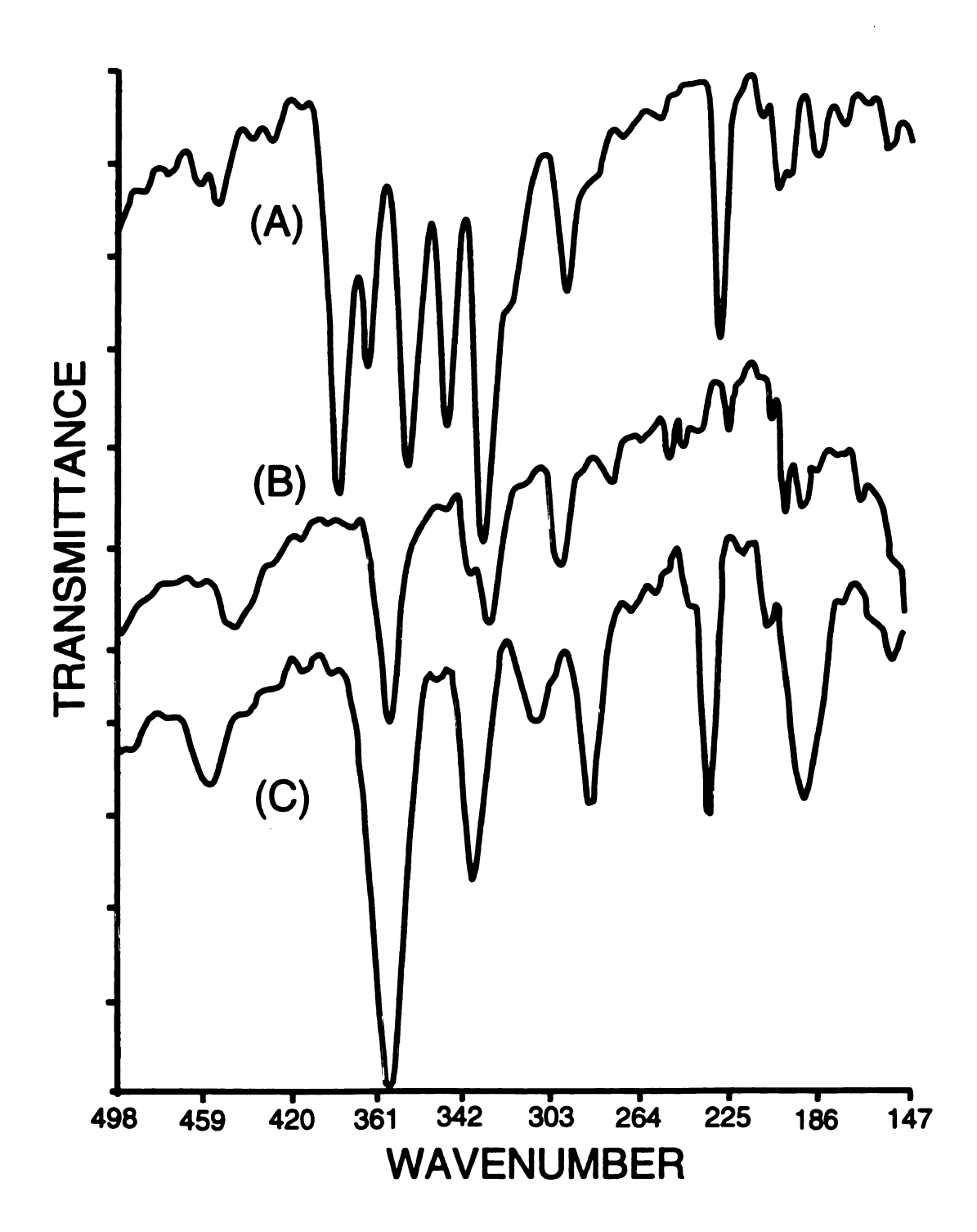


Figure 4-6. Far-IR spectral Data for (A) $(Ph_4P)_2[Pt(As_3S_5)_2](I)$, (B) $(Ph_4P)_2K[Pt_3(AsS_4)_3]\cdot 1.5$ $H_2O(II)$, and (C) $(Ph_4P)_2K[Pd_3(AsS_4)_3]\cdot 3$ MeOH(III).

161

Table 4-12. Far-IR spectral Data for $(Ph_4P)_2[Pt(As_3S_5)_2](I)$, $(Ph_4P)_2K[Pt_3(AsS_4)_3]\cdot 1.5$ H₂O(II), and $(Ph_4P)_2K[Pd_3(AsS_4)_3]\cdot 3$ MeOH(III).

Compounds	Infrared	Raman
I	401(s), 388(m)	305(w), 337(m), 301(m)
	369(s), 351(s)	288(w), 234(s), 182(m)
	334(m), 298(w)	177(m), 160(w)
	231(m), 203(w)	
II	449(w), 377(m)	383(w), 365(m), 336(m)
	331(m, sh), 300(m)	318(s), 297(w), 284(w)
	280(w), 194(w)	269(w), 236(s)
		210(m), 185(m)
III	456(w), 375(s)	391(w), 359(m)
	336(m), 308(w)	307(s), 259(w)
	284(m), 233(m, sh)	208(w), 190(w)
	191(m)	176(w), 157(m)

^{*} s: strong, m; medium, w: weak, sh: shoulder.

FT-Raman spectra of (I), (II), and (III) were also collected. There are a number of peaks in the range between 150 to 400 cm⁻¹. The specific assignments were difficult since these peaks can be assigned to either the As-S or M-S vibration modes. One interesting observation is that we did not see the S-S stretching mode (expected

around 480 cm⁻¹) in either $(Ph_4P)_2K[Pt_3(AsS_4)_3](II)$ or $(Ph_4P)_2K[Pd_3(AsS_4)_3](III)$

Thermal Gravimetric Analysis (TGA) results for all compounds are summarized in Table 4-13 and shown in Figure 4-7 and 4-8. Table 4-13. TGA Data for (Ph₄P)₂[Pt(As₃S₅)₂](I), (Ph₄P)₂K[Pt₃(AsS₄)₃] · 1.5H₂O(II), and (Ph₄P)₂K[Pd₃(AsS₄)₃] · 3MeOH(III).

Compound	Temp. range (°C)	Weight loss (%)
(Ph ₄ P) ₂ [Pt(As ₃ S ₅) ₂]	120 - 550	56.1
(Ph ₄ P) ₂ K[Pt ₃ (AsS ₄) ₃]·1.5H ₂ O	90 - 155	2.0
	330 - 500	45.5
	580 - 800	13.5
(Ph ₄ P) ₂ K[Pd ₃ (AsS ₄) ₃]·3MeOH	50 - 125	3.0
	326 - 530	47.5
	570 - 800	12.8

(Ph₄P)₂[Pt(As₃S₅)₂] showed a one step weight loss of 56.1 % in the temperature range of 120 - 550 °C. The black residue obtained from the decomposition contains Pt, As and S in the 2:1.5:1 ratio. There known phases with Pt/As/S. For are no $(Ph_4P)_2K[Pt_3(AsS_4)_3]\cdot 1.5H_2O$ (II) the 2 % weight loss in the temperature range of 90 - 150 °C is due to the loss of the water molecule. The compound loses 45.5 % of its weight in the second step. For (Ph₄P)₂K[Pd₃(AsS₄)₃]·3MeOH (III) the 3.0 % weight loss in the temperature 50 - 125 °C could be due to the loss of methanol

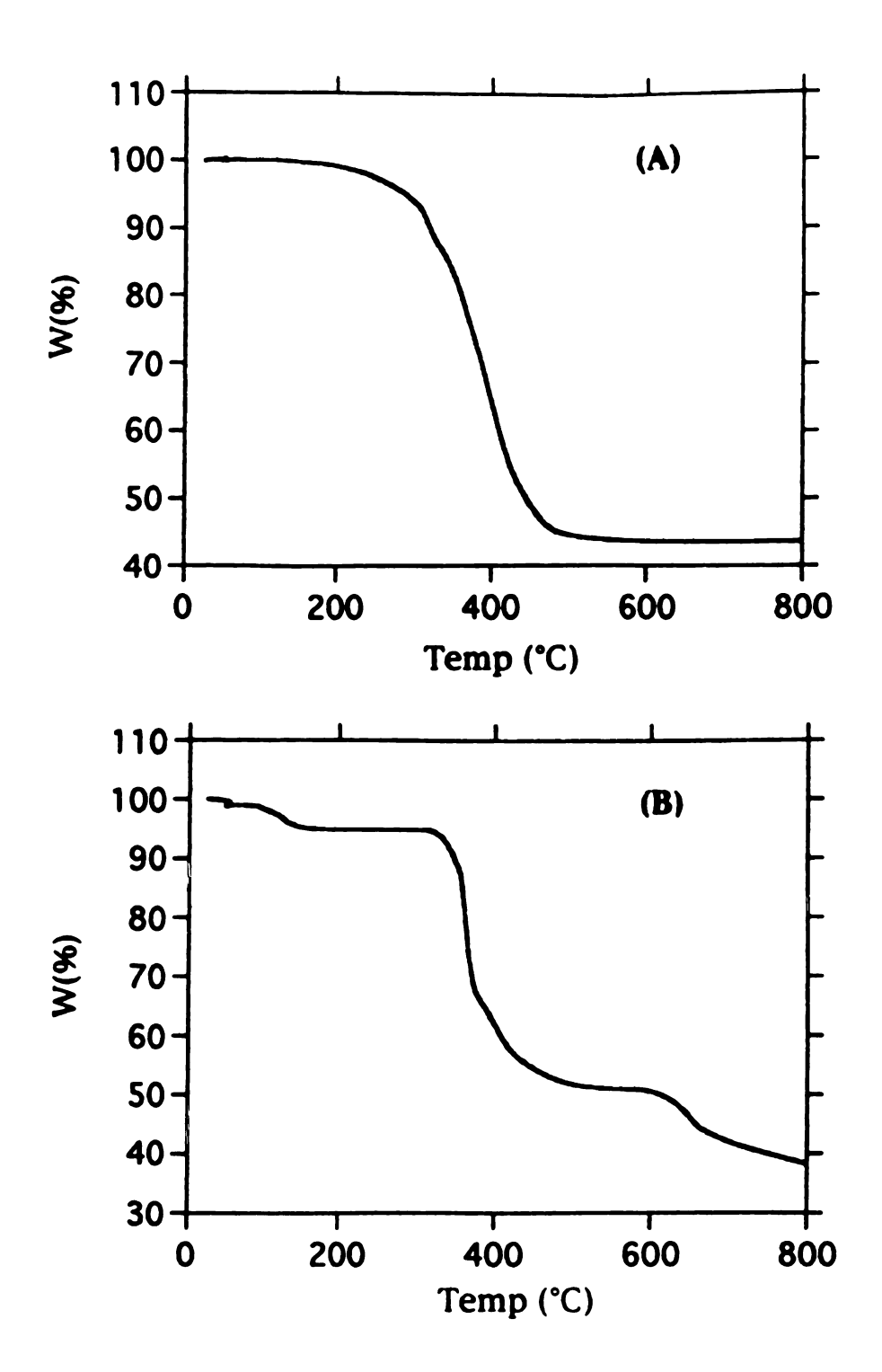


Figure 4-7. TGA diagrams of (A) $(Ph_4P)_2[Pt(As_3S_5)_2](I)$, (B) $(Ph_4P)_2K[Pt_3(AsS_4)_3]\cdot 1.5 H_2O(II)$.

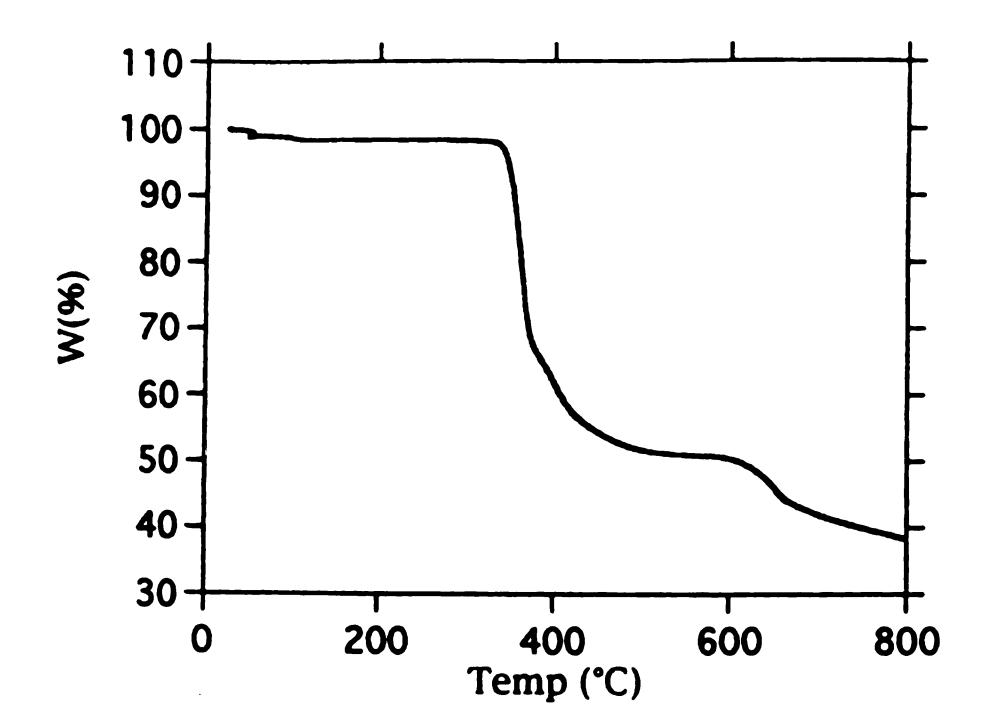


Figure 2-9. TGA diagram of $(Ph_4P)_2K[Pd_3(AsS_4)_3]\cdot 1.5 H_2O(III)$.

molecules. In the next step of weight loss, (III) loses 47.5 % of its mass, as in the case of (II). In both (II) and (III), mass loss continues above 800 °C. The final residue for both (II) and (III), appears by SEM/EDS analysis, contains to K/Pt/As/S and K/Pd/As/S in the similar 1:3:2:1.5 ratio. There are no known quaternary K/Pt/As/S phases.

Three group 10 metal/ As_xQ_y (Q = S, Se) compounds have been synthesized through hydro(methano)thermal reactions. The most unexpected outcome of these reactions is the redox chemistry and the Pt-As bond formation. Attempts to prepare the Pd analog of the $[PtAs_6S_{10}]^{2-}$ anion were unsuccessful due to the fact that Pd^4+ compounds are both thermodynamically and kinetically unstable. Similar to previous observations in metal polychalcogenide chemistry, cation size is very important in determining the type of clusters found in the product. These compounds have so far proven to be inaccessible by conventional solution reactions due to the fact that no common soluble thioarsenate source is available. It is, however, entirely possible that these types of clusters may be accessible if a suitable thioarsenate anion is used.

The structure of $[Pt_3(AsS_4)_3]^{3-}$ is of particular interest in that $[Pt(S_4)_2]^{2-}$ -like fragments can be recognized in the structure. Such fragments reinforce our previous statement that, conceptually, thioarsenic polyanions are similar to polysulfide ligands. With the introduction of the trivalent As atoms the complexity of the product

will no doubt increase dramatically due to an increase in possible connectivity.

In conclusion, the successful hydro(solvo)thermal synthesis of $(Ph_4P)_2[Pt(As_3S_5)_2](I)$, $(Ph_4P)_2K[Pt_3(AsS_4)_3]\cdot 1.5H_2O(II)$, and (Ph₄P)₂K[Pd₃(AsS₄)₃]·3MeOH(III), indicates that not only polymeric solid state compounds, but also formation of large clusters is also possible in the metal/As_xS_y system. The discovery of the new ligands, [As₃S₅]³- and [AsS₄]³-, in these compounds suggests that in addition to the already complex condensation equilibria between the various $[As_x S_y]^{z}$ species, redox reactions also exist in the reaction media. Therefore, the thioarsenate systems are much more complicated in nature than the pure polychalcogenide solutions. three novel clusters reported here represent innovative extensions of the long known platinum/palladium polysulfide chemistry. That coupled with the observation of novel bonding, such as Pt-As bond, justifies further investigations in this area of chemistry. The fact that familiar fragments can be recognized in the [Pt₃(AsS₄)₃]³- make this chemistry even more exciting by virtue of the enormous structure types reported in the metal polychalcogenide chemistry. The introduction of a trivalent As atom in a polychalcogenide chain generates additional structural complexity that is not possible with polychalcogenides only. This forecasts the development of exciting higher-order clusters and solid state chemistry with thioarsenates.

REFERENCES

- 1. (a) Hartley, F. R. The Chemistry of Platinum and Palladium,
 Applied Science Publishers, London, UK, 1973. b) Belluco, U.
 Organometallic and Coordination Chemistry of Platinum,
 Academic Press, London, UK, 1974.
- (a) Roundhill, D. M. Comprensive Coordination Chemistry Vol. 5
 351-531, Pergamon Press, London, UK, 1987. (b) Troitskaya,
 A. D. Shmakova, E. L. Russ. J. Inorg. Chem. (Engl. Transl.) 1971,
 16, 872.
- (a) Jones, P. E.; Katz, L. J. Chem. Soc. Chem. Commun. 1967, 779-783.
 (b) Schmidt, M. Angew. Chem. Int. Ed. Engl. 1973, 12, 445-455.
 (c) Spangenberg, M. Bronger, W. Z. Naturforsch. 1978, 33b, 482-484.
- 4. Kim, K.-W., Kanatzidis, M. G. Inorg. Chem. 1993, 32, 4161-4163.
- 5. Ansari, M. A.; Ibers, J. A. Inorg. Chem. 1989, 28, 4068-4069.
- (a) Sheldrick, W. S. Z. Anorg. Allg. Chem. 1988, 562, 23-30. (b) Sheldrick, W. S.; Hauser, H.-J. Z. Anorg. Allg. Chem. 1988, 557, 98-104. (c) Sheldrick, W. S.; Braunbeck, H. G. Z. Naturforsch. 1989, 44b. 851-852. (d) Parise, J. B. Science 1991, 251, 293-294. (e) Parise, J. B. J. Chem. Soc., Chem. Commun. 1990, 1553-1554.

- (a) Liao, J.-H.; Kanatzidis, M. G. J. Am. Chem. Soc. 1990, 112, 7400-7402.
 (b) Liao, J.-H.; Kanatzidis, M. G. Inorg. Chem. 1992, 31, 431-439.
 (c) Kim, K.-W. Kanatzidis, M. G. J. Am. Chem. Soc. 1992, 114, 4878-4883.
 (d) Dinhgra, S.; Kanatzidis, M. G. Science, 1992, 258, 1769-1772.
 (e) Kim, K.-W.; Kanatzidis, M. G. J. Am. Chem. Soc. 1993, 115, 5871-5872.
- (a) Soghomonian, V.; Chen, Q.; Haushalter R. C.; Zubieta, J.;
 O'Connor, C. J. Science, 1993, 259, 1596-1599. (b)
 Soghomonian, V.; Chen, Q.; Haushalter R. C.; Zubieta, J. Inorg.
 Chem. 1994, 33, 1700-1704. (c) Warren, C. J.; Dhingra, S. S.; Ho,
 D. M.; Haushalter R. C.; Bocarsly, A. B. Inorg. Chem. 1994, 33, 2704-2711. (d) Khan. M. I.; Lee, Y.-S.; O'Connor, C. J.; Haushalter R. C.; Zubieta, J. Inorg. Chem. 1994, 33, 3855-3856.
- 9. Chou, J.-H.; Kanatzidis, M. G. Inorg. Chem. 1994, 33, 1001-1002.
- 10. Sheldrick, W. S.; Kaub, J. Z. Naturforsch. 1985, 40b, 19-21.
- Sheldrick, G. M. In Crystallographic Computing 3; Sheldrick, G.
 M.; Kruger, C.; Goddard, R., Eds.; Oxford University Press: Oxford,
 U.K., 1985; pp 175-189.
- 12. TEXSAN: Single Crystal Structure Analysis Package, Version5.0, Molecular Structure Corp., Woodland, TX.
- 13. Walker, N.; Stuart, D. Acta Crystallogr. 1983, 39A, 158-166.
- (a) Sheldrick, W. J.; Kaub, J. Z. Naturforsch. 1985, 40b, 1130-1133.
 (b) Porter, E. J.; Sheldrick, G. M. J. Chem. Soc. Dalton.

- Trans. 1971, 3130-3134. (c) Zank, G. A.; Rauchfuss, T. B.; Wilson, S. R. J. Am. Chem. Soc. 1984, 106, 7621-7623.
- 15. CERIUS: Single Crystal Structure Analysis Software, Version 5.0, Molecular Simulations Inc. Cambridge, UK.
- (a) Mohammed, A.; Müller, U. Z. Anorg. Allg. Chem. 1985, 523,
 45-53. (b) Sinning, H.; Müller, U. Z. Anorg. Allg. Chem. 1988,
 564, 37-44.
- 17. Wiess, J. Z. Anorg. Allg. Chem. 1986, 542, 137-143.
- 18. Müller, A.; Krickemeyer, E.; Bögge, H. Angew. Chem. Int. Ed. Engl. 1986, 25, 272-272.
- 19. Müller, A.; Schmitz, K.; Krickemeyer, E.; Bögge, H. Angew. Chem. Int. Ed. Engl. 1986, 25, 453-454.
- 20. Müller, A.; Schimanski, J.; Schimanski, U.; Bögge, H. Z. Naturforsch. 1985, 40b, 1277-1288.

CHAPTER 5

HYDROTHERMAL SYNTHESIS OF M/As_XQ_Y (M = Hg²⁺, Q = S, Se) COMPOUNDS. SYNTHESIS AND CHARACTERIZATION OF $(Ph_4P)_2[Hg_2As_4S_9](I), \ (Me_4N)[HgAs_3S_6](II), \\ (Me_4N)[HgAsSe_3](III), \ (Et_4N)[HgAsSe_3](IV), \ and \\ (Ph_4P)_2[Hg_2As_4Se_{11}](V).$

171 ABSTRACT

 $(Ph_4P)_2[Hg_2As_4S_9]$ (I), $(Me_4N)[HgAs_3S_6]$ (II), $(Me_4N)[HgAsSe_3]$ (III), $(Et_4N)[HgAsSe_3]$ (IV), and $(Ph_4P)_2[Hg_2As_4Se_{11}]$ (V) were hydrothermally using mixtures synthesized b y of HgCl₂/2K₃AsS₃/2Ph₄PBr(Me4NCl), HgCl₂/3K₃AsSe₃/4Me₄NCl(Et₄NBr, Ph₄PBr), respectively, in sealed Pyrex tubes. The structures were determined by single-crystal X-ray diffraction analysis. (Ph₄P)₂[Hg₂As₄S₉] crystallizes in the monoclinic space group P2₁/c (No. 14) with a = 10.119(2)Å, b = 18.010(4)Å, c = 14.932(3)Å, $\beta =$ $103.98(2)^{\circ}$, Z = 4, $V = 2640(2)^{4}$. [Hg₂As₄S₉]_n²ⁿ has a onedimensional polymeric chain structure consisting of trigonal planar Hg²⁺ and linear [As₄S₉]⁶⁻ units formed by corner sharing [AsS₃]³⁻ units. (Me₄N)[HgAs₃S₆] crystallizes in the monoclinic space group C2/c (No. 15) with a = 18.607(7)Å, b = 7.126(1)Å, c = 26.524(6), $\beta =$ 91.87(2)°, Z = 8, $V = 3515(3)Å^3$. The anionic [HgAs₃S₆]_nⁿ possesses a two-dimensional layered structure with distorted tetrahedral Hg²⁺ and corner sharing AsS3³ units. The Me₄N+ cations are located The interlayer distance is 9.303Å. between the layers. (Me₄N)[HgAsSe₃] and (Et₄N)[HgAsSe₃] both crystallize in the monoclinic space group P2₁/n (No. 14) with a = 7.115(1)Å, b =17.464(5)Å, c = 9.356(2)Å, $\beta = 91.34(1)^{\circ}$, Z = 4, V = 1162.2(7)Å³ for the former and a = 7.175(2)Å, b = 18.907(4)Å, c = 10.897(3)Å, $\beta =$ 99.56(2)°, Z = 4, $V = 1457(1)Å^3$ for the latter. They have the same one-dimensional chain-like anionic framework with trigonal planar Hg²⁺ and [AsSe₃]³⁻ units. (Ph₄P)₂[Hg₂As₄Se₁₁] crystallizes in the triclinic space group P-1 (No. 2) with a = 10.329(2)Å, b = 17.017(3)Å,

c=17.485(3)Å, $\alpha=92.70(1)$, $\beta=105.73(1)$ °, $\gamma=103.71(1)$, Z=2, V=2853(1)Å 3 . [Hg₂As₄Se₁₁] $_n^{2n}$ also possess a one-dimensional chain-like structure consisting of both trigonal-planar and tetrahedral Hg²⁺ ions. It too contains a unique [As₄Se₁₁] 6 ligand which binds to four Hg²⁺ ions. The solid state optical and infrared spectra of these compounds are reported.

1. Introduction

Recently, research carried out in this group and others has shown that the hydro(solvo)thermal technique is a useful synthetic tool toward the synthesis of novel transition and main group metal polychalcogenides that are often inaccessible by traditional solution methods. $^{1-3}$ Parise and co-workers also adopted this methodology to investigate the Sb_xS_y system and have reported some very interesting results. 4

We have extended this chemistry to explore the possibility of applying the hydrothermal technique to systems containing metal atoms, $[AsS_3]^{3-}$ and organic counterions R_4E^+ (E=P, R=Ph; E=N, R=alkyl) and have successfully synthesized several new metal thioarsenate compounds, including $[InAs_3S_7]^{2-}$, $[BiAs_6S_{12}]^{3-}$, $[SnAs_4S_9]^{2-}$, $[NiAs_4S_8]^{2-}$, $[Mo_2O_2As_2S_7]^{2-}$, $[Pt(As_3S_5)_2]^{2-}$, $[Pt_3(AsS_4)_3]^{3-}$. The structures of these compounds range from molecular to one-dimensional chains to two-dimensional layers. In these compounds the $[AsS_3]^{3-}$ anion shows a facile condensation ability that results in higher nuclearity $[As_xS_y]^{n-}$ units which are found coordinated to the metal cations.

Here we will explore if this chemistry can be extended to the Hg/As_xQ_y (Q = S, Se) systems. In this chapter, we describe the synthesis and characterization of five new compounds, $(Ph_4P)_2[Hg_2As_4S_9](I)$, $(Me_4N)[HgAs_3S_6](II)$, $(Me_4N)[HgAs_3S_6](II)$, $(Et_4N)[HgAs_3S_6](IV)$, and $(Ph_4P)_2[Hg_2As_4S_{e_11}](V)$.

2. Experimental Section

2.1. Reagents

Chemicals in this work, other than solvents, were used as obtained: (i) selenium powder, ~ 100 mesh, 99.5% purity, Mercury chloride, HgCl₂, 99.5% purity, tetraphenylphosphonium bromide, Ph₄PBr, 99% purity, tetramethylammonium chloride, Me₄NCl, 99% purity, tetraethylammonium bromide, Et₄NBr, 99% purity, Aldrich Chemical Company, Inc., Milwaukee, WI; (ii) arsenic sulfide, As₂S₃, 100 mesh, 99% purity, arsenic selenide, As₂Se₃, 200 mesh, 99% purity, Cerac Inc. Milwaukee WI; (iii) potassium metal, analytical reagent, Mallinckrodt Inc., Paris, KY; (iv) Methanol, anhydrous, Mallinckrodt Inc., Paris, KY; diethyl ether, ACS anhydrous, EM Science, Inc., Gibbstown, NJ.

2.2. Physical Measurements

for details see chapter 2.

2.3. Synthesis

All syntheses were carried out under a dry nitrogen atmosphere in a vacuum atmosphere Dri-Lab glovebox except were specifically mentioned.

K3AsS3 (K3AsSe3) was synthesized by using stoichiometric amounts of alkali metal, arsenic sulfide(selenide), and sulfur(selenium) in liquid ammonia. The reaction gives a yellow (orange) brown powder upon evaporation of ammonia.

(Ph₄P)₂[Hg₂As₄S₉](I): A Pyrex tube (~ 4 mL) containing HgCl₂ (0.087 g, 0.5 mmol), K₃AsS₃ (0.144 g, 0.5 mmol), Ph₄PBr (0.419 g, 1 mmol) and 0.3 mL of water was sealed under vacuum and kept at 130 °C for one week. The large pale yellow transparent rod-like crystals that formed were isolated in MeOH and washed with ether. (Yield = 84.5%, based on Hg) Semiquantitative microprobe analysis of several single crystals gave P:Hg:As:S = 1:1.2:1:7.

(Me4N)[HgAs₃S₆](II): A mixture of HgCl₂ (0.087 g, 0.5 mmol), K₃AsS₃ (0.144 g, 0.5 mmol) and Me₄NCl (0.110 g, 1 mmol) was sealed under vacuum with 0.3-0.5 mL of water in a Pyrex tube(4 mL). The reaction was run at 130 °C for one week. The large pale yellow transparent crystals were isolated in H₂O and washed with methanol and diethyl ether. (Yield = 75.7 % based on Hg) Semiquantitative microprobe analysis of several single crystals gave Hg:As:S = 1:3:9. The presence of tetramethylammonium cations was confirmed by infrared spectroscopy.

(Me4N)[HgAsSe3](III): An amount of 0.03 g (0.1 mmol)

HgCl2, 0.13 g (0.3 mmol) K3AsSe3, 0.07 g (0.6 mmol) Me4NCl were

thoroughly mixed and sealed in a thick-wall Pyrex tube with 0.3 mL

of H2O. The reaction was run at 110 °C for 2 days. The products

were isolated by dissolving the excess starting material and KCl with

H2O and methanol and then washing with anhydrous ether to give

O-O5 g of yellow rod-like crystals (55 % yield based on Hg). Semi
antitative microprobe analysis on single crystals gives

tetramethylammonium cations was confirmed by infrared spectroscopy.

(Et₄N)[HgAsSe₃](IV): An amount of 0.03 g (0.1 mmol) HgCl₂, 0.13 g (0.3 mmol) K₃AsSe₃, 0.13 g (0.6 mmol) Et₄NBr were thoroughly mixed and sealed in a thick-wall Pyrex tube with 0.3 mL of H₂O. The reaction was run at 110 °C for 2 days. The products were isolated as above to give 0.065 g of yellow-orange rod-like crystals (yield = 55 % based on Hg) Semi-quantitative microprobe analysis of several single crystals gives as the formula Hg₁As_{1.2}Se_{3.3}. The presence of the tetraethylammonium cations was confirmed by infrared spectroscopy.

 $(Ph_4P)_2[Hg_2As_4Se_{11}](V)$: An amount of 0.03 g (0.1 mmol) $HgCl_2$, 0.14 g (0.3 mmol) K_3AsSe_3 , 0.24 g (0.6 mmol) Ph_4PBr were thoroughly mixed and sealed in a thick-wall Pyrex tube with 0.5 mL of H_2O . The reaction was run at 110 °C for one week. The dark-red chunky crystal were isolated as above.(0.076 g Yield = 76 %, based on Hg). Semi-quantitative microprobe analysis of several single crystals gives as the formula $P_1Hg_1As_{2.8}Se_{7.3}$.

2.4 X-ray crystallography

(Ph₄P)₂[Hg₂As₄S₉](I): Single-crystal X-ray diffraction data were collected on a P3 Nicolet four-circle diffractometer by using the -2θ scan mode and graphite monochromated Mo Kα radiation at -100 °C. During the structure refinement, we found the position of the S5 atom very close to the special position (1/2, 1, 1). However, fixing the S5 atom in (1/2, 1, 1) resulted in an increased temperature

factor, with the As2-S5 bond distance becoming too short. A better refinement as well as a more reasonable As-S distance was obtained if the S5 atom was displaced away from the special position. The S5 atom was finally refined with 0.5 occupancy. The As2 and the S4 atoms were also found to be disordered between two sites, as a result of the S5 deviation, and the occupancy of the two sites were refined to be 0.47 and 0.53 respectively. The positions of all hydrogen atoms were calculated by using a C-H distance of 0.96Å. The scattering contribution of the hydrogen atoms was included in the structure factor calculation; but their positions were not refined.

 $(Me_4N)[HgAs_3S_6](II)$: Single-crystal X-ray diffraction data were collected at -100 °C on a Rigaku AFC6 diffractometer (Mo K α radiation) by using the ω -20 scan mode.

 $(Me_4N)[HgAsSe_3](III)$: Single-crystal X-ray diffraction data were collected with a Nicolet P3 four-circle automated diffractometer with a graphite-crystal monochromater at -100 °C. The data were collected by the θ -2 θ scan technique.

(Et₄N)[HgAsSe₃](IV): Single-crystal X-ray diffraction data were collected with a Nicolet P3 four-circle automated diffractometer with a graphite-crystal monochromater at -100 °C. The data were collected by the θ -2 θ scan technique.

(Ph4P)₂[Hg₂As₄Se₁₁](V): The same procedure described ≥ above was used..

None of the crystals showed any significant intensity decay as judged by three check reflections measured every 150 reflections throughout the data collection. The space groups were determined from systematic absences and intensity statistics. The structures were solved by using the direct method technique of SHELXS-869 and refined by the full-matrix least-squares techniques of the TEXSAN¹⁰ software package of crystallographic programs. An empirical absorption correction based on ψ -scans was applied to each data set, followed by a DIFABS¹¹ correction to the isotropically refined structure. All non-hydrogen atoms except nitrogen and carbon were refined anisotropically. All calculations were performed on a VAXstation 3100 Model 76 computer.

The complete data collection parameters and details of the structure solutions and refinements are given in Tables 5-1 and 5-2. The fractional atomic coordinates, average temperature factors and their estimated standard deviations are given in Tables 5-3, 4, 5, 6, 7.

Table 5-1. Crystallographic Data for $(Ph_4P)_2[Hg_2As_4S_9](I)$, $(Me_4N)[HgAs_3S_6](II)$

	I	II
Formula	C48H40P2Hg2As4S9	C4H ₁₂ NHgAs ₃ S ₆
F. w.	1666.89	691.37
a, Å	10.119(2)	18.607(7)
b, Å	18.010(3)	7.126(1)
с, Å	14.932(3)	26.524(6)
α, deg.	90.00	90.00
β, deg.	103.98(2)	91.87(2)
γ, deg.	90.00	90.00
Z, V, Å ³	4, 2640(2)	8, 3515(2)
Space Group	$P2_1/n$ (No. 14)	C2/c (No. 15)
color, habit	pale yellow, plate	pale yellow, plate
D _{calc} , g/cm ³	2.01	2.62
Radiation	Μο Κα	Μο Κα
μ, cm ⁻¹	180.27	150.14
2θ _{max} , deg.	45.0	45.0
Absorption Correction	ψ scan	ψ scan
Transmission Factors	0.14-1.00	0.16-1.00
Index ranges	$0 \le h \le 11, 0 \le k \le 20,$	$0 \le h \le 22, \ 0 \le k \le 8$
	-17 ≤ l ≤ 17	$-30 \le l \le 30$
No. of Data coll.	4148	3567
Unique reflections	3624	3362
•		

Data Used	2028	1820	
$(F_o^2 > 3\sigma(F_o^2))$			
No. of Variables	188	116	
Final Ra/Rwb, %	5.8/4.7	7.2/9.3	

^a R= $\Sigma(|F_0|-|F_c|)/\Sigma|F_0|$, ^b R_w= $\{\Sigma_w(|F_0|-|F_c|)^2/\Sigma_w|F_0|^2\}^{1/2}$

181
Table 5-2. Crystallographic Data for (Me₄N)[HgAsSe₃](III), (Et₄N)[HgAsSe₃](IV), and (Ph₄P)₂[Hg₂As₄Se₁₁)](V)

	III	I V	V
Formula	C ₄ H ₁₂ NHgAsSe ₃	C ₈ H ₂₀ NHgAsSe ₃	C ₄₈ H ₄₀ P ₂ H _{g2} As ₄
			Se ₁₁
F. w.	586.40	642.40	2247.45
a, Å	7.115(1)	7.175(2)	10.329(2)
b, Å	17.464(5)	18.907(4)	17.017(3)
c, Å	9.356(2)	10.897(3)	17.485(3)
α, deg.	90.00	90.00	92.70(1)
β, deg.	91.34(1)	99.56(2)	105.73(1)
γ, deg.	90.00	90.00	103.71(1)
Z, V, Å ³	4, 1162.2(7)	4, 1457(1)	2, 2853(1)
Space Group	P21/n(No 14)	P21/n(No.14)	P-1 (No. 2)
color, habit	yellow, block	yellow, block	red, block
D _{cal} , g/cm ³	3.35	2.93	2.62
Radiation	Μο Κα	Μο Κα	Μο Κα
μ, cm ⁻¹	253.12	201.93	147.06
2θ _{max} , deg.	45.00	45.00	45.00
Absorption	ψ scan	ψ scan	ψ scan
Correction			
Transmission	0.15-1.00	0.14-1.00	0.15-1.00
Factors			

		182	
Index ranges	$0 \le h \le 8$	$0 \le h \le 8$	$-12 \le h \le 12,$
	$0 \le k \le 19$	$0 \le k \le 21$	$0 \le k \le 19,$
	$-11 \le l \le 11$	$-12 \le l \le 12$	$-19 \le l \le 19$
No. of Data coll.	1785	2222	8126
Unique	1161	1991	4277
reflections			
Data Used	772	1574	4277
$(F_o^2 > 3\sigma(F_o^2))$			
No. of Variables	66	8 2	364

^a R= $\Sigma(|F_0|-|F_c|)/\Sigma|F_0|$, ^b R_w= $\{\Sigma_w(|F_0|-|F_c|)^2/\Sigma_w|F_0|^2\}^{1/2}$

Final R^a/R^{b} , % 3.5/2.6 3.0/3.1 6.7/7.1

Table 5-3. Selected Atomic Coordinates and Estimated Standard Deviations (esd's) of (Ph₄P)₂[Hg₂As₄S₉]

atom	X	Y	Z	B_{eq}^{a} , (A^2)
Hg1	1.09698(1)	0.91918(7)	0.94178(7)	2.14(4)
As1	0.7588(2)	0.9214(2)	0.9457(2)	1.8(1)
As2	0.4474(5)	0.9172(4)	0.9665(6)	1.6(3)
As2B	0.4819(5)	0.9018(3)	1.0356(6)	2.0(6)
S 1	0.6242(6)	0.8317(4)	0.9861(5)	3.3(3)
S2	0.8856(6)	0.8478(4)	0.8794(4)	2.7(3)
S 3	1.0965(7)	1.0543(3)	0.9155(4)	2.7(3)
S4	0.295(1)	0.836(1)	0.911(2)	3.1(5)
S4B	1.308(1)	0.858(1)	1.033(1)	2.6(5)
S 5	0.547(1)	1.0060(8)	1.0739(9)	3.0(1)
P1	0.2239(6)	0.0809(4)	0.4147(4)	2.3(3)
C1	0.359(2)	0.132(1)	0.386(1)	1.8(5)
C2	0.412(2)	0.111(1)	0.310(1)	1.6(4)
C3	0.503(2)	0.157(1)	0.285(2)	3.1(6)
C4	0.541(2)	0.224(1)	0.329(2)	2.3(5)
C5	0.500(2)	0.242(1)	0.406(2)	2.5(5)
C6	0.408(2)	0.197(1)	0.431(1)	1.9(5)
C7	0.069(2)	0.121(1)	0.351(1)	1.6(5)
C8	0.066(2)	0.195(1)	0.334(2)	2.4(5)
C9	-0.055(2)	0.227(1)	0.284(2)	3.5(6)
C10	-0.172(3)	0.182(2)	0.242(2)	4.2(6)
C11	-0.165(3)	0.108(2)	0.265(2)	3.7(6)

C12	-0.046(2)	0.079(2)	0.319(1)	2.6(5)	
C13	0.227(2)	-0.013(1)	0.382(1)	1.5(4)	
C14	0.255(2)	-0.071(2)).449(2)	3.0(5)	
C15	0.257(3)	-0.145(2)	0.417(2)	4.5(7)	
C16	0.233(3)	-0.164(2)	0.324(2)	4.0(6)	
C17	0.205(2)	-0.102(2)	0.255(2)	3.8(6)	
C18	0.200(2)	-0.031(1)	0.289(1)	2.1(5)	
C19	0.239(2)	0.087(1)	0.535(1)	2.5(5)	
C20	0.130(2)	0.115(1)	0.568(2)	3.1(6)	
C21	0.144(2)	0.119(1)	0.663(2)	3.1(6)	
C22	0.260(2)	0.096(1)	0.725(2)	3.2(6)	
C23	0.369(2)	0.072(2)	0.693(2)	3.5(5)	
C24	0.359(2)	0.067(2)	0.596(2)	3.8(6)	

^a $B_{eq}=(4/3)[a^2B_{11} + b^2B_{22} + c^2B_{33} + ab(\cos\gamma)B_{12} + ac(\cos\beta)B_{13} + bc(\cos\alpha)B_{23}]$

Table 5-4. Selected Atomic Coordinates and Estimated Standard Deviations (esd's) of (Me₄N)[HgAs₃Se₆]

atom	X	Y	Z	$B_{eq}^{a}, (A^2)$
Hg	0.76646(7)	1.0918(2)	0.55382(6)	1.77(5)
As1	0.7375(2)	0.0086(5)	0.6852(1)	1.4(1)
As2	0.7929(2)	0.6042(4)	0.5675(1)	1.3(1)
As3	0.7899(2)	0.4780(4)	0.6916(1)	1.3(1)
S1	0.8404(4)	0.377(1)	0.5208(3)	1.3(1)
S2	0.8427(4)	0.621(1)	0.7601(3)	2.0(4)
S 3	0.6861(5)	0.166(1)	0.6221(3)	2.0(4)
S 4	0.8352(4)	0.184(1)	0.7058(4)	2.2(4)
S 5	0.8468(5)	0.839(1)	0.5305(3)	1.6(3)
S 6	0.8693(4)	0.599(1)	0.6385(3)	1.8(3)
N	0.037(2)	0.130(6)	0.627(2)	6(1)
C1	0.016(6)	-0.04(2)	0.651(5)	17(1)
C2	-0.011(6)	0.20(1)	0.590(5)	16(1)
C3	0.110(4)	0.134(9)	0.607(30	2(1)
C4	0.034(4)	0.30(1)	0.670(4)	11(1)

^a $B_{eq}=(4/3)[a^2B_{11} + b^2B_{22} + c^2B_{33} + ab(\cos\gamma)B_{12} + ac(\cos\beta)B_{13} + bc(\cos\alpha)B_{23}]$

186
Table 5-5. Selected Atomic Coordinates and Estimated Standard
Deviations (esd's) of (Me₄N)[HgAsSe₃]

atom	X	Y	Z	$B_{eq}^{a}, (A^2)$
Hg	0.13217(9)	0.95396(6)	0.1684(1)	1.27(4)
As	-0.3584(2)	0.9499(1)	0.1158(2)	1.1(1)
Se(1)	0.4031(2)	0.8567(1)	0.1456(2)	1.3(1)
Se(2)	-0.1535(2)	0.9060(1)	0.3058(2)	1.3(1)
Se(3)	-0.1813(2)	0.9077(1)	-0.0860(2)	1.3(1)
N	0.633(2)	0.167(1)	0.389(2)	1.1(3)
C(1)	0.583(2)	0.087(2)	0.428(3)	2.8(4)
C(2)	0.678(2)	0.171(2)	0.243(3)	2.7(5)
C(3)	0.470(2)	0.217(1)	0.415(3)	2.5(4)
C(4)	0.790(3)	0.193(2)	0.481(3)	3.0(5)

^a $B_{eq}=(4/3)[a^2B_{11} + b^2B_{22} + c^2B_{33} + ab(\cos\gamma)B_{12} + ac(\cos\beta)B_{13} + bc(\cos\alpha)B_{23}]$

187
Table 5-6. Selected Atomic Coordinates and Estimated Standard
Deviations (esd's) of (Et4N)[HgAsSe3]

atom	X	Y	Z	$B_{eq}^{a}, (A^2)$
Hg	0.15460(6)	0.53578(2)	0.14957(5)	0.84(2)
As	-0.3457(1)	0.53887(6)	0.1045(1)	0.54(4)
Se(1)	0.4274(2)	0.62365(6)	0.1415(1)	0.92(5)
Se(2)	0.2009(2)	0.41131(6)	0.0591(1)	0.77(5)
Se(3)	-0.1051(2)	0.56705(6)	0.2776(1)	0.76(5)
N	0.239(1)	0.1731(5)	0.831(1)	0.9(2)
C(1)	0.252(2)	0.1645(6)	0.695(1)	1.0(2)
C(2)	0.136(1)	0.1077(6)	0.868(1)	0.8(2)
C(3)	0.438(2)	0.1790(6)	0.911(1)	1.1(2)
C(4)	0.137(2)	0.2410(6)	0.854(1)	0.7(2)
C(5)	0.344(2)	0.2260(6)	0.640(1)	1.6(2)
C(6)	0.107(2)	0.1047(7)	1.000(1)	2.2(3)
C(7)	0.572(2)	0.1196(6)	0.899(1)	1.4(2)
C(8)	-0.064(2)	0.2447(7)	0.787(1)	2.0(3)

^a $B_{eq}=(4/3)[a^2B_{11} + b^2B_{22} + c^2B_{33} + ab(\cos\gamma)B_{12} + ac(\cos\beta)B_{13} + bc(\cos\alpha)B_{23}]$

188

Table 5-7. Selected Atomic Coordinates and Estimated Standard

Deviations (esd's) of (Ph₄P)₂[Hg₂As₄Se₁₁]

atom	X	Y	Z	B_{eq}^{a} , (A^2)
Hg(1)	0.2290(1)	0.13758(8)	0.36837(8)	2.30(5)
Hg(2)	0.2230(1)	0.33493(9)	0.24541(9)	3.09(6)
As(1)	-0.0881(3)	0.2007(2)	0.3865(2)	2.0(1)
As(2)	-0.1573(3)	0.3269(2)	0.2369(2)	1.8(1)
As(3)	0.5554(3)	0.1267(2)	0.3187(2)	2.5(1)
As(4)	0.4518(3)	0.2530(2)	0.1624(2)	2.5(1)
Se(1)	0.1818(3)	0.1233(2)	0.2111(2)	2.4(1)
Se(2)	0.4725(3)	0.1135(2)	0.4292(2)	2.2(1)
Se(3)	0.0100(3)	0.0924(2)	0.4149(2)	2.6(1)
Se(4)	0.0109(3)	0.3891(2)	0.1748(2)	2.0(1)
Se(5)	0.3794(4)	0.3727(2)	0.1525(2)	4.0(2)
Se(6)	0.2872(3)	0.3090(2)	0.3911(2)	2.0(1)
Se(7)	-0.1121(3)	0.1940(2)	0.2469(2)	2.3(1)
Se(8)	-0.3453(3)	0.2963(2)	0.1153(2)	2.7(1)
Se(9)	0.3617(3)	0.0595(2)	0.2071(2)	2.9(1)
Se(10)	0.0973(3)	0.3249(2)	0.4349(2)	2.5(1)
Se(11)	0.5528(3)	0.2670(2)	0.3049(2)	2.4(1)
P(1)	0.5671(7)	0.3389(4)	0.6809(4)	1.4(3)
P(2)	0.1153(7)	0.1936(4)	0.8649(4)	1.4(4)
C (1)	0.700(2)	0.364(2)	0.632(2)	1.3(5)
C (2)	0.677(3)	0.321(2)	0.555(2)	1.5(2)
C(3)	0.778(3)	0.346(2)	0.518(2)	2.1(6)
C (4)	0.899(3)	0.412(2)	0.549(2)	1.7(5)

C(5)	0.914(3)	0.453(2)	0.623(2)	2.2(6)
C(6)	0.815(3)	0.430(2)	0.664(2)	2.3(6)
C(7)	0.457(3)	0.407(2)	0.660(2)	1.6(5)
C(8)	0.448(3)	0.448(2)	0.593(2)	2.3(6)
C(9)	0.360(3)	0.500(2)	0.577(2)	3.0(7)
C(10)	0.285(3)	0.513(2)	0.632(2)	2.4(6)
C(11)	0.293(3)	0.472(2)	0.696(2)	3.4(7)
C(12)	0.379(3)	0.419(2)	0.710(2)	3.2(7)
C(13)	0.645(3)	0.350(2)	0.786(2)	1.6(5)
C(14)	0.703(3)	0.432(2)	0.826(2)	1.9(6)
C(15)	0.772(3)	0.439(2)	0.907(2)	2.8(6)
C(16)	0.776(3)	0.373(2)	0.949(2)	2.6(6)
C(17)	0.716(3)	0.296(2)	0.909(2)	3.5(7)
C(18)	0.649(3)	0.282(2)	0.832(2)	2.0(6)
C(19)	0.478(3)	0.232(2)	0.649(2)	1.8(6)
C(20)	0.549(3)	0.178(2)	0.652(2)	1.8(6)
C(21)	0.475(3)	0.095(2)	0.630(2)	3.4(7)
C(22)	0.334(3)	0.074(2)	0.613(2)	2.4(6)
C(23)	0.258(3)	0.130(2)	0.607(2)	2.7(6)
C(24)	0.326(3)	0.213(2)	0.627(2)	2.3(6)
C(25)	0.250(3)	0.138(3)	0.878(2)	2.1(6)
C(26)	0.335(3)	0.138(2)	0.956(2)	1.9(6)
C(27)	0.442(3)	0.101(2)	0.968(2)	2.5(6)
C(28)	0.460(3)	0.058(2)	0.900(2)	3.9(8)
C(29)	0.373(3)	0.055(2)	0.826(2)	3.1(7)
C(30)	0.269(3)	0.093(2)	0.814(2)	3.0(7)
C(31)	0.012(2)	0.160(2)	0.932(2)	1.4(5)

C(32)	0.005(2)	0.215(2)	0.992(2)	1.5(5)	
C(33)	-0.075(3)	0.186(2)	1.040(2)	2.2(6)	
C(34)	-0.141(3)	0.106(2)	1.037(2)	1.9(6)	
C(35)	-0.126(3)	0.050(2)	0.979(2)	3.4(7)	
C(36)	-0.050(3)	0.079(2)	0.925(2)	2.9(7)	
C(37)	0.193(2)	0.302(1)	0.889(1)	0.7(5)	
C(38)	0.108(3)	0.354(2)	0.877(2)	2.3(6)	
C(39)	0.167(3)	0.437(2)	0.888(2)	3.7(7)	
C(40)	0.310(3)	0.468(2)	0.910(2)	3.4(7)	
C(41)	0.401(3)	0.420(2)	0.922(2)	2.7(6)	
C(42)	0.335(3)	0.333(2)	0.909(2)	2.7(6)	
C(43)	0.016(3)	0.177(2)	0.763(2)	1.7(5)	
C(44)	0.042(3)	0.232(2)	0.709(2)	.19(6)	
C(45)	-0.028(3)	0.219(2)	0.632(2)	2.9(7)	
C(46)	-0.134(3)	0.150(2)	0.598(2)	2.9(7)	
C(47)	-0.163(3)	0.096(2)	0.651(2)	2.2(6)	
C(48)	-0.093(3)	0.107(2)	0.730(2)	3.1(7)	

^a $B_{eq}=(4/3)[a^2B_{11} + b^2B_{22} + c^2B_{33} + ab(\cos\gamma)B_{12} + ac(\cos\beta)B_{13} + bc(\cos\alpha)B_{23}]$

The compounds were examined by X-ray powder diffraction for the purpose of phase purity and identification. Accurate dhk1 spacings (Å) were obtained from the powder patterns recorded on a calibrated (with FeOCl as internal standard) Phillips XRG-3000 computer-controlled powder diffractometer with graphite-monochromated Cu Kα radiation operating at 35 kV and 35 mA. The data were collected at a rate of 0.12°/min. Based on the atomic coordinates obtained from the X-ray single crystal diffraction studies, X-ray powder patterns for all compounds were calculated by the software package CERIUS.¹¹ Calculated and observed X-ray powder patterns that show d-spacings and intensities of strong hkl reflections are complied in tables 5-8 to 5-12.

Table 5-8. Calculated and Observed X-ray Powder Diffraction Pattern of (Ph₄P)₂[Hg₂As₄S₉](I).

h	k	l	d _{calc} (Å)	d _{obs} (Å)	I/I _{max} (obs, %)
0	1	1	11.29	11.28	100
0	2	0	9.00	9.00	1 4
0	2	0	8.21	8.21	7
0	0	2	7.24	7.23	26
0	2	2	5.64	5.64	6
0	1	3	4 66	4.66	1 4
0	4	0	4.50	4.50	9
2	1	1	4.22		
0	5	1	3.49		
3	0	-3	3.07		
3	4	0	2.647	2.64	5

Table 5-9. Calculated and Observed X-ray Powder Diffraction Pattern of (Me₄N)[HgAs₃S₆](II).

h	k	l	d _{calc} (Å)	d _{obs} (Å)	I/I _{max} (obs, %)
0	0	2	13.2	13.2	7
2	0	0	9.298	9.29	100
2	0	-2	7.73	7.72	10
1	1	-1	6.47		
2	0	-4	5.48	5.48	7
4	0	0	4.65	4.64	8
4	0	-2	4.43	4.42	7
3	1	2	4.37	4.36	10
0	2	1	3.53		
2	2	0	3.32		
2	0	8	3 08	3.08	10
4	0	8	2.65		

Table 5-10. Calculated and Observed X-ray Powder Diffraction Pattern of (Me₄N)[HgAsSe₃](III).

h	k	1	d _{calc} (Å)	d _{obs} (Å)	I/I _{max} (obs, %)
0	2	0	8.73	8.73	8 5
0	1	1	8.24	8.23	100
1	1	0	6.58	6.58	12
0	2	1	6.38	6.37	58
1	0	-1	5.72	5.72	10
1	2	-1	4.79	4.78	10
1	3	0	4 50	4.50	12
0	4	1	3.95	3.95	28
1	1	2	3.77	3.76	37
1	2	2	3.53		
2	1	1	3.24	3.24	14
0	1	3	3.07	3.07	16
2	3	1	2.87	2.87	11
2	2	-2	2.720	2.720	15
2	2	2	2.665	2.665	11
1	3	3	2.546	2.546	11
2	5	0	2.492	2.491	19
0	7	2	2.202		
2	4	-3	2.084		

Table 5-11. Calculated and Observed X-ray Powder Diffraction Pattern of (Et4N)[HgAsSe3](IV).

h	k	l	d _{calc} (Å)	d _{obs} (Å)	I/I _{max} (obs, %)
0	2	0	9.45	9.44	72
0	1	1	9.34	9.33	100
0	2	1	7.10	7.09	19
1	1	0	6.62	6.62	9
0	3	1	5.43	5.43	10
1	2	-1	5.31	5.30	9
0	1	2	5.16		
0	4	1	4.32	4.32	25
0	3	2	4.09	4.09	9
1	1	2	3.89	3.89	18
0	1	3	3.52	3.51	10
2	1	1	3.16	3.16	9
2	2	-2	3.04	3.04	10
2	3	1	2.857		
1	4	-3	2.778		
1	3	3	2.709	2.708	7

Table 5-12. Calculated and Observed X-ray Powder Diffraction Pattern of (Ph₄P)₂[Hg₂As₄Se₁₁](V).

h	k	l	d _{calc} (Å)	d _{obs} (Å)	1/1 _{max} (obs, %)
0	0	1	16.71	16.7	1 6
0	1	-1	12.47	12.46	50
0	1	1	11.06	11.05	100
1	0	-1	9.62	9.62	8
1	-1	0	9.42	9.41	10
0	0	2	8.35	8.35	20
0	2	0	8.20	8.20	18
1	0	1	7.44	7.43	8
0	2	2	5.53	5.53	13
0	4	0	4.10		
3	-1	-3	3.26		
2	-6	0			

3. Results and Discussion

3.1 Syntheses and description of structures

(Ph₄P)₂[Hg₂As₄S₉](I) was prepared by heating HgCl₂ with K₃A₅S₃ and Ph₄PBr in H₂O at 130 °C. The pale-yellow crystals that formed in 2-3 days do not dissolve in common polar organic solvents. such as DMF or CH₃CN, indicative of a polymeric compounds. The structure was determined by X-ray single-crystal analysis. The compound contains a one-dimensional chain structure consisting of trigonal planar Hg²⁺ ions and linear [As₄S₉]⁶⁻ units formed by corner sharing of the $[AsS_3]^{3-}$ units. The $[Hg_2As_4S_9]_n^{2n-}$ chains are parallel to the crystallographic a-axis and separated by Ph₄P⁺ cations, see Figure 5-1. The chains can also be viewed as assembled by Hg₂As₂S₄ eight-membered puckered rings arranged side-by-side. Inside each ring resides a center of symmetry; see Figure 5-2. We have seen the [As4S9]⁶- units before in (Ph4P)₂[SnAs4S9] (in Chapter 2), however the bonding mode here is different. Instead of two Sn⁴⁺ centers, it now is bonded to four Hg²⁺ centers. The different bonding mode, once again, demonstrates the structural diversity of the thioarsenate The Hg²⁺ is in a trigonal-planar environment with bond angles of S2-Hg-S3 at 119.01(3)°, S2-Hg-S at 121.69(3)°, S3-Hg-S4 at 119.28(2)°. The average Hg-S bonding distance, at 2.470(4)Å, is comparable to the mean bond length, at 2.49Å of other trigonal planar mercury compounds like BaHgS2¹² and Na₂Hg₃S₄.¹³ The average As-S distance of 2.277(8)Å, and the average

Table 5-13. Selected Distances (Å) in (Ph₄P)₂[Hg₂As₄S₉] with Standard Deviations in Parentheses.^a

Hg - S2	2.475(6)	Hg - S3	2.465(7)
Hg - S4	2.470(8)	As1 - S1	2.287(8)
As1 - S2	2.236(8)	As1 - S3	2.272(6)
As2 - S1	2.325(9)	As1 - S4	2.22(2)
As2 - S5	2.32(1)		

Table 5-14. Selected Angles (Deg) in (Ph₄P)₂[Hg₂As₄S₉] with Standard Deviations in Parentheses.^a

S2 - Hg - S3	119.01(3)	S2 - Hg - S4	111.22(3)
S3 - Hg - S4	128.04(3)	S1 - As1 - S2	98.0(3)
S1 - As1 - S3	100.9(2)	S2 - As1 - S3	101.9(2)
S1 - As2 - S4	94.9(6)	S1 - As2 - S5	100.3(4)
S4 - As2 - S5	123.1(8)		

^aThe estimated standard deviations in the mean bond lengths and the mean bond angles are calculated by the equation $\sigma l = \{\Sigma_n(l_n - 1)^2/n(n-1)\}^{1/2}$, where l_n is the length (or angle) of the nth bond, l the mean length (or angle), and n the number of bonds.

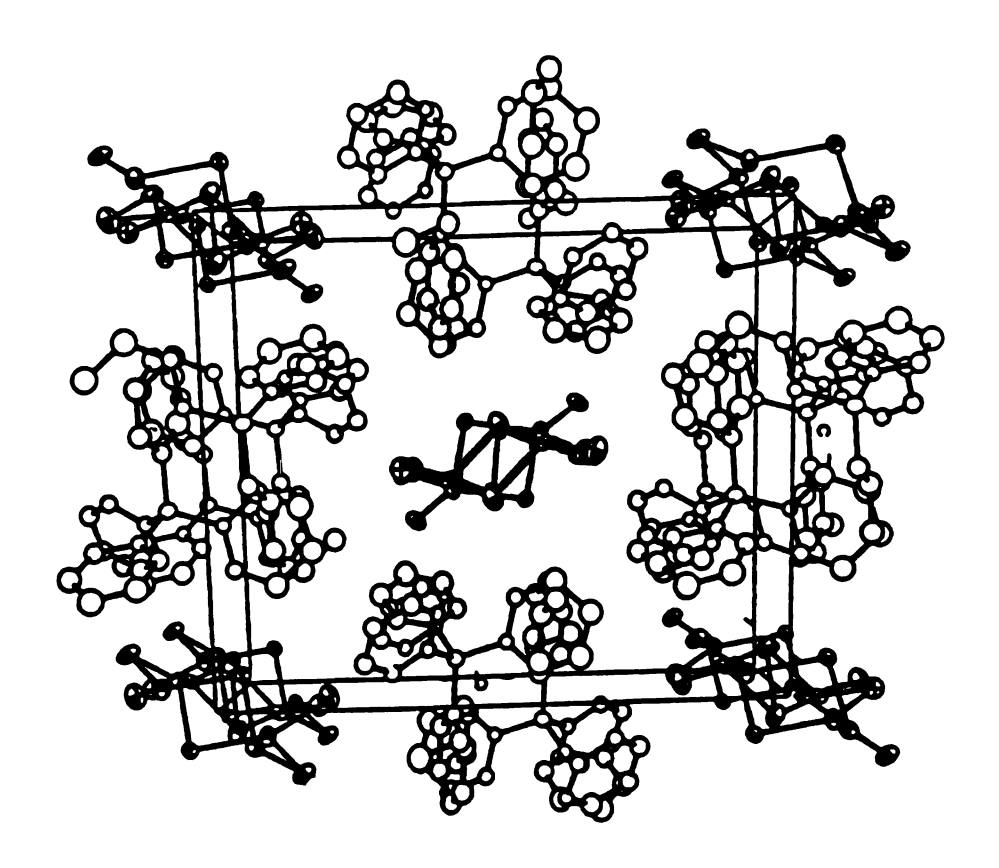


Figure 5-1. Packing diagram of (Ph₄P)₂[Hg₂As₄S₉].

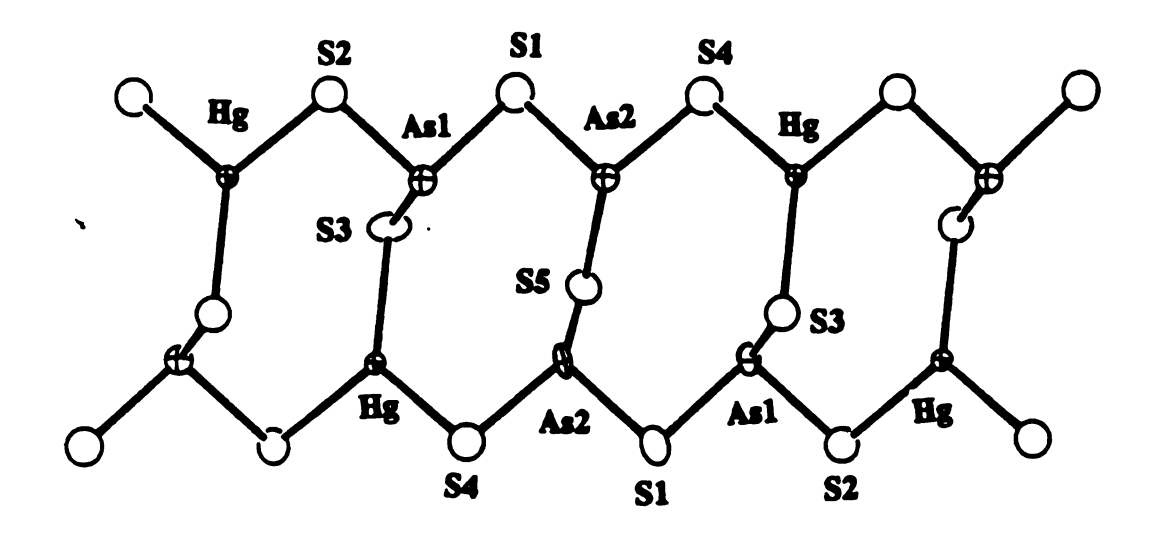


Figure 5-2. Structure and labeling scheme of one $[Hg_2As_4S_9]_n^{2n}$ chain.

S-As-S angles at 100.1(3)°, are well within the normal range found in other arsenic/sulfide compounds.¹⁴ Selected bond distances and bond angles are contained in Tables 5-13 and 5-14.

(Me₄N)[HgAs₃S₆](II) was prepared under conditions similar to those used for (I), but with a longer reaction time (one week). The compound has a unique two-dimensional layered structure where layers of the $[HgAs_3S_6]_{n}^{n}$ covalent framework sandwich Me_4N^+ cations; see Figure 5-3. The interlayer distance is 9.303Å. The [HgAs₃S₆]_nⁿ- framework is composed of tetrahedral Hg²⁺ atoms and polymeric $[As_3S_6]_n^{3n}$ units formed by corner sharing AsS_3^{3} units, See Figure 5-4. The Hg²⁺ ions is in a severely distorted tetrahedral environment as indicated by the bond angles around Hg atoms that range from 94.1(2)° to 138.2(3)°. The Hg-S bond distances are divided into a set of two long bonds at 2.620(8)Å and 2.768(8)Å and a set of two short bonds at 2.445(9)Å and 2.431(8)Å. This distortion is the result of the ligand effect. Selected bond distances and bond angles are contained in Tables 5-15 and 5-16. The Hg-Hg distance is 3.674(3)Å. Both $(Ph_4P)_2[Hg_2As_4S_9]$ and $(Me_4N)[HgAs_3S_6]$ feature new striking thioarsenate polyanions. Both the finite [As4S9]6- and infinite $[As_3S_6]_n^{3n}$, which are shown schematically below, are new species whose formation results from condensation of simpler building block $[AsS_3]^{3-}$. The $[As_3S_6]_n^{3n-}$ represents a "ring-opening" polymerization product of the cyclic [As₃S₆]³- unit observed in $[Bi(As_3S_6)_2]^{3-}$ (see chapter 2).

Several types of rings created as the result of the unusual bonding mode of the infinite $[As_3S_6]_n^{3n}$ range from the large $HgAs_5S_6$ twelve membered ring to the medium $HgAs_3S_4$ and $Hg_2As_2S_4$ eight membered rings to the smallest Hg_2S_2 four membered rings. These ring are all puckered in such way to ensure that the S atoms all point into the gallery region.

(Me₄N)[HgAsSe₃](III) and (Et₄N)[HgAsSe₃](IV) are synthesized with similar reactant ratios and reaction conditions. The rationale for using the small organic cations was the hope that similar higher dimensionality compounds comparable to those in the Hg/As_xS_y system could be obtained. Compounds (III) and (IV) have the same one-dimensional anionic chains composed of trigonal planar Hg²⁺ ions and [AsSe₃]³⁻ units; see Figure 5-5. In order to maintain the same anionic framework and accommodate the large Et₄N+ cations the *b* and *c* axes of (IV) increase by about 1.5Å while the *a* axis remains almost unchanged. The β angle of compound (IV), at 99.56(2)°, also differs from that of the (III), at 91.34(2)°.

203
Table 5-15. Selected Distances (Å) in (Me₄N)[HgAs₃S₆](II) with Standard Deviations in Parentheses.^a

Hg - S1	2.620(8)	Hg - S1	2.768(8)
Hg - S3	2.445(9)	Hg - S5	2.431(8)
As1 - S2	2.263(9)	As1 - S3	2.206(9)
As1 - S4	2.260(9)	As2 - S1	2.263(9)
As2 - S5	2 199(9)	As2 - S6	2.324(9)
As3 - S2	2.279(9)	As3 - S4	2.285(9)
As3 - S6	2.244(9)		

^aThe estimated standard deviations in the mean bond lengths and the mean bond angles are calculated by the equation $\sigma l = \{\Sigma_n(l_n - 1)^2/n(n-1)\}^{1/2}$, where l_n is the length (or angle) of the nth bond, l the mean length (or angle), and n the number of bonds.

Table 5-16. Selected Angles (Deg) in (Me₄N)[HgAs₃S₆](II) with Standard Deviations in Parentheses.^a

S1 - Hg - S1	94.1(2)	S1 - Hg - S3	114.8(3)
S1 - Hg - S5	98.9(2)	S1 - Hg - S3	94.0(3)
S1 - Hg - S5	108.2(3)	S3 - Hg - S5	138.2(3)
S2 - As1 - S4	101.0(4)	S2 - As1 - S3	91.6(3)
S3 - As1 - S4	103.1(4)	S1 - As2 - S5	96.4(3)
S1 - As2-S6	101.2(3)	S5 - As2 - S6	95.7(3)
S2 - As3 - S4	97.6(3)	S2 - As3 - S6	93.1(3)
S4 - As3 - S6	102.0(3)		

The estimated standard deviations in the mean bond lengths and the mean bond angles are calculated by the equation $\sigma l = \{\Sigma_n(l_n - 1)^2/n(n-1)\}^{1/2}$, where l_n is the length (or angle) of the nth bond, l the mean length (or angle), and n the number of bonds.

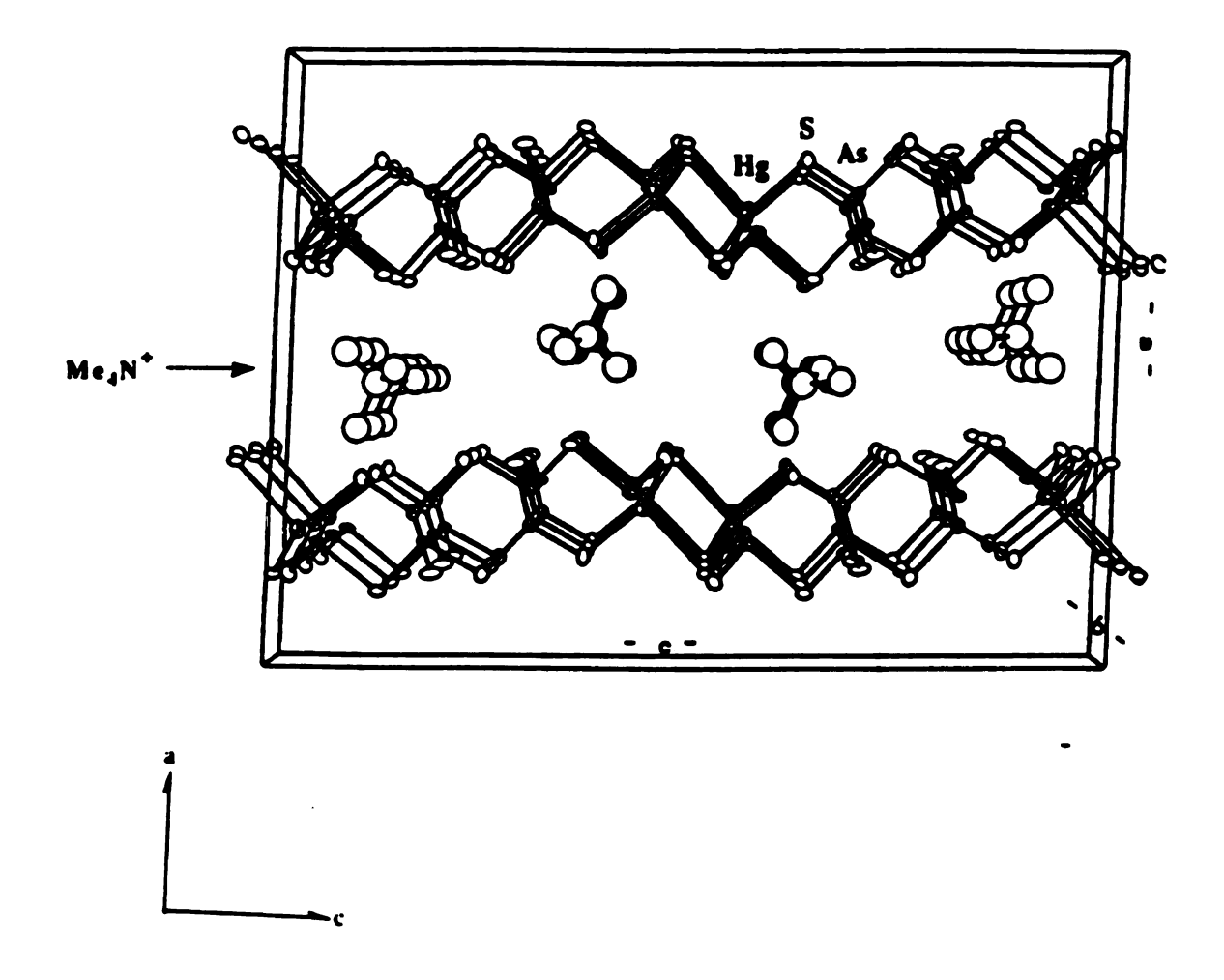


Figure 5-3. Packing diagram of (Me₄N)[HgAs₃S₆].

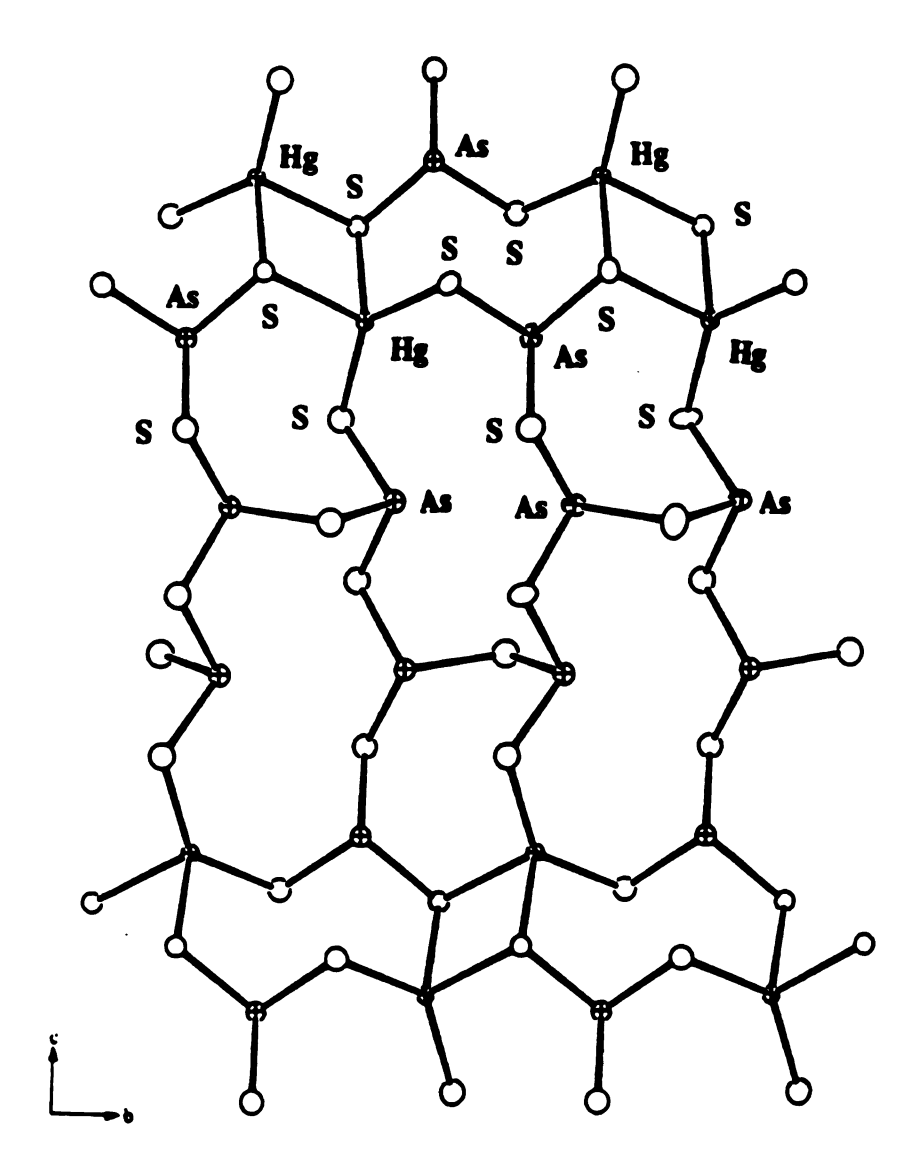
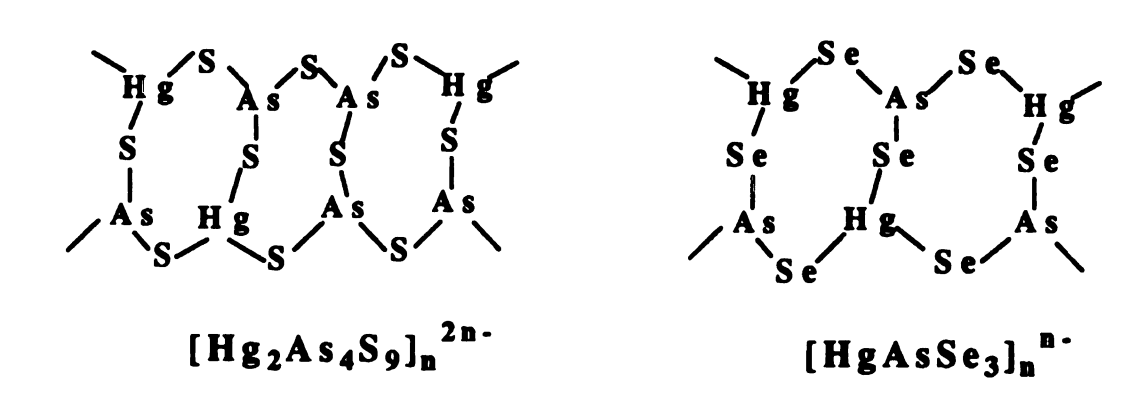


Figure 5-4. Structure and labeling scheme of one $[HgAs_3S_6]_n^n$ layer.

The $[HgAsSe_3]_n^{n-}$ has a one-dimensional chainlike structure that is very similar to that of the $[Hg_2As_4S_9]_n^{2n-}$ (see Figure 5-1). We see the similar $Hg_2As_2Q_4$ eight-membered puckered rings in both structures. The main difference in these two structures, shown in the following scheme, is that in $[Hg_2As_4S_9]_n^{2n-}$, with large $[As_4S_9]_6$ -ligands, the eight-membered rings do not connect to each other; in $[HgAsSe_3]_n^{n-}$, with smaller $[AsSe_3]_3$ - ligands, the eight-membered ring share two common edges, see Figure 5-6.



The Hg²⁺ is in a trigonal-planar environment with bond angles of Se1-Hg-Se2 at 115.25(6)°, Se1-Hg-Se3 at 119.34(5)°, Se2-Hg-Se3 at 124.70(5)°. The average As-S distance of 2.391(3)Å, and the average S-As-S angles at 96.79(6)° are well within the normal range found in other arsenic/selenide compounds¹⁵. Selected bond distances and bond angles are given in Table 5-17.

Table 5-17. Selected Distances (Å) and Angles (Deg) in (Me₄N)[HgAsSe₃] (III) and (Et₄N)[HgAsSe₃] (IV) with Standard Deviations in Parentheses.^a

(Me ₄ N)[HgAsSe ₃] (III)		(Et ₄ N)[HgAsSe ₃] (IV)	
Hg - Sel	2.582(2)	Hg - Sel	2.580(1)
Hg - Se2	2.572(2)	Hg - Se2	2.594(1)
As1 - Se3	2.563(3)	Hg - Se3	2.575(1)
As - Se1	2.373(3)	As - Se1	2.366(2)
As - Se2	2.398(3)	As - Se2	2.400(2)
As - Se3	2.411(3)	As- Se3	2.396(2)
Se1-Hg-Se2	115.32(8)	Se1-Hg-Se2	115.18(4)
Se1-Hg-Se3	119.21(6)	Se1-Hg-Se3	119.47(4)
Se2-Hg-Se3	124.93(7)	Se2-Hg-Se3	124.47(4)
Se1-As-Se2	96.7(1)	Se1-As-Se2	96.72(5)
Se1-As-Se3	105.7(1)	Se1-As-Se3	91.43(5)
Se2-As-Se3	99.38(9)	Se2-As-Se3	90.81(5)
Hg-Sel-As	95.49(9)	Hg-Se1-As	104.81(6)
Hg-Se2-As	89.94(9)	Hg-Se2-As	98.15(6)
Hg-Se3-As	91.39(9)	Hg-Se3-As	98.82(6)

^aThe estimated standard deviations in the mean bond lengths and the mean bond angles are calculated by the equation $\sigma l = \{\Sigma_n(l_n - 1)^2/n(n-1)\}^{1/2}$, where l_n is the length (or angle) of the nth bond, l the mean length (or angle), and n the number of bonds.

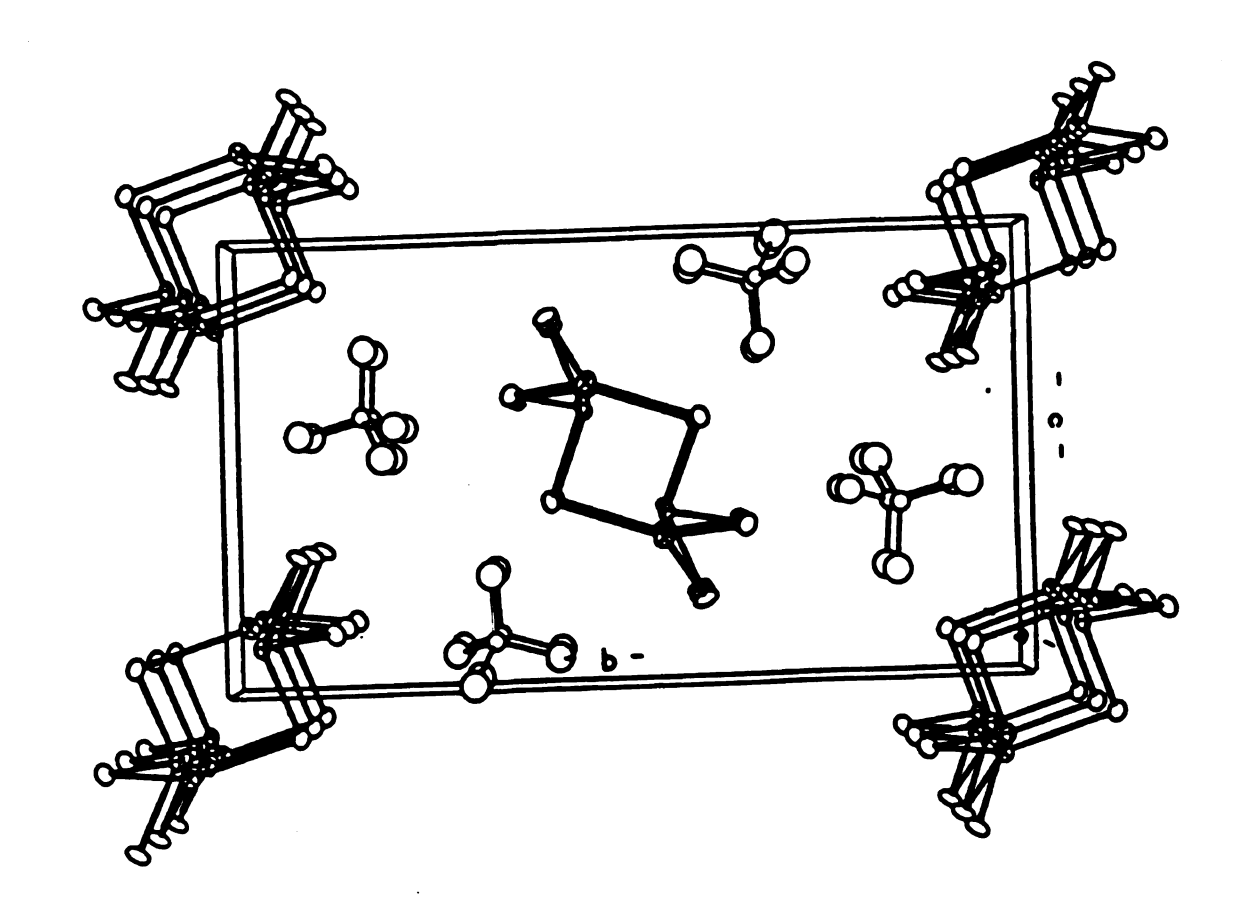


Figure 5-5. Packing diagram of (Me₄N)[HgAsSe₃].

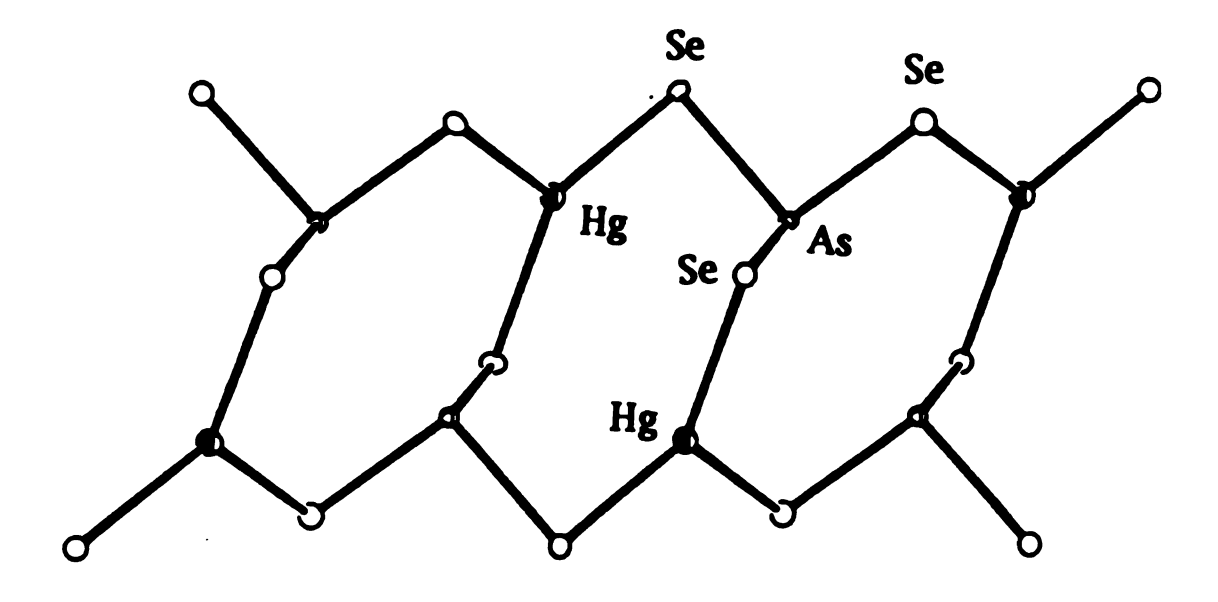


Figure 5-6. Structure and labeling scheme of one $[HgAsSe_3]_n^n$ -chain.

The compound (Ph₄P)₂[Hg₂As₄Se₁₁](V) was prepared by heating HgCl₂ with K₃A₅Se₃ and Ph₄PBr in H₂O at 130 °C. structure was determined by X-ray single-crystal analysis. This compound also contains one-dimensional chains consisting of both trigonal-planar and tetrahedral Hg²⁺ ions and [As₄Se₁₁]⁶⁻ units. The $[Hg_2As_4Se_{11}]_{n^2}^{n-1}$ chains are parallel to the crystallographic a axis and separated by Ph₄P+ cations; see Figure 5-7. These chains can also be viewed as assembled by connecting the clusters Hg2As4Se10 through monoselenide; see Figure 5-8. There are two kinds of Hg²⁺ ions in Hg(1) is coordinated in a distorted tetrahedral the chains. arrangement to four selenides with the Se-Hg-Se angles range from 96.5(1)° to 128.2(1)°. Hg(2) is in a distorted trigonal-planar environment with bond angle of Se4-Hg-Se5 at 109.1(1)°, Se4-Hg-Se6 at 124.9(1)°, Se5-Hg-Se6 at 129.9(1)°. The average As-Se distance and the average Se-As-Se angle are within the normal range found in the other arsenic/selenide compounds¹⁵ The unique feature of this compound is the [As4Se₁₁]⁶- ligand each bonded to four Hg²+ The [As4Se₁₁]⁶- ligand represents a new selenoarsenate ions. These [As4Se₁₁]⁶- units can be viewed as the oxidative polyanion. addition product of the [As4Se9]6- and two Se2-. We have seen the sulfide analogue, [As4S9]6-, previously in the Hg/As_xS_y system and see no reason why the selenoarsenic ligand, [As4Se9]6-, should not exist. The isolation of the (Me₄N)[HgAsSe₃], (Et₄N)[HgAsSe₃], and (Ph₄P)₂[Hg₂As₄Se₁₁] indicates that As_xSe_y polyanions are similar, yet quite different from the As_xS_y anions and one should not think of them just as the seleno- analog of the sulfide system. Selected bond distances and bond angles are contained in Tables 5-18 and 5-19.

Table 5-18. Selected Distances (Å) in (Ph₄P)₂[Hg₂As₄Se₁₁] with Standard Deviations in Parentheses.^a

Hg1 - Se1	2.648(4)	Hg1 - Se2	2.589(3)
Hg1 - Se3	2.570(3)	Hg1 - Se6	2.820(3)
Hg2 - Se4	2.602(3)	Hg2 - Se5	2.587(4)
Hg2 - Se6	2.540(4)	Se1 - Se9	2.378(5)
Se2 - As3	2.316(5)	Se3 - As1	2.317(5)
Se4 - As2	2.362(4)	Se5 - As4	2.329(5)
Se6 - Se10	2.357(4)	Se7 - As1	2.381(5)
Se7 - As2	2.420(5)	Se8 - As2	2.389(5)
Se8 - As4	2.423(4)	Se9 - As3	2.389(5)
Se10 - As1	2.425(4)	Se11 - As3	2.417(5)
Sel1 - As4	2.403(5)		

^aThe estimated standard deviations in the mean bond lengths and the mean bond angles are calculated by the equation $\sigma l = \{\Sigma_n(l_n - 1)^2/n(n-1)\}^{1/2}$, where l_n is the length (or angle) of the nth bond, l the mean length (or angle), and n the number of bonds.

Table 5-19. Selected Angles (Deg) in (Ph₄P)₂[Hg₂As₄Se₁₁] with Standard Deviations in Parentheses.^a

Sel-Hgl-Se2	106.8(1)	Sel-Hgl-Se3	114.6(1)
Se1-Hg1-Se6	96.5(1)	Se2-Hg1-Se3	128.2(1)
Se2-Hg1-Se6	102.06(9)	Se3-Hg1-Se6	102.7(1)
Se4-Hg2-Se5	100.9(1)	Se4-Hg2-Se6	124.9(1)
Se5-Hg2-Se6	129.9(1)	Hg1-Se1-Se9	97.0(1)
Hg1-Se2-As3	99.4(1)	Hg1-Se3-As1	100.7(1)
Hg2-Se4-As2	102.0(1)	Hg2-Se5-As4	93.6(1)
Hg1-Se6-Hg2	98.8(1)	Hg1-Se6-Se10	100.5(1)
Hg2-Se6-Se10	104.4(1)	As1-Se7-As2	93.4(2)
As2-Se8-As4	102.7(1)	Se1-Se9-As3	105.4(1)
Se6-Se10-As1	107.4(2)	As3-Se11-As4	98.3(2)
Se3-As1-Se7	98.7(2)	Se3-As1-Se10	107.3(2)
Se7-As1-Se10	100.3(2)	Se4-As2-Se7	100.3(1)
Se4-As2-Se8	94.1(2)	Se7-As2-Se8	99.4(1)
Se2-As3-Se9	105.3(2)	Se2-As3-Se11	97.8(2)
Se9-As3-Se11	100.2(2)	Se5-As4-Se8	98.0(2)
Se5-As4-Se11	98.9(2)	Se8-As4-Se11	102.4(2)

^aThe estimated standard deviations in the mean bond lengths and the mean bond angles are calculated by the equation $\sigma l = \{\Sigma_n(l_n - 1)^2/n(n-1)\}^{1/2}$, where l_n is the length (or angle) of the nth bond, l the mean length (or angle), and n the number of bonds.

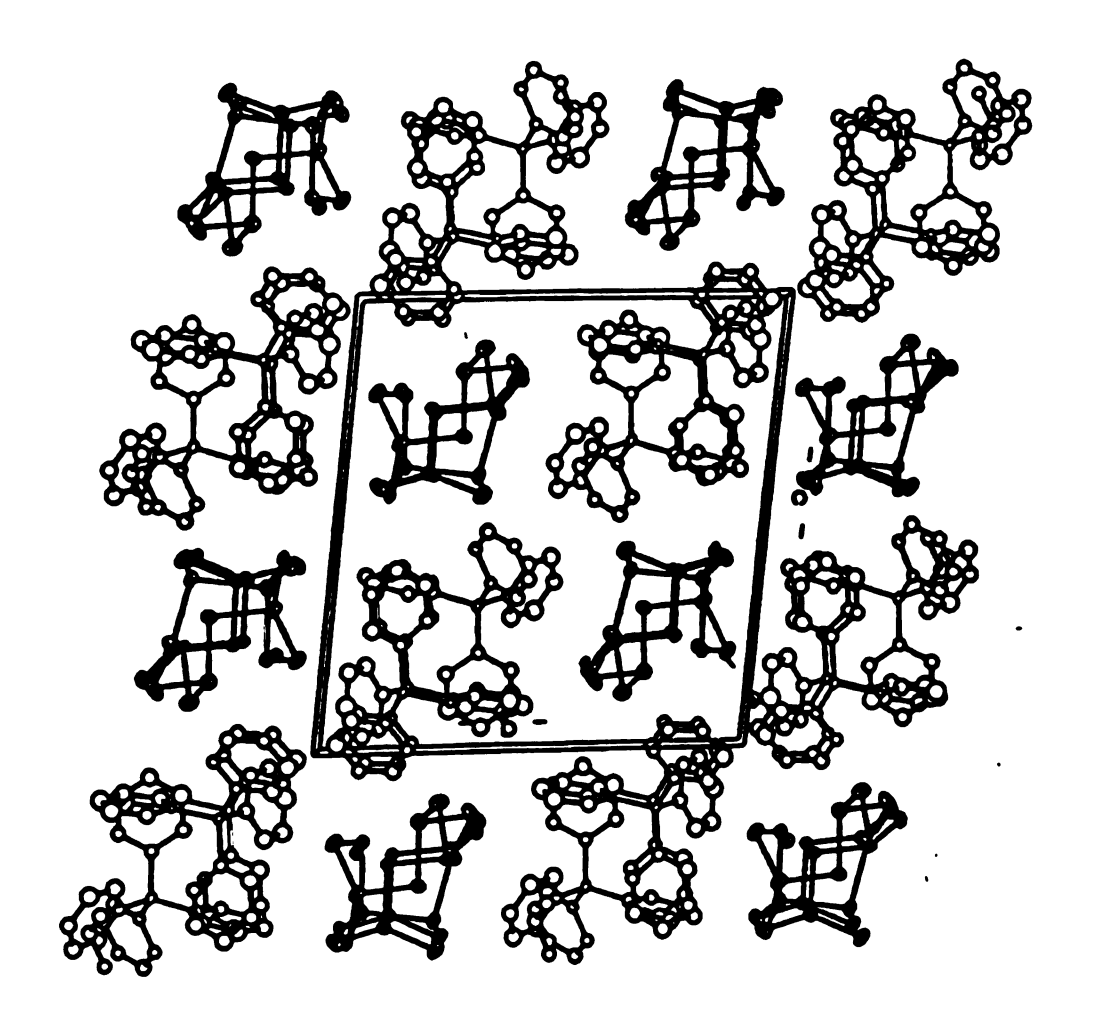


Figure 5-7. Packing diagram of (Ph₄P)₂[Hg₂As₄Se₁₁].

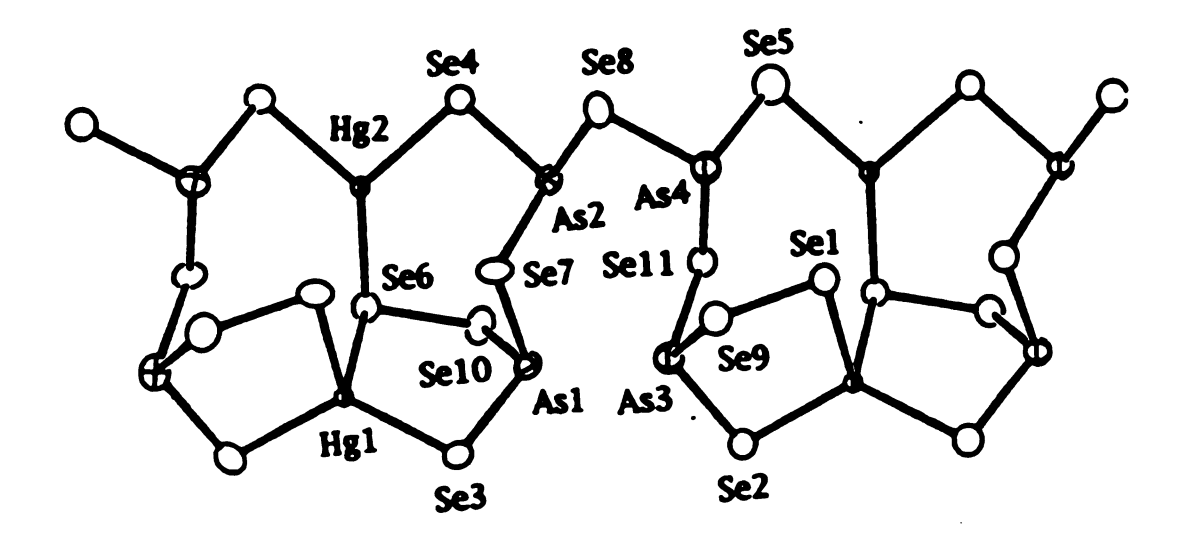


Figure 5-8. Structure and labeling scheme of one $[Hg_2As_4Se_{11}]_n^{2n}$ chain.

3.2 Physicochemical studies

In the far-IR region all complexes reported here exhibit spectral absorptions due to As-S and M-S stretching vibrations as shown in Figures 5-9 and 5-10. Observed absorption frequencies of all the complexes are given in Table 5-20.

Table 5-20. Frequencies (cm⁻¹) of Raman and Infrared Spectral Absorptions of (Ph₄P)₂[Hg₂As₄S₉] (I), (Me₄N)[HgAs₃S₆] (II), (Me₄N)[HgAsSe₃] (III), (Et₄N)[HgAsSe₃] (IV), and (Ph₄P)₂[Hg₂As₄Se₁₁] (V).

Compounds	Infrared	Raman
(Ph ₄ P) ₂ [Hg ₂ As ₄ S ₉]	383(m, sh), 362(m)	
	328(s), 301(m)	
	284(w), 263(s)	
	252(s)	
$(Me_4N)[HgAs_3S_6]$	362(s, sh), 269(s)	
·	226(w), 188(m)	
	178(m),	
(Me ₄ N)[HgAsSe ₃]	268(m), 249(m, sh)	268(w), 252(m), 246(m)
	178(m, sh)	178(s)
(Et4N)[HgAsSe3]	268(m), 249(m, sh)	268(w), 252(m), 246(m)
	178(m, sh)	178(s)
$(Ph_4P)_2[Hg_2As_4Se_{11}]$	273(s), 249(s, sh)	273(w), 249(s), 231(m)
	220(s), 181(m)	217(s), 203(m), 160(m)
	162(m, sh)	

^{*} s: strong, m; medium, w: weak, sh: shoulder.

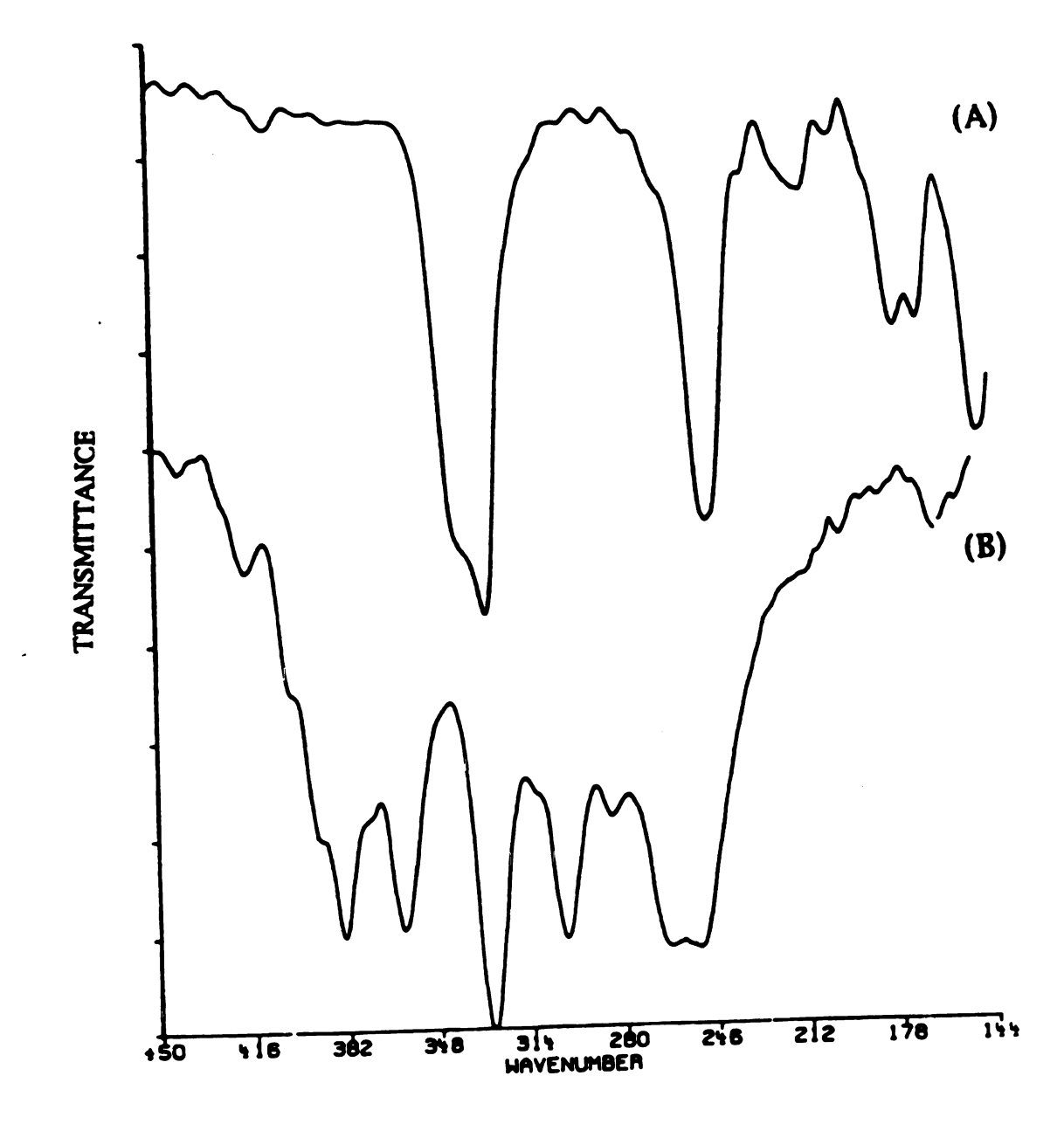


Figure 5-9. Far-IR spectra of (A) $(Ph_4P)_2[Hg_2As_4S_9](I)$, (B) $(Me_4N)[HgAs_3S_6](II)$.

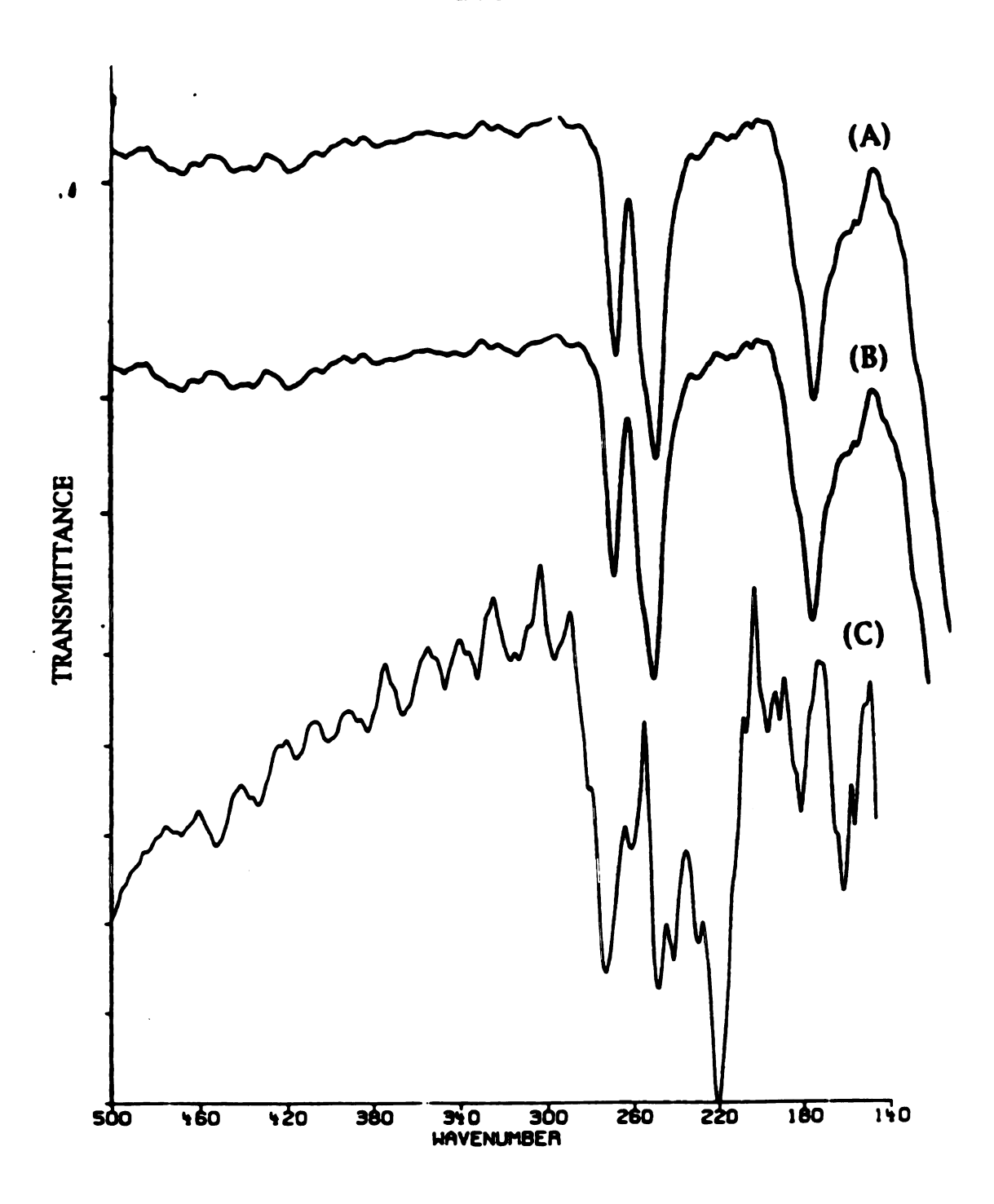


Figure 5-10. Far-IR spectra of (A) $(Me_4N)[HgAsSe_3](III)$, (B) $(Et_4N)[HgAsSe_3](IV)$, and (C) $(Ph_4P)_2[Hg_2As_4Se_{11}](V)$.

In the Far-IR of (Ph₄P)₂[Hg₂As₄S₉], and (Me₄N)[HgAs₃S₆], the peaks in the region of 200-400 cm⁻¹ could be attributed to As-S vibration modes. Similar assignments have been made in the far-IR spectra of other known thioarsenic complexes. 16 It should be noted that it is difficult to interpret the far-IR spectra of compounds (I) and (II) without ambiguity. The major difficulty in assigning the observed IR spectra of these compounds arises from the fact that As-S and Hg-S stretching frequencies fall in the same low frequency region of 200-400 cm⁻¹. The additional peak in the IR spectra for (Me₄N)[HgAs₃S₆] at 188 cm⁻¹ might be assigned as a Hg-S stretching The Far-IR spectra of (Me₄N)[HgAsSe₃] and vibration. (Et₄N)[HgAsSe₃] are identical. The peaks at 268 and 249 cm⁻¹ can be assigned to the As-Se vibration mode. The remaining lower energy peak at 173 cm⁻¹ might be a Hg-Se stretching vibration. A similar assignment can also be derived for the (Ph₄P)₂[Hg₂As₄Se₁₁] compound. The peaks between 200-300 cm⁻¹ can be assigned to As-Se and Se-Se vibration modes and those at 181 and 162 cm⁻¹ can be assigned to Hg-Se stretching vibrations.

Raman spectra of (III), (IV), and (V) were also recorded, but those of (I) and (II) were not because a large diffuse reflectance which obscures the area from 2000 cm⁻¹ to 200 cm⁻¹. We see that the Raman data of (III) and (IV) have a one to one correspondence with peaks in the infrared data with the exception of the 249 cm⁻¹ peak in the infrared spectra which is resolved into two peaks in the Raman spectra. Assignments made to the infrared spectra can also be applied in the Raman spectra.

Thermal Gravimetric Analysis (TGA) results for all compounds are summarized in Table 5-21 and the graphs are shown in Figures 5-11, 5-12, and 5-13. Above 650 °C, all compounds of (I)-(V) completely lost mass without leaving any ternary Hg/As/S(Se) or binary Hg/S(Se) phases. During pyrolysis, redox reactions must have occurred between Hg²⁺ metal ions and $[As_xQ_y]^{n-}$ (Q = S, Se) to form volatile Hg and As_xQ_y (Q = S, Se) phases. For compounds (II), (III), and (IV) there are two step weight losses. The first step can be attributed to the loss of the organic cations, probably as R₃N and R₂S or R₂Se, while the final step is due to the loss of Hg and $As_xS(Se)_y$. Table 5-21. TGA Data for (Ph₄P)₂[Hg₂As₄Se₃] (I), (Me₄N)[HgAs₃Se₃] (II), (Et₄N)[HgAsSe₃] (IV), and (Ph₄P)₂[Hg₂As₄Se₁₁] (V).

Compound	Temp. range (°C)	Weight loss (%)
(Ph ₄ P) ₂ [Hg ₂ As ₄ S ₉]	230 - 485	98.1
$(Me_4N)[HgAs_3S_6]$	230 - 300	30.0
	300 - 525	68.5
(Me ₄ N)[HgAsSe ₃]	148 - 260	22.2
	260 - 610	76.0
(Et4N)[HgAsSe3]	150 - 250	31.1
	250 - 550	67.1
(Ph ₄ P) ₂ [Hg ₂ As ₄ Se ₁₁]	310 - 630	98.2

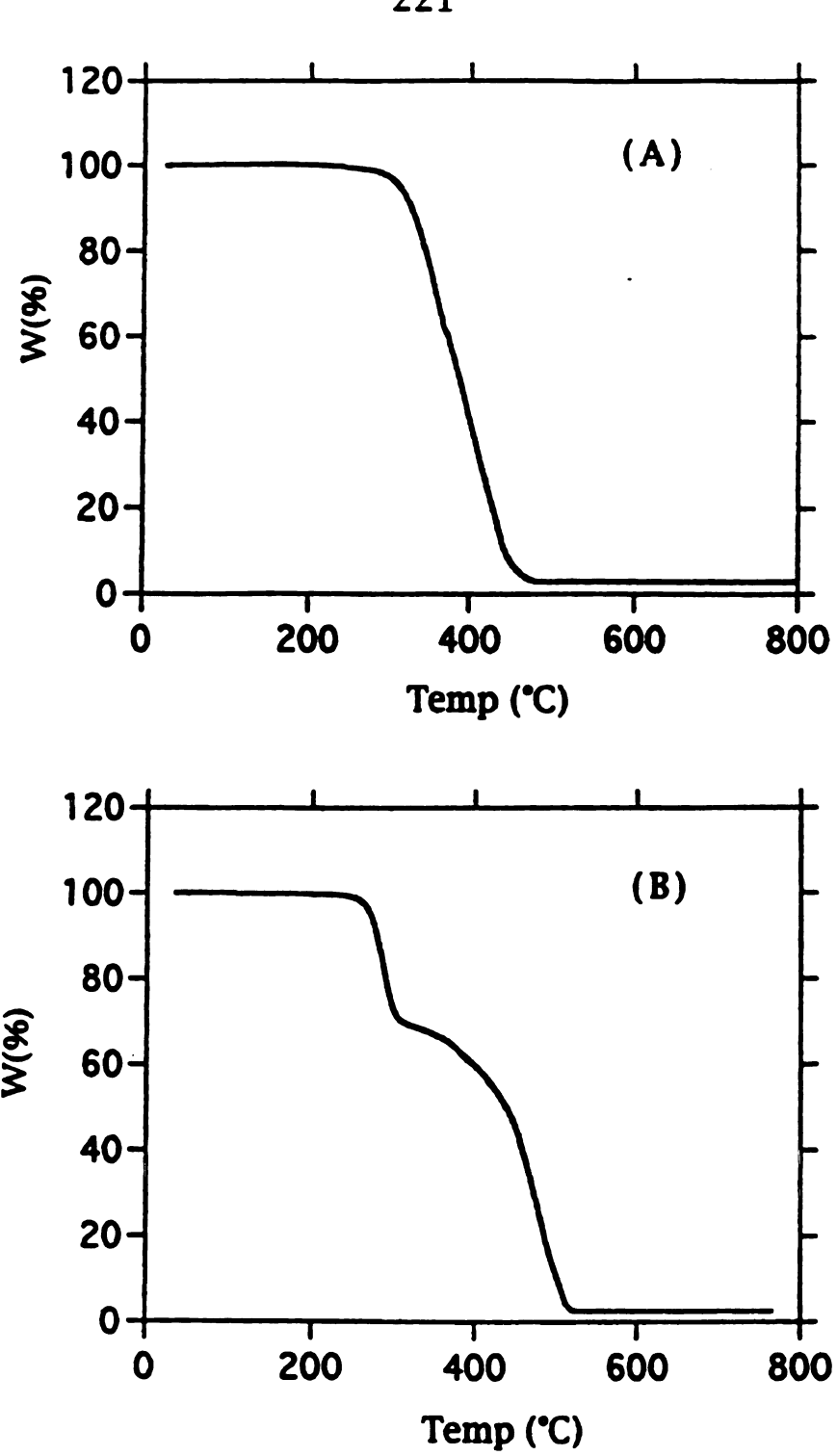


Figure 5-11. TGA diagrams of (A) $(Ph_4P)_2[Hg_2As_4S_9](I)$, (B) $(Me_4N)[HgAs_3S_6](II)$.

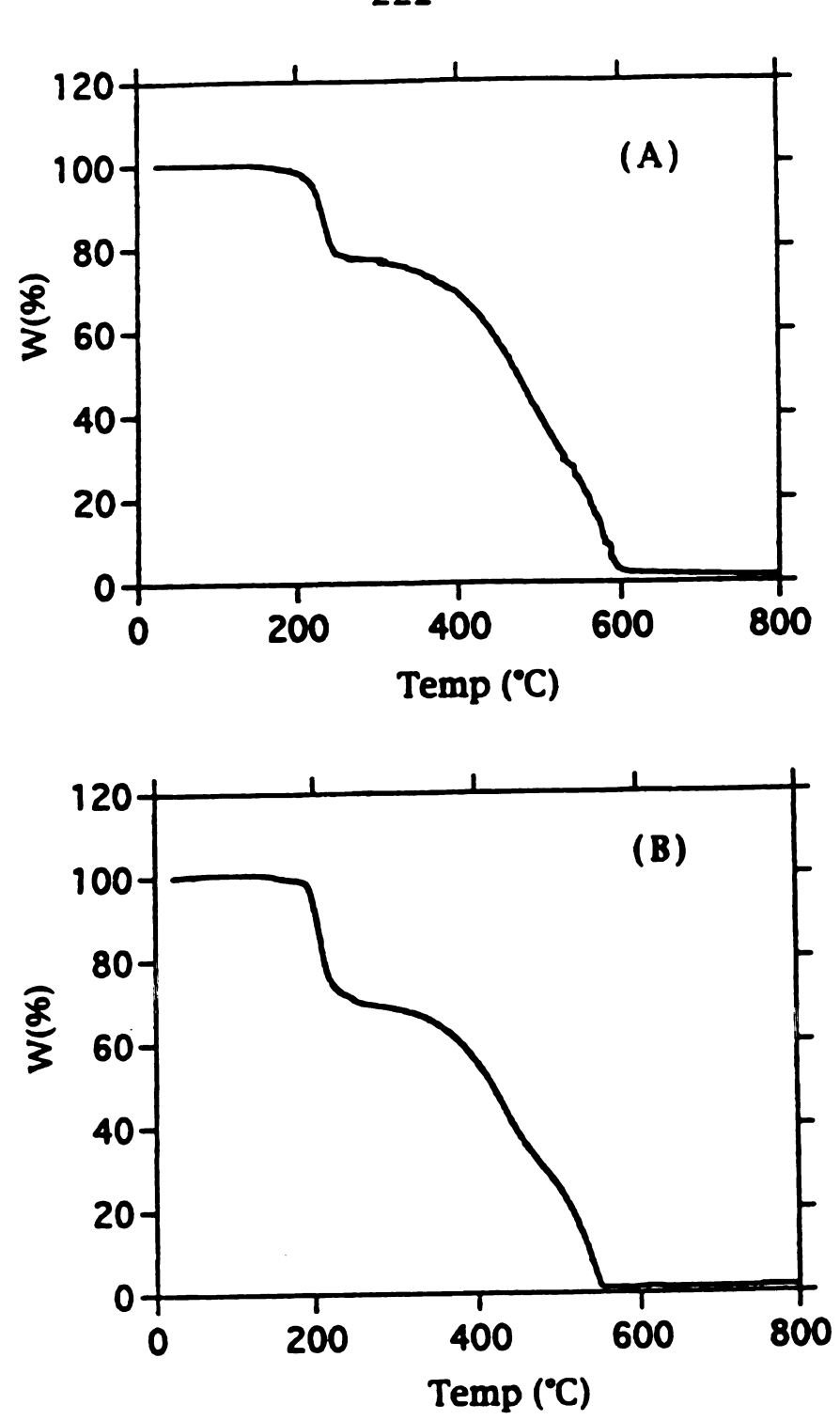


Figure 5-12. TGA diagrams of (A) (Me₄N)[HgAsSe₃](III), (B) (Et₄N)[HgAsSe₃](IV).

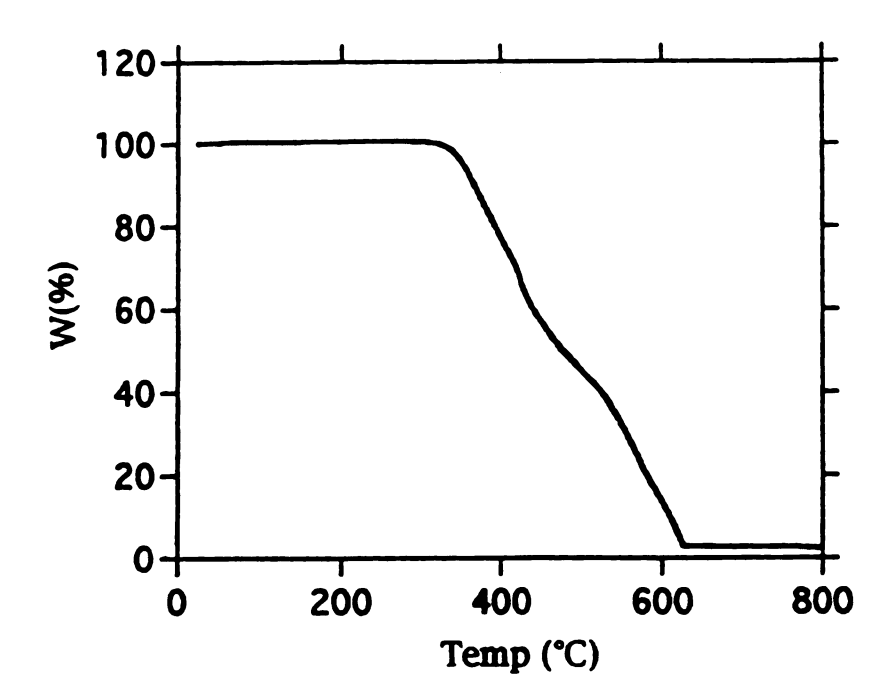


Figure 5-13. TGA diagram of (Ph₄P)₂[Hg₂As₄Se₁₁](V).

The optical properties of compounds (I) - (V) were assessed by studying the UV/near-IR reflectance spectra of the materials. The spectra confirmed they are wide bandgap semiconductors by revealing the presence of sharp optical gaps as shown in Figures 5-14, 5-15, and 5-16. The optical absorption spectra of $(Ph_4P)_2[Hg_2As_4S_9]$ and $(Me_4N)[HgAs_3S_6]$ exhibit an intense, steep absorption edge from which the bandgap, E_g , can be assessed at 2.9 and 2.8 eV respectively. The spectra of (III) - (V) also shows similar absorption edges with corresponding bandgaps of 2.4 eV for $(R_4N)[HgAsSe_3]$ (R = Me, Et) and 2.5 eV for $(Ph_4P)_2[Hg_2As_4Se_{11}]$. The absorption is probably due to a charge-transfer transition from a primarily sulfur-based valence band to a mainly mercury-based conduction band.

Based on the findings reported here, it appears that the relative solubilities of the various products determine the actual $[As_xQ_y]^{n-}$ (Q=S, Se) species formed by condensation reactions of $[AsS_3]^{3-}$. This behavior is reminiscent of the polychalcogenide complexes mentioned earlier, where metal preference, product solubility and solvent are the key factors that control product crystallization.¹⁷ The condensation equilibria are most likely catalyzed by protonation reaction of the terminal sulfide groups. If true, different products are expected from similar reactions performed under aprotic solvents. It is interesting to point out the correlation that exists between the counterion size and the metal coordination number in the Hg/As_xS_y system. The large Ph_4P^+ cations afford a one-dimensional chain structure with the

Figure 5-14. Optical absorption spectra of (A) $(Ph_4P)_2[Hg_2As_4S_9](I)$, (B) $(Me_4N)[HgAs_3S_6](II)$.

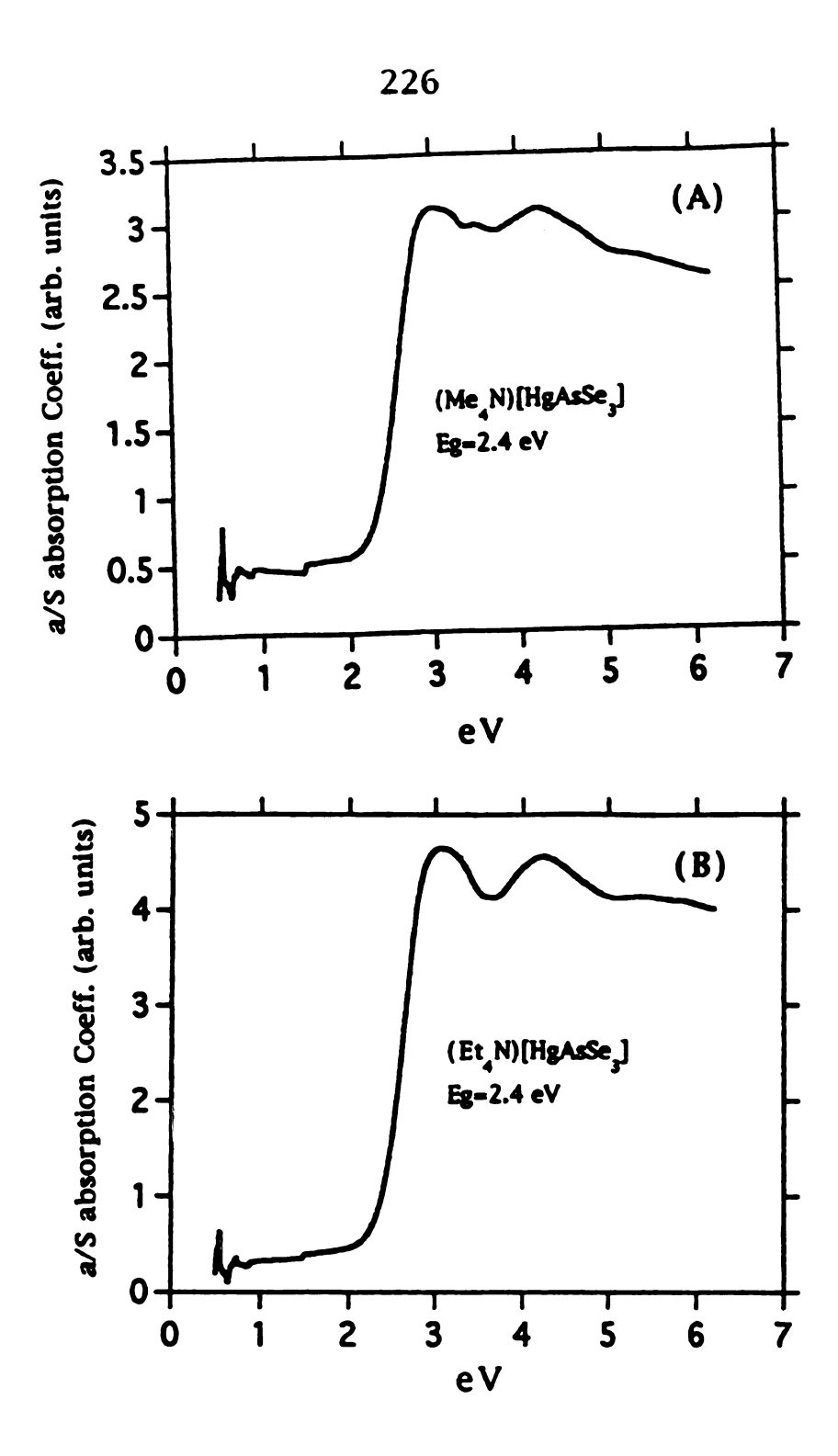


Figure 5-15. Optical absorption spectra of (A) (Me₄N)[HgAsSe₃](III), (B) (Et₄N)[HgAsSe₃](IV).

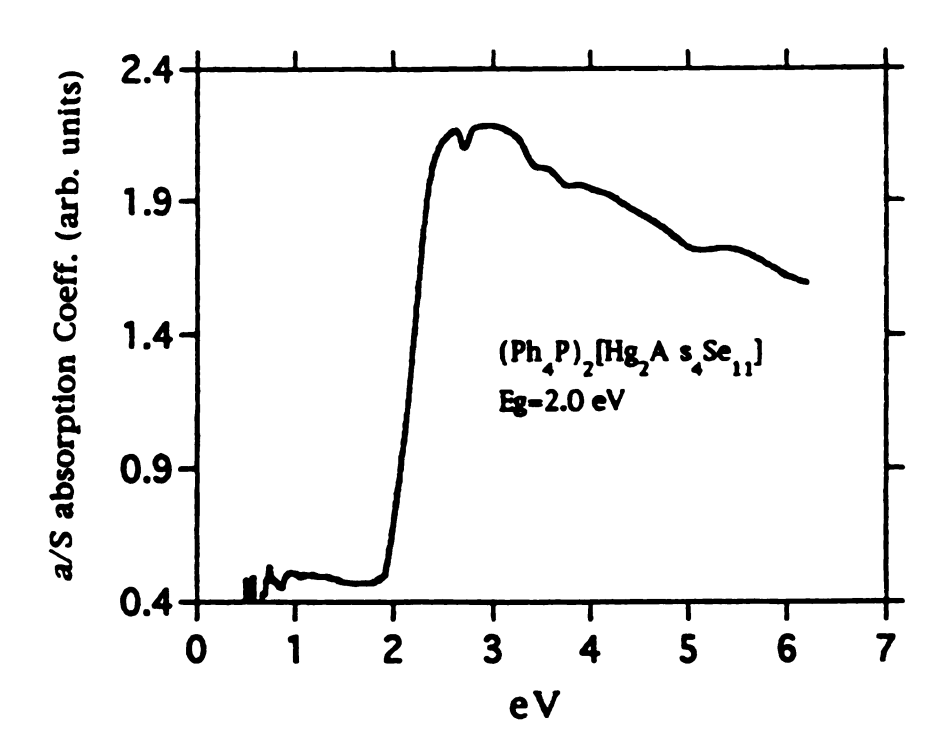


Figure 5-16. Optical absorption spectrum of (Ph₄P)₂[Hg₂As₄Se₁₁](V).

Hg atoms adopting the trigonal-planar geometry, while the small Me₄N⁺ cations produce a layered structure where the Hg atoms can assume tetrahedral coordination. This behavior is reminiscent of similar counterion size effects observed in silver polyselenides 18 where the coordination number of Ag in [Ag_xSe_y]ⁿ anions varied inversely with the size of counterion. Furthermore. the dimensionality of the structures in (Ph4P)2[Hg2As4S9] and $(Me_4N)[HgAs_3S_6]$, as well as in $(Ph_4P)_2[InAs_3S_7]$ and (Me₄N)₂Rb[BiAs₆S₁₂], is consistent with the view expressed earlier, that small cations tend to stabilize higher dimensionality anionic M/Q frameworks than corresponding large cations. 19 This, however, is not yet an established trend, and one can certainly find cases (especially in zeolites) where a given cation may give rise to different structure types or different cations give rise to the same framework. cation size/structure correlation seems to be stronger when the stoichiometry of the anionic M/Q framework is the same from cation to cation.²⁰ We did not see this type of cation dependence in the Hg/As_xSe_y system. The reason may be because of simple crystal packing forces: the As-Se distance is longer than the As-S distance. These distance differences may result "[Hg2As4Se9]2-" chains generate more empty space than As-S chain to be able to pack with Ph₄P⁺ cations, and in order to get good packing the system rearranges to form [As4Se₁₁]⁴- units. We also like to point out that isolation of compounds (III) (IV) and (V) desmonstrates that the $[As_xSe_y]^{n-}$ anions are very different from the $[As_xS_y]^{n-}$ anions. This observation is consistent with our knowledge from the the metal chalcogenide chemistry that polyselenides and polytellurides are not

just an extension of the polysulfides. Although the condensation process probably also occurs in the $[As_xSe_y]^{n-}$ system, the solubilities of different $[As_xSe_y]^{n-}$ polyanions may be different from those of the $[As_xS_y]^{n-}$ anions. The $Hg_2As_2Q_4$ (Q=S, Se) eight-membered ring appears to be a very stable fragment as we see it in both $[Hg_2As_4S_9]^{2-}$ and $[HgAsSe_3]^{-}$.

In summary, the employment of the hydrothermal technique in the organic cation/ M^{n+}/AsQ_3^{3-} (Q = S, Se) system has successfully produced novel metal/arsenic/sulfide(Selenide) covalent frameworks. Further investigations are in process to delineate the factors responsible for influencing the dimensionality of the final products and to achieve three-dimensional frameworks.

REFERENCES

- (a) Liao, J.-H.; Kanatzidis, M. G. Inorg. Chem. 1992, 31, 431-439.
 (b) Liao, L.-H.; Kanatzidis, M. G. J. Am. Chem. Soc. 1990, 112, 7400-7402.
 (c) Huang, S.-P.; Kanatzidis, M. G. J. Am. Chem. Soc. 1992, 114, 5477-5478.
 (d) Kim, K.-W.; Kanatzidis, M. G. J. Am. Chem. Soc. 1992, 114, 4878-4883.
 (e) Dhingra, S. S.; Kanatzidis, M. G. Science, 1992, 258, 1769-1772.
- (a) Sheldrick, W. S. Z. Anorg. Allg. Chem. 1988, 562, 23-30. (b)
 Sheldrick, W. S.; Hanser, H.-J. Z. Anorg. Allg. Chem. 1988, 557, 98-104. (c) Sheldrick, W. S.; Hanser, H.-J. Z. Anorg. Allg. Chem. 1988, 557, 105-110.
- (a) Wood, P. T.; Pennington, W. T.; Kolis, J. W. Inorg. Chem.
 1993, 32, 129-130. (b) Wood, P. T.; Pennington, W. T.; Kolis, J. W. J. Chem. Soc. Chem. Commun. 1993, 25, 235-236.
- 4. (a) Parise, J. B. Sicence, 1991, 251, 293-294. (b) Parise, J. B.; Ko, Y. Chem. Mater. 1992, 4, 1446-1450.
- 5. Chou, J.-H.; Kanatzidis, M. G. Inorg. Chem. 1994, 33, 1001-1002.
- 6. Chou, J.-H.; Kanatzidis, M. G. maniscript in preparation.
- 7. Chou, J.-H.; Kanatzidis, M. G. Inorg. Chem. 1994, In press..
- 8. (a) Wendlandt, W. W.; Hecht, H. G. "Reflectance Spectroscopy",
 Interscience Publishers, 1966. (b) Kotüm, G. "Reflectance

- Spectroscopy", springer Verlag, New York, 1969. (c) Tandon, S. P.; Gupta, J. P. Phys. Stat. Sol. 1970, 38, 363-367.
- Sheldrick, G. M. In Crystallographic Computing 3; Sheldrick, G.
 M.; Kruger, C.; Goddard, R., Eds.; Oxford University Press: Oxford,
 U.K., 1985; pp 175-189.
- 10. TEXSAN: Single Crystal Structure Analysis Package, Version5.0, Molecular Structure Corp., Woodland, TX.
- 11. Walker, N.; Stuart, D. Acta. Crystallogr. 1983, 39A, 158-166.
- 12. Rad, H. D.; Hoppe, R. Z. Anorg. Allg. Chem. 1981, 483, 18-25.
- 13. Siewert, B.; Müller, U. Z. Anorg. Allg. Chem. 1991, 595, 211-215.
- (a) Sommer, H.; Hoppe, R. Z. Anorg. Allg. Chem. 1977, 430, 199.
 (b) Sheldrick, W. S.; Kaub, J. Z. Naturforsch. 1985, 40b, 571-573.
 (c) Jerome, J. E.; Wood, P. T.; Pennington, W. T.; Kolis, J. W. Inorg. Chem. 1994, 33, 1733-1734.
- (a) Sheldrick, W.; Häusler, H.-J. Z. Anorg. Allg. Chem. 1988, 561, 139-148.
 (b) Sheldrick, W.; Kaub, J. Z. Anorg. Allg. Chem. 1986, 535, 179-185.
 (c) O'Neal, S. C.; Pennington, W. T.; Kolis, J. W. J. Am. Chem. Soc. 1991, 113, 710-712.
 (d) O'Neal, S. C.; Pennington, W. T.; Kolis, J. W. Inorg. Chem. 1992, 31, 888-894.

- (a) Mohammed, A.; Müller, U. Z. Anorg. Allg. Chem. 1985, 523,
 45-53. (b) Sinning, H.; Müller, U. Z. Anorg. Allg. Chem. 1988,
 564, 37-44.
- 17. Kanatzidis, M. G.; Huang, S.-P. Coord. Chem. Rev. 1994, 130, 509-621.
- 18. Huang, S.-P.; Kanatzidis, M. G. Inorg. Chem. 1991, 30, 1455-1466.
- 19. Kim, K.-W.; Kanatzidis, M. G. J. Am. Chem. Soc. 1992, 114, 4878-4883.
- 20. Kanatzidis, M. G. In Proceeding of the 7th International Symposium on Inorganic Ring Systems, Banff, Canada, 1994, *Phosphorous, Silicon, and Sulfur*, in press.

CHAPTER 6

HYDRO(METHANO)THERMAL SYNTHESIS OF M/As_xQ_y (M = Ag²⁺, Q = S, Se) COMPOUNDS. SYNTHESIS AND CHARACTERIZATION OF β -Ag₃AsSe₃(I), (Me₃NH)[Ag₃As₂Se₅](II), K₅[Ag₂As₃Se₉](III), and K[Ag₃As₂S₅](IV).

ABSTRACT

β-Ag₃AsSe₃(I) and (Me₃NH)[Ag₃As₂Se₅](II) were synthesized hydrothermally from a mixture of AgBF₄/3K₃A₅S_{e₃} and $AgBF_4/3K_3AsSe_3/Me_3NHCl$, while $K[Ag_3As_2S_5](III)$ and K₅[Ag₂As₃Se₉](IV) were synthesized methanothermally from a mixture of AgBF4/3K3AsSe3 and AgBF4/3K3AsS3, respectively. structures were determined by single-crystal X-ray diffraction analysis. β-Ag₃AsSe₃(I) crystallizes in orthorhombic space group Pnma (No. 62) with a = 8.111(1)Å, b = 11.344(2)Å, c = 20.728(3)Å, Z= 8, V = 1907(1)Å³. The compound is a new allotrope of the known Ag3AsSe3 and has a complicated three-dimensional structure composed of three and four coordinated Ag+ ions and [AsSe₃]³- units. (Me₃NH)[Ag₃As₂Se₅] crystallizes in the triclinic space group P-1 (No. 2) with a = 10.549(2)Å, b = 11.476(4)Å, c = 6.549(3)Å, $\alpha = 104.94$, $\beta = 104.94$ $107.41(2)^{\circ}$, $\gamma = 88.78$, Z = 4, $V = 2640(2)^{\circ}$. The [Ag₃As₂Se₅]_nⁿmacroanion has a very complicated two-dimensional layered structure composed of tetrahedral Ag+ ions and [As2Se5]4- units. The compound K₅[Ag₂As₃Se₉] crystallizes in the orthorhombic space group Pnma with a = 12.599(2)Å, b = 12.607(4)Å, c = 14.067(3)Å, Z = 12.607(4)Å, C = 14.067(3)Å, C = 14.067(3)Å 8. V = 2234(1)Å³. The [Ag₂As₃Se₉]_n⁵ⁿ macroanion has a twodimensional layered structure with tetrahedral Ag+ ions and two different selenoarsenate units, [AsSe4]3- and [As2Se5]4-. The K[Ag₃As₂S₅] also crystallized in orthorhombic space group Pnma with a = 19.210(2)Å, b = 16.867(2)Å, c = 6.3491(7)Å, Z = 8, V =2057.2(7)Å³. The [Ag₃As₂S₅]_nⁿ- macroanion also possesses a twodimensional layered structure with tetrahedral Ag+ ions and two

different thioarsenate ligands, $[AsS_3]^{3-}$ and $[As_3S_7]^{5-}$. The solid state optical and vibrational spectra of these compounds are reported.

1. Introduction

Recently, by hydrothermal synthesis, our exploration of the system R_4E^+ (R = alkyl, Ph, E = N, P)/ M^{n+}/AsS_3^{3-} led to the synthesis of several novel metal thioarsenate compounds, including $[InAs_3S_7]^{2-}$, $[BiAs_6S_{12}]^{3-}$, $[HgAs_3S_6]^ [Hg_2As_4S_9]^{2-}$, $[Pt(As_3S_5]_2]^{2-}$, $[Pt_3(AsS_4]_3]^{3-}$. In these compounds the $[AsS_3]^{3-}$ anion shows a facile condensation ability that results in high nuclearity $[As_xS_y]^{n-}$ units, see Eq. 1-4, which are found coordinated to the metal cations.

$$AsS_3^{3-} + AsS_3^{3-} = [As_2S_5]^{4-} + S^{2-}$$
 (Eq. 1)

$$[As_2S_5]^{4-}$$
 + AsS_3^{3-} = $[As_3S_7]^{5-}$ + S^{2-} (Eq. 2)

$$[As_3S_7]^{5-}$$
 + AsS_3^{3-} = $[As_4S_9]^{6-}$ + S^{2-} (Eq. 3)

$$[As_3S_7]^{5}$$
 = $[As_3S_6]^{3}$ + S^{2} (Eq. 4)

We achieved, however, little success when $M^{n+} = Ag^+$. In our initial work with silver, we repeatedly got the known Ag_3AsS_3 (proustite) compound, without incorporation of the cations. We then decided to explore the corresponding selenoarsenate anions by using $[AsSe_3]^{3-}$ as a reactant. The chemistry of selenoarsenic polyanions is not well developed, but the $[AsSe_3]^{3-}$ units are known to occur in solid state compounds, the so-called sulfosalts, as in Ag_3AsSe_3 and $TlAsSe_3$.

W. S. Sheldrick and co-workers have shown that the hydrothermal technique provides an easy route to prepare a large number of ternary As/Se compounds by simply reacting an alkali metal carbonate with a binary mixed 15/16 phase.⁴⁻⁹ For example:

$$M_2CO_3 + As_2Se_3 = \frac{130 \text{ °C/H}_2O}{MAsSe_3} = M = K, Rb, Cs$$

The MAsSe₃ (M = K, Rb, Cs) contain selenoarsenate anions, $[AsSe_3]^{n-}$, in which the arsenic atom is bonded to a monoselenide and a diselenide into infinite single chains.

In the field of solution chemistry, it was found that WSe₄²- and MoSe₄²- attack As₄Se₄ cages to form (Ph₄P)₂[W₂(μ-Se)₃(AsSe₅)₂] and (Ph₄P)₂[Mo(AsSe₅)₂].¹⁰ Both compounds contain two unusual [AsSe₅]³- groups as capping ligands. It was also found that [As₄Se₆]²can oxidatively decarbonylate to Mo(CO)₆ and W(CO)₆ to form $(Ph_4P)_2[M(CO)_2(As_3Se_3)_2]$ (M = Mo, W).¹¹ The chemistry of these molecular complexes was all done in polar solvents at ambient From the structures of (Ph₄P)₂[Hg₂As₄S₉], temperature. $(Me_4N)_2[HgAs_3Se_6]$, $(Me_4N)[HgAsSe_3]$, $(Et_4N)[HgAsSe_3]$, and (Ph₄P)₂[Hg₂As₄Se₁₁], (see chapter 5) we learned that thioarsenate ligands and selenoarsenate ligands form different $[As_xS_y]^{n-}$ and $[As_xSe_y]^{n-}$ species from condensation reactions and behave differently toward metal ions. With this in mind, we investigated the system Ag/As_xSe_y hoping that it would be different from the Ag/As_xS_y system. During this investigation we found that if we used methanol instead of water as a solvent we could avoid formation of the Ag_3AsQ_3 (Q = S, Se)(proustite) compound. We report here the synthesis, structural characterization, and optical properties of four novel Ag/As_xQ_y (Q = S, Se) compounds, $\beta-Ag_3AsSe_3(I)$, (Me₃NH)[Ag₃As₂Se₅](II), K₅[Ag₂As₃Se₉](III), and K[Ag₃As₂S₅](IV) from hydrothermal and methanothermal synthesis.

2. Experimental Section

2.1 Reagents

Chemicals in this work other than solvents were used as obtained: (i) selenium powder, ~ 100 mesh, 99.5% purity, Sliver tetrafloroboride, AgBF4, 99.5% purity, trimethylammonium chloride, Me₃NHCl, 99% purity, tetramethylammonium chloride, Me₄NCl, 99% purity, tetraethylammonium bromide, Et₄NBr, 99% purity, Aldrich Chemical Company, Inc., Milwaukee, WI; (ii) arsenic sulfide, As₂S₃, 100 mesh, 99% purity, arsenic selenide, As₂Se₃, ~200 mesh, 99% purity, Cerac Inc. Milwaukee WI; (iii) potassium metal, analytical reagent, Mallinckrodt Inc., Paris, KY; (iv) Methanol, anhydrous, Mallinckrodt Inc., Paris, KY; diethyl ether, ACS anhydrous, EM Science, Inc., Gibbstown, NJ.

2.2 Physical Measurements

The instruments and experimental setups for Infrared measurements, optical diffuse reflectance measurements, and quantitative microprobe analysis on SEM/EDS are the same as those reported in Chapter 2. Differential Thermal Analysis (DTA) was

performed with a computer-controlled Shimadzu DTA-50 thermal analyzer. The single crystals (~ 10.0 mg total mass) were sealed in Quartz ampules under vacuum. An empty Quartz ampule of equal mass was sealed and placed on the reference side of the detector. The samples were heated to the desired temperature at 10 °C/min, held isothermal for 10 min and then cooled at 10 °C/min to room temperature. The reported DTA temperatures are peak temperature. The DTA samples were examined by powder X-ray diffraction after the experiments.

2.3 Syntheses

All syntheses were carried out under a dry nitrogen atmosphere in a vacuum atmosphere Dri-Lab glovebox except were specifically mentioned.

K 3 A s S 3 (K 3 A s S e 3) was synthesized by using stoichiometric amounts of alkali metal, arsenic sulfide(selenide), and sulfur(selenium) in liquid ammonia. The reaction gives a yellow (orange) brown powder upon evaporation of ammonia.

β-Ag₃AsSe₃(I): A Pyrex tube (~ 4 mL) containing AgBF₄ (0.02 g, 0.1 mmol), K₃AsSe₃ (0.144 g, 0.3 mmol), Et₄NBr (0.10 g, 0.6 mmol) and 0.3 mL of water was sealed under vacuum and kept at 110 °C for one day. Large black needle-like crystals with metallic shine were isolated by washing the excess starting material and KCl with H₂O, MeOH and anhydrous ether. (Yield = 84.5%, Based on Ag). The infrared spectroscopy indicated the absence of organic cations. Semiquantitative microprobe analysis on single crystals gave

Ag₃As₁Se₃; however, the XRD did not match with any known Ag₄As₅Se ternary phases. The procedures were later modified to prepare this product in the absence of organic cations. The optimized reaction ratio of $1AgBF_4/3K_3AsSe_3$ gave a yield close to 99% based on Ag. Given that another compound with the formula Ag_3AsSe_3 is known, we will refer to (I) as β -Ag₃AsSe₃ and to the known phase as α -Ag₃AsSe₃.

(Me₃NH)[Ag₃As₂Se₅](II): A Pyrex tube (~4 mL) containing AgBF₄ (0.02 g, 0.1 mmol), K₃AsSe₃ (0.144 g, 0.3 mmol), Me₄NCl (0.10 g, 0.6 mmol) and 0.3 mL of water was sealed under vacuum and kept at 110 °C for one day. The large dark-red transparent plate-like crystals that formed were isolated by washing with H₂O, MeOH and anhydrous ether. (Yield = 99%, Based on Hg). Although we started with Me₄N+ as the cation the presence of Me₃NH+ cations was confirmed with infared spectroscopy and was further proved by synthesizing the compound with Me₃NH+ as the counterion. Semiquantitative microprobe analysis on single crystals gave Ag₂As₁Se₂.

K₅[Ag₂As₃Se₉](III): A Pyrex tube (~ 4 mL) containing AgBF4 (0.02 g, 0.1 mmol), K₃AsSe₃ (0.144 g, 0.3 mmol), Ph₄PBr (0.419 g, 1 mmol) and 0.5 mL of methanol was sealed under vacuum and kept at 110 °C for one week. Large black block-like crystals were isolated by removing the excess starting material and KCl with H₂O, MeOH and anhydrous ether(yield = 75% based on Ag). Quantitative microprobe analysis on single crystals gave K_{2.1}Ag₁As_{1.6}Se_{3.9}. The procedure was later modified to avoid the use of organic counterions.

The optimized reaction ratio of AgBF4/K₃AsSe₃ is 1:3 with the yield close to 90% based on Ag.

K[Ag₃As₂S₅](IV): A Pyrex tube (~4 mL) containing AgBF4 (0.02 g, 0.1 mmol), K₃AsS₃ (0.144 g, 0.3 mmol), Ph₄PBr (0.419 g, 1 mmol) and 0.5 mL of methanol was sealed under vacuum and kept at 110 °C for one week. Large brown-yellow chunky crystals were isolated by washing the excess starting material and KCl with H₂O, MeOH and anhydrous ether (yield = 65% based on Ag). Quantitative microprobe analysis on single crystals gave K₁Ag_{2.5}As_{1.6}S_{4.5}. The procedure was later modified to avoid the use of organic counterions. The optimized reaction ratio of AgBF4/K₃AsS₃ is 1:3 with the yield close to 85% based on Ag.

2.4 X-ray crystallography

Single-crystal X-ray diffraction data of all four compounds were collected at 23 °C with a Rigaku AFC6 diffractometer equipped with a graphite-crystal monochromator. The data were collected with a $\theta/2\theta$ scan technique. None of the four crystals showed a significant intensity decay as judged by three check reflections measured every 150 reflections through the data collection. Space groups were determined from systematic absences and intensity statistics. The structures were solved by the direct methods of SHELXS- 86^{12} and refined by the full-matrix least-squares techniques of the TEXSAN¹³ software package of crystallographic programs. An empirical absorption correction based on ψ -scans was applied to each

data set, followed by a DIFABS¹⁴ correction to the isotropically refined structures. All nonhydrogen atoms except carbon and nitrogen were eventually refined anisotropically. All calculations were performed on a VAXstation 3100/76 computer.

The complete data collection parameters and details of the structure solutions and refinements are given in Tables 6-1 and 6-2. The fractional atomic coordinates, average temperature factors, and their estimated standard deviations are given in Tables 6-3, 6-4, 6-5, and 6-6.

Table 6-1. Crystallographic Data for β -Ag₃AsSe₃(I) (Me₃NH)[Ag₃As₂Se₅](II).

	I	II
Formula	Ag ₃ AsSe ₃	C ₃ H ₁₀ NAg ₃ As ₂ Se ₅
F. w.	635.41	928.25
a, Å	8.111(1)	10.549(1)
b, Å	11.344(2)	11.477(2)
c, Å	20.728(3)	6.5491(8)
α, deg.	90.00	104.94(1)
β, deg.	90.00	107.40(8)
γ, deg.	90.00	88.78(1)
Z, V, A^3	12, 1907(1)	2, 729.6(4)
Space Group	Pnma(No. 62)	P-1(No.2)
color, habit	Black, needle	Dark red, plate
D _{calc} , g/cm ³	6.64	4.22
Radiation	Μο Κα	Μο Κα
μ, cm ⁻¹	311.11	207.65
$2\theta_{\text{max}}$, deg.	45.0	45.0
Absorption Correction	ψ scan	ψ scan
Transmission Factors	0.86-1.04	0.80-1.32
Index ranges	$0 \le h \le 12, 0 \le k \le 22,$	$0 \le h \le 13$, $-14 \le k \le 14$,
	0≤1≤9	-8 <u>≤</u> 1 <u><</u> 8
No. of Data coll.	1791	2027
Unique reflections	1676	1901
Data Used	760	997
$(F_0^2 > 3\sigma(F_0^2))$		
No. of Variables	106	107
Final Ra/Rwb, %	6.7/7.9	4.4/4.7

^a R= Σ (|Fo|-|Fc|)/ Σ |Fo|, ^b R_w={ Σ w(|Fo|-|Fc|)²/ Σ w|Fo|²} 1/2.

Table 6-2. Crystallographic Data for $K_5[Ag_2As_3Se_9](III)$ $K[Ag_3As_2S_5](IV)$.

	III	IV
Formula	K5Ag2As3Se9	KAg3As2S5
F. w.	1346.65	672.55
a, Å	12.599(2)	19.210(2)
b, Å	12.607(3)	16.867(2)
с, Å	14.067(3)	6.3491(7)
α, deg.	90.00	90.00
β, deg.	90.00	90.00
γ, deg.	90.00	90.00
Z, V, Å ³	8, 2234(1)	8, 2057.2(7)
Space Group	Pnma(No. 62)	Pnma(No. 62)
color, habit	Black, block	Yellow brown, needle
D _{calc} , g/cm ³	4.00	4.34
Radiation	Μο Κα	Μο Κα
μ, cm ⁻¹	215.77	133.00
$2\theta_{\text{max}}$, deg.	45.0	45.0
Absorption Correction	ψ scan	ψ scan
Transmission Factors	0.51-1.00	0.89-1.18
Index ranges	$0 \le h \le 14, 0 \le k \le 14,$	$0 \le h \le 18, 0 \le k \le 21,$
<u>-</u>	0 <u>≤</u> 1≤15	0 <u>≤</u> 1 <u><</u> 7
No. of Data coll.	1856	1723
Unique reflections	1703	1627
Data Used	843	768
$(F_0^2 > 3\sigma(F_0^2))$		
No. of Variables	97	106
Final Ra/Rwb, %	4.0/4.5	4.0/4.7

^a R= $\Sigma(|F_0|-|F_c|)/\Sigma|F_0|$, ^b R_w={ $\Sigma_w(|F_0|-|F_c|)^2/\Sigma_w|F_0|^2$ } 1/2.

Table 6-3. Selected Atomic Coordinates and Estimated Standard Deviations (esd's) of β -Ag₃AsSe₃(I).

atom	X	Y	Z	B _{eq} a, (A ²)
Ag1	0.6435(6)	-0.0180(4)	0.6779(2)	1.5(2)
Ag2	0.3314(5)	0.1101(4)	0.7155(2)	1.6(2)
Ag3	0.8779(6)	-0.0348(4)	0.5601(2)	1.4(2)
Ag4	0.7139(6)	0.0714(4)	0.4424(2)	1.9(2)
Ag5	0.7766(9)	-0.2500	0.6312(4)	1.3(3)
Se1	0.613(1)	0.2500	0.7120(4)	0.7(4)
Se2	0.988(1)	-0.2500	0.5318(4)	1.1(4)
Se3	0.1200(7)	0.0889(6)	0.6187(3)	1.0(3)
Se4	0.4164(7)	-0.0962(5)	0.7686(3)	0.8(3)
Se5	0.454(1)	-0.2500	0.6095(4)	0.9(4)
Se6	0.6009(7)	0.0837(5)	0.5629(3)	1.1(3)
As1	0.748(1)	0.2500	0.6078(4)	0.6(4)
As2	0.220(1)	0.2500	0.5539(5)	0.7(4)
As3	0.287(1)	-0.2500	0.7082(6)	1.3(4)

^a $B_{eq}=(4/3)[a^2B_{11} + b^2B_{22} + c^2B_{33} + ab(\cos\gamma)B_{12} + ac(\cos\beta)B_{13} + bc(\cos\alpha)B_{23}].$

Table 6-4. Selected Atomic Coordinates and Estimated Standard Deviations (esd's) of (Me₃NH)[As₃As₂Se₅](II).

atom	X	Y	Z	$B_{eq} a, (A^2)$
Ag(1)	0.8318(3)	0.1222(2)	0.2789(4)	3.1(1)
Ag(2)	0.6153(2)	-0.0699(2)	-0.025(4)	2.8(1)
Ag(3)	0.9225(3)	0.1580(2)	0.8225(4)	3.8(1)
Se(1)	0.7384(3)	0.2691(2)	0.5915(4)	1.7(1)
Se(2)	1.0396(3)	0.2355(3)	0.2506(4)	1.8(1)
Se(3)	0.5991(3)	0.1693(3)	-0.0333(4)	1.8(1)
Se(4)	0.6182(3)	-0.2114(2)	-0.4170(4)	1.5(1)
Se(5)	0.8387(3)	-0.1161(3)	0.2712(4)	1.8(1)
A s(1)	0.5867(3)	0.1183(3)	0.5867(4)	1.5(1)
A s(2)	1.1818(3)	0.0856(2)	0.3646(4)	1.5(1)
N	1.235(2)	0.424(2)	0.805(4)	2.8(5)
C(1)	1.271(3)	0.501(3)	0.687(5)	4.0(7)
C(2)	1.332(4)	0.422(4)	1.005(6)	6.2(9)
C(3)	1.105(5)	0.452(4)	0.855(7)	6.7(9)

^a $B_{eq} = (4/3)[a^2B_{11} + b^2B_{22} + c^2B_{33} + ab(\cos\gamma)B_{12} + ac(\cos\beta)B_{13} + bc(\cos\alpha)B_{23}].$

Table 6-5. Selected Atomic Coordinates and Estimated Standard Deviations (esd's) of $K_5[Ag_2As_3Se_9](III)$.

atom	X	Y	Z	$B_{eq}^{a}, (A^2)$
Ag	0.2369(1)	0.0892(2)	0.7118(2)	2.16(9)
Se1	0.3547(3)	-0.2500	0.5712(3)	1.5(2)
Se2	0.2825(2)	0.2500	0.8258(3)	1.2(1)
Se3	0.0358(2)	0.0958(2)	0.6494(2)	1.4(1)
Se4	0.2853(2)	-0.1001(2)	0.7974(2)	1.6(1)
Se5	0.0741(3)	-0.2500	0.6552(3)	2.1(2)
Se6	0.3781(2)	0.1025(2)	0.5681(2)	1.6(1)
As1	0.2481(2)	-0.2500	0.7051(3)	1.1(1)
As2	-0.0365(2)	0.2500	0.7165(2)	0.9(1)
As3	0.4835(2)	0.2500	0.6010(3)	1.3(2)
K 1	0.1787(4)	-0.0718(4)	0.4961(4)	2.3(3)
K2	0.9796(4)	0.0801(4)	0.1694(4)	2.2(2)
К3	0.1707(6)	0.2500	0.4897(7)	2.2(4)

^a $B_{eq}=(4/3)[a^2B_{11} + b^2B_{22} + c^2B_{33} + ab(\cos\gamma)B_{12} + ac(\cos\beta)B_{13} + bc(\cos\alpha)B_{23}].$

Table 6-6. Selected Atomic Coordinates and Estimated Standard Deviations (esd's) of K[Ag₃As₂S₅](IV).

atom	X	Y	Z	B_{eq}^{a} , (A^2)
Agl	0.6851(1)	0.3690(1)	0.0892(4)	3.1(1)
Ag2	0.7332(1)	0.5239(1)	-0.0909(4)	4.2(1)
Ag3	0.8572(1)	0.3669(1)	-0.1605(3)	3.3(1)
As1	0.7870(2)	0.2500	0.4088(6)	1.0(1)
As2	0.5884(1)	0.4603(1)	0.5950(4)	1.2(1)
As3	0.6069(2)	0.2500	0.5118(6)	1.0(1)
K	0.4786(3)	0.3776(3)	0.0894(9)	1.8(2)
S 1	0.3806(4)	0.2500	-0.119(1)	1.4(4)
S2	0.8151(3)	0.3558(4)	0.209(1)	1.4(3)
S 3	0.6071(3)	0.4913(3)	0.256(1)	1.2(2)
S 4	0.5232(3)	0.3456(3)	0.579(1)	1.1(2)
S 5	0.6914(3)	0.4075(3)	-0.311(1)	1.2(3)
S 6	0.6068(5)	0.2500	0.161(1)	1.6(4)

^a $B_{eq}=(4/3)[a^2B_{11} + b^2B_{22} + c^2B_{33} + ab(\cos\gamma)B_{12} + ac(\cos\beta)B_{13} + bc(\cos\alpha)B_{23}].$

The compounds were examined by X-ray powder diffraction for the purpose of phase purity and identification. Accurate d_{hk1} spacings (Å) were obtained from the powder patterns recorded on a calibrated (with FeOCl as internal standard) Phillips XRG-3000 computer-controlled powder diffractometer with graphite-monochromated Cu K α radiation operating at 35 kV and 35 mA. The data were collected at a rate of 0.12° /min. Based on the atomic coordinates from the X-ray single crystal diffraction study, X-ray powder patterns for all compounds were calculated by the software package CERIUS.¹⁴ Calculated and observed X-ray powder patterns that show d-spacings and intensities of strong hkl reflections are complied in Tables 6-7 to 6-10.

Table 6-7. Calculated and Observed X-ray Powder Diffraction Pattern of β -Ag₃AsSe₃(I).

_					
h	k	l	d _{calc} (Å)	d _{obs} (Å)	I/I_{max} (obs. %)
$\overline{1}$	0	2	6.38	6.38	13
0	1	3	5.90		
0	2	0	5.67	5.67	27
1	0	3	5.26	5.25	47
1	1	3	4.77	4.77	1 4
2	0	0	4.06	4.05	3 8
2	1	0	3.82	3.82	77
1	0	5	3.69	3.69	1 2
2	1	2	3.58	3.58	10
0	0	6	3.45	3.45	3 4
1	0	6	3.18	3.17	10
1	2	5	3.09	3.09	1 7
1	3	3	3.07	3.07	97
1	1	6	3.06	3.06	65
2	0	5	2.90	2.90	5 4
0	4	0	2.83	2.83	1 4
2	1	5	2.79	2.79	30
0	3	5	·		
1	2	6	2.77	2.77	4 5
2	3	2	2.67	2.67	5 5
1	3	5	2.64	2.64	28
1	4	2	2.59	2.59	67
0	0	8			
2	2	5	2.58	2.58	79
2	3	3	2.56	2 56	100
1	4	3	2.49	2.49	36
1	3	6	2.43	2.43	15
3	2	2	2.36	2.35	65
0	2	8			
	4	1	2.30	2.30	3 2
2 3 3	2	3			
3	0	5	2.264	2.264	40
0	5	1	2.255	2.255	10
3	2	4	2.205	2.206	78
2	4	3		-	

	_				_	
3	3	1	2.187	2.187	18	
2	3	6	2.159	2.158	25	
3	0	6	2 129	2.13	92	
1	3	8	2.064	2.063	20	
1	2	9				
3	0	7	1.996	1.994	10	
2	5	0	1.980	1.980	25	
1	3	9	1.910	1.910	8 5	
4	2	0				
1	2	10	1.891	1.891	50	
0	6	0				
3	3	6	1.855	1.855	25	
4	2	3	1.840	1.840	10	
4	3	2	1.761			
4	3	3	1 730			
2	5	6	1.717	1.717	10	
2	3	10	1.658	1.658	20	
0	6	6	2.000	_,,,,	_ •	
<u> </u>						

Table 6-9. Calculated and Observed X-ray Powder Diffraction Pattern of K₅[Ag₂As₃Se₉](III).

h	k	l	d_{calc} (Å)	d_{obs} (Å)	I/I_{max} (obs., %)
0	1	1	9.39	9.38	31
0	0	2	7.03	7.03	67
0	2	0	6.30	6.30	1 4
2	0	0			
1	0	2	6.14	6.14	28
2	1	1	5.23	5.23	1 1
2	0	2	4.69	4.68	1 8
1	0	3	4.39	4.39	15
0	3	1	4.02	4.01	10
1	3	1	3.83	3.83	3 4
3	0	2	3.60	3.59	15
1	3	2	3.47	3.46	15
2	3	1	3.39		
1	1	4	3.27		
4	0	0	3.15	3.15	11
2	3	2	3.13	3.13	70
0	3	3			
2	0	4	3.07	3.07	3 5
1	3	3	3.03	3.03	100
4	0	2	2.87	2.87	57
1	0	5	2.74	2.73	50
3	3	2			
1	3	4	2.63		
2	0	5	2.57	2.57	10
1	3	5	2.30	2.30	1 2
4	3	3	2.22	2.22	15
0	6	0	2 10	2 10	5 5
3	3	5	2.04	2.04	15
1	3	6	2.02	-	-
5	3	3	1.963	1.963	24
6	3	0	1.878	1.878	22

Table 6-9. Calculated and Observed X-ray Powder Diffraction Pattern of K₅[Ag₂As₃Se₉](III).

_				 	
h	k	l	d _{calc} (Å)	d_{obs} (Å)	I/I _{max} (obs, %)
0	1	1	9.39	9.38	3 1
0	0	2	7.03	7.03	67
0	2	0	6.30	6.30	1 4
2	0	0			
1	0	2	6.14	6.14	28
2	1	1	5.23	5.23	1 1
2	0	2	4.69	4.68	18
1	0	3	4.39	4.39	1 5
0	3	1	4.02	4.01	10
1	3	1	3.83	3.83	3 4
3	0	2	3.60	3.59	1 5
1	3	2	3.47	3.46	1 5
2	3	1	3.39		
1	1	4	3.27		
4	0	0	3.15	3.15	1 1
2	3	2	3.13	3.13	70
0	3	3			
2	0	4	3.07	3.07	3 5
1	3	3	3.03	3.03	100
4	0	2	2.87	2.87	5 7
1	0	5	2.74	2.73	50
3	3	2			
1	3	4	2.63		
2	0	5	2.57	2.57	10
1 4	3	5	2.30	2.30	1 2
4	3	3	2.22	2.22	15
0	6	0	2 10	2 10	5 5
	3	5	2.04	2.04	15
3 1	3	6	2.02		
5	3	3	1.963	1.963	24
_6	3	0	1.878	1.878	22

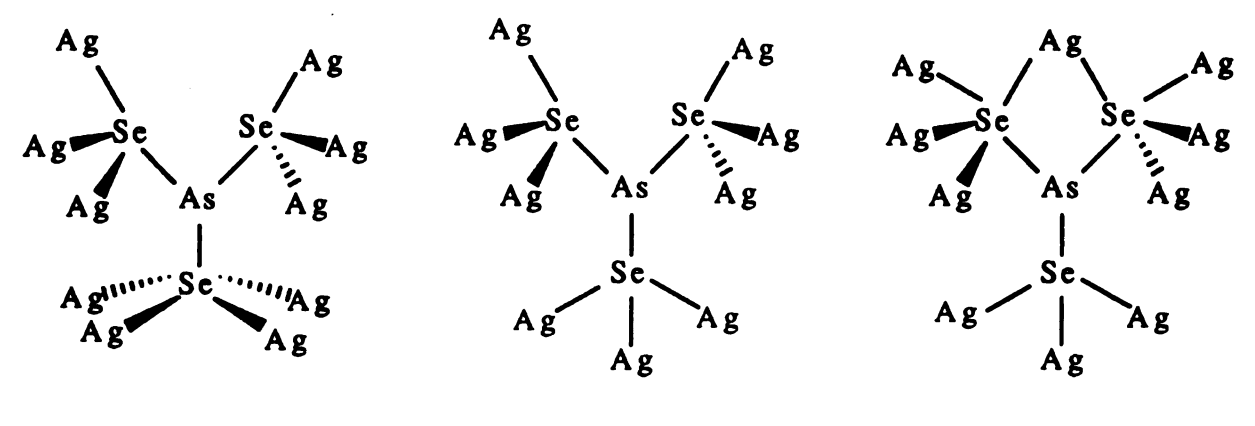
Table 6-10. Calculated and Observed X-ray Powder Diffraction Pattern of K[Ag₃As₂S₅](IV).

h	k	l	d _{calc} (Å)	d _{obs} (Å)	I/I_{max} (obs. %)
2	0	0	9.60	9.60	100
0	2	0	8.43	8.42	14
2	2	0	6.33	6.32	8
1	0	1	6.02	6.01	10
2	0	1	5.29	5.29	1 4
2	1	1	5 05		
1	3	1	4 11	4 11	10
4	1	1	3.73	3.73	13
5	0	1	3.28	3.28	3 5
5	1	1	3.22	3.22	19
2	5	0	3.18	3.19	10
1	1	2	3.08	3.08	25
6	2	0	2.99	2.99	10
1	5	1	2.94	2.94	67
6	0	1	2.86	2.86	18
5	3	1	2.83	2.83	20
4	4	1			
3	1	2	2.80	2.80	10
1	3	2	2.73	2.73	1 4
6	4	0	2.55	2.55	5 4
7	0	1	2.51	2.51	10
1	4	2			
3	4	2	2 35	2.35	3 5
0	8	0	2.10	2.10	10

3. Results and Discussion

3.1 Syntheses and description of structures

 β -Ag₃AsSe₃(I) was originally synthesized with tetraethylammoninum cations present in the reaction mixture. Although the synthesis can be accomplished without the organic cations, only microcrystalline powder can be obtained. Single crystals were only obtained upon addition of tetraethylammoninum chloride. The role of the cations is still unclear, but it may act as a mineralizer. The structure was solved by single-crystal x-ray diffraction analysis. β -Ag₃AsSe₃(I) has a very complicated three-dimensional dense-packed structure; see Figures 6-1, 6-2, and 6-3. The basic building block is the [AsSe₃]³⁻ units which engage in several very complex bonding modes in linking the Ag⁺ ions together; see Scheme 6-1.



Scheme 6-1

The Ag⁺ atoms are found in several different coordination environments. The geometry around Ag(1), Ag(3), and Ag(4) is distorted trigonal planar with normal Ag-Se bond distances (2.665Å). The tetrahedral geometry around the Ag(2) is slightly distorted with

two long Ag(2)-Se(1) bonds, at 2.785(7) and 2.812(8)Å, and two normal Ag-Se bonds, at 2.651(6) and 2.676(7)Å. The Se-Ag(2)-Seangles range from 92.8(3)° to 124.3(3)°. The tetrahedral environment around the Ag(5) is highly distorted with two very long Ag-Se "bonds" at 2.939(7)Å, and two normal Ag-Se bonds at 2.663(7) and 2.681(9)Å. The Se-Ag(5)-Se angles range from 72.8(3)° to 120.0(3)°. Detailed bond distances and angles are given in Tables 6-The major difference between this compound and the well known sulfosalt, α-Ag₃AsSe₃ is that in the latter the Ag⁺ ions are coordinated to three Se atoms; see Figure 6-1(B). The geometry around the Ag atoms in the α-form can best be described as bent-T shaped with the Se-Ag-Se angles ranging from 159° to 85°. bent-T centers all point toward the same direction with the result that crystallization occurs in the acentric space group, R3c (No. 161). In our compound which is centrosymmetric, β-Ag₃AsSe₃(I), the Ag⁺ ions are both three- and four- coordinated. This is consistent with the fact that the density of β -Ag₃AsSe₃ is 0.12 g/cm³ higher than that of α -Ag₃AsSe₃.

This compound may have eluded mineralogists for such long time because it may be meta-stable given the mild conditions under which it was synthesized. Traditional sulfosalt synthetic conditions typically involve heating stiochiometric amount of elements at temperatures in excess of 1000 °C. The β-Ag₃AsSe₃(I), however, was synthesized from AgBF₄/3K₃AsSe₃, hydrothermally at 110 °C in one day, suggestive that it is only a kinetically stable phase. In a way, this suggestion is quite puzzling when we consider that β-Ag₃AsSe₃ is

Table 6-11. Selected Distances (Å) in β -Ag₃AsSe₃ with Standard Deviations in Parentheses.^a

Ag1 - Ag2	3.021(6)	Ag1 - Ag2	3.053(5)
Ag1 - Ag3	3.101(6)	Ag1 - Ag5	3.005(6)
Ag1 - Se4	2.778(5)	Ag1 - Se4	2.630(5)
Ag1 - Se6	2.671(7)	Ag2 - Se1	2.785(7)
Ag2 - Se1	2.812(8)	Ag2 - Se3	2.651(6)
Ag2 - Se4	2.676(7)	Ag3 - Ag4	3.028(6)
Ag3 - Ag5	2.969(5)	Ag3 - Se2	2.664(5)
Ag3 - Se3	2.702(7)	Ag3 - Se6	2.619(6)
Ag4 - Se3	2.593(7)	Ag4 - Se5	2.670(7)
Ag4 - Se6	2.663(7)	Ag5 - Se2	2.681(9)
Ag5 - Se4	2.939(7)	Ag5 - Se5	2.659(9)
Sel - Asl	2.421(9)	Se2 - As2	2.451(9)
Se3 - As2	2.408(9)	Se4 - As3	2.389(7)
Se5 - As3	2.450(9)	Se6 - As1	2.418(8)

^aThe estimated standard deviations in the mean bond lengths and the mean bond angles are calculated by the equation $\sigma l = \{\Sigma_n(l_n - 1)^2/n(n-1)\}^{1/2}$, where l_n is the length (or angle) of the nth bond, l the mean length (or angle), and n the number of bonds.

Table 6-12. Selected Angles (Deg) in β -Ag₃AsSe₃ with Standard Deviations in Parentheses.^a

Se4-Ag1-Se4	99.5(2)	Se4-Ag1-Se6	131.0(2)
Se4-Ag1-Se6	129.1(2)	Sel-Ag2-Sel	102.1(2)
Se1-Ag2-Se3	124.3(3)	Se1-Ag2-Se4	107.3(2)
Se1-Ag2-Se3	92.8(3)	Se1-Ag2-Se4	115.8(3)
Se3-Ag2-Se4	113.5(3)	Se2-Ag3-Se3	109.4(3)
Se2-Ag3-Se6	139.6(3)	Se3-Ag3-Se6	110.3(2)
Se3-Ag4-Se5	127.0(3)	Se3-Ag4-Se6	132.3(3)
Se5-Ag4-Se6	99.3(3)	Se2-Ag5-Se4	107.3(3)
Se2-Ag5-Se4	107.3(3)	Se2-Ag5-Se5	119.9(4)
Se4-Ag5-Se4	72.8(3)	Se4-Ag5-Se5	120.0(3)
Ag2-Se1-Ag2	69.5(3)	Ag2-Se1-Ag2	145.5(3)
Ag2-Se1-Ag2	100.4(2)	Ag2-Se1-As1	113.2(3)
Ag3-Se2-As2	86.0(3)	Ag5-Se2-As2	96.8(4)
Ag2-Se3-As2	97.8(3)	Ag3-Se3-As2	112.8(3)
Ag4-Se3-As2	94.9(3)	Ag1-Se4-As3	99.7(2)
Ag2-Se4-As3	108.1(2)	Ag4-Se5-As3	93.1(3)
Ag1-Se6-As1	85.9(3)	Ag3-Se6-As1	89.2(3)
Ag4-Se6-As1	103.4(3)	Sel-Asl-Se6	97.0(3)
Se6-As1-Se6	102.6(4)	Se2-As2-Se3	100.0(3)

^aThe estimated standard deviations in the mean bond lengths and the mean bond angles are calculated by the equation $\sigma l = \{\Sigma_n(l_n - 1)^2/n(n-1)\}^{1/2}$, where l_n is the length (or angle) of the nth bond, l the mean length (or angle), and n the number of bonds.

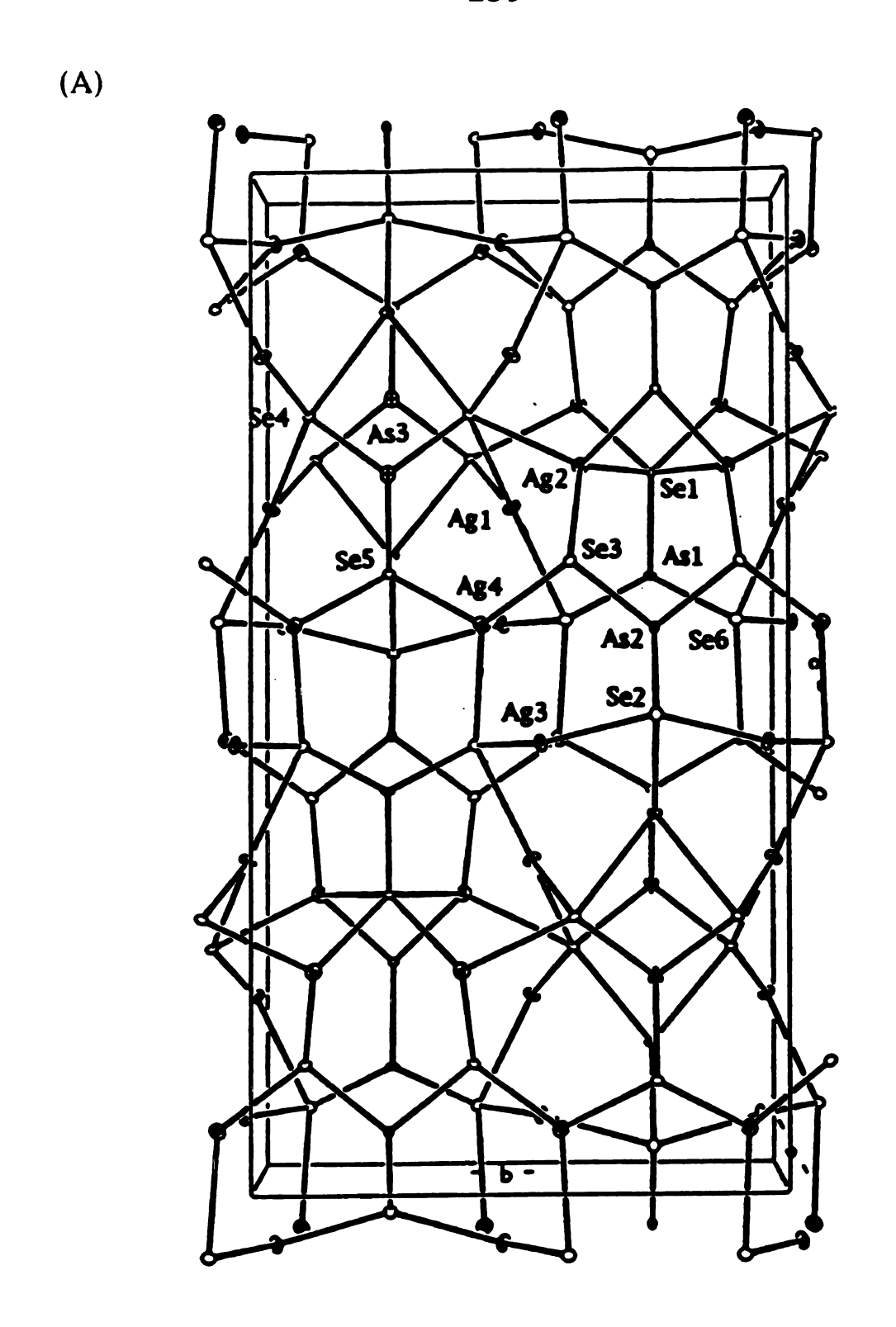
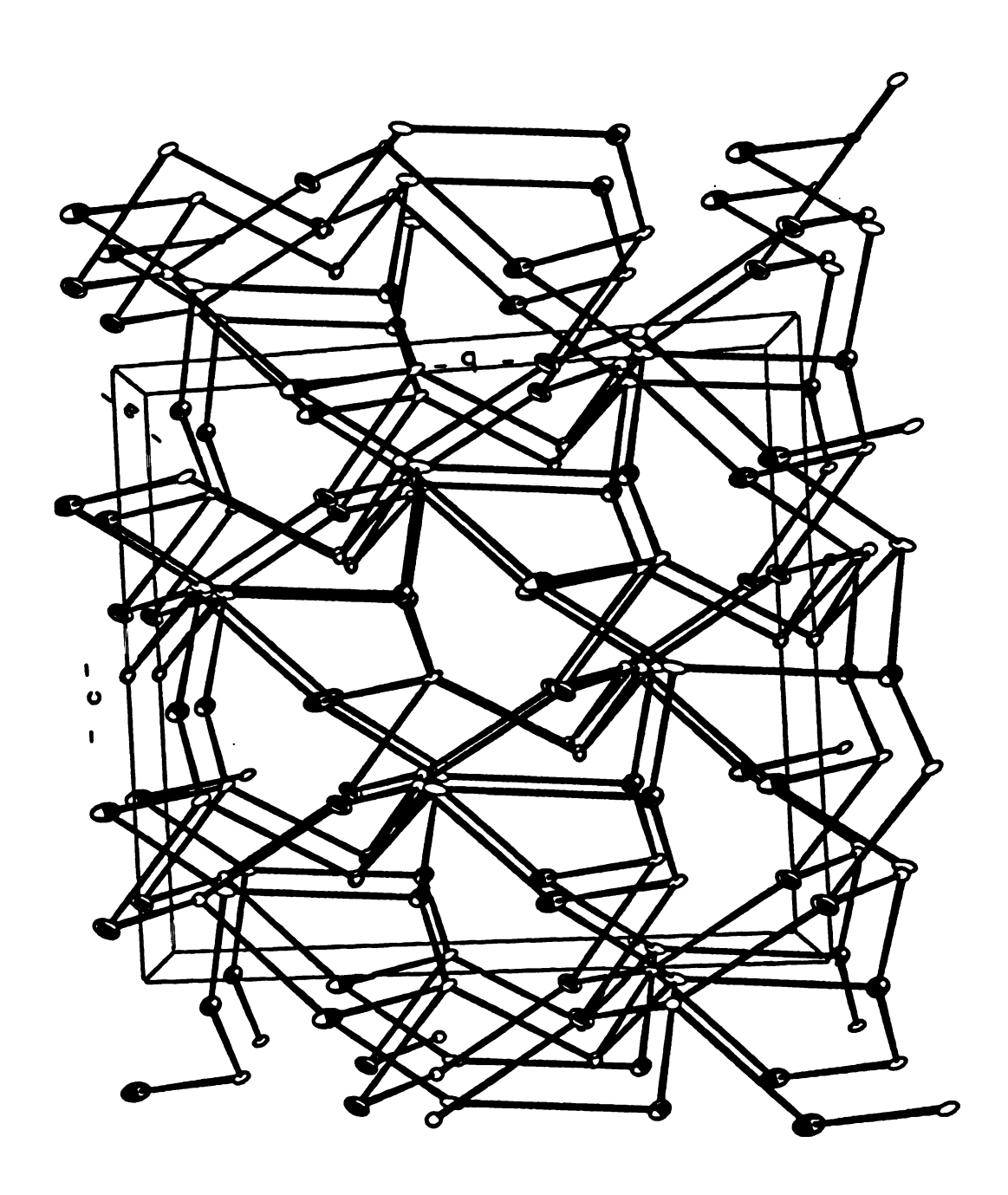


Figure 6-1. Structure and labeling scheme of Ag₃AsSe₃. (A) β -form. (B) α -form.

(B)



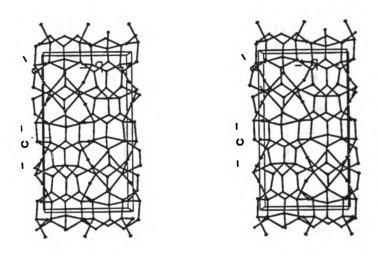


Figure 6-2. Stereoview of the β -Ag₃AsSe₃ (I).

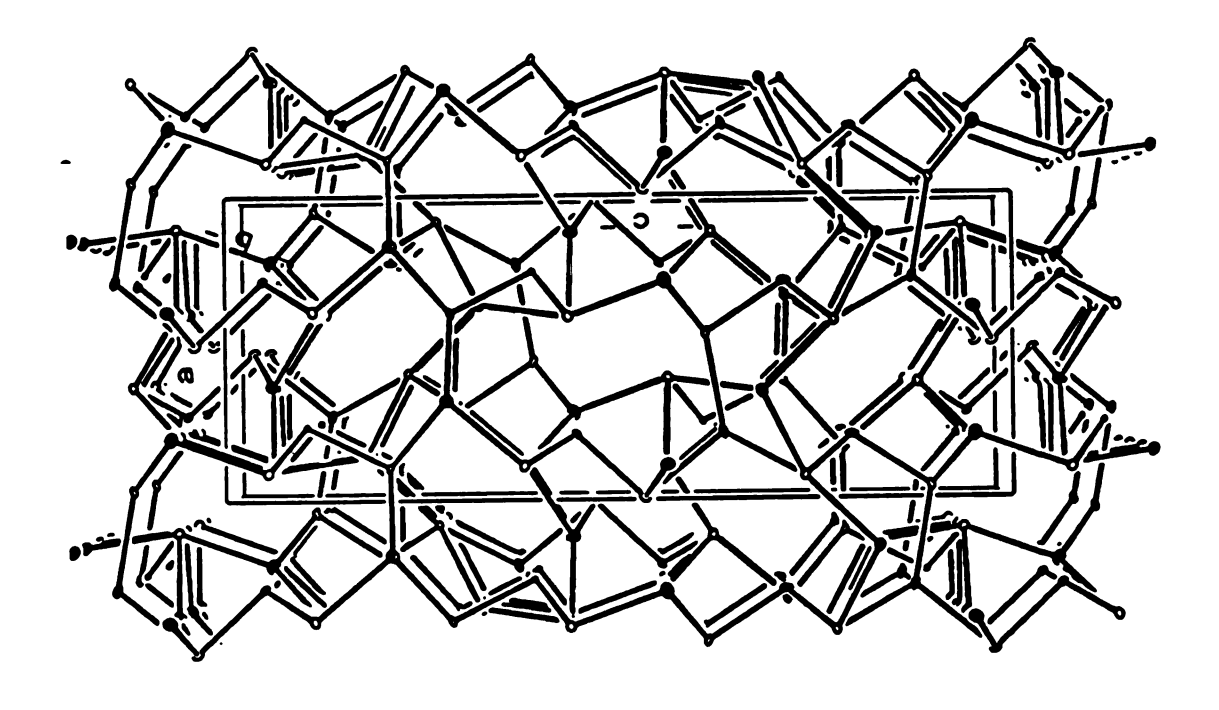
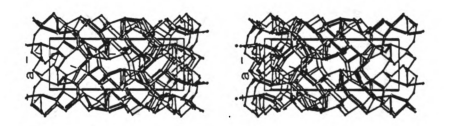
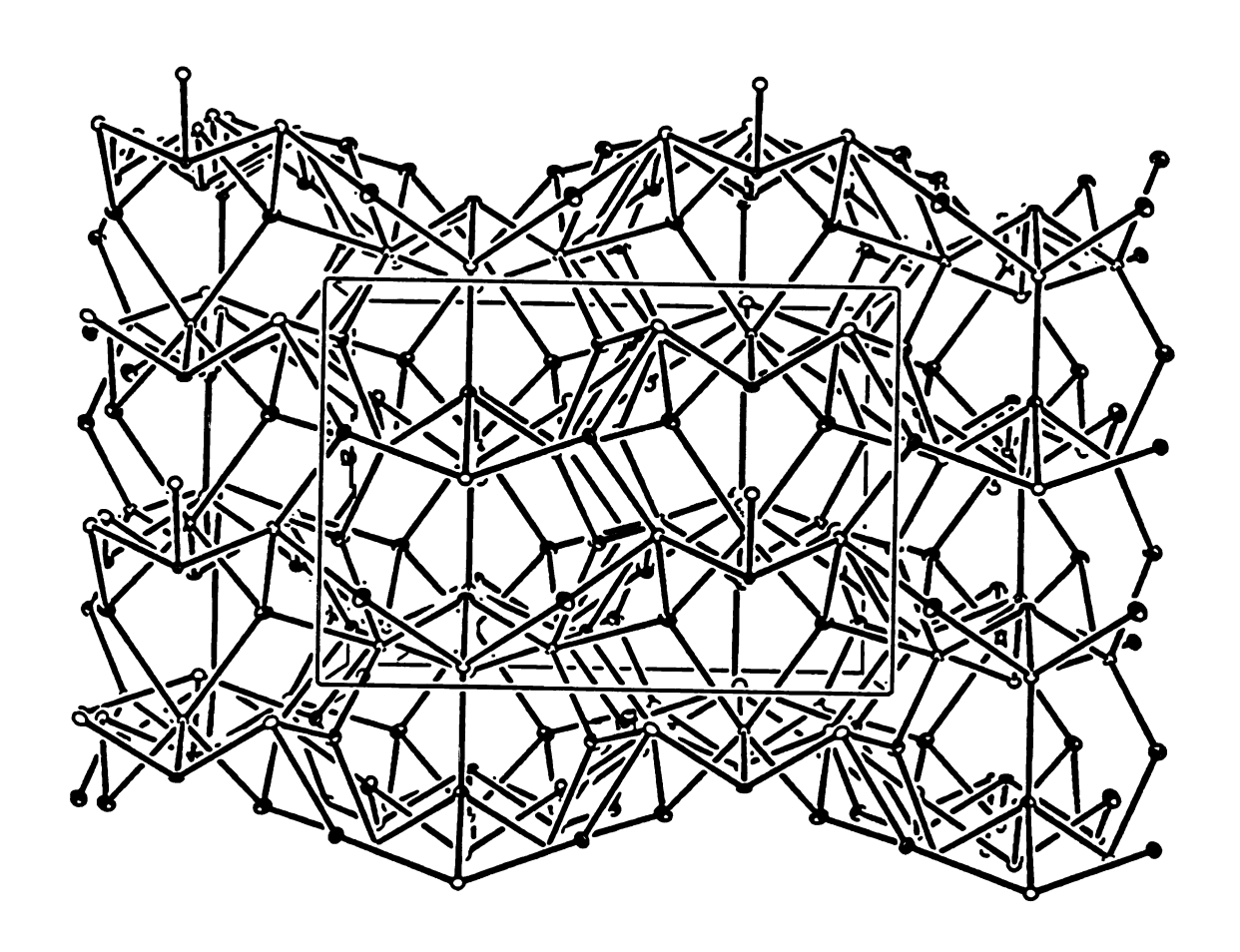


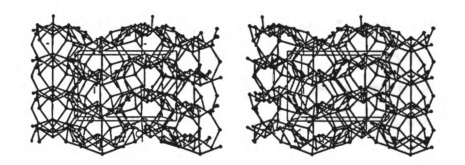
Figure 6-3. Packing diagrams of β -Ag₃AsSe₃(I). (A) view down the b-axis. (B) Stereoview down the b-axis. (C) view down the c-axis. (D) stereoview down the c-axis.

(B)



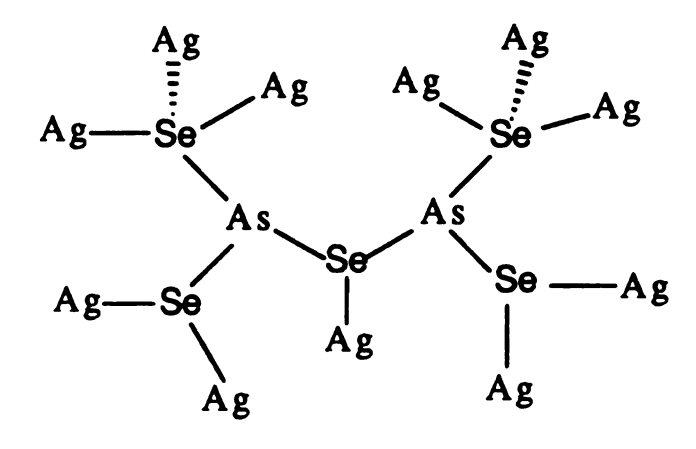


(D)



more dense and thus could represent a high pressure modification of α-Ag₃AsSe₃.

The compound (Me₃NH)[As₃As₂Se₅](II) was first synthesized by heating AgBF₄ with K₃As₈Se₃ and Me₄NCl in H₂O at 110 °C for one day. Although we started with Me₄N+ as the counterion, the presence of Me₃N H+ cations was confirmed with infared spectroscopy. Other similar-sized organic cations were also tried, without success, in anticipation of obtaining the same anionic framework, an indication that the Me₃N H+ ion was playing a templating role for compound (II). The anions [As₃As₂Se₅]_nⁿ-possess a very complicated two-dimensional layered structure consisting of tetrahedral Ag+ and [As₂Se₅]⁴- units formed by two corner-sharing trigonal pyramidal [AsSe₃]³-; see Figures 6-4 and 6-5. Each of the [As₂Se₅]⁴- units engages in a remarkably complex multidentate coordination with 11 Ag+ centers using all five of their selenium atoms; see Scheme 6-2.



Scheme 6-2

The coordination geometry of the Ag(1) and Ag(2) atoms is distorted tetrahedral with the Se-Ag-Se bonds angles ranging from 85.9(1)° to 119.8(1)°. The average Ag-Se distance, at 2.725(5)Å, is normal for tetrahedral Ag+ ions. The Ag(3) atom is coordinated to three Se atoms and the lone electron pair of an As atom. This is the first time we observed the lone pair of the As atom to be involved in metal binding. Recently, a similar bonding arrangement was also observed in KCu₂AsS₃ where Cu(1) and Cu(2) were tetrahedrally coordinated to three S atoms and the lone pair of an As atom. The Ag(3)-As distance is 2.844(4)Å. The geometry of the Ag(3) can be described as either distorted trigonal planar, without the As atom, or distorted tetrahedral, with the As atom. Only one of the two As atoms in [As₂Se₅]⁴- is interacting with a Ag center. The average As-Se distance, at 2.410(4)Å, and Se-As-Se angles, at 99.0(1) are normal compared to those in the known As/Se compounds.¹⁵ The shortest Ag-Ag distances are 2.889(5) and 3.012(3)Å. Detailed distances and angles are summarized in Tables 6-13 and 6.14.

The $[Ag_3As_2Se_5]_n^{n-}$ layers are formed in such way that all the lone pairs of the selenium atoms are pointed away from the layers. The trimethylammonium cations, Me₃NH⁺, are located in the gallery region, yielding an interlayer distance of 11.47 Å. Interestingly, the hydrogen atoms bonded to the nitrogen in the Me₃NH⁺ ion point toward the layers, suggesting the presence of hydrogen bonding to the selenides, see Figure 6-6. The closest Se-H distances are Se(3)-H1 and Se(5)-H1 at 3.016Å and 2.739Å, respectively, which are much shorter than the van der Waals contact of 3.35 Å. The Me₃NH⁺

Table 6-13. Selected Distances (Å) (with Standard Deviations in Parentheses^a) in the [Ag₃As₂Se₅]¹- layer.

Ag1 - Ag2	3.012(3)	Ag1 - Se1	2.713(4)	
Ag1 - Se2	2.650(4)	Ag1 - Se3	2.830(4)	
Ag1 - Se5	2.722(4)	Ag2 - Ag2	2.889(5)	
Ag2 - Se3	2.802(4)	Ag2 - Se3	2.653(4)	
Ag2 - Se4	2.790(4)	Ag2 - Se5	2.638(4)	
Ag3 - Se1	2.611(4)	Ag3 - Se2	2.620(4)	
Ag3 - Se5	2.770(4)	Ag3 - As2	2.844(4)	
Sel - Asl	2.370(4)	Se2 - As2	2.376(4)	
Se3 - As1	2.369(4)	Se4 - As1	2.475(4)	
Se4 - As2	2.469(4)	Se5 - As2	2.395(4)	

^aThe estimated standard deviations in the mean bond lengths and the mean bond angles are calculated by the equation $\sigma l = \{\Sigma_n(l_n - 1)^2/n(n-1)\}^{1/2}$, where l_n is the length (or angle) of the nth bond, l the mean length (or angle), and n the number of bonds.

Table 6-14. Selected Angles (Deg) (with Standard Deviations in Parentheses^a) in the [Ag₃As₂Se₅]¹- layer.

Sel-Agl-Se2	108.6(1)	Sel-Agl-Se3	85.9(1)
Se1-Ag1-Se5	116.7(1)	Se2-Ag1-Se3	108.9(1)
Se2-Ag1-Se5	119.8(1)	Se3-Ag1-Se5	111.6(1)
Se3-Ag2-Se3	116.1(1)	Se3-Ag2-Se4	106.4(1)
Se3-Ag2-Se5	115.2(1)	Se3-Ag2-Se4	100.2(1)
Se3-Ag2-Se5	113.0(1)	Se4-Ag2-Se5	103.7(1)
Se1-Ag3-Se2	124.7(1)	Se1-Ag3-Se5	120.7(1)
Se1-Ag3-As2	100.8(1)	Se2-Ag3-Se5	93.2(1)
Se2-Ag3-As2	119.7(1)	Se5-Ag3-As2	95.0(1)
Ag1-Se1-As1	94.2(1)	Ag1-Se1-As2	91.2(1)
Ag3-Se2-As2	108.1(1)	Ag1-Se3-As1	119.0(1)
Ag2-Se3-As1	108.2(1)	Ag2-Se4-As1	88.6(1)
As1-Se4-As2	110.9(1)	Sel-Asl-Se3	100.1(1)
Se1-As1-Se4	96.3(1)	Se3-As1-Se4	102.9(2)
Ag3-As2-Se2	116.2(1)	Ag3-As2-Se4	139.6(1)
Ag3-As2-Se5	99.5(1)	Se2-As2-Se4	91.5(1)
Se2-As2-Se5	98.5(1)	Se4-As2-Se5	104.9(1)

^aThe estimated standard deviations in the mean bond lengths and the mean bond angles are calculated by the equation $\sigma l = \{\Sigma_n(l_n - 1)^2/n(n-1)\}^{1/2}$, where l_n is the length (or angle) of the nth bond, l the mean length (or angle), and n the number of bonds.

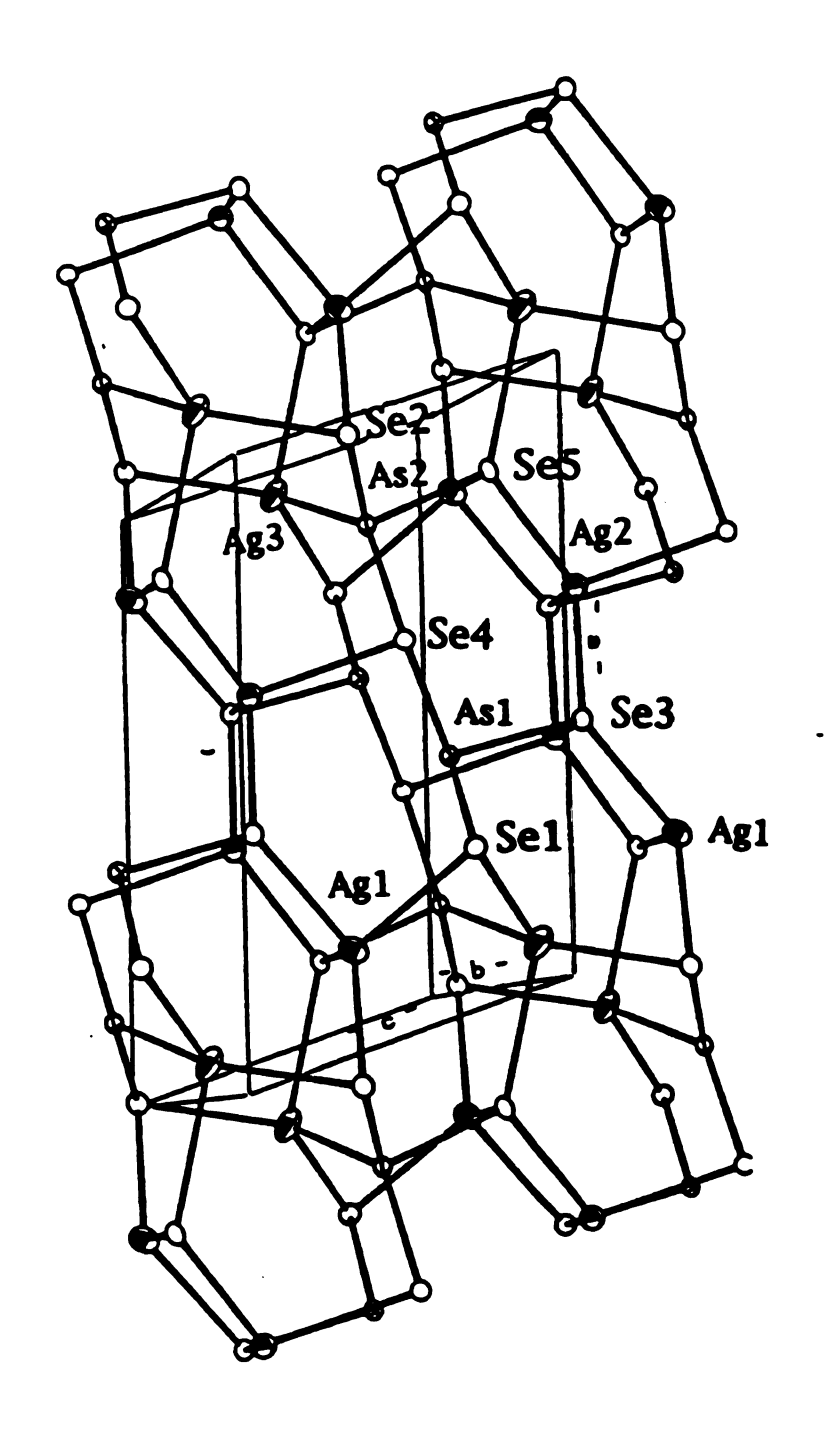
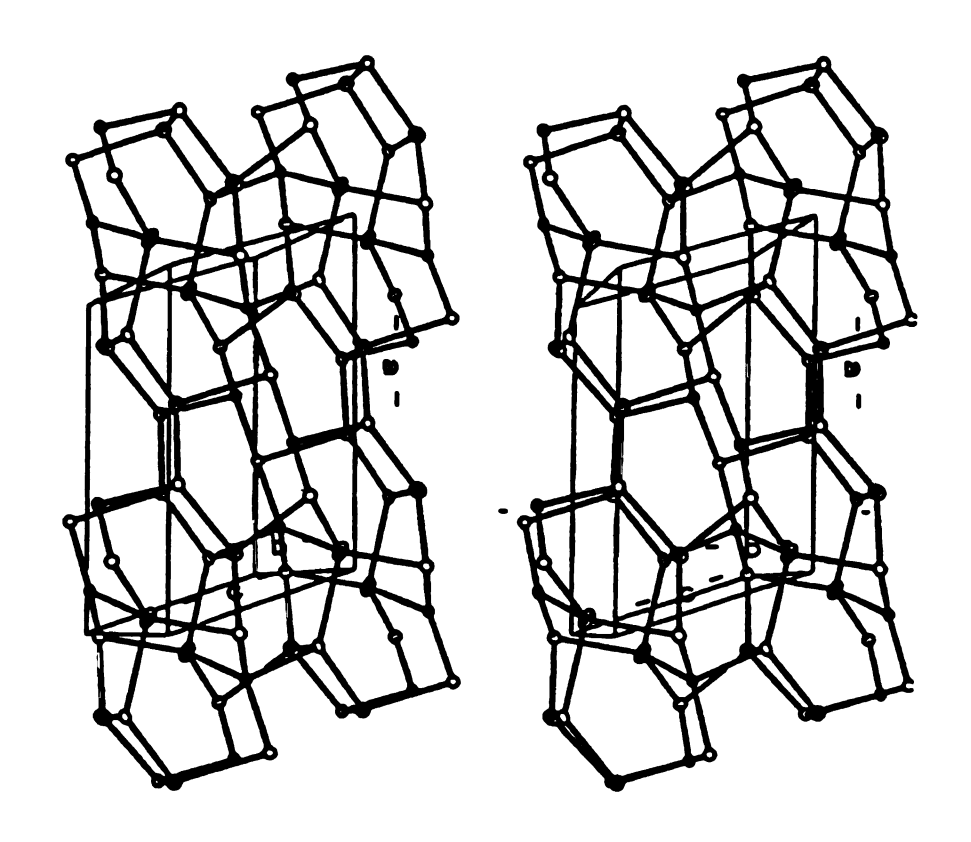


Figure 6-4. (A). Structure and labeling scheme of one [Ag₃As₂Se₅]-layer. (B) Stereoview.



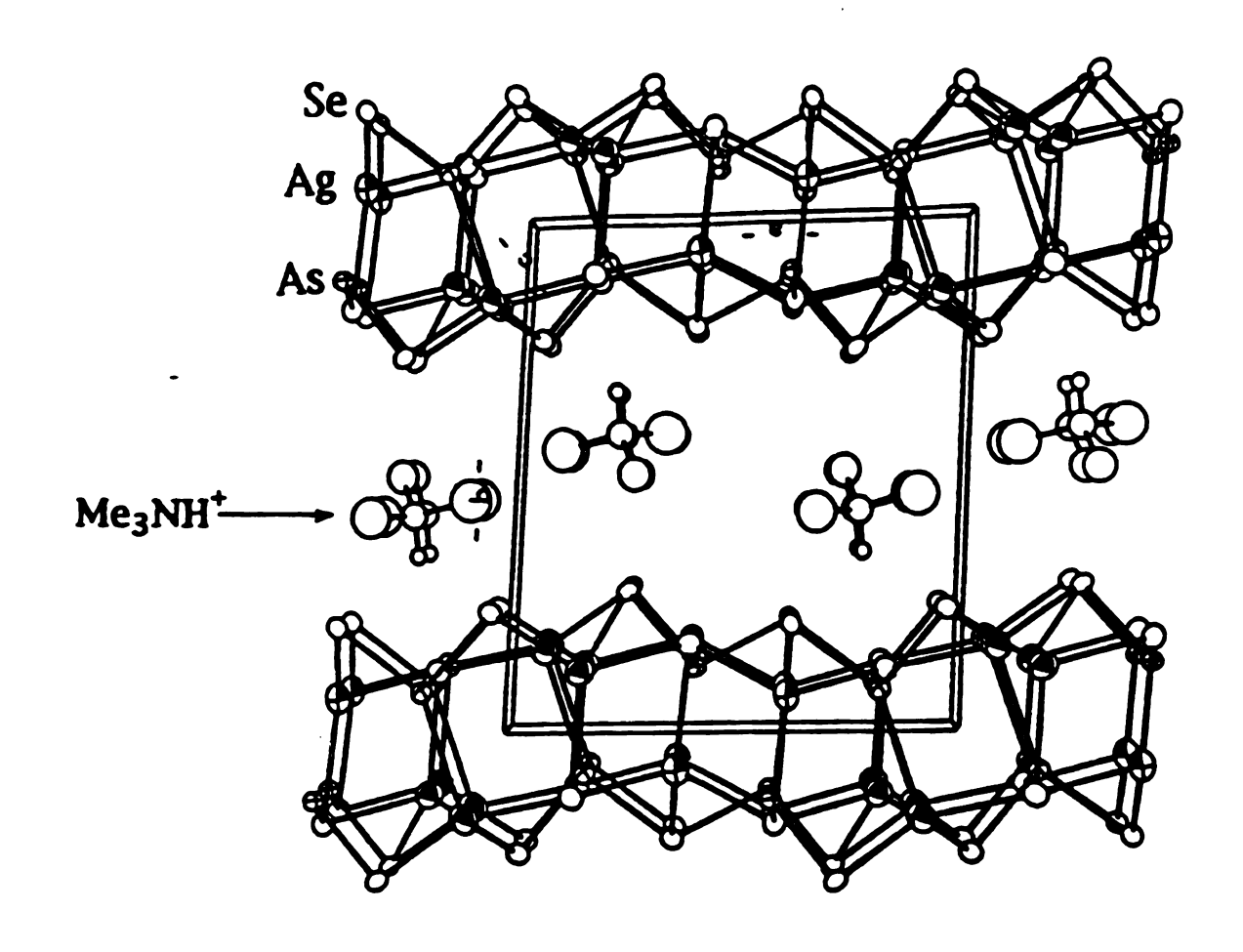
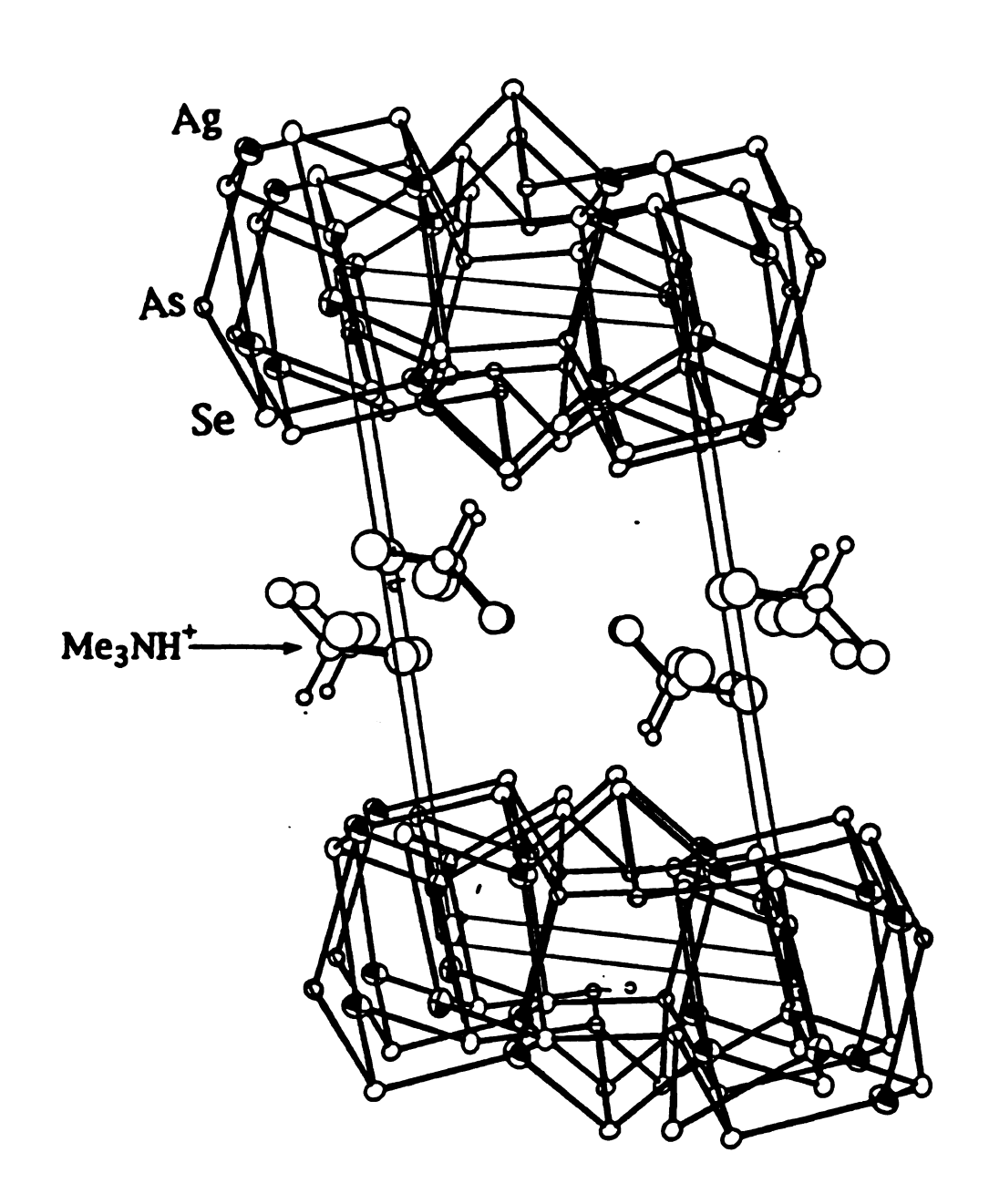


Figure 6-5. Packing diagrams of $(Me_3NH)[Ag_3As_2Se_5](II)$. (A) view down the c-axis. (B) view down the a-axis.

(B)



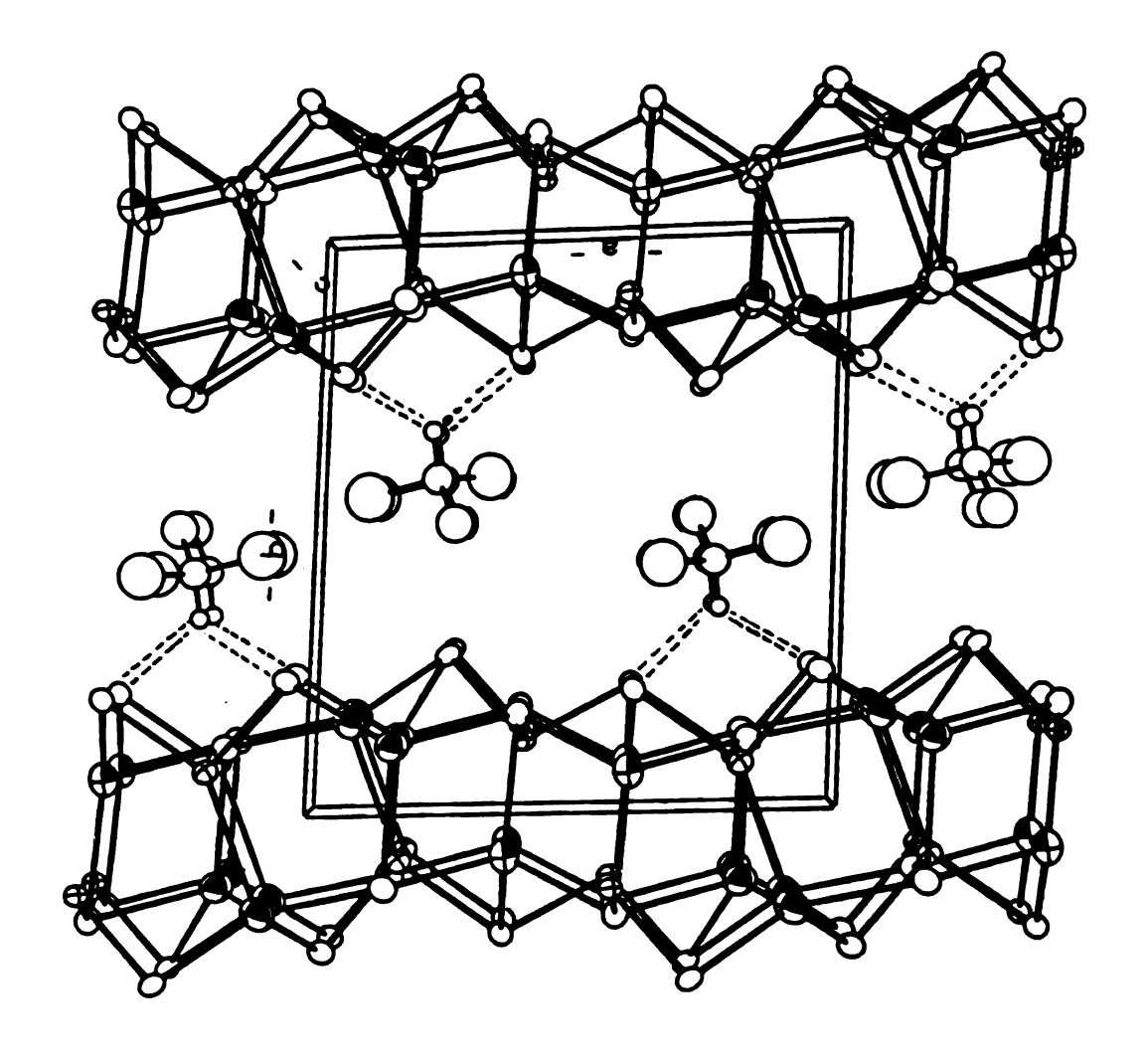
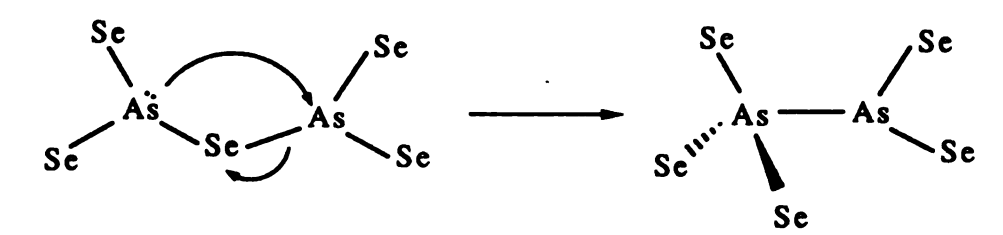


Figure 6-6. Packing diagram of (Me₃NH)[Ag₃As₂Se₅](II) showing the hydrogen bonding between the Se and H.

cations may act as structure directing agents and cause this compound to form even in the presence of a very large excess of Me₄N⁺. Several attempts to perform ion-exchange with this compound did not succeed.

The compound K₅[Ag₂As₃Se₉](III) was prepared by heating a mixture of AgBF4 and K3AsSe3 in methanol at 110 °C for several days. Similar reactions with the other alkali metal salts of $A_3A_5Se_3$ (A = Na, Rb) did not yield isostructural A₅[Ag₂As₃Se₉] compounds, indicating a templating role of K⁺. The [Ag₂As₃Se₉]_n⁵ⁿ- macroanion has a unique two-dimensional layered structure with tetrahedral Ag+ ions and two different types of selenoarsenate ligands, [AsSe₄]³- and [As₂Se₅]⁴-; see Figures 6-7 and 6-8. This [As₂Se₅]⁴ unit in (III) is different from the [As₂Se₅]⁴- unit found in (Me₃NH)[Ag₃As₂Se₅](II). They are structural isomers. The [As₂Se₅]⁴- unit In (III) can be viewed as the internal two-electron transfer (shown below) product of the $[As_2Se_5]^{4-}$ unit found in $(Me_3NH)[Ag_3As_2Se_5](II)$. The formal oxidation state of the four-coordinated As atom can be asigned as 4+ while the three-coordinated As atom is 2+. Kolis et al. have synthesized various arsenic selenides, 16 including the discrete [As₂Se₅]⁴- in superheated ethylenediamine.



The structure of $[Ag_2As_3Se_9]_n^{5n}$ can be described as chains of $[Ag_2As_2Se_5]^{2}$ linked by tetrahedral $[AsSe_4]^{3}$ units; see Figure 6-7. A

Table 6-15. Selected Distances (Å) of K₅[Ag₂As₃Se₉] with Standard Deviations in Parentheses.^a

Ag - Se2	2.648(3)	Ag - Se3	2.683(3)
Ag - Se4	2.742(3)	Ag - Se6	2.699(3)
Se1 - As1	2.313(6)	Se2 - As2	2.346(3)
Se4 - As1	2.340(3)	Se5 - As1	2.302(5)
Se6 - As3	2.331(3)	As2 - As3	2.580(5)
K1 - Se1	3.329(6)	K1 - Se2	3.321(7)
K1 - Se3	3.514(6)	K1 - Se3	3.403(6)
K1 - Se4	3.567(7)	K1 - Se5	3.434
K1 - Se6	3.489(6)	K2 - Se1	3.294(6)
K2 - Se3	3.385(6)	K2 - Se4	3.380(5)
K2 - Se4	3.476(5)	K2 - Se5	3.337(6)
K2 - Se6	3.247(6)	K2 - Se6	3.588(6)
K3 - Se3	3.423(8)	K3 - Se4	3.346(9)
K3 - Se6	3.392(7)		

^aThe estimated standard deviations in the mean bond lengths and the mean bond angles are calculated by the equation $\sigma l = \{\Sigma_n(l_n - 1)^2/n(n-1)\}^{1/2}$, where l_n is the length (or angle) of the nth bond, l the mean length (or angle), and n the number of bonds.

Table 6-16. Selected Angles (Deg) of [Ag₂As₃Se₉]⁵ with Standard Deviations in Parentheses.^a

Se2-Ag-Se3	112.3(1)	Se2-Ag-Se4	110.6(1)
Se2-Ag-Se6	105.2(1)	Se3-Ag-Se4	112.4(1)
Se3-Ag-Se6	112.1(1)	Se4-Ag-Se6	103.65(9)
Ag-Se2-As2	93.3(1)	Ag-Se3-As2	105.1(1)
Ag-Se4-As1	114.5(1)	Ag-Se6-As3	106.0(1)
Se1-As1-Se4	109.6(1)	Se1-As1-Se5	107.8(2)
Se4-As1-Se4	107.7(1)	Se4-As1-Se5	111.1(1)
Se2-As2-Se3	105.9(1)	Se2-As2-Se3	110.2(2)
Se3-As2-Se3	111.3(1)	Se3-As3-As2	98.2(1)
Se6-As3-Se6	105.8(2)	Se6-Se3-As2	98.2(1)

^aThe estimated standard deviation in the mean bond lengths and the mean bond angles are calculated by the equation $\sigma l = \{\Sigma_n(l_n - 1)^2/n(n-1)\}^{1/2}$, where l_n is the length (or angle) of the nth bond, l the mean length (or angle), and n the number of bonds.

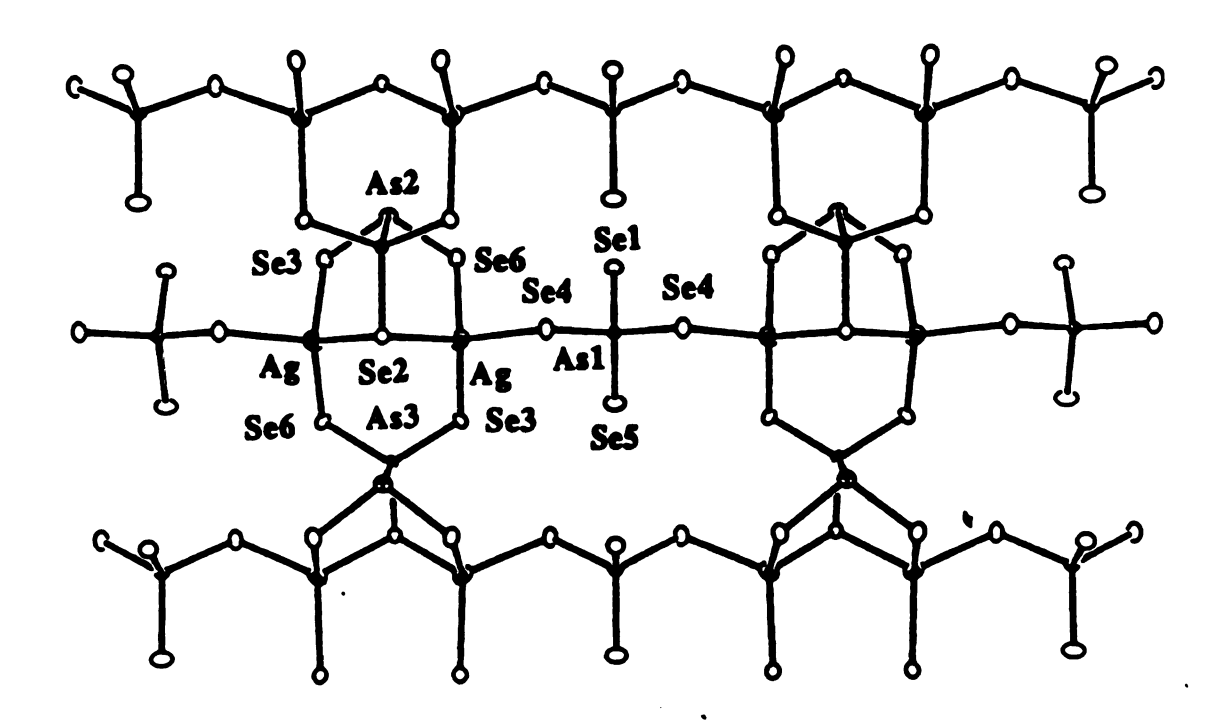


Figure 6-7. Structure and labeling scheme of one $[Ag_2As_3Se_9]n^5n$ -layer.

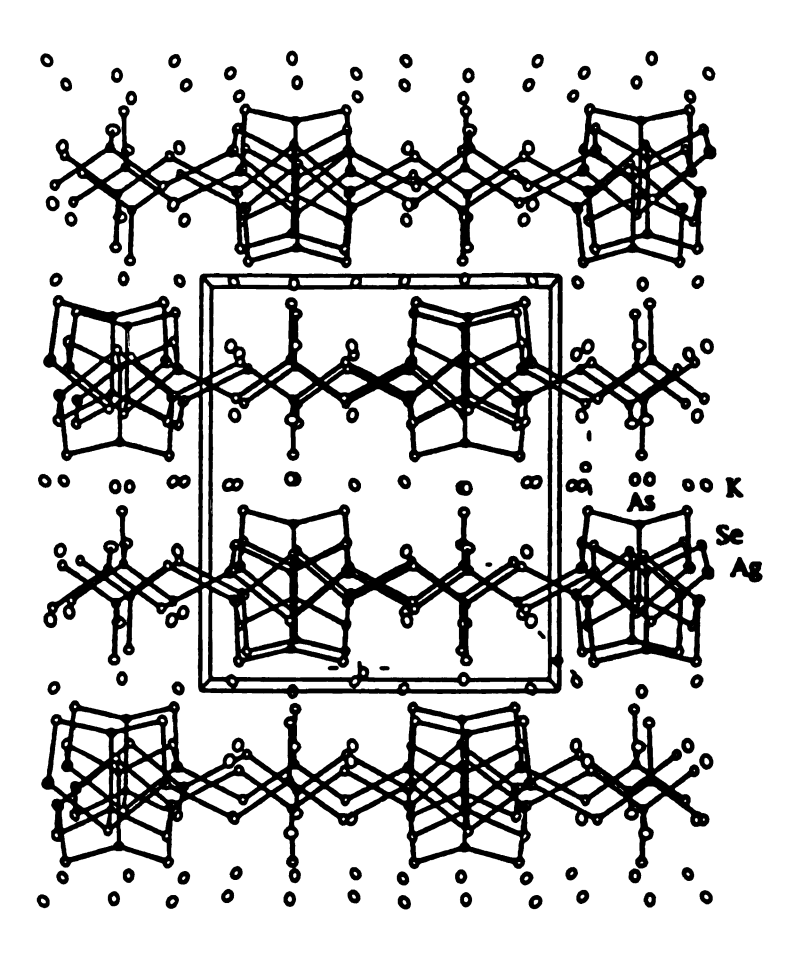
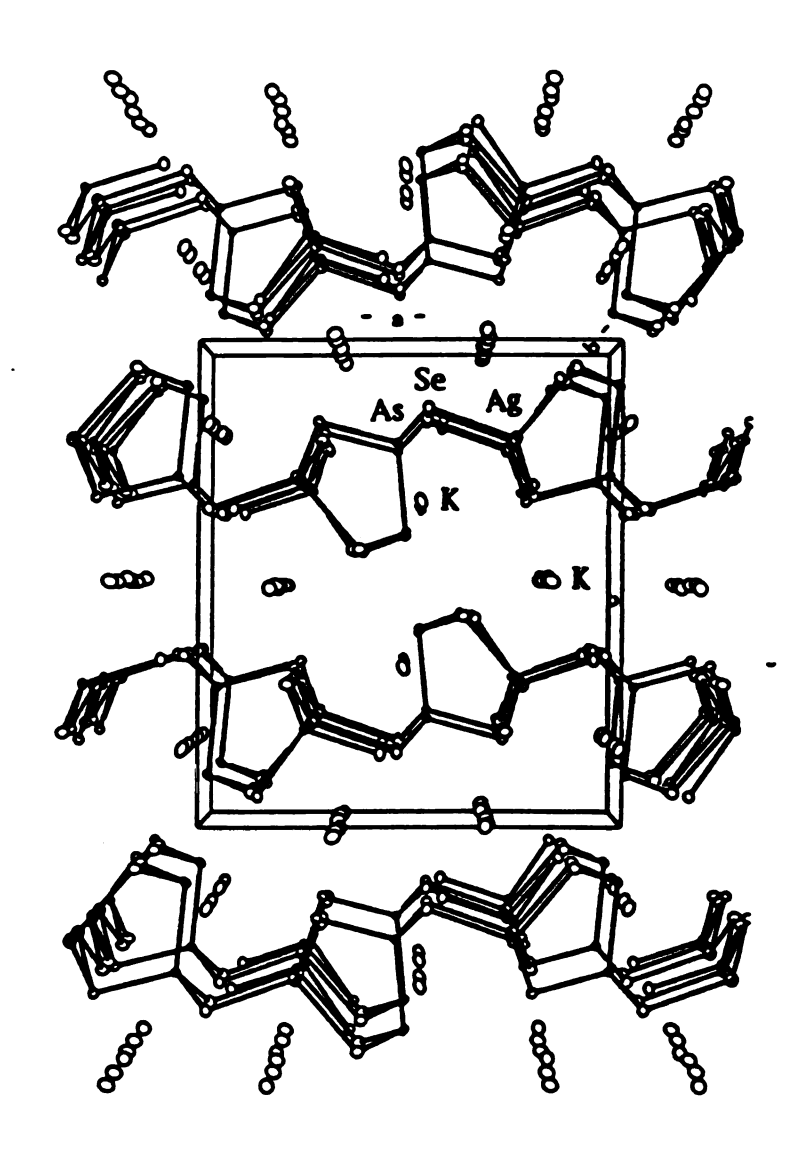


Figure 6-8. Packing diagram of $K_5[Ag_2As_3Se_9]$. (A) view down the a-axis. (B) view down the b-axis.



more descriptive formula of the compound would be $[Ag_2(As_2Se_5)(AsSe_4)]$. A unique feature of this compound is its mixed-valent As^3+/As^5+ character. The Ag^+ ion is in a distorted tetrahedral environment with the Se-Ag-Se angles ranging from $103.65(9)^\circ$ to $112.4(1)^\circ$. The average Ag-Se distance is normal at 2.693(3)Å. The average As-Se distance in the As(III) unit (i.e. $[As_2Se_5]^{4-}$), at 2.344(6)Å, is slightly longer than that of the As(V) unit (i.e. $[AsSe_4]^{3-}$), at 2.318(6)Å, as expected.

The residual negative charge on the Se atoms leads to short K-Se distances due to the high electrostatic attraction. The geometry of seven-coordinated K(1) can best be described as trigonal prismatic with one of the faces capped by the seventh Se, see Figure 6-9. The K(1)-Se distances range from 3.321(7)Å to 3.567(7)Å. The K(2) atom is also seven-coordinated with a capped trigonal antiprismatic The K(2)-Se distances range from 3.247(6)Å to environment. The six-coordinated K(3) has a distorted trigonal 3.588(6)Å. prismatic geometry with the K(3)-Se distances ranging from 3.346(9)Å to 3.423(8)Å. The detailed bond distances and angles are summarized in Tables 6-15 and 6-16. The [AsSe₄]³⁻ only uses two of its four Se atoms to coordinate to Ag atoms and leaves the other two Se atoms as terminal selenides. The result of this bonding mode creates large 16 member rings where the K cations reside.

K[Ag₃As₂S₅](IV) was synthesized by heating various ratios of AgBF₄, and K₃AsS₃ in methanol at 110 °C. Initial experiments in the Ag/As_xS_y system, with water as solvent always yielded the mineral

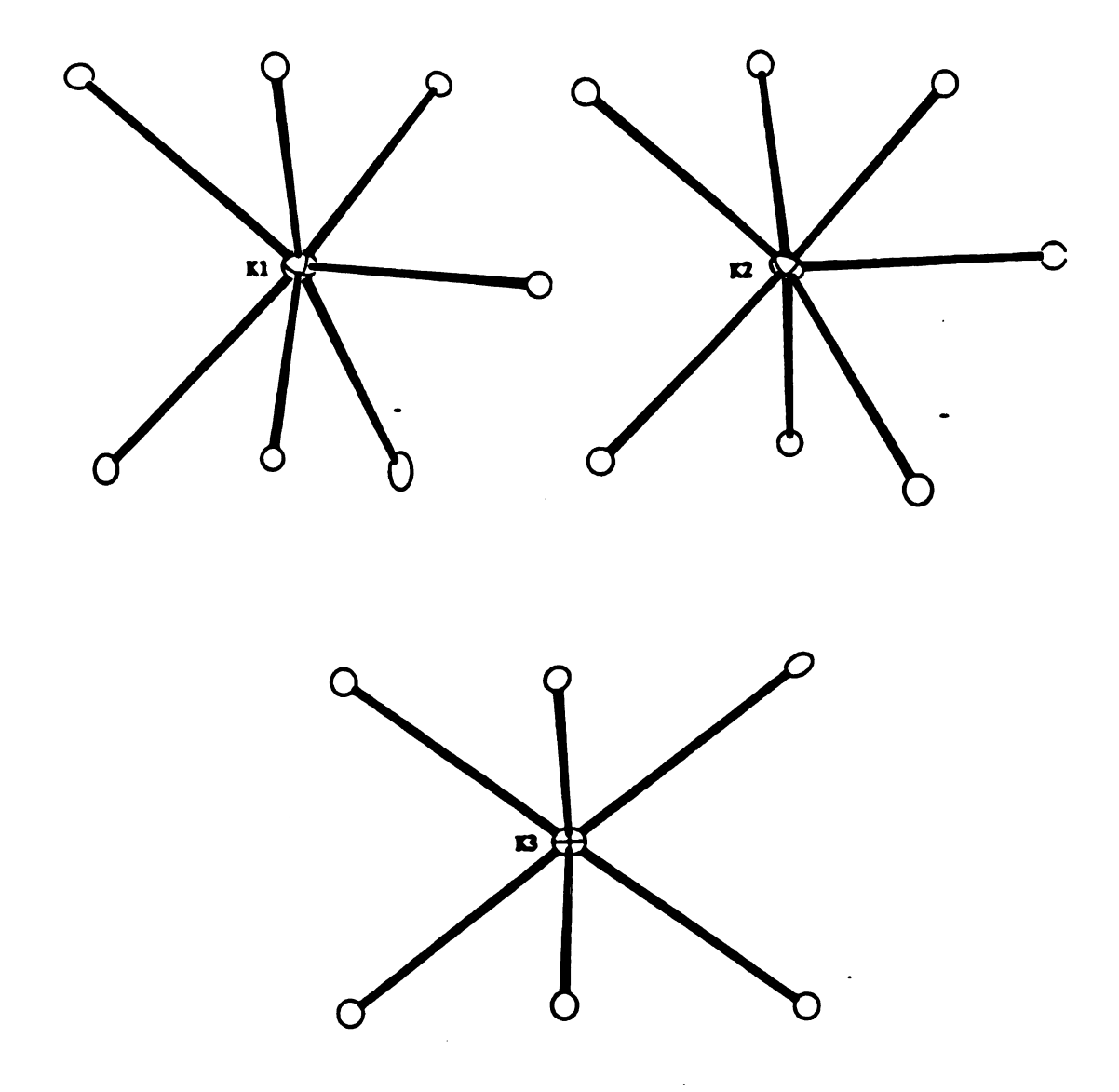
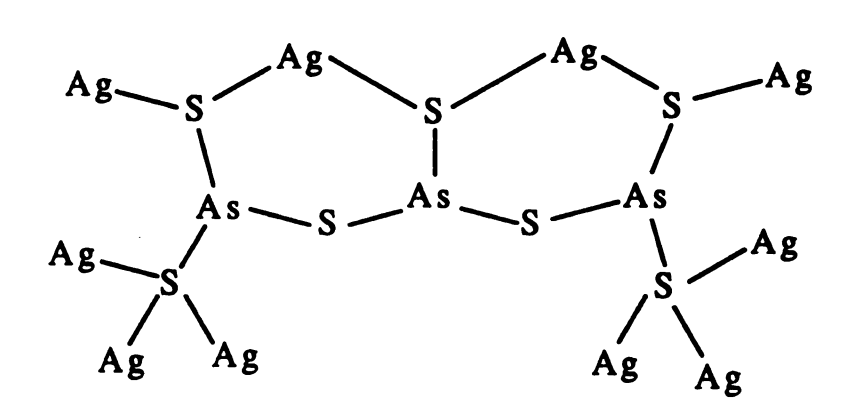


Figure 6-9. The coordination environments of K^+ in $K_5[Ag_2As_3Se_9]$. The open circles represent Se atoms.

proustite(Ag₃AsS₃). By simply changing the solvent from water to methanol we totally avoided the sulfosalt and obtained the new quanternary phase. The structure contains unique two-dimensional layers. Each layer has a very complicated structure consisting of formally Ag⁺ ions linked by a series of linear [As₃S₇]⁵⁻ units and pyramidal [AsS₃]³⁻ units; see Figures 6-10 and 6-11. Although the [As₃S₇]⁵⁻ units have been observed before in [InAs₃S₇]²⁻, the binding mode is totally different in K[Ag₃As₂S₅](IV). In [InAs₃S₇] n^{2n} , the [As₃S₇]⁵⁻ unit uses five of its terminal sulfur atoms to connect two In³⁺ centers, while in [Ag₃As₂S₅] n^{n} , the [As₃S₇]⁵⁻ units are bonded to 10 Ag⁺ centers, see Scheme 6-3.



Scheme 6-3

A more descriptive formula of the compound would be $K_2[Ag_6(AsS_3)(As_3S_7)]$. There are three kinds of Ag atoms in the lattice. The Ag(1) atom is in a distorted tetrahedral geometry with the S-Ag-S angles ranging from $101.5(2)^\circ$ to $118.0(2)^\circ$ while the Ag(2) and Ag(3) atoms are trigonal-planar coordinated to three S

atoms. The Ag(2) atom is more distorted than that of the Ag(3) atom with S-Ag(2)-S angles that range from 100.9(2) to 155.1(1)°. The S-Ag(3)-S angles range from 110.8(2)° to 125.8(2)°. The distortion is probably due to the ligand constrain. The average tetrahedral Ag(1)-S distance, at 2.638(6)Å, is longer than the expected average trigonal-planar Ag(2)-S and Ag(3)-S distances of 2.558(7)Å and 2.498(6)Å, respectively. The average As-S distances and S-As-S angles are normal at 2.268(6)Å and 99.5(2)°.17 The K atom is seven-coordinated with the K-S distances ranging from 3.150(8)Å to 3.522(8)Å. The coordination environment of K is irregular and can best be described as a capped trigonal antiprism, see Figure 6-12. Detailed distances and angles are summarized in Tables 6-17 and 6-18.

Table 6-17. Selected Distances (Å) in K[Ag₃As₂S₅] with Standard Deviations in Parentheses.^a

Ag1 - Ag2	2.996(3)	Ag1 - Ag2	3.139(3)
Ag1 - S2	2.620(6)	Ag1 - S3	2.758(6)
Ag1 - S5	2.624(6)	Ag1 - S6	2.550(6)
Ag2 - S2	2.568(7)	Ag2 - S5	2.538(7)
Ag2 - S5	2.569(7)	Ag3 - S1	2.461(6)
Ag3 - S2	2.488(6)	Ag3 - S3	2.545(6)
As1 - S1	2.238(9)	As1 - S2	2.255(6)
As2 - S3	2.246(6)	As2 - S4	2.307(6)
As2 - S5	2.252(6)	As3 - S4	2.317(6)
As3 - S6	2.231(8)	K - S1	3.150(8)
K - S2	3.413(8)	K - S3	3.299(8)
K - S3	3.522(8)	K - S4	3.269(8)
K - S4	3.395(8)	K - S6	3.302(9)

^aThe estimated standard deviations in the mean bond lengths and the mean bond angles are calculated by the equation $\sigma l = \{\Sigma_n(l_n - 1)^2/n(n-1)\}^{1/2}$, where l_n is the length (or angle) of the nth bond, l the mean length (or angle), and n the number of bonds.

Table 6-18. Selected Angles (Deg) in the [Ag₃As₂S₅]¹- ion with Standard Deviations in Parentheses.^a

S2-Ag1-S3	118.0(2)	S2-Ag1-S5	104.9(2)
S2-Ag1-S6	116.3(2)	S3-Ag1-S5	102.2(2)
S3-Ag1-S6	101.5(2)	S5-Ag1-S6	113.3(3)
S2-Ag2-S5	103.0(2)	S2-Ag1-S5	100.9(2)
S5-Ag1-S5	155.1(1)	S1-Ag1-S2	122.4(2)
S1-Ag3-S3	125.8(2)	S2-Ag3-S3	110.8(2)
S1-As1-S2	98.2(2)	S1-As1-S2	98.2(2)
S2-As1-S2	104.6(4)	S3-As2-S4	103.9(2)
S3-As2-S5	101.9(2)	S4-As2-S5	99.1(2)
S4-As3-S4	88.2(3)	S4-As3-S6	100.6(6)
S4-As3-S6	100.6(6)	Ag3-S1-As1	101.1(2)
Ag1-S2-As1	90.1(2)	Ag2-S2-As1	105.1(2)
Ag3-S2-As1	131.9(3)	Ag1-S3-As2	106.3(2)
Ag3-S3-As2	93.5(2)	As2-S4-As3	102.4(2)
Ag2-S5-As2	96.8(2)	Ag2-S5-As2	97.7(2)
Ag1-S6-As3	100.3(3)		

^aThe estimated standard deviations in the mean bond lengths and the mean bond angles are calculated by the equation $\sigma l = \{\Sigma_n(l_n - 1)^2/n(n-1)\}^{1/2}$, where l_n is the length (or angle) of the nth bond, l the mean length (or angle), and n the number of bonds.

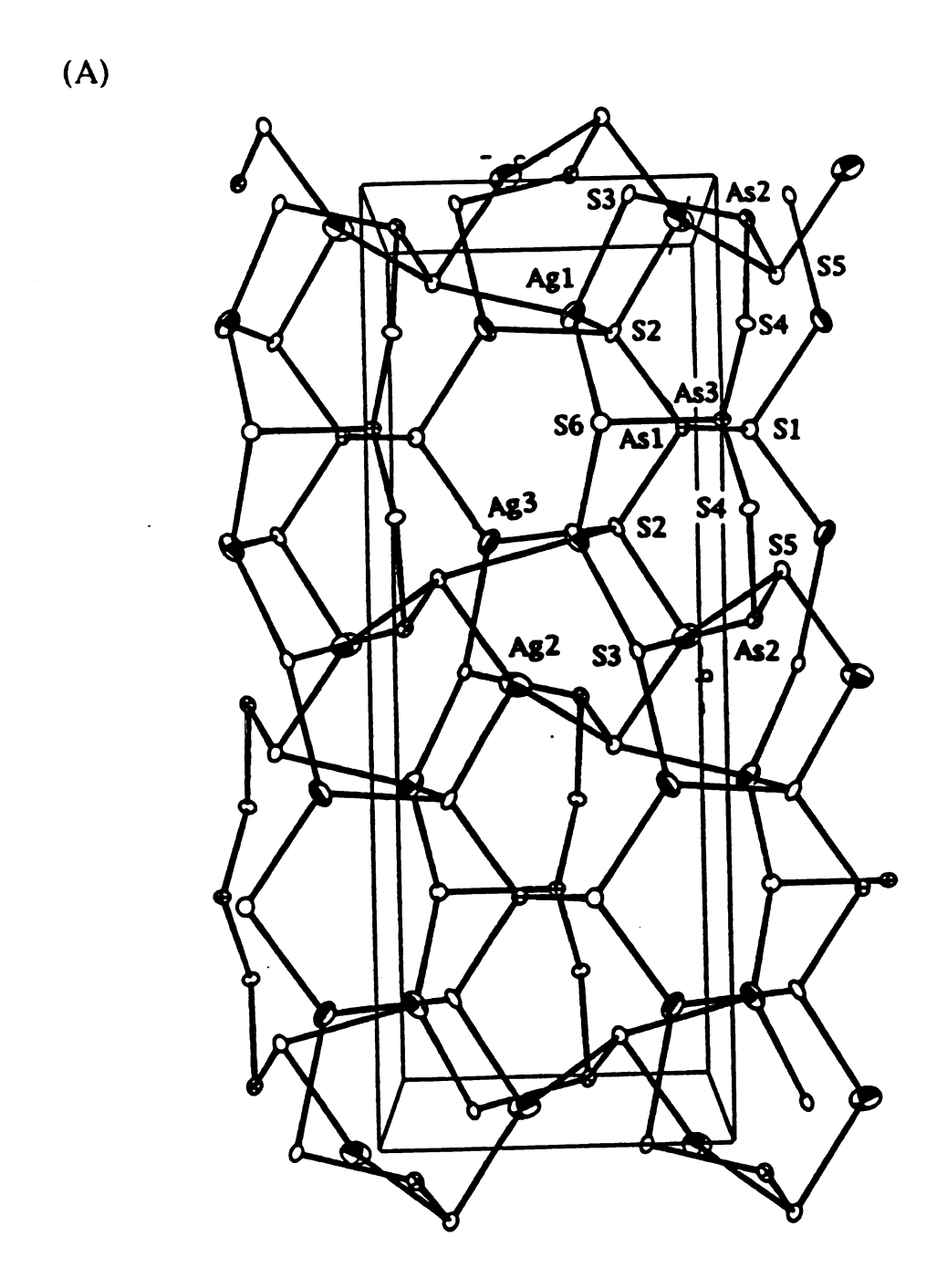
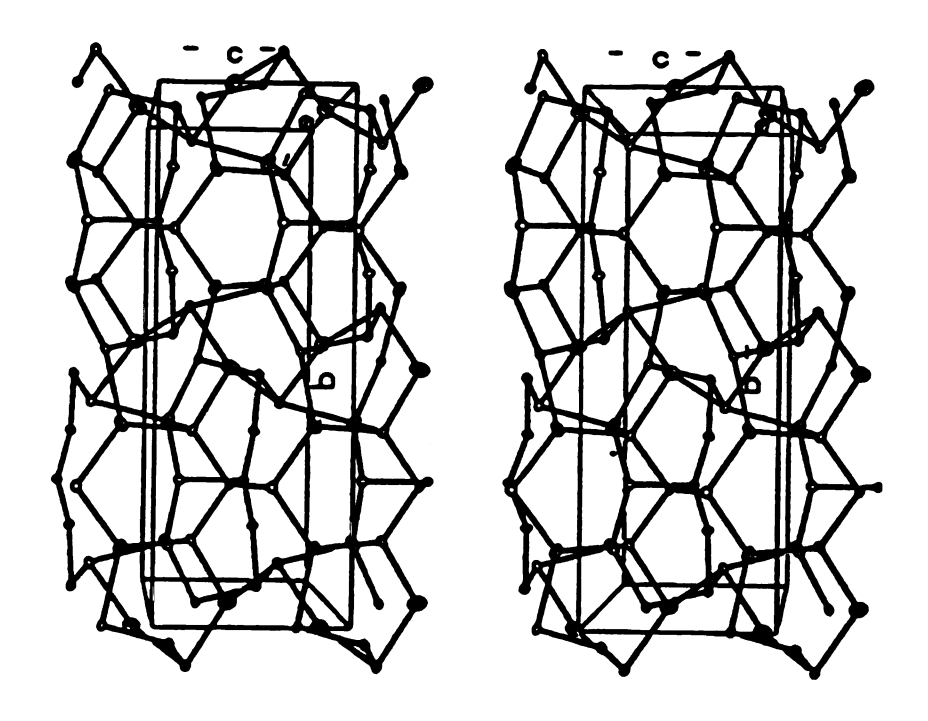


Figure 6-10. (A) Structure and labeling scheme of one $[Ag_3As_2S_5]_n^n$ layer. (B) Stereoview.



All the second s

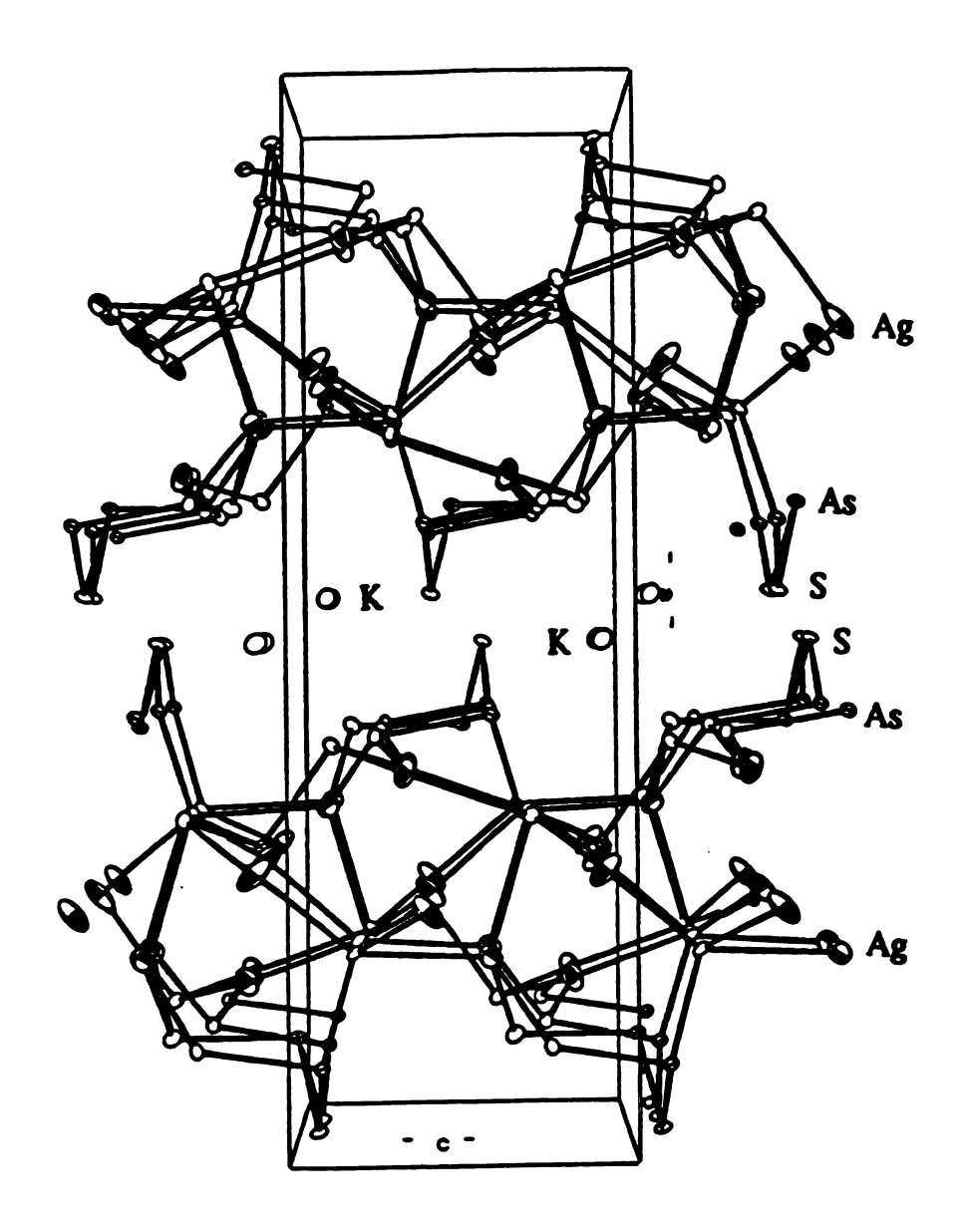
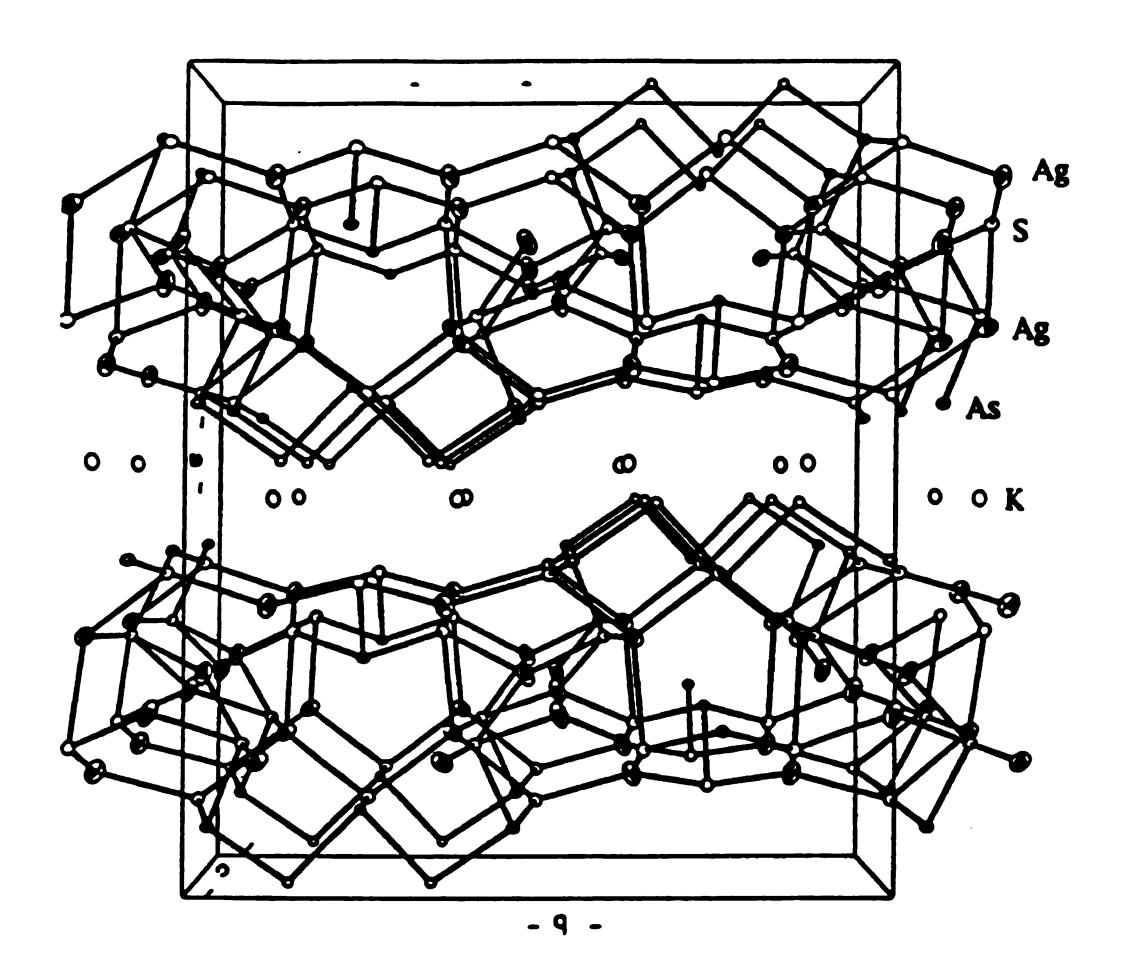


Figure 6-11. Packing diagram of $K[Ag_3As_2S_5]$. (A) view down the baxis. (B) view down the c-axis.

(B)



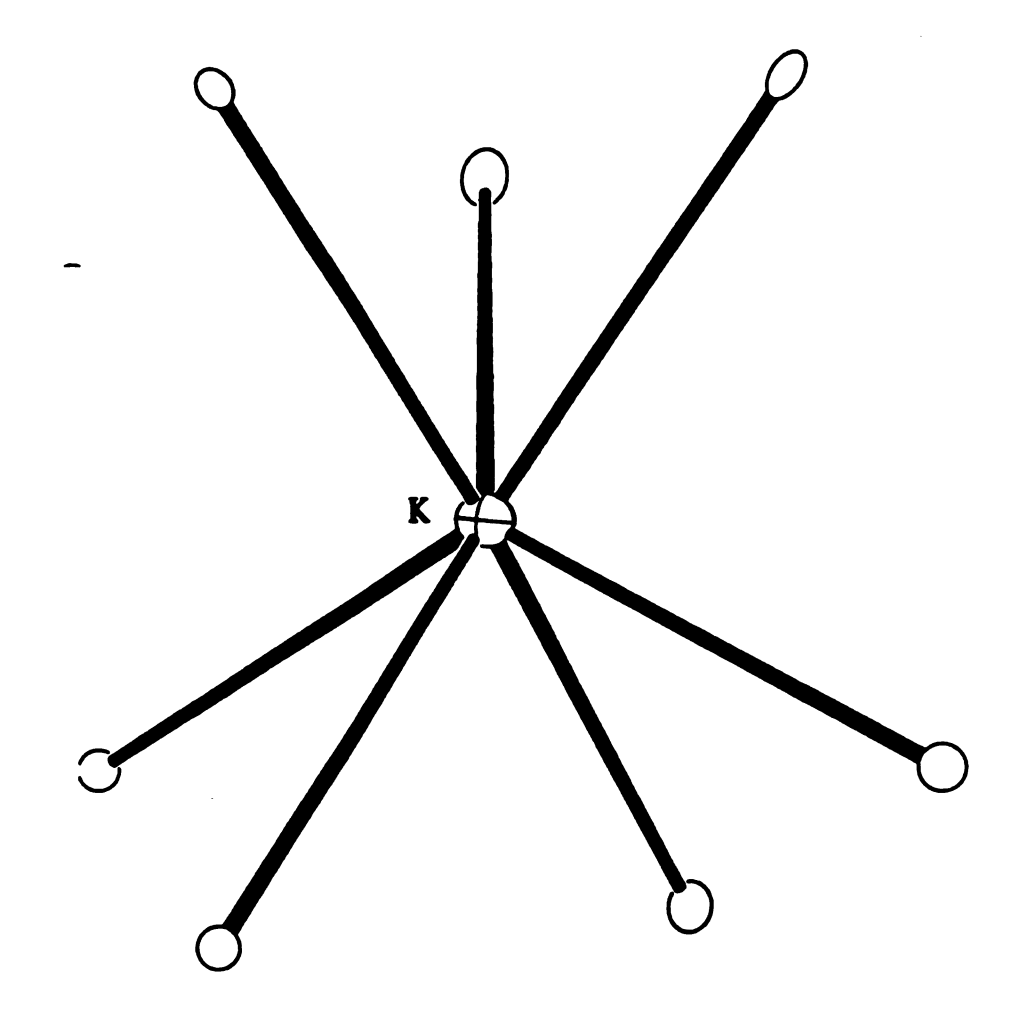


Figure 6-12. The coordination environments of K^+ in $K[Ag_3As_2S_5]$. The open circles represent S atoms.

3.2 Physicochemical studies

In the far-IR region complexes (I)-(III) exhibit spectral absorptions due to As-Se and Ag-Se stretching vibrations while complex (IV) show spectral absorptions due to As-S and Ag-S stretching vibrations; see Figures 6-13 and 6-14. Observed absorption frequencies of all the complexes are given in Table 6.19.

Table 6.19. Frequencies (cm⁻¹) of Raman and Infrared Spectral Absorptions of β -Ag₃AsSe₃ (I), (Me₃NH)[Ag₃As₂Se₅] (II), K₅[Ag₂As₃Se₉] (III), and K[Ag₃As₂S₅] (IV).

Compounds	Infrared	Raman
β-Ag ₃ AsSe ₃	246(s, br), 232(s)	243(s), 209(m), 167(m)
	171(m), 157(m)	
	142(m),	
(Me ₃ NH)[Ag ₃ As ₂ Se ₅]	269(s), 258(s)	273(s), 260(s), 246(m)
	248(s, sh), 219(s)	234(w), 215(m), 175(w)
	161(m, br)	
K ₅ [Ag ₂ As ₃ Se ₉]	293(s, sh), 282(s)	294(m), 272(m), 265(m)
	264(m), 242(w)	236(m), 210(s), 178(m)
	177(m, br), 155(m)	
K[Ag ₃ As ₂ S ₅]	336(s, br), 252(m)	373(s), 336(m), 317(m)
	247(m),190(w)	218(m, br),
	225(m), 205(m)	

^{*} s: strong, m; medium, w: weak, sh: shoulder, br : broad.

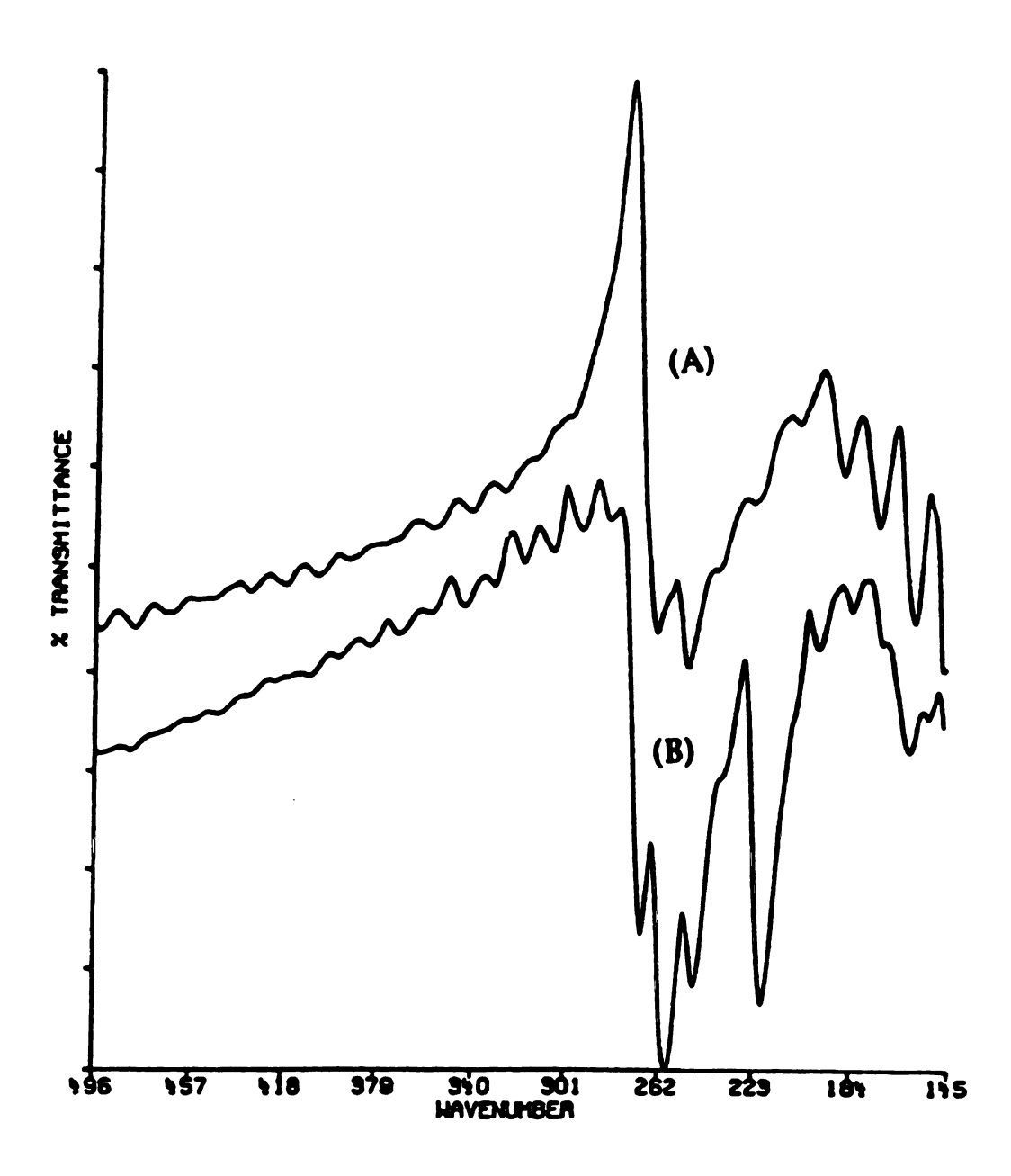


Figure 6-13. Far-IR spectra of (A) β -Ag₃AsSe₃, (B) (Me₃NH)[Ag₃As₂Se₅].

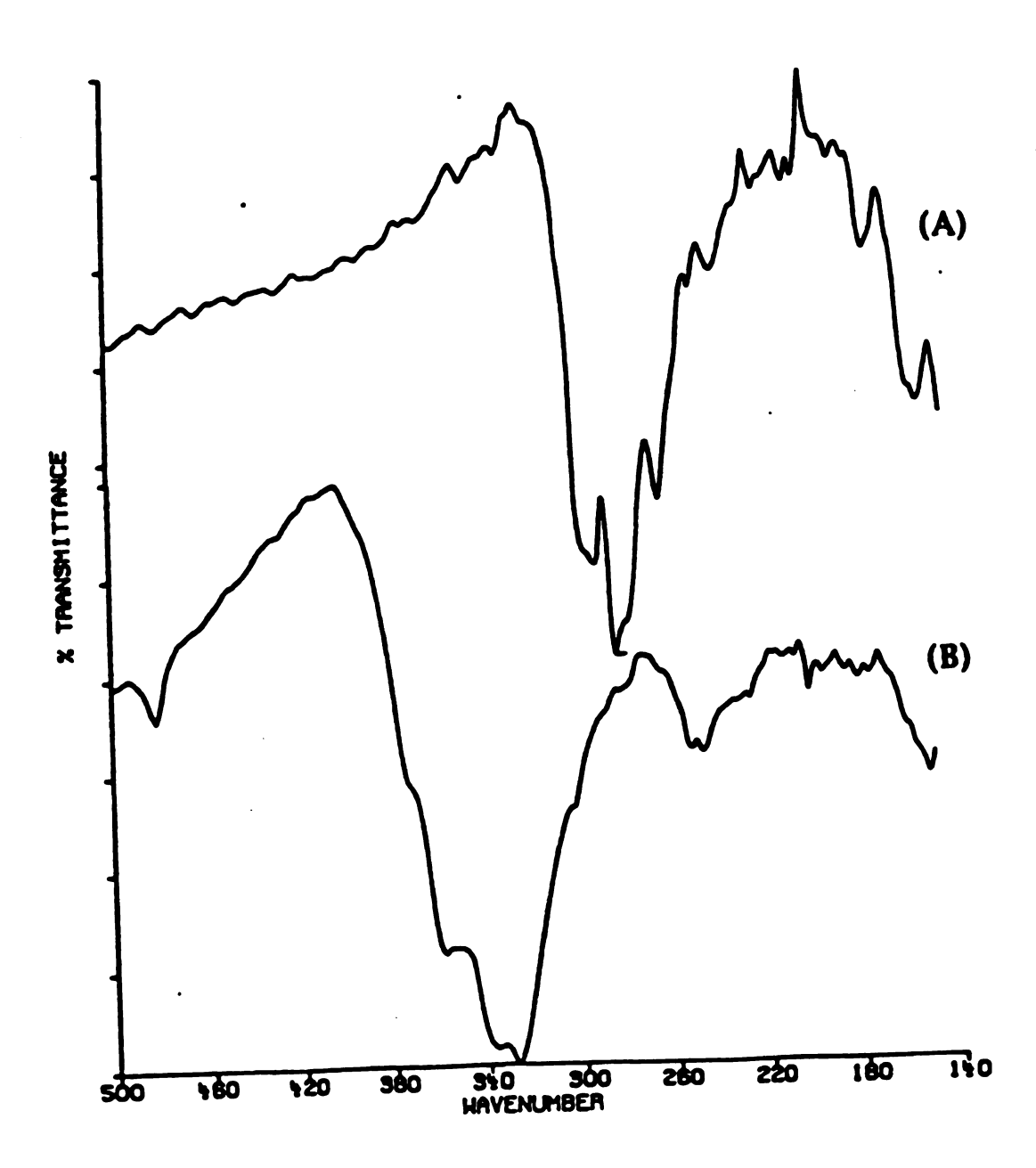


Figure 6-14. Far-IR spectra of (A) $K_5[Ag_2As_3Se_9]$, (B) and $K[Ag_3As_2S_5]$.

In the Far-IR spectra of β-Ag₃AsSe₃ (I), (Me₃NH)[Ag₃As₂Se₅] (II), and K₅[Ag₂As₃Se₉] (III), the peaks in the region of 200-300 cm⁻¹ could be attributed to As-Se vibration modes. Similar assignments have been made in the far-IR spectra of other known thioarsenic complexes. 18 In addition, a medium-intensity band around 170-150 cm⁻¹ was found in all compounds. This might result from an Ag-Se stretching vibration. The Far-IR spectrum of K[Ag₃As₂S₅] (IV) showed a strong-intensity broad band at around 340 cm⁻¹ and a weak-intensity band at 250 cm⁻¹. The former can be assigned to an As-S stretching vibration¹⁹ while the latter might be due to a Ag-S stretching vibration. The major difficulty in assigning correctly the observed IR spectra of these compounds arises from the fact that As-Q and Ag-Q (Q = S, Se) stretching frequencies fall in the same low frequency region of 150-350 cm⁻¹

The Raman spectra of (I), (II), (III) and (IV) were also recorded. In (I), (II), and (III) the peaks in the region of 200-300 cm⁻¹ could be assigned to As-Se vibrations while the lower energy peak around 170 cm⁻¹ could result from Ag-Se vibrational modes. A similar assignment for (IV) can be applied to the Raman spectrum as was done for its Far-IR spectrum.

The optical properties of compound (I) - (IV) were assessed by studying the UV/near-IR reflectance spectra of the materials. The spectra confirmed they are semiconductors by revealing the

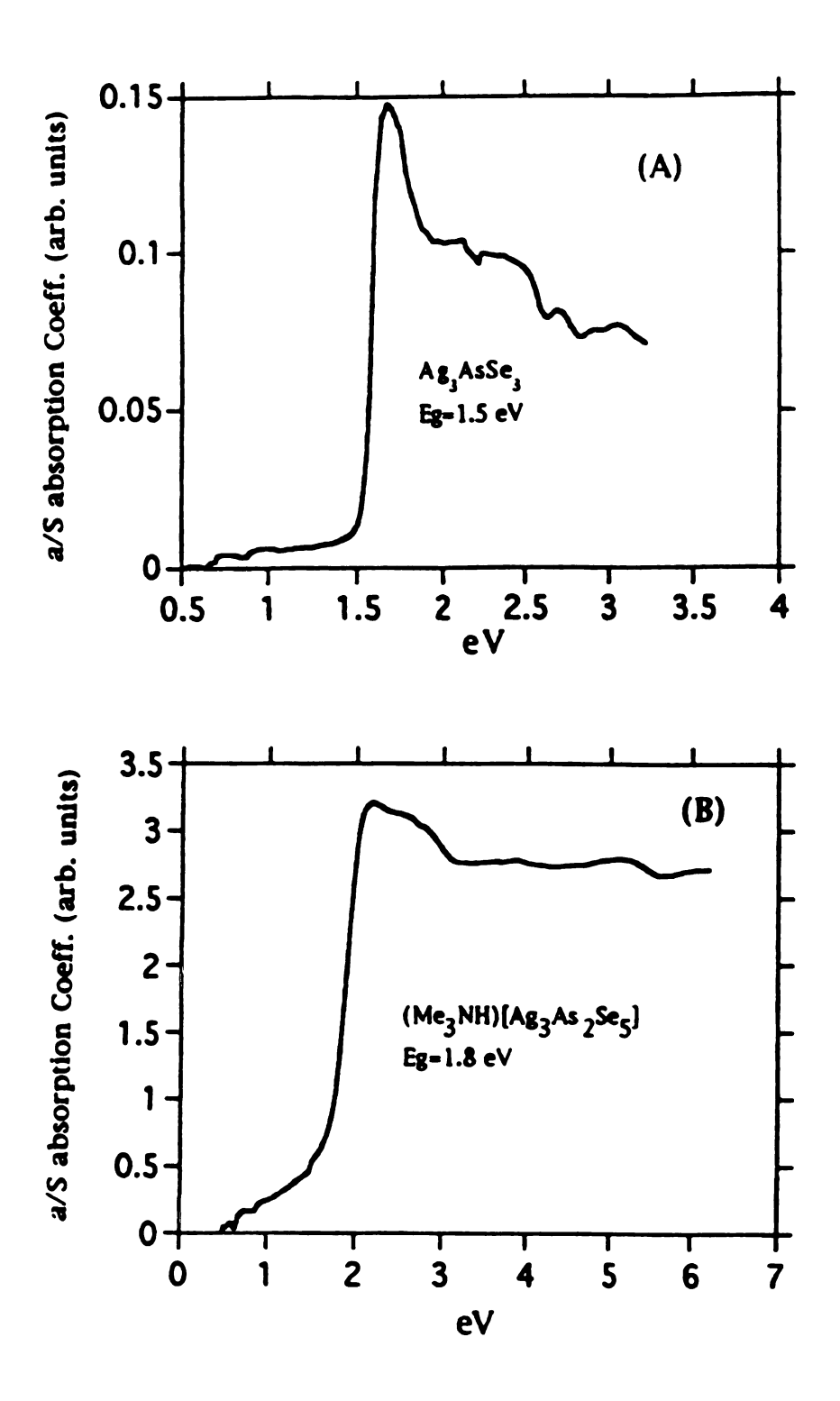


Figure 6-15. Optical absorption spectra of (A) β -Ag₃AsSe₃(I) and (B) (Me₃NH)[Ag₃As₂Se₅](II).

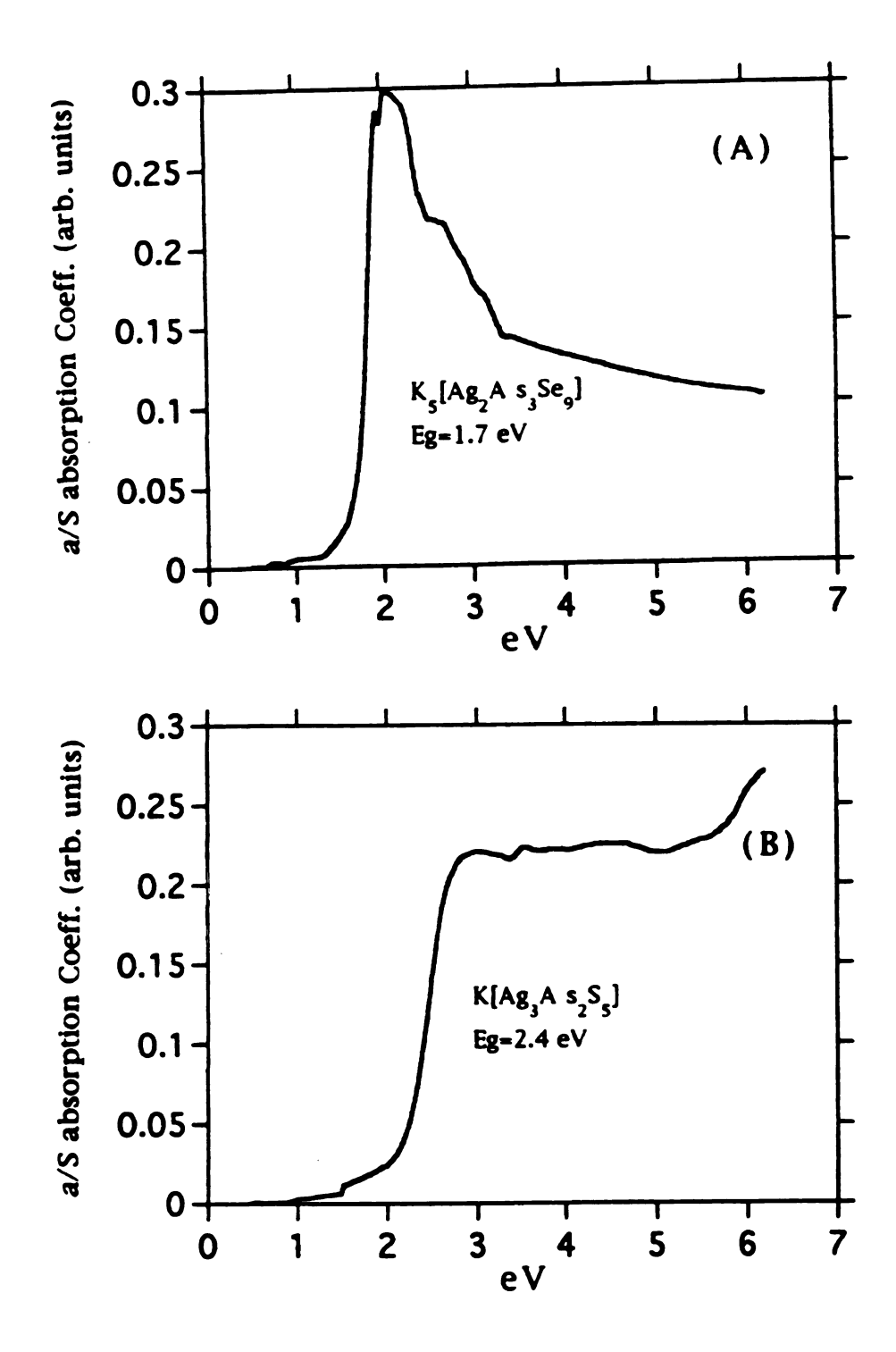


Figure 6-16. Optical absorption spectra of (A) $K_5[Ag_2As_3Se_9](III)$ and (B) $K[Ag_3As_2S_5](IV)$.

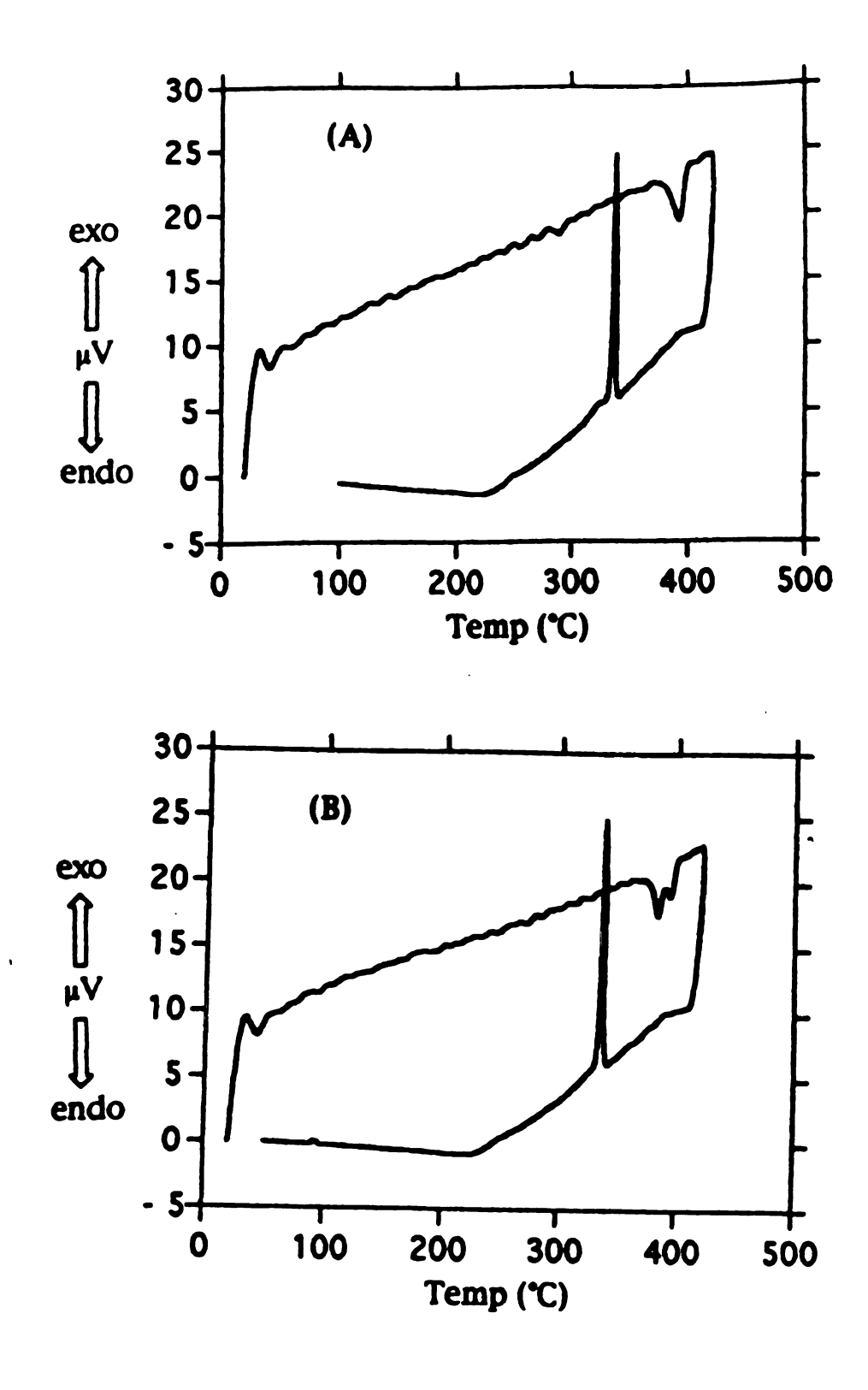


Figure 6-17. DTA data of β -Ag₃AsSe₃(I). (A) First cycle. (B) Second cycle

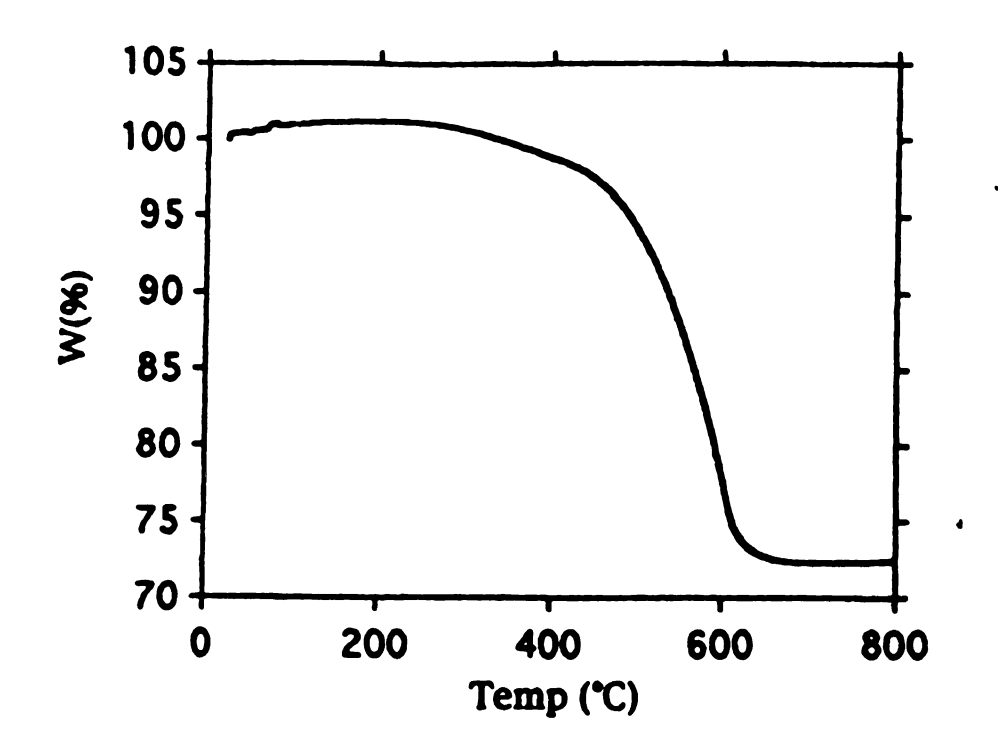


Figure 6-18. TGA diagram of β -Ag₃AsSe₃(I).

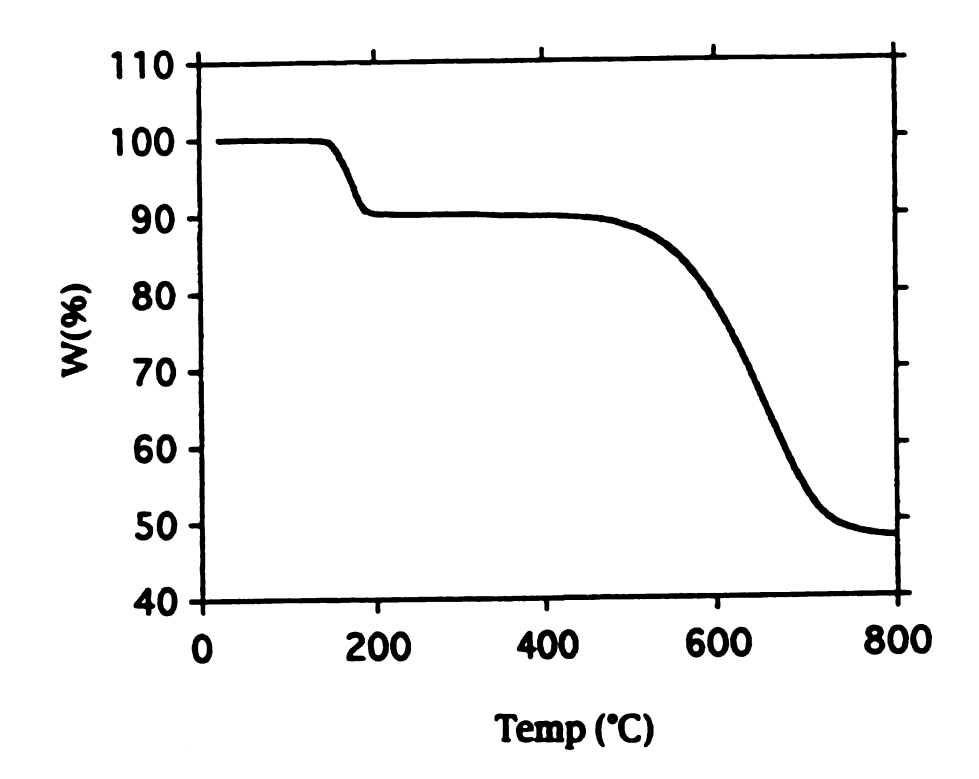


Figure 6-19. TGA diagram of (Me₃NH)[Ag₃As₂Se₅].

presence of sharp optical gaps as shown in Figures 6-15 and 6-16. The bandgaps are 1.5, 1.8, 1.7, and 2.4 eV, respectively. An $(\alpha h v)^2$ vs. E plot in the 1.5 to 1.7 eV region of the spectrum of β -Ag₃AsSe₃ gives a linear section, see figure 6-15, which suggests the presence of a direct band-gap in this material. It is tempting to suggest that the sharp absorption feature in the spectrum is excitonic in origin, but additional experiments would be required to prove this. The 1.5 eV band-gap of β -Ag₃AsSe₃ lies in the optimal region for efficient absorption of solar radiation, which coupled with the three-dimensional structure of this material, suggests that it may possess significant photoconductivity.

The thermal behavior of β -Ag₃AsSe₃ was investigated with differential thermal analysis (DTA), see Figure 6-17. The DTA thermogram, first cycle, showed a melting point, at 396 °C, and a crystallization point, at 342 °C. A second cycle, revealed two melting points, at 391 °C and 396 °C, and the same crystallization point, at 342 °C. The XRD of the DTA residue indicated that β -Ag₃AsSe₃ transformed into the known α -Ag₃AsSe₃ with Ag₂Se as a minor product. This observation was also comfirmed by the TGA experiment where β -Ag₃AsSe₃, see Figure 6-18, started to lose mass around 250 °C to give Ag₂Se.

The thermal stability of (Me₃NH)[Ag₃As₂Se₅] (II) was studied by thermal gravimetric analysis (TGA). There are two weight loss steps in the temperature range of 140-200 and 430-770 °C; see Figure 6-19. (Me₃NH)[Ag₃As₂Se₅] loses its organic cations as Me₃N and H₂Se in the first step. The layer integrity, however, is not maintained and the products at the end of the first weight loss were found to be, by X-ray powder diffraction, a mixture of α-Ag₃AsSe₃ and AgAsSe₂. The second weight loss corresponds to the loss of As₂Se₃ and the final decomposition product is pure Ag₂Se(Ag₂Se-120, naumannite)²⁰ by X-ray powder diffraction. The final weight loss observed from the TGA diagram was in excellent agreement with the theoretical value.

In conclusion, the synthesis of new ternary and quaternary compounds, β -Ag₃AsSe₃ (I), (Me₃NH)[Ag₃As₂Se₅] (II), K₅[Ag₂As₃Se₉] (III), and K[Ag₃As₂S₅] (IV), has proven that the hydro(solvo)thermal technique is a very powerful yet simple synthetic route to new silver arsenic sulfide and selenide compounds. The isolation of β -Ag₃AsSe₃, alone, implies that there are more new low temperature phases, in sulfosalts, waiting to be discovered and chemists should take another look at this alternative synthetic route.

REFERENCES

- 1 Chou, J.-H.; Kanatzidis, M. G. Inorg. Chem. 1994, 33, 1001-1002.
- 2. Chou, J.-H.; Kanatzidis, M. G. Chem. Mater. 1995, 7, 5-8.
- 3. Chou, J.-H.; Kanatzidis, M. G. Inorg. Chem. 1994, 33, 5372-5373.
- 4. Sheldrick, W. S.; Haüsler, H.-J. Z. Anorg. Allg. Chem. 1988, 557, 98-104.
- 5. Sheldrick, W. S.; Haüsler, H.-J. Z. Anorg. Allg. Chem. 1988, 557, 105-111.
- 6. Sheldrick, W. S.; Haüsler, H.-J. Z. Anorg. Allg. Chem. 1988, 561, 139-148.
- 7. Sheldrick, W. S.; Haüsler, H.-J. Z. Anorg. Allg. Chem. 1988, 561, 149-156.
- 8. Sheldrick, W.; Kaub, J. Z. Anorg. Allg. Chem. 1986, 535, 114-118.
- 9. Sheldrick, W.; Kaub, J. Z. Anorg. Allg. Chem. 1986, 535, 179-185.
- O'Neal, S. C.; Pennington, W. T.; Kolis, J. W. J. Am. Chem. Soc.1991, 113, 710-712.
- 11. O'Neal, S. C.; Pennington, W. T.; Kolis, J. W. *Inorg. Chem.* 1992, 31, 888-894.

- Sheldrick, G. M. In Crystallographic Computing 3; Sheldrick, G.
 M.; Kruger, C.; Goddard, R., Eds.; Oxford University Press: Oxford,
 U.K., 1985; pp 175-189.
- 13. TEXSAN: Single Crystal Structure Analysis Package, Version 5.0, Molecular Structure Corp., Woodland, TX.
- 14. Walker, N.; Stuart, D. Acta Crystallogr. 1983, 39A, 158-166.
- (a) Sheldrick, W.; Häusler, H.-J. Z. Anorg. Allg. Chem. 1988, 561, 139-148.
 (b) Sheldrick, W.; Kaub, J. Z. Anorg. Allg. Chem. 1986, 535, 179-185.
 (c) O'Neal, S. C.; Pennington, W. T.; Kolis, J. W. J. Am. Chem. Soc. 1991, 113, 710-712.
 (d) O'Neal, S. C.; Pennington, W. T.; Kolis, J. W. Inorg. Chem. 1992, 31, 888-894.
- 16. Drake, G. W.; Kolis, J. W. Coord. Chem. Rev. 1994, 137, 131-178.
- 17. (a) Sommer, H.; Hoppe, R. Z. Anorg. Allg. Chem. 1977, 430, 199.
 (b) Sheldrick, W. S.; Kaub, J. Z. Naturforsch. 1985, 40b, 571-573. (c) Jerome, J. E.; Wood, P. T.; Pennington, W. T.; Kolis, J. W. Inorg. Chem. 1994, 33, 1733-1734.
- 18. Christian, B. H.; Gillespie, R. J.; Sawyer, J, F, *Inorg. Chem.* 1981, 20, 3410-3420.
- (a) Mohammed, A.; Müller, U. Z. Anorg. Allg. Chem. 1985, 523,
 45-53. (b) Sinning, H.; Müller, U. Z. Anorg. Allg. Chem. 1988,
 564, 37-44.

20. JCPDS International Center for Diffraction Data, Powder Diffraction File 24-1044.

CHAPTER 7

CONCLUSIONS

In this work we have developed the hydro(solvo)thermal method for making various metal/As_xQ_y (Q = S, Se) compounds. Although the hydro(solvo)thermal technique has been known for many years, the current interest of applying this technique to inorganic synthesis is focused on solid state compounds. We hope our work will change the misconception that hydro(solvo)thermal chemistry is applicable only to metal oxides, silicates, etc. 2

The remarkable feature exhibited by the compounds described in this dissertation is the complex condensation reactions exhibited by the thioarsenate and selenoarsenate polyanions.(see eq 1-4)

$$AsS_2SH^{2-} + AsS_2SH^{2-} = [As_2S_5]^{4-} + H_2S$$
 (Eq. 1)

$$[As_2S_5]^{4-} + H_2S = [As_2S_4SH]^{3-} + HS^{1-}$$
 (Eq. 2)

$$[As_2S_4SH]^{3}$$
 + AsS_2SH^{2} = $[As_3S_7]^{5}$ + H_2S (Eq. 3)

$$[As_3S_7]^{5}$$
 + H_2S [As₃S₆SH]⁴ + HS^{1} (Eq. 4)

These condensation reactions were probably catalyzed by the protonation of the terminal sulfur groups. The list of various $[As_xQ_y]^{n-}$ (Q = S, Se) polyanions found in this work is shown in Tables 7-1 and 7-2. Their structures and their bonding modes are shown in Tables 7-3, 7-4, and 7-5.

Table 7-1 Various $[As_xS_y]^{n-}$ polyanions.

Ligand	Solvent	Compound
$[AsS_3]^{3}$	methanol	$K_2[Ag_6(AsS_3)(As_3S_7)]$
[AsS ₄] ³ -	water, methanol	$(Ph_4P)_2K[M_3(AsS_4)_3]$
		(M=Pt, Pd)
[As ₂ S ₅] ⁴ -	water	$(Me_4N)_2[Mo_2O_2(As_2S_5)S_2]$
$[As_3S_5]^{3}$	water	$(Ph_4P)_2[Pt(As_3S_5)_2]$
$[As_3S_6]^{3-}$	water	$(Me_4N)_2Rb[Bi(As_3S_6)_2],$
		$(Me_4N)[HgAs_3S_6]$
[As ₃ S ₇] ⁵ -	water, methanol	$K_2[Ag_6(AsS_3)(As_3S_7)],$
		$(Ph_4)_2[InAs_3S_7]$
[As ₄ S ₈] ⁴ -	water	$(Ph_4P)_2[NiAs_4S_8]$
[As4S9] ⁶⁻	water	(Ph ₄ P) ₂ [Hg ₂ As ₄ S ₉],
		(Ph ₄ P) ₂ [SnAs ₄ S ₉]

Table 7-2 Various $[As_xSe_y]^{n-}$ polyanions.

Ligand	Solvent	Compound
[AsSe ₃] ³ -	water	(Me4N)[HgAsSe3],
		(Et4N)[HgAsSe3]
[As2Se5]4-a	water	$(Me_3NH)[Ag_3As_2Se_5]$
[As ₂ Se ₅] ^{4- b}	methanol	$K_5[Ag_2As_3Se_9]$
[As4Se ₁₁] ⁶ -	water	$(Ph_4P)_2[Hg_2As_4Se_{11}]$

Table 7-3. Various $[As_xQ_y]^{n-}$ (Q = S, Se) anions found in this work.

$\left[AsQ_3\right]^{3}$	Q As.
[AsSe ₄] ³⁻	Se — Se
[AsS ₄] ³⁻	S As. As
$\left[\mathrm{As}_{2}\mathrm{Q}_{5}\right]^{4-}$	As, As, Q
[As ₃ S ₅] ³⁻	SIN As S AsS
[As ₃ S ₆] ³⁻	
[As ₃ S ₇] ⁵⁻	S As, As, As, S As, S
[As ₄ S ₈] ⁴⁻	S S S S S S S S S S S S S S S S S S S
[As ₄ S ₉] ⁶⁻	S S S S S S S S S S S S S S S S S S S
[As ₄ Se ₁₁] ⁶ -	Se
[As ₃ S ₆] _n ³ⁿ⁻	S S S S S S S S S S S S S S S S S S S

Table 7-4. Different binding modes found in the $[As_xQ_y]^{n-}$ anions.

Table 7-5. Some other known $[As_xQ_y]^{n-}$ (Q = S, Se, Te) anions.

[AsS ₈]	S As S S
$[As_2S_6]^{2^-}$ (Q=S, Se, Te)	$Q \xrightarrow{As} Q \xrightarrow{Q} Q$ $Q \xrightarrow{As} Q$
[As ₄ S ₆] ²⁻ (Q=S, Se, Te)	Q As Q As Q
[As ₆ S ₁₂] ⁶⁻	S S S S S S S S S S S S S S S S S S S

We believe that the $[As_xS_y]^{n-}$ and $[As_xSe_y]^{n-}$ polyanions are very similar to the polychalcogenide ligands, and that they are so versatile that their coordination chemistry towards metal ions is vast; see Table 7-4. This can in part be attributed to the coordination preference of the metal ions. By adjusting their coordination modes, to the demands of the metal ions and the packing requirements of the counterions, different compounds can be derived from the same $[As_xQ_y]^{n-}$ anion. Of course, all these uncertainties also undermine our ability to predict the structures. The solubilities of these cation/M/ $[As_xS_y]^{n-}$ compounds also cannot be ignored; if a certain

compound has low solubility, it is going to crystallize out first, thus often leading to kinetically stable, rather than thermodynamically stable products. We also like to point out that there is the possibility for redox chemistry in the reaction media when M = Pt, $Pd.^3$ These redox reactions resulted in the unusual Pt-As bond formation in [Pt(As₃S₅)]²- and indicate the chemistry of thioarsenate ligands is as, more, complicated than their counterparts, the polychalcogenide ligands. The fact that familiar fragments, such as $[Pt(Q_4)_2]^{2-}$, can be recognized in $[Pt_3(A_5S_4)_3]^{3-}$, make this chemistry even more exciting by virtue of the enormous number of structure types reported in the metal polychalcogenide chemistry. We are fortunate to have studied the chemistry of metal polychalcogenide for the past six years and the knowledge gained in those years will no doubt be very helpful in the continuing exploratory work of the metal/As_xQ_y systems.⁴

At this stage, at least two directions may be taken to further investigate the field. Metal/As_xSe_y and Metal/As_xTe_y chemistry must be explored due to the fact learned from metal polychalcogenide chemistry that heavy polychalcogenide chemistry is very different from the polysulfide chemistry.⁵ Other cations must be explored in more detail. We have not had very much success with cations other than the Ph₄P⁺. In order to achieve our initial goal, three-dimensional framework compounds, small organic cations are probably our best bet.

REFERENCES

- Several review articles dealing with different aspects of hydrothermal research are available, see (a) Laudise, R. A. Inorg. Chem. 1962, 3, 1-47. (b) Demianets, L. M.; Lobachev, A. N. in Crystallization Process under Hydrothermal Conditions, A. N. Lobachev Ed.; Consultants Bureau, New, York, 1973.
- (a) Liebau, F. Structural Chemistry of Silicates; Springer: New York, 1985.
 (b) Day, V. W.; Klemperer, W. G.; Mainz, V. V.; Millar, D. M. J. Am. Chem. Soc. 1985, 107, 8262-8264.
 (c) Cotton, F. A.; Wilkinson, G. Advanced Inorganic Chemistry; John Wiley & Sons: New York, 1988, pp 421-430.
 (d) Barrer, R. M. Hydrothermal Chemistry of Zeolites, Academic Press, New York, 1982.
- 3. Chou, J.-H.; Kanatzidis, M. G. Inorg. Chem. 1994, in press.
- Some examples: (a) Liao, J.-H.; Kanatzidis, M. G. J. Am. Chem. Soc. 1990, 112, 7400-7402. (b) Liao, J.-H.; Kanatzidis, M. G. Inorg. Chem. 1992, 31, 431-439. (c) Kim, K.-W. Kanatzidis, M. G. J. Am. Chem. Soc. 1992, 114, 4878-4883. (d) Dinhgra, S.; Kanatzidis, M. G. Science, 1992, 258, 1769-1772. (e) Kim, K.-W.; Kanatzidis, M. G. J. Am. Chem. Soc. 1993, 115, 5871-5872.
- Several review articles dealing with polyselenide and polytelluride ligands are available, see:(e) Roof, L. C.; Kolis, J. W. Chem. Rev. 1993, 93, 1037-1080. (c) Huang, S.-P.; Kanatzidis, M. G. Coord. Chem. Rev. 1994, 597-624.

